



รายงานวิจัยฉบับสมบูรณ์

โครงการ การตอบสนองของป่าทวีปต่อการเปลี่ยนแปลงและ
ความแปรปรวนของสภาพภูมิอากาศตามแนวละตitud: กรณีศึกษาของ
แปลงพลวัตบนเส้นลองจิจูดที่ 101 องศาตะวันออก



โดย รองศาสตราจารย์ ดร. พันธนา ตอเงิน และคณะ
มีนาคม 2564

รายงานວິຈัยຈັບສົມບູຮັນ

ໂຄຮກການ ການຕອບສັອງຂອງປ່າທິວໄປຕ່ອກເປີ່ຍແປລັງແລະ ຄວາມແປປ່ວນຂອງສກພຸມມີອາກາສຕາມແນວລະຕິຈຸດ: ກຣີນີ້ສຶກໜາຂອງແປລັງ ພລວັດບັນເສັ້ນລອງຈິຈຸດທີ 101 ອອງສາຕະວັນອອກ

ຄະະຜູ້ວິຈัย

1. ອອງສາສຕຣາຈາຍ ດຣ. ພັນທາ ຕອເງິນ	ຈຸ່າພາລັງກຣົນໆມໍາຫວີທີຍາລັຍ
2. ອອງສາສຕຣາຈາຍ ດຣ. ວົງຄໍ ຈັນທຣ	ມໍາຫວີທີຍາລັຍເກະຊາດສູງ
3. ອອງສາສຕຣາຈາຍ ດຣ. ສກລວຮຣນ ທ່າວໄຊຍ	ຈຸ່າພາລັງກຣົນໆມໍາຫວີທີຍາລັຍ
4. ດຣ. ດັຕຣທິພຍໍ ຮອດທັກນາ	ຈຸ່າພາລັງກຣົນໆມໍາຫວີທີຍາລັຍ

ສັບສົນໂດຍສໍາໜັກງານຄະະກຽມກາຮ່າງສົ່ງເສີມວິທີຍາສາສູງ ວິຈය ແລະ ນວັດກຽມ
(ສກສວ.)

(ຄວາມເຫັນໃນรายงานນີ້ເປັນຂອງຜູ້ວິຈය ສກສວ. ໄນຈໍາເປັນຕົ້ນເຫັນດ້ວຍເສມອໄປ)

Final Report

The Response of Typical Forests to Climate Change and Climate Variability along A Latitudinal Gradient: A Case Study on E101 Longitude Dynamic Plots Belt

การตอบสนองของป่าทั่วไปต่อการเปลี่ยนแปลงและความแปรปรวนของสภาพภูมิอากาศตาม
แนวละติจูด: กรณีศึกษาของแปลงพลาตบันเลี้นลงจิจูดที่ 101 องศาตะวันออก

Principal Investigator	Associate Professor Pantana Tor-ngern, Ph.D. Chulalongkorn University
Project duration	3 December 2018 – 2 December 2021
Co-investigators	Associate Professor Wirong Chanthorn, Ph.D. Kasetsart University Assistant Professor Sakonvan Chawchai, Ph.D. Chulalongkorn University Chadtip Rodtassana, Ph.D. Chulalongkorn University
Chinese investigators	Associate Professor Yajun Chen, Ph.D. Chinese Academy of Sciences Professor Zhenghong Tan, Ph.D. Hainan University Associate Professor Ke Wei, Ph.D. Chinese Academy of Sciences Associate Professor Hua Lin, Ph.D. Chinese Academy of Sciences Associate Professor Peili Fu, Ph.D. Chinese Academy of Sciences Assistant Professor Shubin Zhang, Ph.D. Chinese Academy of Sciences Shankar Panthi, Ph.D. Chinese Academy of Sciences

Executive Summary

The main objectives of this research collaboration between Thailand and China are to investigate the past responses of tree growth to climate change, the present responses of forests to variation in climate and the vulnerability and resilience of forests, and the future impacts of climate change on forest biomass, productivity, and diversity. We attempted to complete the studies as proposed; however, there were many obstacles resulting from the Covid-19 pandemic that significantly hampered the collaborative work. Nevertheless, we managed to perform many studies in Thai forests with remote collaboration from Chinese researchers, resulting in five publications in peer-reviewed international journals with good impact factors (at least Q1 SCOPUS), one manuscript being under reviewed in an international journal (Q1 SCOPUS), and one manuscript under preparation. Based on our findings from various studies, we found that the typical forests in this region respond differently to variations in climatic and environmental factors, including air temperature and relative humidity, rainfall, and soil moisture across seasons. Site conditions involving canopy development associated with forest successional stages may play critical role in such different responses among the forests from similar climate region. We also performed extensive measurements on the vulnerability of tropical tree species to drought in Thai forests. We managed to obtain similar data on vulnerability to drought of trees in two Chinese forests from our partner and synthesized them with our data to gain some insights into adaptive strategies of these species which would imply their likelihood to survive under future climate change. Here, we summarize the main findings from these studies that were published or submitted to international, peer-reviewed journals.

1. Tree rings could provide long term trend for the carbon fixation capacity and climate change. However, due to the lack of ring boundary for most tropical tree species and difficulty in cross-dating, the tree ring study in tropical region is limited to a few species. *Choerospondias axillaris* is a tropical species that has never been studied for tree rings in Thailand. To investigate the dendrochronological potential of *C. axillaris*, this study focused on the growth-climate relationship and long-term growth trend of *C. axillaris* at Mosingto forest dynamic plot, Khao Yai National Park, east-central Thailand. A chronology with 100 core samples from 56 trees was constructed covering the period 1932 to 2019. Tree-ring width index of *C. axillaris* at Mosingto was positively correlated with precipitation from June, July and October of current year ($p<0.05$), indicating that the growth of *C. axillaris* is mainly controlled by moisture availability in the monsoon season. However, there was no significant correlation between tree ring index of *C. axillaris* and temperature. The long-term growth trend of *C. axillaris* showed an increasing trend from 1932 to 1984 but showed a slightly decreasing trend from 1985 to 2019. Our study will provide an important insight into the growth-climate relationships in tropical regions.
2. Deforestation has created heterogeneous patches of old-growth and secondary forests throughout Southeast Asia, posing challenges for understanding the hydrological and carbon cycles. In addition to changes in species composition, environmental conditions differ across successional stages which in turn can influence forest water use and productivity. Here, we investigated leaf-level area-based photosynthesis (A_{area}) and

stomatal conductance (g_s) of 11 tree species dominating an old-growth (OF; >200 years), an intermediate (IF; ~44 years), and a young forest (YF; ~4 years) in Thailand during both the wet and dry season. Specifically, we compared A_{area} and g_s and assessed the sensitivity of g_s to vapor pressure deficit (VPD). We also examined relationships between gas exchange parameters and key functional leaf traits, including leaf mass per area (LMA), nitrogen (N), phosphorus (P), and chlorophyll concentration. All three forests showed comparable A_{area} and g_s in the wet season, whereas significantly lower values were observed in IF during the dry season. All forest stages displayed similar sensitivity of g_s to VPD. Among the leaf functional traits considered, LMA, N and P were significantly higher in YF compared to the other two successional stages. Our results suggested that forest succession may not influence gas exchange, rather, canopy development associated with forest stage produced the main effect. Furthermore, the young forest was the most active in resource acquisition with its high LMA and leaf nutrient concentrations, which could result in high photosynthetic rates. However, low soil water availability in YF possibly limit the gas exchange rates thereby making them similar to those in the old-growth forest. These findings highlight the potential effects of canopy characteristics inherent in successional forests on water and carbon exchanges between trees and the atmosphere and their sensitivity to atmospheric drought. These results call for the need for further studies to identify the main factors influencing forest productivity during secondary succession in the tropics, particularly in the Southeast Asian region where such information is lacking.

3. Soil respiration (SR) in forests contributes significant carbon dioxide emissions from terrestrial ecosystems and is highly sensitive to environmental changes, including soil temperature, soil moisture, microbial community, surface litter and vegetation type. Indeed, a small change in SR may have large impacts on the global carbon balance, further influencing feedbacks to climate change. Thus, detailed characterization of SR responses to changes in environmental conditions is needed to accurately estimate carbon dioxide emissions from forest ecosystems. However, data for such analyses are still limited, especially in tropical forests of Southeast Asia where various stages of forest succession exist due to previous land-use changes. In this study, we measured SR and some environmental factors including soil temperature (ST), soil moisture (SM) and organic matter content (OM) in three successional tropical forests in both wet and dry periods. We also analyzed the relationships between SR and these environmental variables. Results showed that SR was higher in the wet period and in older forests. While no response of SR to ST was found in younger forest stages, SR of the old-growth forest significantly responded to ST, plausibly due to the non-uniform forest structure, including gaps, that resulted in a wide range of ST. Across forest stages, SM was the limiting factor for SR in the wet period whereas SR significantly varied with OM in the dry period. Overall, our results indicated that the responses of SR to environmental factors varied temporally and across forest succession. Nevertheless, these findings are still preliminary and call for detailed investigations on SR and its variations with environmental factors in Southeast Asian tropical forests where patches of successional stages dominate.
4. Sapwood area is an important parameter for estimating canopy transpiration in the forest water cycle. However, sapwood area highly varies across species and forest ecosystems,

and is difficult to measure directly. Therefore, species- and site-specific allometric equations are needed to estimate sapwood area of all trees in a forest. Here, we conducted a comprehensive campaign to measure sapwood thickness and estimate sapwood area of 14 common tree species in a successional forest in Thailand. These data represent the first comprehensive measurements of sapwood area in Southeast Asian successional forests growing under diverse environmental conditions in terms of soil moisture and canopy density. The results show that a power function can significantly explain the relationship between sapwood area and stem size, represented by diameter at breast height (DBH), in all species in both primary and secondary forests. Interestingly, a single equation could describe the sapwood area ~ DBH relationship in all species and forest stages, except for *Dipterocarpus gracilis*, an emergent, dominant species in the primary forest. The latter showed slower growth in sapwood area once the trees reached a DBH of approximately 30 cm. Overall, our results can benefit future studies that estimate canopy transpiration of tropical forests with similar conditions as in our study sites.

5. Due to large-scale abandoned agricultural areas in Southeast Asia, secondary tropical forest successions commonly comprise various forest stages, resulting in multiple characteristics and inherent environmental conditions. Such spatial heterogeneity challenges the study of how these forests respond to environmental changes, especially under the predicted increasing climatic water stress. Therefore, the information of trees' response to changing environments is still lacking in tropical forests, especially in Southeast Asia. To fill this knowledge gap, we investigated the seasonal variations in leaf water status and drought tolerance of dominant tree species in three tropical forests with different ages, ranging from 5 to > 200 years old, and located in Khao Yai National Park, Thailand. Seasonal variation in leaf water status differed among the successional stages with trees in young and intermediate sites demonstrating a 30% increase in apparent water stress between the wet and dry season. Even though vulnerability to embolism curves revealed that trees in old-growth forest was potentially more sensitive to declining leaf water status than intermediate and young forests, trees in old-growth forest were predicted to loss less than 5% of their hydraulic capacity as opposed to 13% for the trees in the other sites. Moreover, a large variation in the capacity to tolerate drought was observed among the study species even within one forest stage. However, same tree species common to all three sites exhibited similar drought tolerance across forest stages. Overall, the results suggested that soil water availability may influence plant water status and drought tolerance of trees. Nevertheless, species with high drought tolerance can remain active regardless of various soil moisture conditions. Our results suggest that the responses to water stress of tree species in different forest ages greatly vary with a tendency of trees in younger sites to be more impacted than trees in older sites. Therefore, evaluating species' performance under water stress should be carefully interpreted. Such information would be beneficial for selecting tree species that could be well adapted to specific environments, thus improving the strategies for managing forests of different ages under a warmer future.

Although the different responses of these typical forests to climatic and environmental factors may not be surprising, our results are among the first evidence from field investigations

in tropical forests of Southeast Asia which are considered the big puzzle in the earth system models. In the final analysis comprising the synthesis among data from Thai and Chinese forests, the result suggested that future droughts may exert different impacts on different forest ecosystems. Species in forests in high elevation and high rainfall regions may be more vulnerable to drought than those in lower altitude and drier sites. Moreover, tall forests may be vulnerable to drought. Such preliminary information, if confirmed later with more data, would provide significant insights into the survival of typical forests in these regions when climate change, such as droughts, occur. Nevertheless, our findings can benefit various sectors in Thailand, especially those related to strategic planning for forest conservation and restoration. For example, governmental or private sectors that are interested in forest restoration may utilize part of our results involving species-specific drought tolerance for selective planting in the designated areas for optimal results. Overall, our results suggest the need to continue exploring the responses of various ecological and plant physiological parameters to the environmental factors across timescale, ranging from sub-daily to interannually, to confirm certain findings as presented here. Additionally, these studies call for support for long-term monitoring of field data to broaden such investigations and extend the analysis to the development of predictive models for future impacts of climate change on these forest ecosystems.

บทสรุปผู้บริหาร

วัตถุประสงค์หลักของความร่วมมือในการทำวิจัยระหว่างไทยและจีนในครั้งนี้คือ เพื่อศึกษาการตอบสนองในด้านของการเจริญเติบโตของต้นไม้ต่อการเปลี่ยนแปลงสภาพภูมิอากาศ การตอบสนองในปัจจุบันของป่าไม้ต่อการแปรผันของสภาพอากาศ รวมไปถึงความเปราะบางและความยืดหยุ่นของป่าไม้ และผลกระทบในอนาคตของการเปลี่ยนแปลงสภาพภูมิอากาศต่อชีวมวล ผลผลิต และความหลากหลายของป่าไม้ โดยการทำวิจัยในครั้งนี้ เรายพยายามที่จะทำการศึกษาตามที่ได้เสนอไว้ อย่างไรก็ตาม การระบาดของไวรัสโคโรนา วิด-19 ก่อให้เกิดอุปสรรคมากมายและส่งผลกระทบอย่างมากต่อการทำางานร่วมกันระหว่างสองประเทศ ทั้งนี้ เรายังได้ดำเนินการทำวิจัยหลายชิ้นในป่าของประเทศไทยพร้อมกับความร่วมมือทางไกลของนักวิจัยจากประเทศไทย จีน ส่งผลให้มีการตีพิมพ์ในวารสารนานาชาติที่มี Impact factor สูง (อย่างน้อยใน Q1 SCOPUS) ด้วยกัน 5 ผลงาน, 1 ผลงานที่อยู่ระหว่างการตรวจสอบในวารสารนานาชาติ (Q1 SCOPUS), และอีก 1 ผลงานที่อยู่ในระหว่างการจัดทำ โดยผลที่ได้จากการวิจัยเหล่านี้ พบว่า ป่าไม้หลายแห่งในภูมิภาคนี้ตอบสนองแตกต่างกันต่อการเปลี่ยนแปลงของปัจจัยทางภูมิอากาศและสภาพแวดล้อม อันประกอบไปด้วยอุณหภูมิ ความชื้นสัมพัทธ์ ปริมาณน้ำฝน และความชื้นในดินของแต่ละฤดูกาล ลักษณะพื้นที่ที่เกี่ยวข้องกับการพัฒนาโครงสร้างของเรือนยอด (Canopy development) ที่มีความสัมพันธ์กับระยะต่าง ๆ ของการเปลี่ยนแปลงแทนที่ของป่าไม้ที่ทำการศึกษา แม้จะมาจากบริเวณที่มีสภาพภูมิอากาศที่คล้ายคลึงกัน นอกจากนี้ เรายังได้ดำเนินการศึกษาความเปราะบางของพันธุ์ไม้ในป่าเขตร้อนต่อสภาพแวดล้อมในป่าหลายแห่งของประเทศไทย อีกทั้ง เรายังได้รับข้อมูลที่มีผลในลักษณะเดียวกันจากป่า 2 แห่งในประเทศไทย และได้วิเคราะห์ข้อมูลดังกล่าวกับข้อมูลของเรานำมาใช้ในการตีความรู้เชิงลึกเกี่ยวกับกลยุทธ์ในการปรับตัวของพันธุ์ไม้เหล่านี้ ที่จะสามารถใช้คาดการณ์ถึงแนวโน้มของการดำเนินชีวิตของพันธุ์ไม้ภายใต้การเปลี่ยนแปลงสภาพภูมิอากาศในอนาคต โดยในที่นี้ เรายังได้สรุปผลสำคัญจากการวิจัยหลายชิ้นที่ได้ตีพิมพ์หรือนำเสนอแล้ว หรือกำลังอยู่ในขั้นตอนของการจัดทำเพื่อนำส่งให้กับวารสารนานาชาติต่อไป

1. วงปีของต้นไม้สามารถบ่งบอกถึงแนวโน้มของการตีความรู้ในระยะยาวต่อการเปลี่ยนแปลงของสภาพภูมิอากาศ แต่เนื่องจากต้นไม้ในป่าเขตร้อนส่วนใหญ่ไม่มีข้อบ่งชี้ของวงปีที่ชัดเจน รวมไปถึงความยุ่งยากในการเปรียบเทียบลักษณะของวงปีโดยการเชื่อมโยง (Cross-dating) การศึกษาวงปีในพื้นที่เขตร้อนจึงจำกัดอยู่กับพันธุ์ไม้เพียงแค่ไม่กี่ชนิด *Choerospondias axillaris* เป็นพันธุ์ไม้เขตร้อนที่ไม่เคยมีการศึกษาวงปีมาก่อนในประเทศไทย เพื่อที่จะศึกษาการล่านุกรมต้นไม้ (Dendrochronology) ของ *C. Axillaris* นั้น งานวิจัยนี้มุ่งเน้นไปที่ความสัมพันธ์ระหว่างการเจริญเติบโตต่อสภาพภูมิอากาศ รวมไปถึงแนวโน้มของการเจริญเติบโตในระยะยาวของ *C. Axillaris* จากแปลงศึกษามอสิงโตในอุทยานแห่งชาติเขาใหญ่ ที่ตั้งอยู่ในภาคกลาง-ตะวันออกของประเทศไทย ด้วยวิธีการตีความรู้เชิงลึกสร้างขึ้นจากแกนไม้จำนวน 100 ตัวอย่างจากต้นไม้ 56 ต้น คลอบคลุมช่วงเวลาตั้งแต่ปี ค.ศ. 1932 - 2019 ผลที่ได้จากการวิจัยนี้ พบว่า ดัชนีความกว้างของวงปี

(Tree-ring width index) ของ *C. Axillaris* ในแปลงมอสิงโตมีความสัมพันธ์เชิงบวกกับปริมาณน้ำฝนในเดือนมิถุนายน กรกฎาคม และตุลาคมของปีปัจจุบัน ($p<0.05$) แสดงให้เห็นว่าการเจริญเติบโตของ *C. Axillaris* นั้น โดยส่วนใหญ่แล้ว เป็นผลมาจากการปริมาณความชื้นในช่วงฤดูมรสุมอย่างไรก็ตาม ไม่มีความสัมพันธ์อย่างมีนัยสำคัญระหว่างดัชนีของ *C. Axillaris* กับอุณหภูมิสำหรับการเจริญเติบโตในระยะเวลาของ *C. Axillaris* มีแนวโน้มที่เพิ่มขึ้น ตั้งแต่ปี ค.ศ. 1932 – 1984 แต่มีแนวโน้มลดลงเล็กน้อยตั้งแต่ปี 1985 – 2019 ทั้งนี้ งานวิจัยชิ้นนี้ได้ให้ข้อมูลเชิงลึกที่สำคัญเกี่ยวกับความสัมพันธ์ระหว่างการเจริญเติบโตและสภาพภูมิอากาศในภูมิภาคเขตต้อน

2. การตัดไม้ทำลายป่าส่งผลให้พื้นที่ป่าดีนิ่งใหญ่กลับเป็นพื้นที่ป่าหลายขั้นทดแทนที่ประกอบไปด้วยป่าสมบูรณ์ (old-growth forest) และป่ารุ่นสอง (secondary forest) หลายช่วงอายุทั่วทั้งภูมิภาค เอเชียตะวันออกเฉียงใต้ ทำให้เกิดความท้าทายในการทำความเข้าใจเกี่ยวกับวัฏจักรของน้ำและคาร์บอนในบริเวณนี้ นอกเหนือจากการเปลี่ยนแปลงขององค์ประกอบของชนิดพื้นธูไม้แล้ว สภาพแวดล้อมของป่าหลายขั้นทดแทนดังกล่าวยังมีความแตกต่างกัน ซึ่งส่งผลกระทบต่อการใช้น้ำ และผลผลิตของป่าไม้ ในงานวิจัยนี้ ได้ศึกษาการสังเคราะห์ด้วยแสงในระดับพื้นที่-ใบ (leaf-level area-based photosynthesis, A_{area}) และค่าการซักนำปากใบ (stomatal conductance, g_s) ของพื้นธูไม้เด่นจำนวน 11 ชนิด จากพื้นที่ป่าสมบูรณ์ (OF; >200 ปี) ป่ารุ่นสองกลาง (IF; ~ 44 ปี) และป่ารุ่นสองระยะเริ่มต้น (YF; ~ 4 ปี) ในระหว่างฤดูฝนและฤดูแล้ง โดยเปรียบเทียบ A_{area} ต่อ g_s และการศึกษาความอ่อนไหวของ g_s ต่อค่าความแตกต่างระหว่างความดันไอ (Vapor pressure deficit, VPD) นอกจากนี้ ยังได้ศึกษาความสัมพันธ์ระหว่างพารามิเตอร์ของการแลกเปลี่ยนกําชของพืชต่อคุณลักษณะเชิงพังค์ชันของใบพืชที่สำคัญ ได้แก่ มวลใบต่อพื้นที่ (leaf mass per area, LMA) ในไตรเจน (N) ฟอสฟอรัส (P) และปริมาณของคลอโรฟิลล์ (Chlorophyll concentration) ผลที่ได้ พบว่า ป่าไม้ทั้ง 3 แห่งมีค่า A_{area} และ g_s ใกล้เคียงกันในฤดูฝน แต่ค่าทั้งสองกลับมีค่าที่ต่ำกว่าอย่างมีนัยสำคัญในแปลง YF ในฤดูแล้ง อีกทั้ง ป่าไม้ทั้ง 3 แห่งนี้มีความอ่อนไหวของ g_s ต่อ VPD ที่คล้ายคลึงกัน ในบรรดาคุณลักษณะเชิงพังค์ชันของใบพืชที่ได้ทำการศึกษานั้น LMA, N, และ P มีค่าสูงกว่าอย่างมีนัยสำคัญในแปลง YF เมื่อเทียบกับป่าขั้นทดแทนอื่น ผลที่ได้จากการวิจัยนี้ แสดงให้เห็นว่า การเปลี่ยนแปลงแทนที่ของป่าไม้อาจไม่ใช่ตัวแปรสำคัญที่ส่งผลกระทบต่อการแลกเปลี่ยนกําชของพืช แต่ผลกระทบนี้อาจเกิดจากการพัฒนาโครงสร้างของเรือนยอด (Canopy development) ที่มีความสัมพันธ์กับระยะต่าง ๆ ของการเปลี่ยนแปลงแทนที่ของป่าไม้ นอกจากนี้ การที่ YF เป็นพื้นที่ที่มีทรัพยากรสูงที่สุด อีกทั้งยังมีค่า LMA และปริมาณธาตุอาหารในใบสูง อาจส่งผลให้อัตราการสังเคราะห์ด้วยแสงสูงขึ้นด้วย อย่างไรก็ตาม น้ำในดินของ YF ที่มีปริมาณต่ำ อาจเป็นตัวการสำคัญในการจำกัดอัตราการแลกเปลี่ยนของกําชของพืช ซึ่งทำให้อัตราการแลกเปลี่ยนดังกล่าวมีค่าที่ใกล้เคียงกับป่าสมบูรณ์ ผลที่ได้จากงานวิจัยนี้ เน้นย้ำถึงผลกระทบที่อาจเกิดขึ้นจากการพัฒนาโครงสร้างของเรือนยอดในป่าหลายขั้น

ทดแทนต่อการแลกเปลี่ยนน้ำและคาร์บอนระหว่างต้นไม้กับบรรยากาศ รวมไปถึงความอ่อนไหวต่อ สภาวะแล้งในชั้นบรรยากาศ ผลลัพธ์เหล่านี้บ่งชี้ให้เห็นถึงความสำคัญของการศึกษาเพิ่มเติม เพื่อที่จะระบุปัจจัยหลักที่มีผลต่อผลผลิตของป่าไม้ในพื้นที่ป่าหลายชั้นทดแทนในเขตต้อน โดยเฉพาะอย่างยิ่งในบริเวณเอเชียตะวันออกเฉียงใต้ ที่องค์ความรู้ดังกล่าวยังคงขาดแคลน

3. การหายใจของดิน (Soil respiration, SR) ในป่า เป็นองค์ประกอบสำคัญในการปล่อยก๊าซ คาร์บอนไดออกไซด์จากการบินเวศบกและมีความอ่อนไหวสูงต่อการเปลี่ยนแปลงของสิ่งแวดล้อม ประกอบไปด้วย อุณหภูมิในดิน ความชื้นในดิน จุลินทรีย์ในดิน เชษชากพืชบริเวณผิวดิน และ ประเภทของพื้นธูพืช อันที่จริงแล้ว การเปลี่ยนแปลงเพียงเล็กน้อยของ SR อาจส่งผลกระทบอย่าง มากต่อสมดุลการบอนของโลก และอาจส่งผลกระทบเพิ่มเติมต่อการเปลี่ยนแปลงสภาพภูมิอากาศ ดังนั้น การศึกษาโดยละเอียดของการตอบสนองของ SR ต่อการเปลี่ยนแปลงทางปัจจัย สภาพแวดล้อมจึงเป็นสิ่งสำคัญ เพื่อให้การคาดการณ์การปล่อยก๊าซการบอนไดออกไซด์จากการบิน เนเวศป่าทำได้อย่างถูกต้อง อย่างไรก็ตาม ข้อมูลสำหรับการวิเคราะห์ดังกล่าวมีอยู่น้อยมาก โดยเฉพาะในป่าเขตต้อนของเอเชียตะวันออกเฉียงใต้ ที่ประกอบไปด้วยพื้นที่ป่าหลายชั่วงอายุจาก การเปลี่ยนแปลงที่ดินในอดีตเพื่อนำไปใช้ประโยชน์ในด้านอื่น ในการศึกษานี้ ได้มีการวัด SR และ ปัจจัยสภาพแวดล้อม ได้แก่ อุณหภูมิในดิน (Soil temperature, ST) ความชื้นในดิน (Soil moisture, SM) และปริมาณอินทรีย์วัตถุในดิน (Organic matter content, OM) ในพื้นที่ป่าหลายชั่วง ทดแทน 3 แห่ง ทั้งในฤดูฝนและฤดูแล้ง นอกจากนี้ ยังมีการวิเคราะห์ความสัมพันธ์ระหว่าง SR กับ ปัจจัยสภาพแวดล้อมดังกล่าวอีกด้วย ผลการศึกษา พบว่ามีค่า SR ที่สูงขึ้นช่วงฤดูฝน และในพื้นที่ ป่าที่มีอายุมากกว่า นอกจากนี้ ยังพบความสัมพันธ์ระหว่าง SR ต่อ ST ในพื้นที่ป่าที่มีอายุมากกว่า ในขณะที่ความสัมพันธ์ดังกล่าวไม่พบในพื้นที่ป่าที่มีอายุต่ำกว่า อาจเป็นเพราะลักษณะโครงสร้าง ของป่าที่เป็นแบบ non-uniform รวมไปถึงช่องว่างของชั้นเรือนยอด ที่ส่งผลให้ช่วงของค่า ST มี ความหลากหลายมากขึ้น สำหรับป่าในแต่ละช่วงอายุนั้น มีค่า SM ที่เป็นปัจจัยจำกัดสำหรับ SR ในช่วงฤดูฝน ในขณะที่ SR เปลี่ยนแปลงไปตาม OM อย่างมีนัยสำคัญในฤดูแล้ง โดยรวมแล้ว การ ค้นพบครั้งนี้แสดงให้เห็นถึงการตอบสนองของ SR ต่อปัจจัยสภาพแวดล้อมที่มีความแตกต่างกัน ออกเป็นตามช่วงเวลาและพื้นที่ป่า อย่างไรก็ตาม ผลที่ได้จากการวิจัยนี้ยังคงเป็นเพียงข้อมูลเบื้องต้น และยังต้องการการศึกษาอย่างละเอียดเกี่ยวกับการเปลี่ยนแปลงของ SR ต่อปัจจัยสภาพแวดล้อม ในบริเวณเอเชียตะวันออกเฉียงใต้ ที่ซึ่งป่าไม้ไปด้วยพื้นที่ป่าเขตต้อนหลากหลาย
4. พื้นที่กระพี้ (Sapwood area) เป็นตัวแปรสำคัญสำหรับการประเมินการคายน้ำในระดับเรือนยอด ในวัฏจักรน้ำของป่า อย่างไรก็ตาม พื้นที่กระพี้มีความแตกต่างอย่างมากในแต่ละชนิดพื้นธู และในแต่ ละระบบเนเวศป่า และเป็นเรื่องยากในการวัดพื้นที่กระพี้ไม้โดยตรง ดังนั้น การใช้สมการ allometry ที่มีความจำเพาะต่อชนิดพื้นธู และพื้นที่ป่า จึงมีความจำเป็นอย่างมากในการประเมิน พื้นที่กระพี้ของต้นไม้ทั้งหมดในป่าพื้นที่หนึ่ง ในงานวิจัยนี้ได้ออกแบบการเก็บตัวอย่างอย่าง

ครอบคลุม สำหรับการวัดความหนาของกระพี้และประเมินพื้นที่กระพี้ จาก 14 พันธุ์ไม้ที่พบได้ ทั่วไปในป่าหลายช่วงอายุของประเทศไทย โดยงานวิจัยนี้ ถือเป็นงานวิจัยแรกในบริเวณเอเชีย ตะวันออกเฉียงใต้ ที่มีการตรวจวัดพื้นที่กระพี้จากป่าหลายชั้นทดแทนที่มีสภาพแวดล้อมที่ หลากหลายในแต่ละช่วงความชื้นในดินและความหนาแน่นของเรือนยอด ผลที่ได้จากการวิจัยนี้ พบว่า power function สามารถใช้เพื่อธิบายความสัมพันธ์ระหว่างพื้นที่กระพี้ต่อขนาดลำต้น โดยวัด จากเส้นผ่านสูงกลางเพียงอก (Diameter at breast height, DBH) ได้อย่างมีนัยสำคัญในทุก ๆ ชนิดพันธุ์ไม้ที่ได้ทำการศึกษา ทั้งในป่าสมบูรณ์และป่ารุ่นสอง ยิ่งไปกว่านั้น สมการที่ได้จากการวิจัย นี้เพียงสมการเดียว สามารถอธิบายความสัมพันธ์ระหว่างพื้นที่กระพี้ไม้ต่อ DBH ของทุกชนิดพันธุ์ และทุกพื้นที่ศึกษาได้ ยกเว้น *Dipterocarpus gracilis* ที่เป็นไม้สูงเด่นและพบได้เฉพาะในป่า สมบูรณ์ ซึ่งชนิดพันธุ์นี้จะมีการเจริญเติบโตของพื้นที่กระพี้ที่ช้ากว่าชนิดอื่น ๆ เมื่อมี DBH อยู่ที่ ประมาณ 30 เซนติเมตร โดยรวมแล้ว ผลที่ได้จากการวิจัยนี้จะเป็นประโยชน์ต่อการงานวิจัยใน อนาคตที่ศึกษาเกี่ยวกับการประเมินการคายน้ำเรือนยอดของป่าเขตต้อนที่มีลักษณะคล้ายคลึงกับ พื้นที่ป่าที่ศึกษาในงานวิจัยนี้

5. สืบเนื่องมาจากพื้นที่เกษตรกรรมขนาดใหญ่ได้ถูกทิ้งร้างไว้หลายแห่งในเอเชียตะวันออกเฉียงใต้ พื้นที่ป่าในเขตภูมิภาคนี้ โดยส่วนใหญ่แล้ว ประกอบไปด้วยป่ารุ่นสองหลายช่วงอายุ ส่งผลให้เกิด ลักษณะเฉพาะที่หลากหลายและสภาพแวดล้อมที่แตกต่างกัน ความหลากหลายเชิงพื้นที่เหล่านี้ถือ เป็นความท้าทายอย่างหนึ่งต่อการศึกษาการตอบสนองของป่าไม้ต่อการเปลี่ยนแปลงสภาพแวดล้อม โดยเฉพาะอย่างยิ่ง ภายใต้สภาวะแล้งในอนาคต ดังนั้น ข้อมูลการตอบสนองของป่าต่อการ เปลี่ยนแปลงสภาพแวดล้อมจึงมีน้อยมาก โดยเฉพาะพื้นที่ป่าในบริเวณเอเชียตะวันออกเฉียงใต้ งานวิจัยนี้จึงได้ทำการตรวจวัดความแตกต่างของสถานะของน้ำในใบ (leaf water status) ต่อการ เปลี่ยนแปลงฤทธิ์ทางเคมีและความหนาแน่นของชนิดพันธุ์เด่นในป่า 3 แห่งที่มีความแตกต่างตามช่วง อายุ ตั้งแต่ 5 ถึง >200 ปี ที่ตั้งอยู่ในอุทยานแห่งชาติเขาใหญ่ของประเทศไทย ผลที่ได้ พบว่า ค่า สถานะของน้ำในใบต่อการเปลี่ยนแปลงของฤทธิ์ทางเคมีความแตกต่างกันในป่าแต่ละช่วงอายุ โดย ต้นไม้ในพื้นที่ป่ารุ่นสองกลาง และป่ารุ่นสองเริ่มต้น แสดงให้เห็นถึงความเครียดน้ำที่เพิ่มขึ้น ประมาณ 30% ระหว่างฤดูฝนและฤดูแล้ง ถึงแม้ว่าต้นไม้ในป่าสมบูรณ์อาจจะมีความอ่อนไหวต่อ การเกิดฟองอากาศในท่อลำเลียง (embolism) จากการลดลงของค่าสถานะของน้ำในใบสูงกว่าป่า ในช่วงอายุอื่น ต้นไม้ในป่าสมบูรณ์นี้ถูกคาดการณ์ว่าจะสูญเสียความสามารถในการลำเลียงน้ำ <5% เมื่อเทียบกับป่าในช่วงอายุอื่น ที่มีค่าตั้งกล่าว >13% นอกจากนี้ ยังพบความแตกต่างอย่างมี นัยสำคัญของความสามารถในการทนแล้งของชนิดพันธุ์เด่นในแต่ละแปลงศักษา อย่างไรก็ตาม ชนิด พันธุ์ที่สามารถพบรได้ในป่าหลายช่วงอายุมีค่าความหนาแน่นที่ใกล้เคียงกัน โดยรวมแล้ว ผลที่ได้จาก งานวิจัยนี้ ชี้ให้เห็นว่า ปริมาณน้ำในดินอาจส่งผลต่อค่าสถานะของน้ำและความหนาแน่นของต้นไม้แต่ ละชนิด อย่างไรก็ตาม ชนิดพันธุ์ที่มีความหนาแน่นได้สามารถคงอยู่ได้โดยภายใต้สภาวะน้ำในดินที่

แตกต่างกัน งานวิจัยนี้ยังบ่งชี้อีกว่า การตอบสนองต่อความเครียดน้ำของมีความแตกต่างกันในป่าแต่ละช่วงอายุ โดยมีแนวโน้มว่า ต้นไม้ในป่าที่มีอายุน้อยกว่าจะได้รับผลกระทบจากความเครียดน้ำมากกว่าต้นไม้ในป่าที่มีอายุมากกว่า ดังนั้น การประเมินประสิทธิภาพของแต่ละชนิดพันธุ์ภายใต้สภาพเครียดน้ำควรตีความอย่างรอบคอบ ซึ่งข้อมูลเหล่านี้จะเป็นประโยชน์สำหรับการเลือกชนิดพันธุ์ที่สามารถปรับตัวให้เข้ากับสภาพแวดล้อมนั้น ๆ ได้ เพื่อเป็นการปรับปรุงกลยุทธ์ในการจัดการป่าที่แตกต่างกันตามช่วงอายุได้อย่างเหมาะสม ภายใต้สภาพภูมิอากาศที่คาดการณ์ว่าจะมีอุณหภูมิสูงขึ้นในอนาคต

แม้ว่าการตอบสนองที่แตกต่างกันของแต่ละพื้นที่ป่าต่อปัจจัยทางสภาพภูมิอากาศและสภาพแวดล้อมไม่ได้ให้ผลลัพธ์ที่มีความแปลกใหม่มากนัก แต่ผลที่ได้จากการวิจัยของเรานี้เป็นหลักฐานชั้นแรก ๆ จากการทำวิจัยในป่าขนาดต่างๆ ที่จะเป็นข้อมูลชิ้นสำคัญสำหรับแบบจำลองระบบโลก (earth system models) ในการวิเคราะห์ส่วนสุดท้ายโดยพิจารณาข้อมูลจากป่าในประเทศไทยและประเทศจีนพบว่า สภาวะแวดล้อมในอนาคตอาจส่งผลกระทบต่อป่าทั่วไปในภูมิภาคนี้ในรูปแบบที่แตกต่างกัน กล่าวคือ ป่าที่อยู่ในที่สูงและมีฝนตกชุกอาจมีความไวต่อสภาวะแวดล้อมมากกว่าป่าที่อยู่ในที่ลุ่มและแห้งแล้งกว่า นอกจากนี้ ป่าไม้ที่มีเรือนยอดสูงก็อาจไม่ทนต่อสภาวะแวดล้อม ผลที่ได้นี้ หากได้รับการยืนยันจากข้อมูลเพิ่มเติม จะช่วยให้ข้อมูลที่สำคัญเกี่ยวกับการอุ่นภูมิภาคในป่าทั่วไปในพื้นที่นี้ เมื่อประสบกับการเปลี่ยนแปลงภูมิอากาศ เช่น สภาวะแวดล้อมอย่างไรก็ได้ ผลที่ได้จากการนี้จะเป็นประโยชน์แก่หน่วยงานที่หลากหลายในประเทศไทย โดยเฉพาะอย่างยิ่งหน่วยงานที่เกี่ยวข้องกับการวางแผนกลยุทธ์ในการอนุรักษ์และฟื้นฟูป่า ยกตัวอย่างเช่น หน่วยงานภาครัฐและเอกชนที่สนใจฟื้นฟูป่าอาจใช้ข้อมูลจากโครงการนี้ในส่วนที่ศึกษาเกี่ยวกับความทันสมัยและของชนิดพันธุ์ต้นไม้ที่แตกต่างกันในอุทยานแห่งชาติเข้าใหญ่ เพื่อช่วยในการคัดเลือกพันธุ์ที่เหมาะสมกับพื้นที่ที่เลือกปลูกทดแทน เพื่อให้ได้ผลที่ดีที่สุด โดยทั่วไปแล้ว ผลที่ได้จากการวิจัยเหล่านี้ บ่งชี้ให้เห็นถึงความสำคัญของการดำเนินการศึกษาอย่างต่อเนื่องสำหรับการตอบสนองของแต่ละระบบในเวศป่าไม้และปัจจัยทางสิริวิทยาของพืชต่อสภาพแวดล้อมในช่วงเวลาต่าง ๆ ตั้งแต่ระดับรายวันจนถึงระดับรายปี เพื่อที่จะยืนยันผลลัพธ์ที่ได้จากการศึกษาต่าง ๆ ของงานวิจัยนี้ ยิ่งไปกว่านั้น งานวิจัยนี้ยังแสดงให้เห็นถึงความสำคัญของการเก็บตัวอย่างภาคสนามในระยะยาว เพื่อให้ได้ข้อมูลของงานวิจัยที่กว้างขึ้นและการวิเคราะห์ข้อมูลที่ละเอียดมากขึ้น นำไปสู่การพัฒนาแบบจำลองต่าง ๆ ในการประเมินผลกระทบของการเปลี่ยนแปลงสภาพอากาศต่อระบบในเวศป่าไม้ในเขตภูมิภาคนี้

Abstract

In monsoon Asia, climate change impacts including changes in rainfall patterns and increased frequency and severity of drought may potentially drive rapid and large-scale shifts in forest structure and species composition. Until now, how and to what extent of such impacts have affected forests in this region is poorly understood due to limited studies. In this project, we performed various studies to investigate the past responses of tree growth to climate change using tree ring analysis and the present responses of various plant physiological and ecological parameters related to water and carbon flow to climate variability. Finally, we combined available data of parameters representing vulnerability to drought of tree species in Thai and Chinese forests and analyze their variation along the latitudinal gradient, with the implication for the possibility of drought tolerance of these forests to predicted increases droughts in the future. Overall, we found that trees in these forests respond differently to environmental factors between seasons. Furthermore, local conditions including canopy development and microclimatic conditions within the forests may affect the responses. These results suggest the need for further investigations that extend the spatial and temporal coverage of these studies to confirm these findings. We produced several publications in peer-reviewed international journal with high impact factors and many graduate students from both partner countries. Results from this study were among the first evidence from field observations in Southeast Asian forests which are considered the puzzle in the earth system models.

บทคัดย่อ

ในเขตรัฐสุเมอเรีย ผลกระทบของการเปลี่ยนแปลงภูมิอากาศ อันได้แก่ การเปลี่ยนแปลงรูปแบบการตกของฝน ความถี่และความรุนแรงของสภาพแล้งที่สูงขึ้น อาจก่อให้เกิดการเปลี่ยนแปลงอย่างรวดเร็วและในวงกว้างของโครงสร้างและองค์ประกอบของพันธุ์ไม้ในป่า อย่างไรก็ตาม ความรู้เกี่ยวกับกลไกและขอบเขตของผลกระทบ ดังกล่าวต่อป่าไม้ในเขตรัฐสุเมอเรียนี้ยังคงมีจำกัด เนื่องจากไม่มีการศึกษามากนัก โครงการนี้ได้ทำการศึกษา งานวิจัยที่หลากหลายเพื่อสำรวจการตอบสนองในอดีตของการเติบโตของต้นไม้ต่อการเปลี่ยนแปลงของ ภูมิอากาศด้วยการวิเคราะห์ปี และการตอบสนองในปัจจุบันของตัวแปรศึกษาเกี่ยวกับสรีรวิทยาพืชและ นิเวศวิทยาหลายตัวที่เกี่ยวข้องกับการเปลี่ยนแปลงของน้ำและคาร์บอนต่อความแปรปรวนของภูมิอากาศ และ สุดท้าย ได้ใช้ข้อมูลของพารามิเตอร์ที่เป็นตัวบ่งชี้ถึงความเปลี่ยนแปลงต่อสภาพแล้งของต้นไม้ชนิดต่างๆ ในป่า ของประเทศไทยและประเทศจีน เพื่อที่หาข้อมูลได้ มากวิเคราะห์ความแปรปรวนของพารามิเตอร์ดังกล่าวตาม แนวโน้มดังนี้ เป็นที่ตั้งของป่าที่เก็บข้อมูลนี้ โดยผลกระทบวิเคราะห์เบื้องต้นดังกล่าวอาจบ่งถึงความเป็นไป ได้ของความสามารถในการทนแล้งของป่าเหล่านี้ภายใต้สภาพแล้งที่ถูกคาดการณ์ว่าจะรุนแรงขึ้น โดยที่ว่าไป แล้ว พบว่าต้นไม้ในป่าที่ศึกษามีการตอบสนองต่อปัจจัยทางสิ่งแวดล้อมต่างกันในแต่ละฤดูกาล นอกจากนี้ สภาพการณ์ของป่า อันได้แก่ โครงสร้างของเรือนยอด และสถานะเชิงจุลภูมิอากาศในป่าแต่ละแห่งก็อาจมี อิทธิพลต่อรูปแบบการตอบสนองดังกล่าวด้วย ผลการศึกษาจากโครงการนี้ชี้ให้เห็นว่าต้องมีการขยายพื้นที่ ศึกษา รวมถึงระยะเวลาและความถี่ในการเก็บข้อมูลของการศึกษาที่หลากหลายนี้เพื่อยืนยันผลที่ได้ คณะผู้วิจัย ได้ผลิตบทความวิจัยที่ได้รับการตีพิมพ์ในวารสารระดับนานาชาติที่มี impact factor สูง และนักศึกษาระดับ บัณฑิตศึกษาหลายคนที่จบการศึกษาจากสถาบันในประเทศไทยและจีน ผลการศึกษาเหล่านี้เป็นหลักฐาน แรกเริ่มที่ได้จากการข้อมูลที่วัดในพื้นที่จริงของป่าในแถบเอเชียตะวันออกเฉียงใต้ซึ่งนับว่ายังเป็นปริศนาใน แบบจำลองระบบโลก

Introduction

The interaction between climate and vegetation has been a great challenge to plant ecologists and earth system modelers. One of the approaches to address this challenge is the Dynamic Global Vegetation Models (DGVMs) (Prentice et al., 2007). The DGVMs utilize ecophysiological principles to simulate distribution of plant functional types which is influenced by biotic (species interaction) and abiotic (climate and physical environments) factors, thus offering knowledge about climate and vegetation in the past, current and future at regional to global scales (Prentice et al., 2007). Furthermore, the DGVMs serve as a component of earth system models and provide dynamic representation of land-surface energy balance and global carbon and water budgets (Bonan 2008). The DGVMs have been widely used to tackle important questions, such as, the impacts of climate change on carbon cycle and biome patterns (Cramer et al., 2001), how land use affects the carbon cycle (Bondeau et al., 2007). Additionally, the DGVMs have been linked with general circulation models (GCMs) to generate fully coupled biosphere-atmosphere models which are essential for studying impacts of climate change on vegetation and, in turn, how changes in vegetation cover affect climate (Raddatz et al., 2007, Brovkin et al., 2009). However, there are some weaknesses in the DGVMs. The first weakness is that they use plant functional types (PFTs), which represent broad categories of plants, to represent vegetation. Typically, the DGVMs only include small sets of plant attributes of PFTs. Such representation largely ignores the mechanistic processes of vegetation that govern the biosphere-atmosphere interaction and therefore may contribute to uncertainties in predicting future climates and their feedback with global vegetation. It is therefore crucial to improve the understanding of mechanistic processes of species and their interactions (i.e., competition versus facilitation) which influence climate feedbacks with forests and the global carbon cycle.

Forests are the hotspots of biodiversity which contain approximately 53,000 tree species (Slik et al., 2015), cover 30% of the earth's land surface, store 45% of terrestrial carbon and are responsible for 50% of the terrestrial net primary productivity (Bonan, 2008). Forest ecosystems serve as the main and persistent terrestrial carbon sink in the global carbon cycle and hence mitigate consequences of climate change, i.e. ongoing rise of atmospheric CO₂ (van Mantgem & Stephenson, 2007; Kurz et al., 2008; Pan, et al., 2011).

Climate change is predicted to have immense and far-reaching effects on the world's forests. While climate events can damage forests in many ways ranging from ice storms to tornadoes and hurricanes, the emphasis here is on climatic water stress, driven by drought and warm temperatures. Accelerating rates and massive forest mortality in association with drought and rising temperature have now been documented recently in all major global biomes (Phillips et al., 2010; McDowell et al., 2011; Hartmann et al., 2015; McDowell et al., 2015; Anderegg et al., 2016). Even worse, forest mortality is expected to increase due to the rising temperature and increasing drought frequency and severity (Dietze & Moorcroft 2011; Lewis et al., 2011; Williams et al., 2013). Such mortality events could lead to dramatic decreases in carbon stored by forests and severely affect animal populations and local economic status dependent on tourism and logging. The consequences of forest mortality include large climate feedbacks (Adams et al., 2012; Jiang et al., 2013; Maness et al., 2013), loss of ecosystem services, impacts

on community composition (Redmond & Barger 2013), soil biochemistry (Cobb et al., 2013) and the availability of fuel wood and food in developing nations (Anderegg et al., 2013). Many tree species appear globally to operate near their hydraulic limits with relatively minimal hydraulic safety margins and thus could be vulnerable to drought (Allen et al., 2010; Choat et al., 2012). Due to their important role in the earth system, understanding how vulnerable the forests are; when, where, and how trees die from climate stress is critical for projections of carbon and water cycling with climate change (Anderegg et al., 2013).

In monsoon Asia, associated effects are the variability of rainfall and storm patterns which increase with increasing temperature anomalies (Loo et al., 2015). A recent study predicted rising temperature (at least 2–4°C) by 2100 (Corlett, 2011), which will incur frequent changes and shifts to up to 70% reduction of monsoon precipitation below normal levels (Schewe & Levermann, 2012) while another suggested that the onset of monsoon over Southeast Asia may be delayed up to 15 days in the future (Ashfaq et al., 2009). Consequences of these shifts in rainfall patterns and elevated temperature is increasing frequency, length and intensity of drought events which will inevitably drive rapid and large-scale shifts in forest structure and species composition (van Mantgem & Stephenson, 2007; Kurz et al., 2008; Pan et al., 2011). In this regard, there is a great need for more robust predictions of the impacts of future climate scenarios on species and communities. Unfortunately, currently available models include a few species in the tropics (Corlett, 2011). Additionally, the current models often extrapolate short-term, leaf-level observations to long-term, canopy-scale responses to climatic variation. For example, models of mass and energy exchanges between forests and the atmosphere incorporate functions describing stomatal closure with increasing atmospheric CO₂ concentration based on leaf-scale measurement (Ball et al., 1987; Sellers et al., 1996; Douville et al., 2000). However, responses at the canopy level may differ (Medlyn et al., 2001; Wullschleger et al., 2002; Ainsworth & Rogers, 2007), making projected changes in annual runoff, the residual between precipitation and forest evapotranspiration debatable (Betts et al., 2007; Tor-ngern et al., 2015). The uncertainty in predicting forest responses is also attributed to poor understanding of the underlying processes of canopy tree responses to climatic variations and the contribution of biodiversity in various forest types to ecosystem functioning. These challenges are central to climate change studies of global terrestrial ecosystems which include forests as the major contribution to climate change mitigation, as recognized in the recent Paris climate agreement (Rogelj & Knutti, 2016).

In this project, our particular interest is the response of canopy trees because they make up the bulk of the forest biomass (Slik et al., 2013). Additionally, with their exposed crowns, canopy trees are the interface between forest and the atmosphere, and are exposed to the macro-climate and changes therein. Canopy trees drive the carbon- water- and nutrient cycles and productivity of the forest (Zuidema et al., 2013), with large consequences for the global carbon cycle (Smith & Dukes, 2013). Yet, canopy trees are poorly studied because it is difficult to access and measure them. We will make use of unique infrastructural combination of a large set of forest canopy cranes as well as long-term forest monitoring plots along 101 degrees east longitude which provide new opportunities for integration and for answering extant and upcoming questions regarding the impact of climate change on forests in the monsoon Asia.

This project aims to close these knowledge gaps by analyzing the effects of climate variability and climate change on forest water and carbon fluxes in typical forests along the E101 longitude dynamic plots belt, covering a wide range of forests in monsoon Asia. Specifically, the main objectives are to study:

- 1) The past responses of tree growth to climate change
- 2) The present responses of forests to variation in climate and the vulnerability and resilience of forests
- 3) The future impacts of climate change on forest biomass, productivity, and diversity.

We performed many studies for the objectives which culminated in publications or manuscripts being in preparation and under review. In this section, we will present the studies separately for each objective. Some of these studies were collaborative between Thailand and China but some were conducted by Thai team only. However, we also present some results that were obtained from forests in China as a synthetic analysis with data from Thai forests.

Objective 1

The past responses of tree growth to climate change

Growth-climate relationships and long-term growth trend of *Choerospondias axillaris* at Mosingto, Khao Yai National Park, Central Thailand
(Surayothee et al. submitted to *Forests* (Q1 SCOPUS) and is under review)

1.1 Introduction

Climate change has a major impact on the natural system worldwide. Evidence from tree-ring can provide the important information for the impact of climate change (Bradley, 1999). Tree-rings is a key ecological indicator for the studies of climate change and environment variability (Zhang, 2015). Tree rings can record a long-term climate in the past, and record environmental signals of the whole lifespan, both directly and indirectly (Speer, 2012). Dendrochronology is one of the scientific methods of dating of tree rings and can make an important contribution and provide fundamental to understand how trees response to environmental changes (Amoroso et al., 2017). The physiological mechanisms of tree radial growth variations is complex, and which might be affected by climatic factors, site conditions, and species characteristic (Fritts, 1976). The sensitivity of tree-ring growth to climate can change over time, which is depending on the severity of climate change (Carrer and Urbinati, 2006). The positive effect and negative effect of climatic factors are recorded by the sequence of wide and narrow rings in trees, respectively.

Tropical forest is a known of biodiversity hotspot and they play an important role in the global carbon cycling (Hughes, 2017). In Southeast Asia, heavy logging leads to deforest and biodiversity decreasing. The extreme event in tropical region is also increasing, which would further influence the tree growth. The main factors influencing tropical tree growth are climate factors (temperature, precipitation, light, moisture and wind), soil factors (texture and structure, soil moisture and nutrients) and topographic factors (elevation, slope and aspect) etc. (Brienen et al., 2016; Pumijumnong, 2013).

Dendrochronology in tropical region is generally a challenge. There are mainly two reasons for the less developed of tree ring study in tropical region. Firstly, climate variations are only slightly different in each season, thus there is the lack of distinct ring boundary in most tree species in tropical region. Secondly, there is no strong limiting climatic factors for the growth of tropical trees, so cross-dating is a challenge for tropical trees. Several techniques can be used to study the response of tropical tree species to climate variation such as tree ring width, cambial activity, wood anatomical analysis and stable isotopes (^{13}C and ^{18}O) (Rozendaal and Zuidema, 2010). However, increasing number of tree species in tropical region have been found to form clear ring boundaries and have dendrochronological potential (Sarutanon et al., 1995; Worbes, 2002; Speer, 2012; Pumijumnong, 2013; Fichtler, 2016). Most of the above study are focusing on conifer trees, not many tropical broad-leaved trees have been successful studied with respect to dendrochronology. In the last decades, there has been an increase in tree ring studies in topical areas (Worbes, 2002). It is of importance to study broad-leaved tree species to better understand the growth-climate relationship in tropical regions since broad-leaved trees play important roles in tropical ecosystems.

Choerospondias axillaris (Anacardiaceae) is a deciduous tree with semi-ring porous wood (Dong and Baas, 1993). *C. axillaris* is widely distributed in tropical Asia (Flora of China), and it is an economically important species in SE Asian countries (Shrestha, 2020).

The tree ring boundary of *C. axillaris* is very distinct, but there is no study to investigate its dendrochronological potential. The aim of this study aims to; (i) to develop tree-ring width chronology of *C. axillaris*; (ii) to investigate the relationship between tree ring width of *C. axillaris* and climatic factors, and (iii) to study long-term growth pattern of this tree species. The present study would help us to better understand the growth-climate relationships for tropical broad-leaved tree species.

1.2 Materials and Methods

1.2.1 Study area and climate

The present study was conducted in Mosingto forest dynamic plot at Khao Yai National Park, in Central Thailand (101°22' E, 14°26' N, 725-815 m above sea level). The plot has been established in the center of Khao Yai National Park, Thailand, where is in broad-leaved, seasonal evergreen forest and briefly deciduous fore. Annual mean temperature is 22.5 ± 0.05 °C and the average annual rainfall is approximately $1,680.72 \pm 3.84$ mm (Brockelman et al., 2011). The wet season is from May to October, and the dry season is from November to April. September is the month with highest precipitation. April is the month with highest temperature and December is the lowest temperature (Figure 1.1).

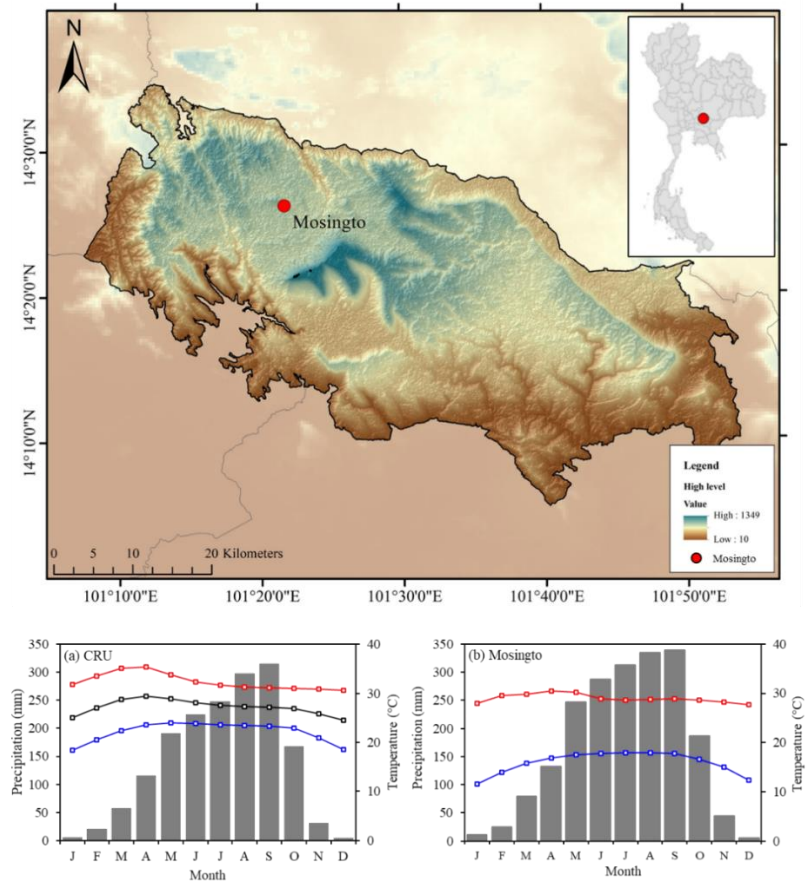


Figure 1.1 Map of the study area (top) and climate diagrams (bottom). (a) monthly maximum temperature (red line), minimum temperature (blue line) and mean temperature (black line) temperature and precipitation data (grey bar) from CRU during 1932 - 2019 and (b) monthly maximum temperature, minimum temperature, and precipitation data from Mosingto climate station during 1994 - 2019.

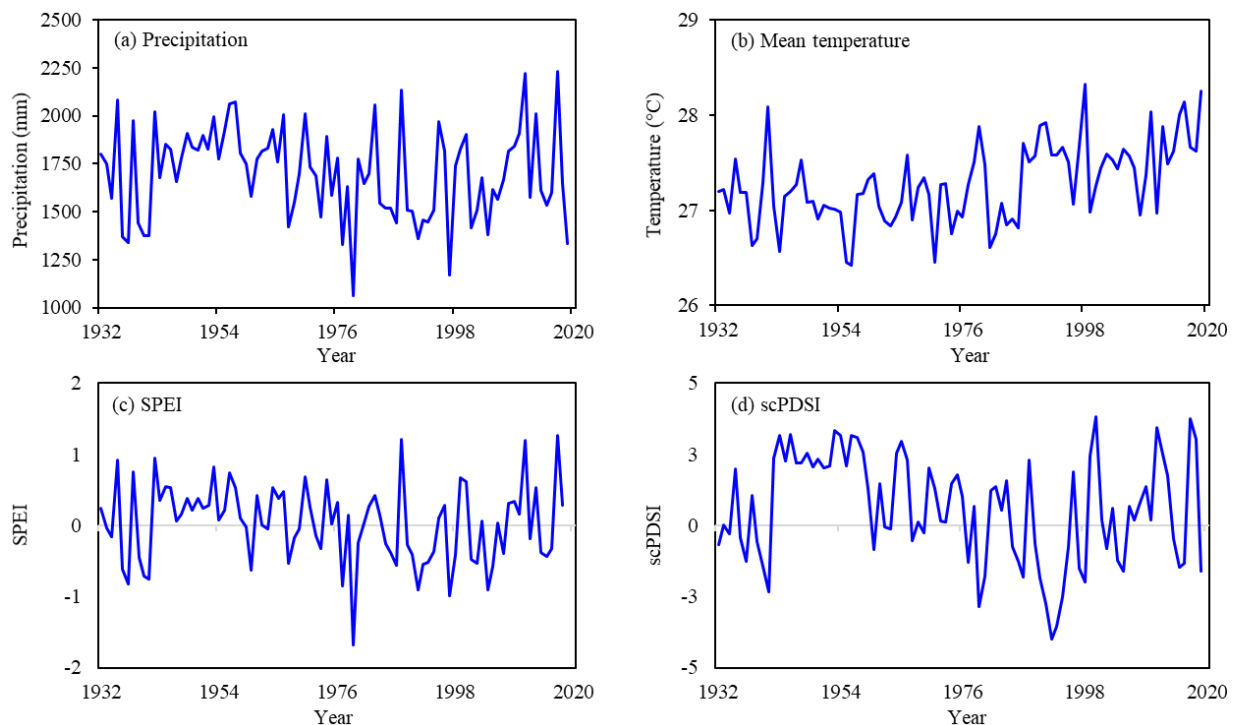


Figure 1.2 Long-term trend of climate data from CRU (blue line) (a) precipitation; (b) mean temperature; (c) Standardized Precipitation-Evapotranspiration Index and (SPEI) (d) self-calibrated Palmer Drought Severity Index (scPDSI), cover the analysis period 1932-2019, only SPEI have time span 1932-2018.

1.2.2 Study species

C. axillaris is a canopy tree up to 30 meters in height, and prefers deep, wet clay or sandy clay soils. The flowering period of *C. axillaris* in Mosingto plot is on January to March and fruiting period is on June to November (Chanthorn and Brockelman, 2008). *C. axillaris* is a dominant canopy species in Mosingto plot.

1.2.3 Sampling, Sample preparation, Tree ring-width measurement and cross-dating

The core samples were collected at breast height level (1.30 m above the ground) for two to three cores per tree by using an increment borer. The sample were dried in the laboratory and were then mounted into the wooden core frame. The dried core samples were polished by progressively finer grades of sandpapers until the ring boundary could be clearly visible, following the standard dendrochronological techniques (Cook et al., 1990). Tree ring widths were measured under a stereomicroscope that connected with the LINTAB (LINTABTM 6, Rinntech Heidelberg, Germany) with a resolution of 0.001 mm.

The cross-dating of tree ring width was done by visual growth pattern matching and statistical tests using the software TSAP-Win (TSAP; Rinntech Heidelberg, Germany). The quality of cross-dating was further assessed with COFECHA software (Tenzin and Dukpa, 2017). Then, the raw tree ring width data were standardized and detrending with cubic smoothing splines (Speer, 2012) by using ‘dplR’ package based on R software (R). Average radial growth rate (AGR), mean sensitivity (MS), and 1st order autocorrelation (AC1) were

computed for standard chronology. The inter-series correlation (Rbar) and the expressed population signal (EPS) were calculated with 30 year moving windows with 15-year overlaps. Rbar is the strength of the common signal in a chronology.

1.2.4 Growth climate relationships

Since there is only short period of available climate data from the Mosingto climate station (1994-2019), climate data from global Climate Research Unit grids (<https://crudata.uea.ac.uk/cru/data/>), including monthly precipitation, maximum temperature, mean temperature, minimum temperature, the self-calibrated Palmer Drought Severity Index (scPDSI) and the Standardized Precipitation-Evapotranspiration Index (SPEI) during the period 1932 - 2019 were used for the climate-growth analysis. However, the climate data from Mosingto station (1994 - 2019) to use to compare the climate patterns with CRU data. The climate data from Mosingto station and from CRU shared similar pattern. The total annual precipitation of CRU data is 1701.70 ± 238.7 mm. The long-term annual mean, maximum and minimum temperature are 27.3, 32.4 and 22.2°C respectively. For Mosingto station, the total annual precipitation is $2,002 \pm 411.9$ mm. and the long-term annual maximum and minimum temperature are 28.97 and 15.92 °C, respectively. The long-term trend of climate of CRU and Mosingto also shared similar pattern. However, Mosingto climate data was more variable than that of the CRU climate data, and precipitation in Mosingto was higher and temperature is lower compared with those of CRU data, respectively. (Figure 1.2).

The growth-climate relationships were analyzed by computing Pearson's correlation coefficients between ring-width chronologies of *C. axillaris* and monthly CRU climate data (maximum temperature, mean temperature, minimum temperature, and annual precipitation) for 17-month time window from the previous August to current December over the period 1932 - 2019. The correlations coefficients between ring-width chronologies with the CRU Standardized Precipitation-Evapotranspiration Index (SPEI) and self-calibrated Palmer Drought Severity Index (scPDSI) were also computed cover the period 1932 - 2019, The relationships between tree-growth and climate responses were analyzed by using SPSS and moving correlation analysis was conducted by using the package “treeclim” (Zang et al., 2015) in R software.

1.2.5 Long-term growth trends

The basal area increment (BAI) was calculated from the raw measurement of ring width data by using the function “bai. Out” in R package dplR (Bunn, 2010), assuming each ring is uniform and in a circular cross-section of the trees. The BAI was calculated according to the following equation (Gauda et al., 2016).

$$BAI = \pi(R^2_t - R^2_{t-1}) \quad (1.1)$$

where R is tree radius and t is the year of tree ring formation. The long-term growth trends were analyzed by using the linear mixing model by using “lme4” package, with year as the fixed effect and core number as the random effect.

1.3 Results

1.3.1 Tree ring chronology characteristic at Mosingto

The core samples of *Choerospondias axillaris* showed distinct ring boundary. The earlywood is characterized by bigger vessels, whereas vessels in the latewood are smaller

(Figure 1.3). The tree-ring width chronology of *C. axillaris* was established by using 100 cores from 56 trees. The length of tree-ring width of *C. axillaris* at Mosingto spanned the period 1932 - 2019 (88 years) with the average growth rate (AGR) of 0.379 mm per year (Table 1). The first-order auto correlation (AC1) was 0.551, indicated that the growth in previous year would influence the growth of current year. The mean sensitivity was 0.412, and the inter-series correlation (Rbar) was 0.297. The expressed population signal (EPS) was 0.968, which passed the recommended criteria, indicating that this chronology is acceptable for dendroclimatic analysis (Figure 1.4).



Figure 1.3 Scanned image of wood core sample of *Choerospondias axillaris*. The white triangle indicated the ring boundary.

Table 1.1 Sampling site characteristics and chronology statistics of *Choerospondias axillaris* at Mosingto, Khaoyai National Park, central Thailand.

Latitude (N°)	Longitude (E°)	Elevation (m)	Core/Trees	Time span	AGR (mm/yr)	MSL (yr)	MS	AC 1	Rbar	EPS	
14.26	101.22	725- 815	100/5 6	1932- 2019	0.379	65	2	0.41	0.5	0.2	0.96

Note: Average growth rate (AGR), Mean segment length (MSL), Mean sensitivity (MS), First-order auto correlation (AC1), Inter-series correlation (Rbar) and Express population signal (EPS).

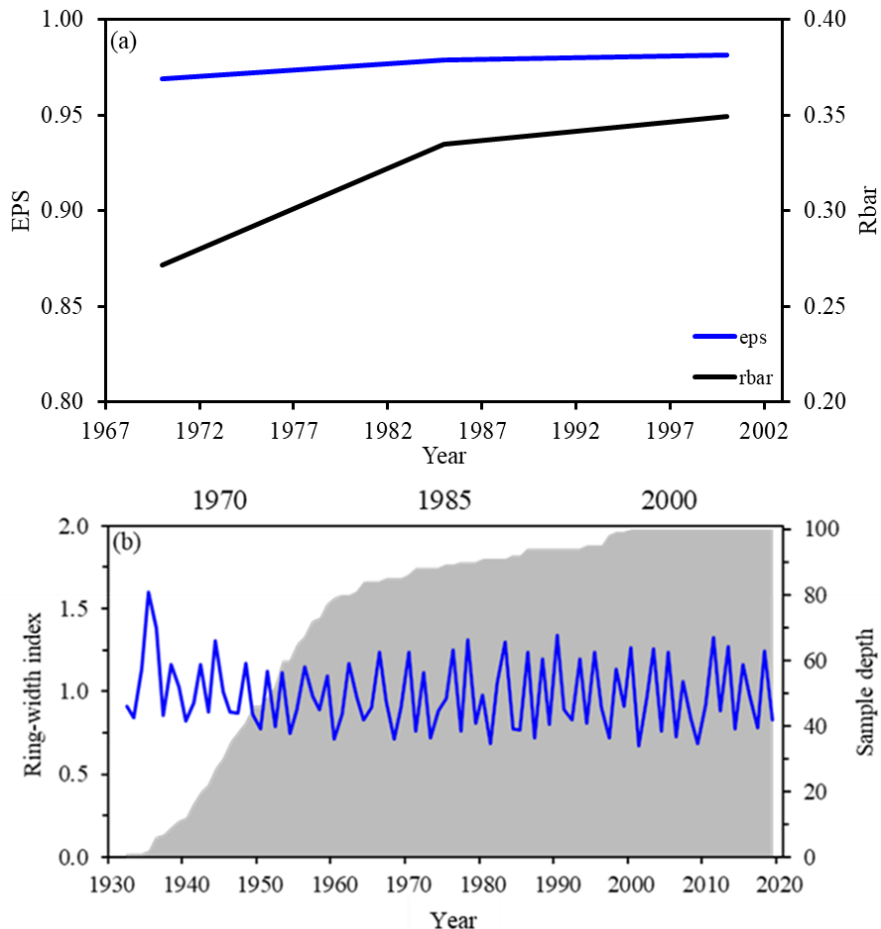


Figure 1.4 The chronology of *C. axillaris* at Mosingto, Khaoyai National Park, Central Thailand. (a) Express population signal and Rbar, and (b) *C. axillaris* chronology (blue line) and sample depth (grey area).

1.3.2 Growth-climate relationships

Tree-ring width index of *C. axillaris* was significantly and positively correlated ($p < 0.05$) with precipitation in June, July and October of current year, however, there is no significant correlations between the tree ring width index and mean temperature throughout the year. The response of tree-ring width index to the SPEI was significantly positive in July to October of current year. Tree-ring width index of *C. axillaris* was significantly and positively correlated with the scPDSI during August to December of current year (Figure 1.5).

The growth-climate correlations were confirmed by moving correlation analysis. There were significant and positive correlations between tree ring width index and precipitation in late monsoon season (July - October) over the analyzed period (1932-2019), the correlation at an early period were weaker and gradually become stronger over the recent decades. However, the correlation between tree ring width index and precipitation in June was significant at the early period but became non-significant during the recent decade. The correlations between mean temperature and tree growth were not stable throughout the analyzed period. The tree-ring index of *C. axillaris* was significantly and negatively correlated with SPEI during the second half of the year (July - December), and this

correlation become stronger in the recent decades (Figure 1.7a). Tree ring index of *C. axillaris* was significantly and positively correlated with scPDSI during August to October during the study period (Figure 1.7b).

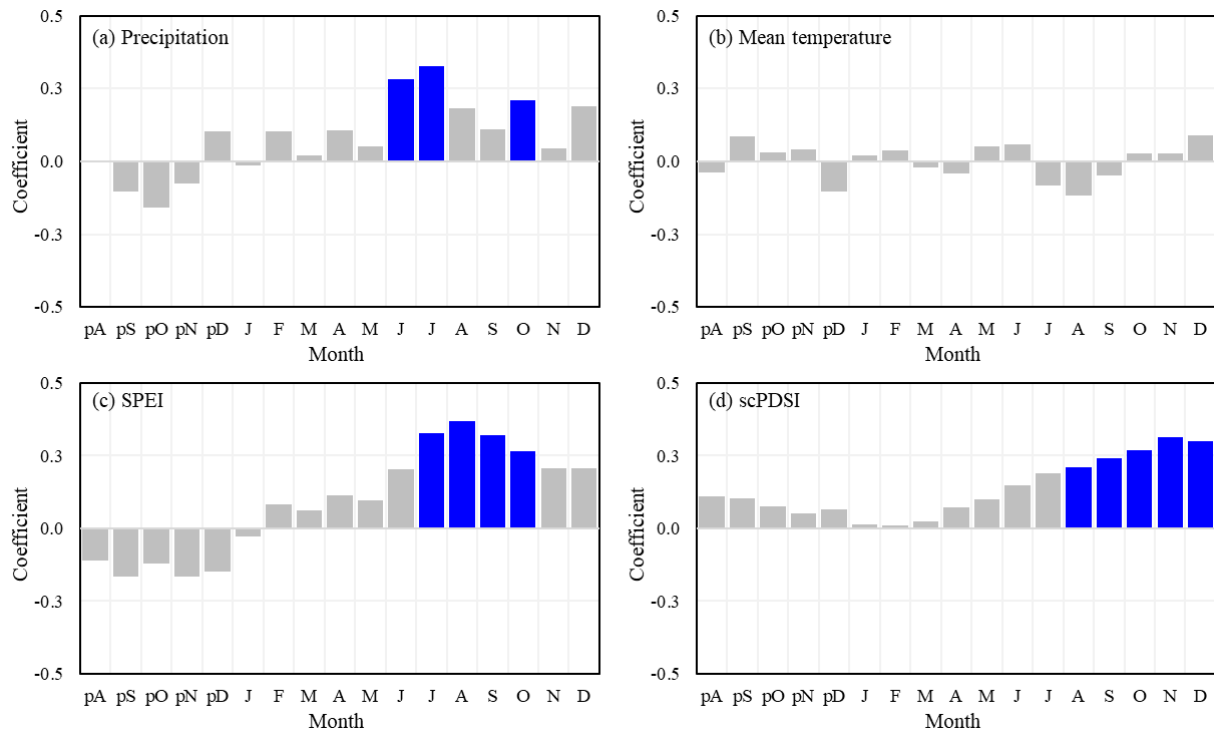


Figure 1.5 Correlation coefficients of *Choerospondias axillaris* tree ring width index with monthly mean climate data. (a) precipitation, (b) mean temperature, (c) Standardized Precipitation-Evapotranspiration Index (SPEI) and (d) self-calibrated Palmer Drought Severity Index (scPDSI) during the period 1932-2019. Blue and grey bars indicate statistically significant ($p < 0.05$) and non-significant ($p > 0.05$) correlation, respectively.

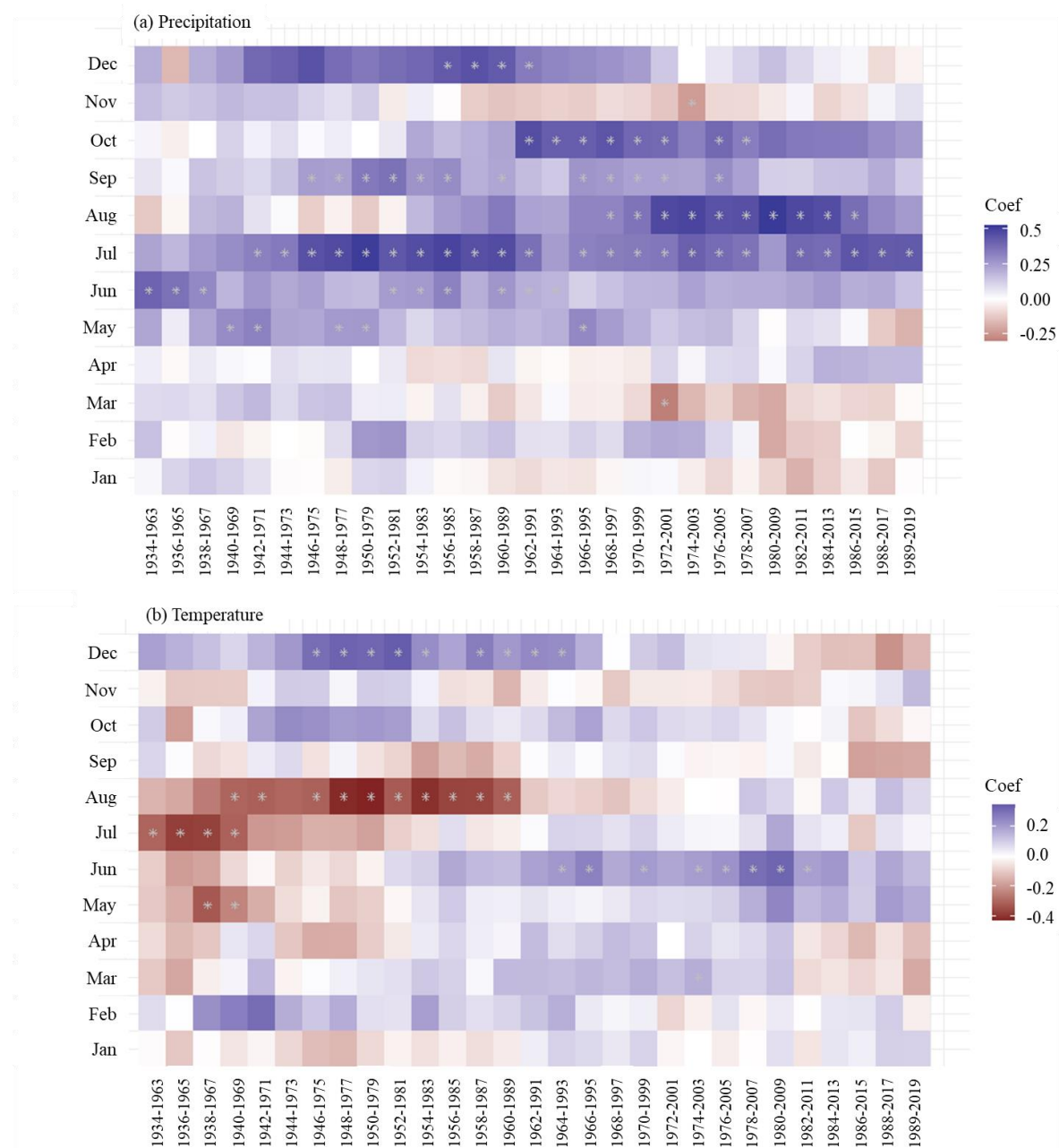
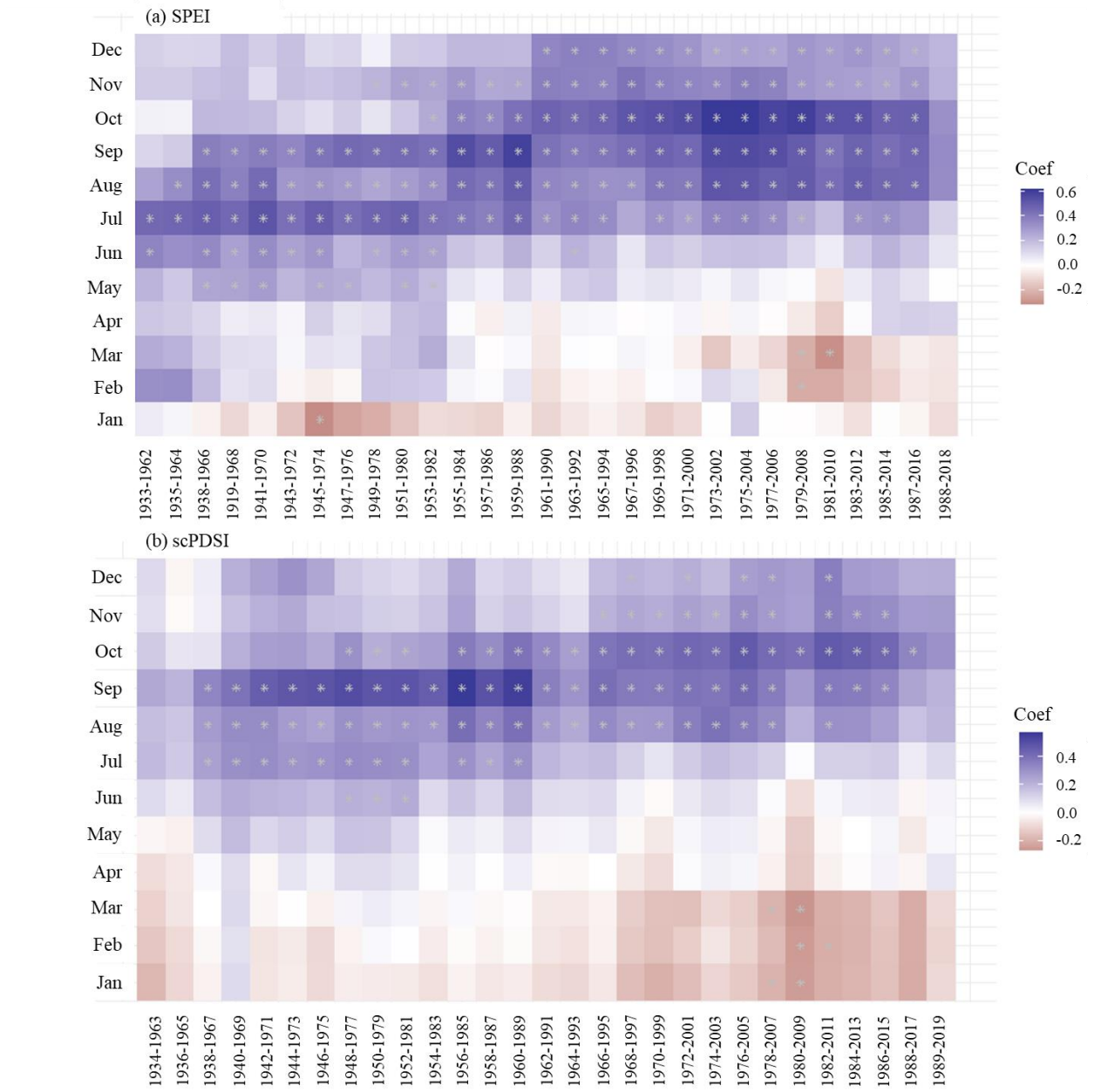


Figure 1.6 Moving correlations between tree ring width index of *Choerospondias axillaris* and (a) precipitation and (b) mean temperature during the period 1934-2019 from Climate Research Unit (CRU). The correlation analysis was carried out in a 30-year window with two-year offset. Color code represents correlation coefficient. Significant correlations are indicated by white asterisks.



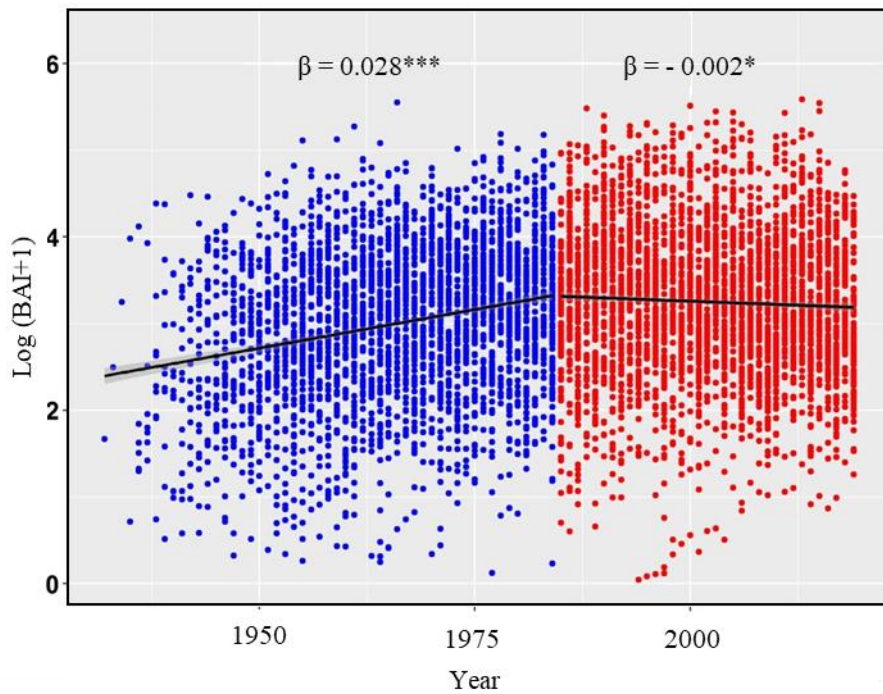


Figure 1.8 Long-term growth trend of *Choerospondias axillaris* at Mosingto during period 1932-1984 (blue point) and 1985-2019 (red point). Black line represents growth trend, “ β ” is slope. Statistically test of the growth trend were indicated by *** $p < 0.001$, * $, p < 0.01$.

1.4 Discussion

1.4.1 *Choerospondias axillaris* chronology characteristic

Our study established a new tree ring chronology for *C. axillaris* spanned from 1932 to 2019. Since there are only few broad-leaved tree species had been studied in tropical region, our study would provide important information about the growth-climate relationships for tropical trees. The average radial growth rate of *C. axillaris* was relatively low (AGR = 0.379 mm/yr) in comparison with other broadleaf tropical species in Thailand. Mean sensitivity is a measure of year-to-year growth variability and is commonly accepted to reflect the sensitivity of growth to high-frequency climatic variations. We observed high value of MS (MS = 0.412) indicating that the growth of *C. axillaris* responds to climate factors. The moderate of first-order autocorrelation indicates that tree growth was influenced by conditions in the preceding year (Fritts, 1976). Inter-series correlation (Rbar) of our study was low during the period 1970-1985, which could be due to fast-growing when the tree was young, buttress and rotten inside etc. The Rbar was higher after 1985, indicating an environmental influence on growth during the recent decades. The express population signal (EPS, 0.968) of this chronology is reliable for dendroclimatic analysis due to the EPS value 0.968 was passed arbitrary threshold vales of cut-off point 0.85 (Speer, 2012).

We found that the tree-ring width chronology *C. axillaris* had a great variation in short period, which might be related to impact of fruit production. There is an inverse relationship between radial growth and fruit production (Knops et al., 2007; Mund et al., 2020). Chanthorn and Brockelman (2008) found that the fruit production in 2004 was a bigger year with abundant seeds were found in the field, whereas the fruit production in 2005 was a smaller year with less

seeds were found in the field. The bigger year in fruit production in 2004 was in accordance with the narrower ring width index (0.76), whereas the smaller year of fruit production in 2005 is in accordance with wider ring width index (1.23). However, since long term of fruit production data is lacking, the relationships between seeds production and radial growth still needs to be further studied.

1.4.2 Growth - climate relationships

Our study found that the growth of *C. axillaris* was mainly limited by moisture availability in the rainy season (Figure 1.5). In another study found that Monsoon precipitation is the liming factor for the growth of Teaks in Myanmar (Zaw et al., 2021). Previous study found that dry season moisture availability during the dry season or dry to wet transition season is the main limiting factor for tree growth in tropical region (Vlam et al., 2013). Pumijumnong and Buajan (2012) found precipitation during the transition from dry to wet season on March was the main factor influencing cambial activity of *C. axillaris* in the same study site with present study. Although the cambial activity of tree species was related to climate in the transition seasons, the maximum growth of tropical tree species mainly occurred in the rainy season from July to August (Hu et al., 2016). We found that the growth of *C. axillaris* was positively correlated with SPEI from July to October and PDSI from August, which further confirmed that the growth was limited by the moisture availability in the rainy season. Previous studies found that radial growth of tropical tree species is negatively correlated with temperature in the dry season and dry to wet transition season in tropical seasonal dry forest (Vlam et al., 2013; Rahman et al., 2018). A higher temperature in the dry season would increase evapotranspiration and induce water deficit (Snyder et al., 2011), which would further limit tree growth. However, we did not find a significant correlation between the radial growth of *C. axillaris* and temperature in the present study. Our study showed that the growth-is stable across different period. The correlations relationships between tree growth and July to October precipitation were consistently and become stronger in recent years., which is similar to results of Rakthai et al. (2020). In addition, internal factor (heredity) and topographic factors (slope, aspect, and elevation) would also impact tree growth-climate relations (Pumijumnong, 2013). The relationships between fruit production and wood radial growth can also impact the growth-climate relationships for *C. axillaris*. Mund et al. (2020) found that fruit production was negatively correlated with the May precipitation, whereas wood growth was positively correlated with May precipitation. Precisely understanding the climate-growth correlations need to include long term fruiting and flowering monitoring in the future.

1.4.3 Long-term growth trend of *Choerospondias axillaris*

Our study revealed that the growth of *C. axillaris* at Mosingto plot, Khao Yai National Park, Thailand showing an increasing trend during 1932-1984, but the growth changed a slightly decreasing trend during 1985-2019. Our results was consistent with previous study in which the growth trend of *Pinus laterri* in Thailand also showed increasing trend during 1951-1984, but decreasing trend during 1985-2017 (He et al., 2004; Rakthai et al., 2020). The decreasing trend of the growth of *C. axillaris* in recent years could be related to increasing of temperature and slightly decreasing of precipitation trend in the present study site (Figure 1.2), which results in drier trend. The increasing trend of temperature and decreasing trend of precipitation could affect the trend of growth in the last decades (Somogyi, 2008). The

decreasing trend of tree species could also be related to the development stage. Most of the adult individuals are rotten inside (personal observation), which could also be an indicator of growth decreasing. In another study revealed that the decreasing in growth rate and productivity decline by cause of an increasing in drought severity (Feeley et al., 2007). van der Sleen et al. (2015) found that no growth was stimulated with the increasing of water use efficiency.

1.5 Conclusion

Our study provided a new chronology of tree-ring data from broad-leaved tropical species, *Choerospondias axillaris* during 1932-2019 from Mosingto forest dynamic plot, Khaoyai National Park, Central Thailand. The growth of *C. axillaris* was mainly limited by moisture availability in the monsoon season. The long-term growth trend of *C. axillaris* showed an increasing trend during 1932-1984 and a slightly decreasing trend from 1985 to 2019, which could be related to the regional climate and/or tree development stage.

#####
Note: This is the manuscript draft before the submission to the journal. The manuscript was revised once and is accepted (as of November 25, 2021). The authors and their affiliations are as follows.

Wisawakorn Surayothee^{1,2,3}, Supaporn Buajan³, Pei-Li Fu^{1,4,*}, Nathsuda Pumijumnong^{3,*}, Ze-Xin Fan^{1,4,5}, Shankar Panthi^{1,4}, Yong-Jiang Zhang⁶, Ya-Jun Chen^{1,5}, Pantana Tor-ngern⁷, Wirong Chanthorn⁸, Anuttara Nathalang⁹, Warren Y. Brockelman⁹

¹ CAS Key Laboratory of Tropical Forest Ecology, Xishuangbanna Tropical Botanical Garden, Chinese Academy of Sciences, Mengla, Yunnan 666303, China

² University of the Chinese Academy of Sciences, Beijing, 100049, China

³ Faculty of Environment and Resource Studies, Mahidol University, Salaya, Phutthamonthon, Nakhon Pathom 73170, Thailand

⁴ Ailaoshan Station of Subtropical Forest Ecosystem Studies, Xishuangbanna Tropical Botanical Garden, Chinese Academy of Sciences, Jingdong, Yunnan, 676209, China

⁵ Center for Plant Ecology, Core Botanical Gardens, Chinese Academy of Sciences, Xishuangbanna 666303, China

⁶ School of Biology and Ecology, University of Maine, Maine, 04469, USA

⁷ Department of Environmental Science, Faculty of Science, Chulalongkorn University, Bangkok 10330, Thailand

⁸ Department of Environmental Technology and Management, Faculty of Environment, Kasetsart University, Bangkok 10900, Thailand

⁹ National Biobank of Thailand, National Science and Technology Development Agency, Pathum Thani 12120, Thailand

*Correspondence: fpl@xtbg.org.cn; nathsuda@gmail.com

Objective 2

The present responses of forests to variation in climate and the vulnerability and resilience of forests

For this objective, we performed many studies to investigate variations of various parameters including leaf gas exchange, leaf traits, soil respiration, sap flow, litterfall and tree hydraulics, across seasons and forest stages. Most of the studies were conducted in Thai forests of various ecological successions. However, the Chinese team also contributed to results' interpretation and revision of manuscripts. In this section, we present the studies separately, some of which were already published whereas the rest is under preparation.

2.1 Investigating leaf gas exchange and functional traits of dominant tree species in successional forests in Thailand (Tor-ngern et al., 2021)

2.1.1 Introduction

Tropical forests play an important role in the biosphere, especially in global water and carbon cycles. Transpiration represents *ca.* 40–90% of the total amount of water emitted to the atmosphere (e.g., Miralles et al., 2011; Jasechko et al., 2013; Wang-Erlandsson et al., 2014; Good et al., 2015) and thus strongly influences hydrology and energy partitioning in terrestrial ecosystems (Bonan, 2008). Tropical forests sequester *ca.* 0.28–1.26 Pg C each year (Hubau et al., 2020) and thus play a critical role in mitigating rising atmospheric carbon dioxide and related climate change impacts. However, widespread deforestation and land use change are rapidly transforming these ecosystems, with over 80 million hectares of natural, old-growth tropical forests being lost since 1990 (FAO and UNEP, 2020). Deforestation and land use change is especially pervasive across Southeast Asia (Zeng et al., 2018; FAO and UNEP, 2020), where large-scale agricultural production and commercial tree plantations have been the main drivers of forest loss (Curtis et al., 2018). However, many of these large-scale operations have been abandoned because of unsustainable practices, leading to the regeneration of secondary forests either through natural or aided processes. Consequently, forests in Southeast Asia are characterized by a patchy mosaic of primary, old-growth forests, and forests at different stages of secondary succession.

Structural attributes, such as canopy height and tree density, vary considerably among forests which in turn can strongly influence the microclimate (Rambo and North, 2009; Jucker et al., 2018) as well as the carbon and water balance in old growth, primary forests, and forests at different stages of secondary succession (Powers and Marin-Spiotta, 2017). Old-growth forests usually contain larger trees and heterogeneous canopy layers, and lower stem density, compared to secondary forests (Chazdon 2014; Chanthorn et al., 2016, 2017; Jucker et al., 2018). Conversely, the intermediate successional stage, namely the “stem exclusion” stage, has a relatively homogeneous canopy and high stem density (Chazdon 2014; Chanthorn et al., 2016, 2017). Variation in canopy height can lead to differences in the convective boundary layer which is responsible for transport of energy and gases from plant surfaces to the atmosphere. Smaller convective boundary layers over early successional forest (stand initiation stage), which are characterized by low canopy height, result in a hotter and drier microclimate, especially during the dry season (Fisch et al., 2004). Additionally, early successional forests have greater variability in their physical environments, including water and light conditions, compared to later successional and old growth forests (Culf et al., 1996). Consequently, species acclimated to early-successional stages tend to have higher gas exchange rates, and higher stomatal conductance and photosynthesis (Hölscher et al., 2006; Vargas and Cordero, 2013;

Mujawamariya et al., 2018). In contrast, the canopy is more homogeneous and shaded in the intermediate, stem exclusion stage (Chazdon et al., 2014; Chanthon et al., 2016, 2017), which constrains gas exchange, especially leaf transpiration (Hardwick et al., 2015).

Environmental gradients during secondary succession can impact the strategies trees use to acquire resources and ultimately lead to differences in tree species richness and composition among different successional forests (Zhang et al., 2012; Chazdon et al., 2014, Chanthon et al., 2016, 2017). Previous studies in humid tropical forests have shown that decreasing light penetration during secondary succession results in changes of leaf traits (Lohbeck et al., 2013, 2015). Most trees in early successional forests are fast-growing species and, according to the leaf economic spectrum (Wright et al., 2004), have leaf traits promoting quick returns on investment in nutrients and carbon (i.e., high specific leaf area and nutrient levels, short lifespan and high metabolic rates). In contrast, trees in old growth forests tend to exhibit conservative strategies (Lohbeck et al., 2013, 2015) with high investments in leaf carbon structures (i.e., high leaf dry matter content). However, in dry tropical forests, the light gradient during succession is less pronounced and these forests are often more water-limited and have higher temperatures which may be stronger factors driving changes in plant communities (Lebrija-Trejos et al., 2010, 2011). In general, trees growing in more xeric conditions tend to exhibit leaf traits with slow returns on resource investment, i.e., have conservative strategies (Reich, 2014). Yet, we still know little about how leaf traits vary during secondary succession in dry tropical forests and how variation in leaf traits and microclimate conditions affect leaf gas exchange measurements (i.e., photosynthesis and transpiration) and ultimately, the growth and productivity of these forests.

In this study, we measured leaf-level gas exchange and plant functional traits of the dominant tree species in a seasonal evergreen forest in Thailand. Measurements were made during both the wet (May–October) and dry (November–April) season as well as within forests representing different stages of succession: a young forest (YF, ~4 years), an intermediate forest (IF, ~44 years) and an old-growth forest (OF, >200 years). Specifically, our study addressed the following questions: (Q1) Does leaf-level gas exchange (photosynthesis and stomatal conductance) differ across successional forests and between seasons? (Q2) Does the sensitivity of stomatal conductance to changes in atmospheric demand vary across different stages of forest succession? (Q3) How do different leaf functional traits relate to leaf gas exchange parameters, and do these relationships change depending on forest stage? Results from this study will improve our understanding of the underlying mechanisms governing water and carbon fluxes in different successional forests as well as assessing how these forests may respond to a hotter, drier future.

2.1.2 Materials and Methods

2.1.2.1 Site description

The study was carried out in Khao Yai National Park (KYNP), a seasonal evergreen forest in Nakhon Ratchasima Province, Thailand (14°26'31" N, 101°22'55" E, 700–800 m asl; Figure 2.1.1). Based on 1994–2018 data, mean annual temperature and precipitation at the site are about 22.4°C and 2,100 mm, respectively. The wet season usually covers the months from May to October while the dry season ranges from November to April, when monthly

precipitation is less than 100 mm (Brockelman et al., 2017). KYNP contains a mosaic of different forest types including old-growth (primary) forests and secondary forests of different ages that have regenerated from old fields within the past 42 years (Jha et al., 2020). In this study, we selected three plots representing different successional stages. The first plot was within the 30-ha Mo Singto forest dynamic plot (Brockelman et al., 2017), a ForestGEO plot in the network of the Centre for Tropical Forest Science (CTFS), Smithsonian Tropical Research Institute. These plots were established using a uniform methodology (Condit, 1998) in which every woody stem ≥ 1 cm DBH is identified, mapped, and measured every five years. This plot represented an old-growth stage (hereafter OF), with the age of at least ca. 200 years. The OF's main canopy height was 20–30 m with some emergent trees being higher than 50 m, a leaf area index (LAI) of 5 and stem density of 1,112 trees ha^{-1} (Chanthorn et al., 2016; Brockelman et al., 2017). Adjacent to the northern edge of this plot, a 1-ha plot in a secondary forest was established in 2003, using the same CTFS methods. This plot (hereafter IF) was in an intermediate successional stage at about 44 years of age and classified as stem exclusion stage. The forest canopy of IF was more homogenous and denser compared to that of OF and had a mean canopy height of 25 m, an LAI of 6, and stem density of 2,052 trees ha^{-1} (Chanthorn et al., 2016). Approximately 3 km away from the OF plot, we established a 2-ha plot in a 4-year-old, early successional forest (hereafter YF). Its mean canopy height was 15 m and stem density of 1,226 trees ha^{-1} . Despite the lack of LAI data, the YF canopy was distinctly sparse compared to the other stages based on visual observation. The IF and YF were classified as “stem exclusion” and “stand initiation” stages, respectively (Chazdon, 2014; Chanthorn et al., 2016, 2017). The soil type of these forests was gray, brown ultisol, but the soils under the IF and YF were degraded by shifting agriculture and burning prior to regeneration (Chanthorn et al., 2016, 2017).

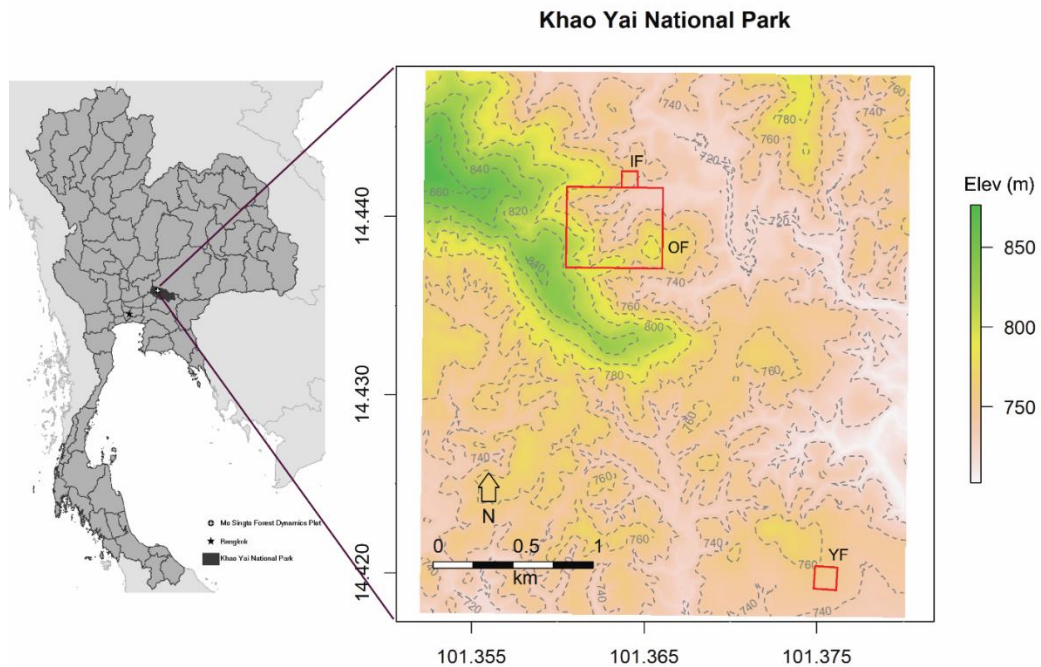


Figure 2.1.1 Study sites include a young (YF), an intermediate (IF) and an old growth (OF) forest in Khao Yai National Park, Thailand.

2.1.2.2 Plant materials and measurements

In each plot, we selected five dominant tree species, based on basal area ranking within the site. The selection resulted in 11 species in total with three species occurring in more than one forest stage: *Syzygium nervosum* in IF and YF, *Schima wallichii* in OF and IF, and *Symplocos cochinchinensis* in all stages. Table 2.1.1 summarizes the selected dominant species in each study site.

Table 2.1.1 Dominant tree species selected for measurements in each forest stage in Khao Yai National Park, Thailand.

Old growth (OF)	Intermediate (IF)	Young (YF)
<i>Dipterocarpus gracilis</i>	<i>Syzygium nervosum</i>	<i>Adinandra integrerrima</i>
<i>Ilex chevalieri</i>	<i>Eurya acuminata</i>	<i>Cratoxylum cochinchinensis</i>
<i>Schima wallichii</i>	<i>Machilus gamblei</i>	<i>Syzygium nervosum</i>
<i>Sloanea signa</i>	<i>Schima wallichii</i>	<i>Syzygium antisepticum</i>
<i>Symplocos cochinchinensis</i>	<i>Symplocos cochinchinensis</i>	<i>Symplocos cochinchinensis</i>

For each species, five trees of similar stem size (diameter at breast height averaged 13.83 ± 2.74 cm (standard deviation) were randomly selected for gas exchange measurements and leaf sample collection. For each tree, we randomly chose three mature and fully expanded leaves with good exposure to sunlight from the lower and outside branches (Kröber et al., 2015). For sampling in the intermediate and old-growth forests, we particularly selected leaves that were always present in light gaps within each canopy to ensure that the leaves received full or substantial sunlight (Fan et al., 2011; Markesteijn et al., 2011; Zhu et al., 2013). Since the canopy could not be accessed directly due to the unavailability of towers or canopy cranes, we had to perform the measurements on cut branches containing the sun-exposed leaves with the stems submerged in a container filled with water. Prior to gas exchange measurements, the stems of individual branches were recut underwater to allow the restoration of the xylem water column (Dang et al., 1997). Within 5 minutes after re-cutting, we placed a leaf in the cuvette for gas exchange measurement to minimize excision-induced effects (Santiago and Mulkey, 2003). Then, we waited for at least 2-3 minutes to allow the leaf to reach small changes in gas exchange over time before logging the data after observing stable gas exchange parameters. Leaf gas exchange measurements were made using a portable photosynthesis system (TARGAS-1, PP Systems, Amesbury, MA, USA). All leaves covered the entire window area of the cuvette which was equal to 4.5 cm^2 . Area-based photosynthetic rate (A_{area} ; $\mu\text{mol m}^{-2} \text{ s}^{-1}$) and stomatal conductance (g_s ; $\text{mmol m}^{-2} \text{ s}^{-1}$) were recorded for each leaf and reported per unit area. All measurements were conducted between 0900 and 1600 h (Marenco et al., 2001). We realized that the measurement period was longer than that often used for gas exchange measurement to avoid stomatal closure which is usually 1–2 hours before and after midday (Brodrribb and Holbrook, 2004; Bianco and Avellone, 2014; Urban et al., 2014). However, because of logistical issues, we utilized sunny conditions between the periods for gas exchange measurements. Nevertheless, we compared both A_{area} and g_s values that were recorded after 1400 h with those recorded during midday (1000-1400 h) on the same day and found no

statistical differences ($p \geq 0.064$). The flow rate was set to 250 ml min⁻¹ (TARGAS-1 Portable Photosynthesis System Operation Manual Version 1.04 2018). Photosynthetically active radiation (PAR; $\mu\text{mol m}^{-2} \text{s}^{-1}$) inside the cuvette was set to 1700 $\mu\text{mol m}^{-2} \text{s}^{-1}$, which corresponded to the light saturation point (data not shown; Hölscher et al., 2006; Zhu et al., 2013). Temperature, relative humidity and CO₂ concentration were not controlled and thus tracking ambient conditions. Because no previous publications reporting gas exchange measurements from this model of portable photosynthesis system were found, we compared our measured values to others made in tropical forests by plotting photosynthesis against stomatal conductance. Although our values are mostly concentrated in the low ranges of photosynthesis and stomatal conductance, they fall within the ranges of values measured by other techniques. We realized that this comparison may not fully justify our measurements, but our main goal was to study the variations among forest stages rather than attempting to quantify absolute gas exchange rates.

Leaf-to-air vapor pressure deficit (VPD; kPa) was recorded for each measurement and used in the sensitivity analysis. Leaf-level gas exchange measurements were performed in both the dry (March 2019, total monthly precipitation = 0.8 mm) and the wet (July 2019, total monthly precipitation = 141.7 mm) seasons. During the wet season campaign, we also collected the leaves on which gas exchange measurements were made to measure leaf functional traits. Leaf functional traits used in this study included leaf mass per area (LMA; g m⁻²), area-based nitrogen (N; g cm⁻²) and phosphorus (P; g cm⁻²) concentration, and chlorophyll concentration (Chl; $\mu\text{g cm}^{-2}$). LMA was calculated as the ratio of leaf dry mass and leaf area (Poorter et al., 2009), measured by ImageJ (Schneider et al., 2012). For chemical analyses of total N and P concentrations, three leaves from each tree were pooled to obtain enough samples (at least 0.1 g) for laboratory analyses. Total N was determined using the Kjeldahl method (Kammerer et al., 1967) and the colorimetric method was used to determine total P (Gales et al., 1966). Chlorophyll concentration was estimated from SPAD values (range 34.3–75.8) which were measured using the SPAD-502 chlorophyll meter (Konica Minolta, Tokyo, Japan). We converted SPAD into Chl using the relationship derived from 13 Neotropical species ($\text{Chl} = \frac{117.1 \times \text{SPAD}}{148.84 - \text{SPAD}}$, $r^2 = 0.89$, SPAD value ≤ 80 ; Coste et al., 2010).

2.1.2.3 Statistical analyses

To test for significant differences in A_{area} and g_s among forest stages and seasons (Q1), we used a General Linear Mixed Model with forest stage and season as fixed factors and species as a random factor. A Tukey's test was applied for post hoc analysis. We conducted regression analyses using exponential decay and logarithmic functions to analyze the sensitivity of g_s to VPD. To compare the sensitivity across forest stages (Q2), we performed the analysis with pooled data from all species within each stage and then analyze the data from species that existed in multiple stages (i.e., *Syzygium nervosum* (IF, YF), *Schima wallichii* (OF, IF) and *Symplocos cochinchinensis* (all stages)). We applied an F-test to compare the regression curves among stages. In these analyses, the sample size was 15 per species, resulting in 75 samples for each stage. We performed a one-way Analysis of Variance (ANOVA) to compare leaf traits, which were only measured in the wet season, across forest stages. We did regression analysis to evaluate the relationships between A_{area} and g_s and the leaf traits and used an Analysis of

Covariance (ANCOVA) to assess variations of significant relationships across forest stages. All analyses of comparisons were done in SPSS (IBM Corp. Released 2013. IBM SPSS Statistics for Windows, Version 22.0. Armonk, NY, USA) and regression analyses were performed in SigmaPlot (version 12.0, Systat Software, Inc., San Jose, CA, USA). In all statistical analyses, we used the significance level of 0.01.

2.1.3 Results

2.1.3.1 Does leaf-level gas exchange differ across successional forests and between seasons?

In general, species in all forest stages had higher A_{area} and g_s in the wet than in the dry season ($p \leq 0.0001$). When combining data from both the wet and dry season, there was no significant difference in A_{area} and g_s among successional forest stages ($p \geq 0.184$). However, when comparing dry-season measurements, there were significant differences in A_{area} and g_s among the forest stages ($p \leq 0.0006$; Figure 2.2 brown bars), whereas there were no differences in the wet season ($p \geq 0.03$; Figure 2.1.2 yellow bars). In the dry season, trees in OF and YF had comparable A_{area} and g_s but higher values than trees in IF (Figure 2.1.2).

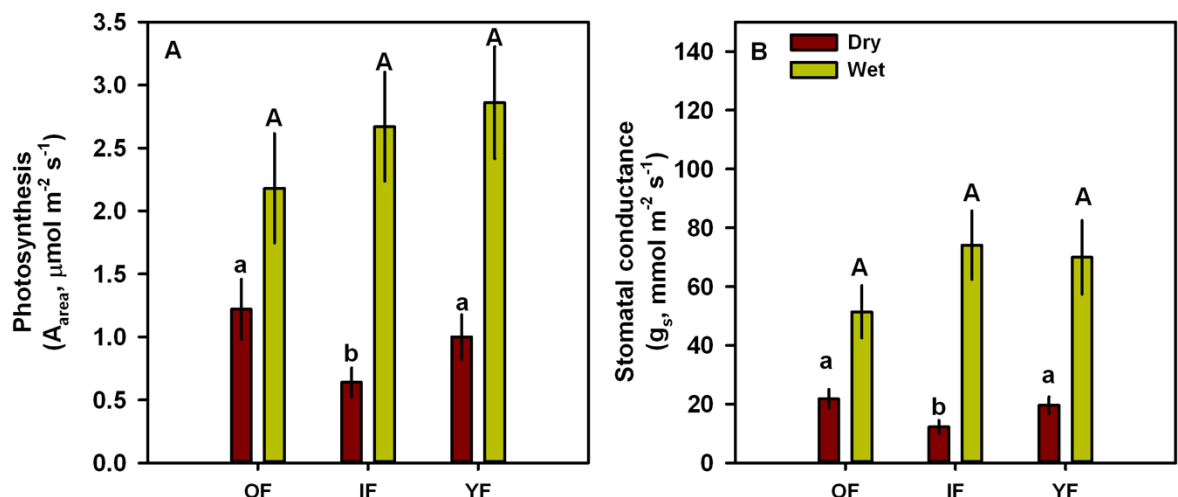


Figure 2.1.2 Overall mean ($\pm 1 \text{ SE}$) leaf-level (A) photosynthesis (A_{area} ; $\mu\text{mol m}^{-2} \text{s}^{-1}$) and (B) stomatal conductance (g_s ; $\text{mmol m}^{-2} \text{s}^{-1}$) in young (YF), intermediate (IF) and old-growth forests (OF) within Khao Yai National Park, Thailand. Measurements were taken in the dry (brown bars) and the wet (yellow bars) season. Different lowercase (uppercase) letters indicate significant difference among forest stages during the dry (wet) season.

For *Schima wallichii* and *Symplocos cochinchinensis*, tree species found in multiple sites, there was no significant difference in A_{area} and g_s among forest stages during the wet season ($p \geq 0.659$; Figure 2.1.3A, B, D, E; yellow bars). However, during the dry season these two species had significantly higher gas exchange rates in OF compared to the younger sites ($p \leq 0.004$, Figure 2.1.3A, B, D, E; brown bars). For *Syzygium nervosum*, which was found in the intermediate and early successional forests, A_{area} and g_s were similar across stages regardless of season (Figure 2.1.3C, F; $p \geq 0.631$).

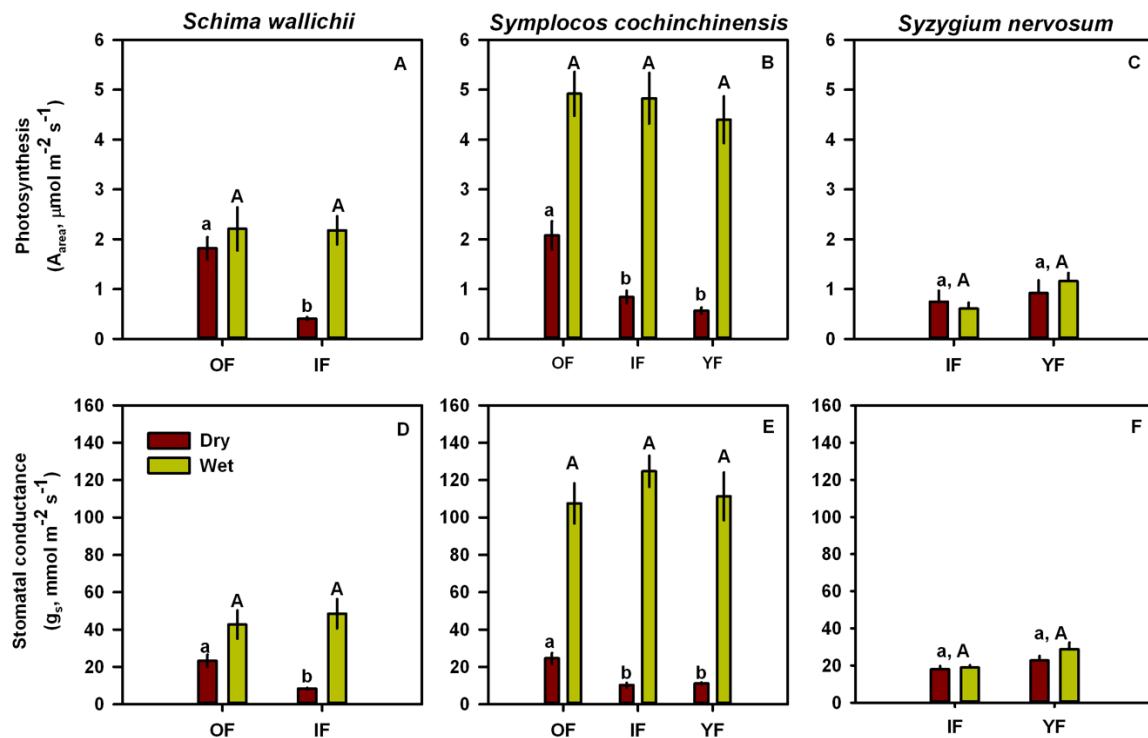


Figure 2.1.3 Mean ($\pm 1 \text{ SE}$) leaf-level (A–C) photosynthesis (A_{area} ; $\mu\text{mol m}^{-2} \text{s}^{-1}$) and (D–F) stomatal conductance (g_s ; $\text{mmol m}^{-2} \text{s}^{-1}$) of species that occurred in multiple forest stages in Khao Yai National Park. Measurements were made during the dry (brown bars) and wet (yellow bars) season. Different lowercase (uppercase) letters indicate significant difference among forest stages during the dry (wet) season.

2.1.3.2 Does the sensitivity of stomatal conductance to changes in atmospheric demand vary across forest succession?

We tested the relationship between g_s and VPD in all tree species using data from both seasons. Various equations have been proposed to explain such relationship, including linear (McCaughey and Iacobelli, 1994), exponential (Dye and Olbrich, 1993) and logarithmic (Oren et al., 1999). We employed these equations in our regression analysis for each species in each stage and found significant results with exponential ($y = a \times \exp(-bx) + c$) and logarithmic ($y = b \times \ln(x) + c$) forms in 10 out of 11 species, which is consistent with previous studies of various tree species (Oren et al., 1999; Mielke et al., 2005; Motzer et al., 2005). No equation could explain the relationship in *Machilus gamblei*. First, we examined the relationship between g_s and VPD in all dominant species within each site. We found that g_s exponentially decreased with VPD in all forests ($p < 0.0001$, $r^2 \geq 0.66$) with no difference among successional stages (Figure 2.1.4A, $F_{2,447} = 1.25$, $p = 0.287$). Next, we further considered the species that occurred in multiple forest stages. A logarithmic decline was the best fit between g_s and VPD for *Syzygium antisepticum*, whereas for *Schima wallichii* and *Symplocos cochinchinensis*, an exponentially decaying function was the best fit (Figure 2.1.4B–D; $p \leq 0.01$). When compared among sites, the relationships between g_s and VPD for these species were similar across forest stages ($p \geq 0.136$).

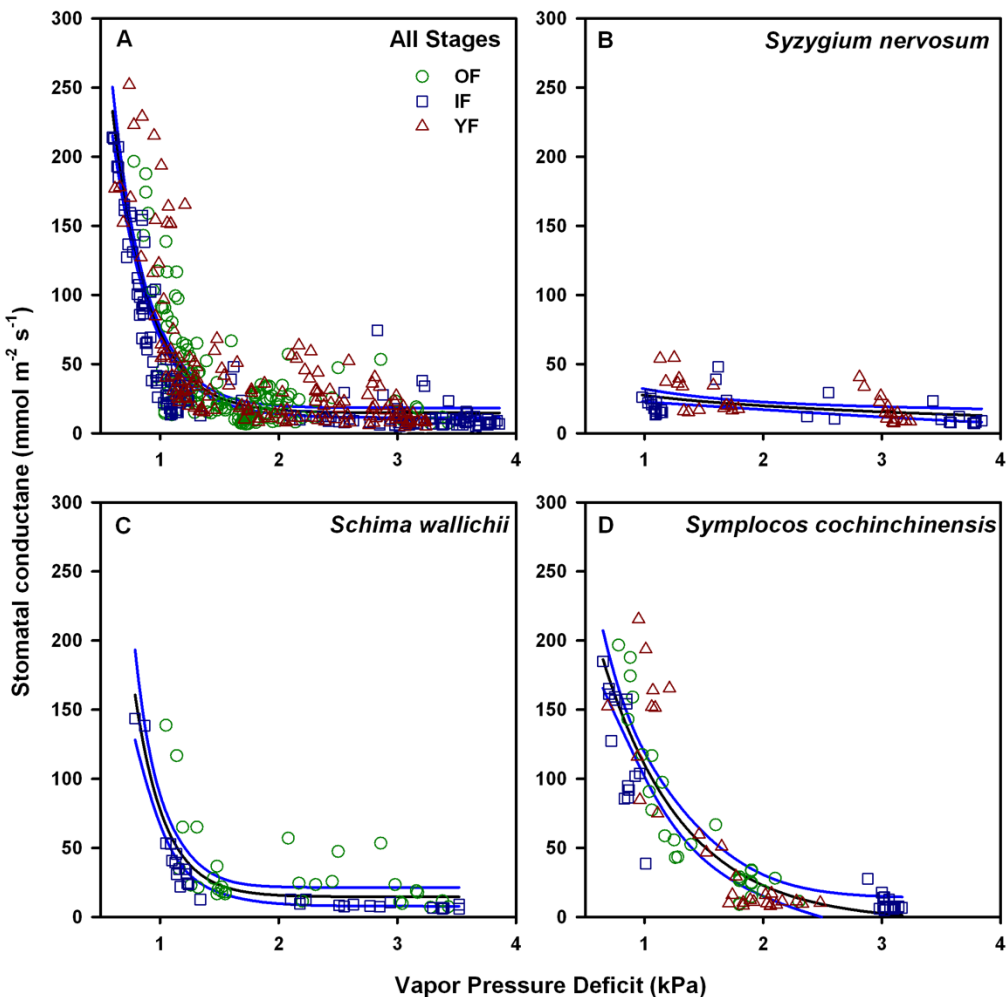


Figure 2.1.4 Relationships between leaf-level stomatal conductance (g_s ; $\text{mmol m}^{-2} \text{s}^{-1}$) and leaf-to-air vapor pressure deficit (VPD; kPa) for (A) all forest stages (B) *Syzygium nervosum*, (C) *Schima wallichii*, and (D) *Symplocos cochinchinensis*. Measurements were made in an old-growth forest (OF, green circles), an intermediate forest (IF, blue squares), and a young forest (YF, red triangles). Black solid lines show the best fits with 95% confidence intervals (blue lines) for pooled data after finding no difference among different stages.

2.1.3.3 How do different leaf functional traits relate to leaf gas exchange parameters and do these relationships change depending on forest stage?

For this research question, we focused on the wet season only due to the availability of data. Across the three forest stages, average LMA, P and N values were higher in YF compared to the two older forests (Figure 2.1.5A–C; $p < 0.0001$). In contrast, there was no significant difference in Chl among the successional forests (Figure 2.1.5D; $p = 0.067$). Next, we explored the relationships between gas exchange parameters and the leaf traits. Of all considered traits, only LMA and N were significantly related with A_{area} and g_s in IF and OF ($p \leq 0.01$). We further compared the relationships between both gas exchange parameters and LMA and N in OF and IF and found no difference between the stages ($p \geq 0.024$). Figure 2.1.6 shows the significant relationships for the pooled data from both OF and IF (black solid lines).

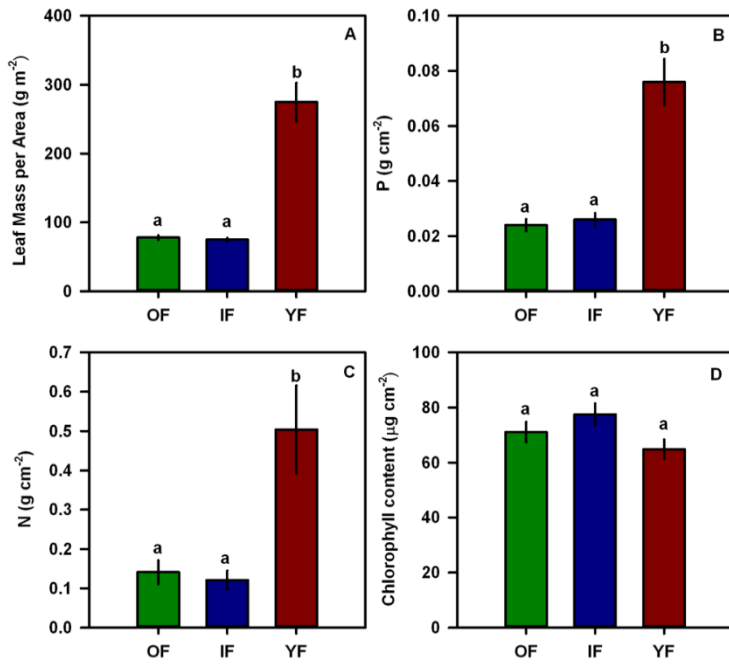


Figure 2.1.5 Mean (\pm SE) (A) leaf mass per area (LMA; g m^{-2}), (B) phosphorus concentration (P; g cm^{-2}), (C) total nitrogen concentration (N; g cm^{-2}) and (D) chlorophyll concentration (Chl; $\mu\text{g cm}^{-2}$) among the old-growth (OF; green bars), intermediate (IF, blue bars), and young (YF, red bars) forest stages. Lower case letters indicate significant differences among forest stages.

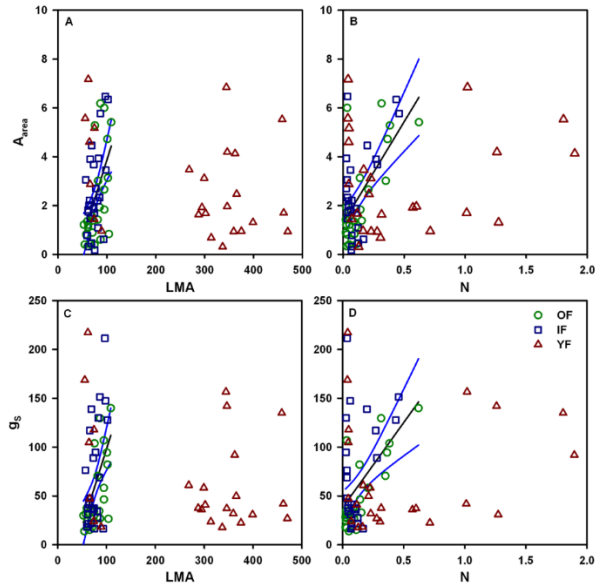


Figure 2.1.6 Linear relationships between photosynthesis (A_{area} ; $\mu\text{mol m}^{-2} \text{s}^{-1}$) and stomatal conductance (g_s ; $\text{mmol m}^{-2} \text{s}^{-1}$) and leaf mass per area (LMA; g m^{-2}) and total nitrogen concentration (N; g cm^{-2}). Measurements were made in an old-growth forest (OF, green circles), an intermediate forest (IF, blue squares), and a young forest (YF, red triangles). Black solid lines show the best fits with 95% confidence intervals (blue lines) for pooled data of OF and IF after finding no difference among the stages. Note that no significant relationships were found in YF.

2.1.4 Discussion

Seasonal variations in both gas exchange parameters were observed at the forest level and at species level. Generally, both A_{area} and g_s were higher in the wet than in the dry season. For all studied species, lower A_{area} and g_s in the dry season corresponded to higher VPD which is consistent with plants closing their stomata in response to increasing atmospheric drought (Cunningham, 2004; Chen et al., 2016). These results suggested that productivity of these successional stages may differ, especially during the dry season when both atmospheric and soil humidity are usually limiting (Harper et al., 2013). However, we found no significant difference in the gas exchange parameters across our successional forests during the wet season. Instead, a significant decrease in the parameters was observed in the intermediate forest (IF) with the highest stem density (2,052 trees ha^{-1} vs. 1,112 trees ha^{-1} and 1,226 trees ha^{-1} in OF and YF, respectively), in the dry season. Such high density induces shading in the canopy with lower variability in LAI (Chazdon, 2014; Chanthorn et al., 2016, 2017) and may limit the gas exchange as previously observed in shade-acclimated trees (Chazdon et al., 1996; Gerardin et al., 2018; Yang et al., 2019). Based on observations, the indifference of gas exchange parameters across stages in the wet season may result from the higher canopy leaves in OF and YF compared to those in the dry season. In other words, the shaded canopy in IF maintained throughout seasons while the canopy in OF and YF varied seasonally, with the greatest difference between seasons in YF. Further measurements of canopy leaf areas should be performed to confirm this point. Overall, our results suggest that the gas exchange rates did not differ across forest succession but were affected by different microclimates induced by different canopy density. Nevertheless, previous reports on gas exchange measurements in various tropical tree species have shown inconclusive evidence on the effects of forest succession on leaf gas exchange rates (Hogan et al., 1995, Coste et al., 2005; Hölscher et al., 2006).

Next, we examined species that grew in multiple successional stages to further investigate the effect of forest succession on gas exchange rates. There were no differences in gas exchange for *Syzygium nervosum* among the forest stages regardless of season. In contrast, *Schima wallichii* and *Symplocos cochinchinensis* exhibited higher gas exchange rates in the old growth forest compared to the two young successional forests during the dry season. The lack of difference in the gas exchange rates of *Syzygium nervosum* may be supported by similar stomatal density ($p = 0.22$, data not shown) across seasons, showing unchanged number of sites available for gas exchange per unit leaf area (Wu et al., 2018). Compared to the rates in the primary forest, lower rates of *Schima wallichii* and *Symplocos cochinchinensis* in the intermediate forest agreed with site-level results of limited gas exchange under shaded canopy while lower rates in the young forest may be attributed to its drier soil (average soil moisture = $23.85 \pm 5.34\%$ in YF vs. $44.54 \pm 8.46\%$ and $38.11 \pm 6.73\%$ in OF and IF, respectively). Nevertheless, further investigations on physiological responses such as tree hydraulic conductivity and architecture should be performed to confirm these results.

Sensitivity of g_s to VPD provides insight into how trees respond to increasing atmospheric drought (i.e., higher temperature combined with low humidity). Trees with greater sensitivity of g_s to VPD, closing stomata more rapidly when air dries, acclimate better to

increasing atmospheric drought compared to those with lower sensitivity. Nevertheless, trees in our successional forests did not show distinct sensitivity of g_s to VPD when considering both the forest level and species level. Most studies investigating the sensitivity of stomatal conductance to VPD in tree species found differences in the relationships across various factors besides species, such as crown height and wood anatomy (Woodruff et al., 2009; Tsuji et al., 2020). However, our data showed similar sensitivities of stomatal conductance to changing vapor pressure deficit across our successional forests, suggesting similar responses of the dominant trees to varying atmospheric humidity throughout the year. This finding may support the observed similarity in the gas exchange rates between the two contrasting forest stages (OF and YF), despite the widely reported results that early successional species usually have greater maximum gas change rates than late-successional ones (Hölscher et al., 2006; Zhu et al., 2013). Regarding the response of stomatal conductance to atmospheric conditions, we further examined the slope parameter in the unified stomatal optimization model (USO; Medlyn et al., 2011) which represents a measure of intrinsic plant water-use efficiency. Wu et al. (2019) showed that the slope parameter significantly varied with leaf mass per area in tropical forests. However, we tested this finding with our data and found an insignificant result ($p = 0.998$), suggesting similar intrinsic water-use efficiency among the dominant trees regardless of LMA. Furthermore, we found no difference in slope parameters across successional forests in the case of species existing in multiple sites ($p \geq 0.66$). Nevertheless, further studies on canopy fluxes should be conducted to confirm such findings because results from leaf-level measurements can obscure those from the canopy level (Tor-ngern et al., 2015).

While similar chlorophyll concentration was observed across all forest stages, LMA, leaf N and P were significantly higher in YF compared to other forest stages. Previous studies indicated that nutrient-poor soils may induce larger allocation of leaf nitrogen into cell walls, increasing LMA but decreasing maximum photosynthesis (Takashima et al., 2004; Hikada and Kitayama 2009). However, we found no significant difference in soil N and P among the forest stages ($p \geq 0.21$; data not shown), suggesting that the soil condition in YF was not nutrient poor compared to the others. Other studies have shown that species with high LMA usually occur in areas with low rainfall and high light and temperature (Niinemets, 2001; Villar and Merino, 2001; Lamont et al., 2002; Wright et al., 2004). This supports our result because trees in YF experience more xeric conditions and higher radiation due to their sparse canopy cover. Higher LMA may be associated with greater accumulation of nutrients in leaves (Kimura et al., 1998) as observed in our data, allowing high photosynthesis under adverse growing conditions, such as low soil moisture as often observed in sparse canopy forests with low leaf area indices (Von Arx et al., 2013). Nevertheless, our results did not show such high photosynthesis in YF which may be limited by the low soil water availability of this site compared to the others.

To gain insight into which leaf traits were linked to tree growth, we explored the relationships between leaf functional traits and gas exchange parameters (A_{area} and g_s) within the different successional forests. Maximum net photosynthesis is usually affected by various leaf traits, such as LMA (Field and Mooney 1986; Reich et al., 1999; Poorter et al., 2009), and leaf nutrient concentrations (Evans, 1989; Reich et al., 1999; Wright et al., 2004). Several studies have reported significantly positive correlations between maximum photosynthesis rate and LMA (Reich et al., 1997; Wright et al., 2004; Quero et al., 2006), leaf N (Reich et al.,

1994; Ellsworth and Reich, 1996; Kull and Niinemets, 1998; Gulias et al., 2003; Hölscher et al., 2006) and P (Hölscher et al., 2006; Zhang et al., 2018). Our results showed that LMA and leaf N were significantly related to the gas exchange rates in IF and OF, although we found no relationships between the rates and leaf P. Comparing the linear dependence of A_{area} and g_s on LMA and N between OF and IF, we found no differences between the trends, which is in contrast to a recent study that showed a lower slope between A_{area} and N in climax species (Zhang et al., 2018). However, the study argued that such difference was relevant to different soil phosphorus concentrations between successional stages, which was not the case for our sites. Interestingly, we observed no significant relationships between maximum gas exchange parameters and any leaf traits in YF. High variations of species-specific data may contribute to the insignificant relationship as seen in clearly separated clusters of data, corresponding to different species within YF. This finding suggests that trees in the young forest (YF) may be more active in resource acquisition, as shown by the large variation in leaf nutrients, and in morphological acclimation through the increased LMA for greater nutrient accumulation. Such acclimation should facilitate high gas exchange rates; however, the different soil water availability may have limited the rates in the young forest. Nevertheless, findings from this study warrant further investigations from different perspectives, including other physiological parameters, such as tree hydraulics and canopy-level measurements, to arrive at firm conclusions.

2.1.5 Conclusions

Varying environmental conditions among different successional forests present a challenge for estimating forest water use and productivity in tropical forests. Such heterogeneity in environmental conditions can strongly influence water and carbon exchanges between the forest canopy and the atmosphere. Our results show that, in general, gas exchange rates between the tree canopy and the atmosphere did not vary across forest stages yet differed among them in the dry season, as a result of changes in canopy density during secondary succession. The similar rates were further supported by similar sensitivity of stomatal conductance to changing atmospheric humidity across forest stages. Our data also suggest that the young forest was highly active in acquiring resources, but such high resource acquisition did not allow high gas exchange rates because of limiting soil water availability. These findings highlight the potential effects of inherent canopy characteristics of successional forests on water and carbon exchanges between trees and the atmosphere. Nevertheless, further studies on canopy level are needed to confirm such findings.

#####
Note: This work was published. Please refer to the publication in the Appendix.

2.2 Different responses of soil respiration to environmental factors across forest stages in a Southeast Asian forest (Rodtassana et al., 2021)

2.2.1 Introduction

The role of climate change in the functioning of forests has been increasingly recognized by the global community. Forests cover about 30% of the global land surface and store ~45% of terrestrial carbon (Bonan 2008). Global forests sequester and store carbon in above- and below-

ground parts (Giardina et al., 2004; Bunker et al., 2005), and they release carbon dioxide (CO_2) back into the atmosphere through respiration by plants and soil. Soil respiration (SR) is an important component of the global carbon cycle, contributing 78–95 Pg of carbon back into the atmosphere annually (Bond-Lamberty and Thomson 2010; Hashimoto et al. 2015). Specifically, SR in forests represents 40–90% of total CO_2 emissions from terrestrial ecosystems (Granier et al. 2000; Schlesinger and Andrews 2000).

Soil respiration is highly sensitive to environmental change because it is influenced by many factors, including soil temperature, soil moisture, the microbial community, surface litter and vegetation type (Jenkinson et al. 1991; Grace 2004; Davidson et al. 2006; Yan et al., 2006; Fekete et al. 2014). In fact, even small changes in SR can incur profound impacts on the global carbon balance, further affecting feedbacks to climate change (Davidson et al. 2006). Despite several studies on SR and its drivers in forests in boreal and temperate regions, such investigations remain elusive in tropical systems, especially in Southeast Asia. Deforestation and land-use change are particularly pervasive across Southeast Asia (Zeng et al., 2018; FAO and UNEP, 2020), where large-scale agricultural production and commercial tree plantations are the main drivers of forest loss (Curtis et al., 2018). However, due to unsustainable practices, such large-scale operations have often been abandoned, leading to the regeneration of secondary forests naturally or artificially. Consequently, forests in Southeast Asia are mostly characterized by patches of primary, old-growth forest and forests at different stages of secondary succession. Such variations in forests may exert different impacts on SR through modifications of environmental factors associated with successional gradients.

Forest succession often modifies microclimatic conditions and biogeochemical cycles (De Kovel et al. 2000; Lebrija-Trejos et al., 2011; Li et al., 2013) and varies with species composition and abundance (Sheil, 2001). Therefore, the driving factors for SR are affected by the forest succession (Raich and Tufekcioglu, 2000). For instance, soil organic carbon, total nitrogen and microbial biomass increase rapidly with secondary forest succession (Jia et al., 2005). The rate of surface litter decomposition has been found to be higher in older successional stages of tropical dry secondary forests (Tolosa et al., 2003). Although several studies have investigated SR and its driving factors in association with forest succession (Yan et al., 2006, 2009; Luo et al. 2012; Han et al., 2015; Huang et al., 2016; Wang et al., 2017; Gao et al., 2020), none of these studies were conducted in tropical forests of Southeast Asia.

To help fill this knowledge gap, we measured SR of three successional forest plots in a seasonal evergreen forest in Thailand. We performed the measurements in the wet (June and September 2020) and the dry (February and March 2021) periods within plots of different stages of succession: young forest (YF, ~5 years), intermediate forest (IF, ~45 years) and old-growth forest (OF, >200 years). The main research questions included (1) Does SR differ across successional forests and among periods of data collection? and (2) Does SR respond to environmental factors including soil organic matter (OM), soil temperature (ST) and soil moisture (SM) and whether these relationships (if any) differ across forest stages? Note that we did not intend to estimate total carbon dioxide efflux from these forests, but rather aimed to investigate the dynamical changes of SR in response to various environmental factors across forest succession.

2.2.2 Materials and Methods

2.2.2.1 Site description

The study was conducted in seasonal evergreen forest at 700–800 m asl in Khao Yai National Park (KYNP), Nakhon Ratchasima Province, Thailand (14°26'31" N, 101°22'55" E; Figure 2.2.1A). According to data spanning 1994–2018, mean annual temperature and precipitation at the site are 22.4 °C and 2,100 mm, respectively (Department of National Parks, Wildlife and Plant Conservation; 25-year means). The wet season lasts from May to October and the dry season from about late October to April, when monthly precipitation is less than 100 mm (Brockelman et al., 2017). During the study, precipitation peaked in September which accounted for 21% (2019) and 26% (2020) of total precipitation in the wet season (data from a rain logger near the study site). Monthly precipitation was 239.2 mm (June 2020), 466.9 mm (September 2020), 33.6 mm (February 2021), and 1.4 mm (March 2021) as shown in Figure 2.2.1B. Using the same criteria as in Brockelman et al. (2017), we identified two data collection periods: the wet period in June through September 2020, when monthly precipitation exceeded 100 mm, and the dry period in February and March 2021.

KYNP contains mostly old-growth (primary) forest with scattered patches of secondary forest at various stages which have regenerated from old fields within the past 50 years (Jha et al., 2020). For this study, we selected three plots representing different stages. The first plot was within the 30-ha Mo Singto forest dynamic plot (Brockelman et al., 2017), a ForestGEO plot in the global network of the Center for Tropical Forest Science (CTFS), Smithsonian Tropical Research Institute (Davies et al., 2021). CTFS plots are established using a uniform methodology (Condit, 1998) in which every woody stem ≥ 1 cm DBH is identified, mapped, and measured every five years. This plot represented an old-growth stage (hereafter OF), with the age of at least ca. 200 years. The OF's mean canopy height was 30 m with some emergent trees being higher than 50 m, a leaf area index (LAI) of 5 and stem density of 1,112 trees ha^{-1} (Chanthorn et al., 2016; Brockelman et al., 2017). Adjacent to the northern edge of this plot, a 1-ha plot in a secondary forest was established in 2003, using the same CTFS methods. This plot (hereafter IF) was at an intermediate successional stage about 45 years of age, classified as the stem-exclusion stage. The forest canopy of IF was more uniform and denser than that of OF and had a mean canopy height of 25 m, an LAI of 6, and stem density of 2,052 trees ha^{-1} (Chanthorn et al., 2016). About 3 km away from the OF plot, we established a 2-ha plot in a 5-year-old, initial stage forest (hereafter YF). Its mean canopy height was 15 m and stem density was 1,226 trees ha^{-1} . Despite the lack of LAI data, the YF canopy was distinctly sparse compared to the other stages based on visual observation. The soil type of these forests was gray, brown ultisol, but the soils under the IF and YF were degraded by shifting agriculture and burning prior to regeneration (Chanthorn et al., 2016, 2017). Based on the preliminary measurement at the sites, bulk density of the soil in IF (averaged 0.93 g cm^{-3}) was lower than that in OF and YF (1.26 and 1.24 g cm^{-3} , respectively). The soil texture at the study plots, measured at 10 cm depth, was classified as sandy clay-loam and clay loam with the highest sand contents in YF plots measured in September 2020 and February 2021 as $64.4 \pm 3.06 \%$ and $56.4 \pm 5.03 \%$, respectively. All study sites (OF, IF and YF) are similar with respect to geology and slope.

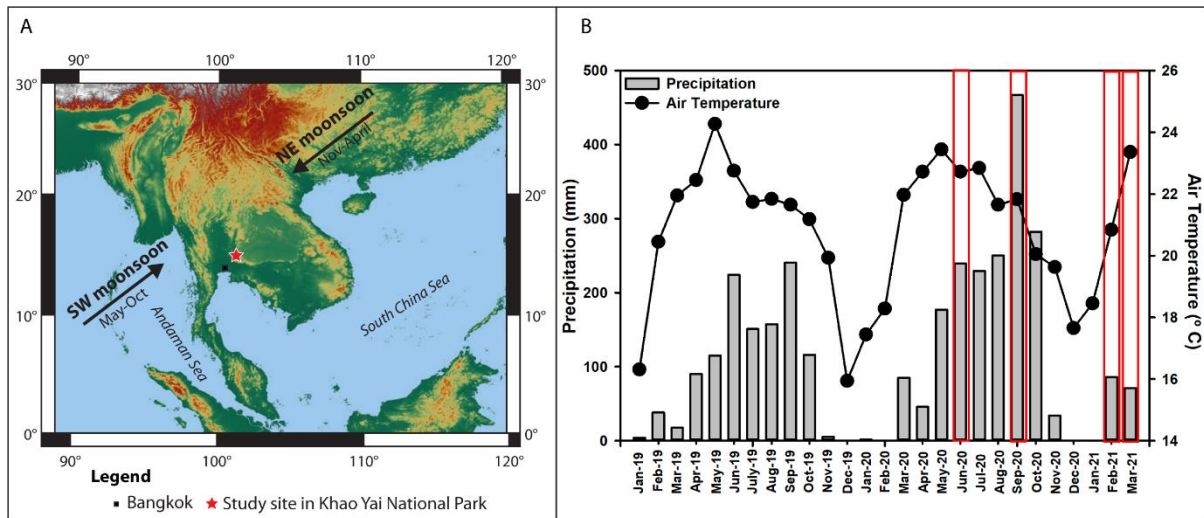


Figure 2.2.1 (A) Location of Khao Yai National Park in Thailand where the study was performed. (B) Monthly total precipitation (mm; bars) and average air temperature (°C; circles) profiles in Khao Yai National Park. Data from January 2019 to December 2020 were obtained from a local station near the old-growth forest (OF) while those from January to March 2021 were from the weather station near the young forest (YF). Red boxes indicate the months in which our measurements were made.

2.2.2.2. Measurements of the study variables

We performed the study in two different periods of contrasting rainfall which we will refer to as ‘wet’ and ‘dry’ periods in the results. In each period, we conducted the measurements twice, each separated by at least a month (Figure 1B, red frames). In each forest stage, we established a 1-ha plot and divided it into $20\text{ m} \times 20\text{ m}$ subplots as shown in Figure A2. Then, we randomly selected six sampling points within the 1-ha plot and measured all study variables concurrently at each point during 1000–1500 h on sunny days. For SR, we used a portable photosynthesis system (TARGAS-1, PP Systems, Amesbury, MA, USA) connected to a soil respiration chamber (SRC-2 Soil Respiration Chamber, PP Systems, Amesbury, MA, USA). In this process, the SR rate, measured in $\text{g CO}_2 \text{ m}^{-2} \text{ h}^{-1}$, was calculated by measuring the rate of increase of CO_2 concentration in the chamber over a period which was set to 60 seconds. Before taking measurements, we installed a soil collar with cross-sectional area of 78 cm^2 , on each selected sampling point at 5-cm depth in the soil, leaving it for at least one hour prior to SR measurement. Before putting the soil respiration chamber on the soil collar, we removed small living plants and coarse litter from the soil surface within the collar to avoid measuring their respiration (Zhou et al., 2007; Peng et al., 2014). Simultaneously, ST was measured using a probe (STP-2 Soil Temperature Probe, PP Systems, Amesbury, MA, USA) at 10-cm depth near the soil collar. Soil moisture was measured at 5-cm depth from the soil surface using a probe (SM150T, DeltaT Devices, London, UK). For each sampling point, all measurements of SR, ST and SM were repeated three times and then averaged to represent each sampling point. In addition, the unit of SR was converted to $\mu\text{molCO}_2 \text{ m}^{-2} \text{ s}^{-1}$ to facilitate the comparisons with other studies which mostly present SR rate in this unit. For the soil analyses, we collected three 3.2-cm diameter soil core samples from each study plot at 10-cm soil depth in the wet season

(September 2020) and the dry season (February 2021). We used a total organic carbon analyzer (Multi N/C 3100, Analytik Jena) to obtain OM values.

2.2.2.3 Statistical analysis

To answer the research questions, we analyzed differences in the measured variables across forest stages and between both periods. Before performing the data analysis, we used the Shapiro-Wilk test and the Levene's test to check for normality and homogeneity of variance, respectively. For the comparison between two collection periods (wet and dry), we employed an independent t-test for the data with normal distribution and Mann-Whitney U test for non-normal data. Then, for each period, we compared the SR, ST, SM, and OM across forest stages by using one-way ANOVA with a Tukey's post hoc analysis for normally distributed data and the Kraskal-Wallis test with pairwise comparisons for non-parametric data. All statistical tests were performed in SPSS (IBM Corp. Released 2013. IBM SPSS Statistics for Windows, Version 22.0. Armonk, NY, USA). For the relationships among the variables, we performed regression analyses in SigmaPlot (version 12.0, Systat Software, Inc., San Jose, CA, USA) with SR as the dependent variable and ST, SM and OM as the independent variables. In all statistical analyses, we used the significance level of 0.05.

2.2.3 Results

Figure 2.2.2 shows data of all measured variables, including soil temperature (ST), soil moisture (SM), soil organic matter (OM) and soil respiration (SR) during both collection periods. In both periods, ST in YF was significantly higher than in IF (Kruskal-Wallis, $H = 8.074, p < 0.05$ and $H = 7.803, p < 0.05$ for wet and dry periods, respectively), although it was not significantly different from that in OF. Soil temperature in all forest stages was significantly lower in the dry period in February and March 2021 (Mann-Whitney U, $U = 164.000, p < 0.0001$, Figure 2.2.2A) with an average of 22.4 ± 1.1 °C (one standard deviation) than in the wet period in June and September 2020 with an average of 23.7 ± 0.7 °C. Variations in SM across successional stages was observed across periods. During the dry period, SM in OF and IF was significantly higher than that in YF (one-way ANOVA, $F = 21.25, p < 0.0001$) whereas in the wet period SM in IF was the highest (one-way ANOVA, $F = 14.31, p < 0.0001$). Overall, SM was significantly higher (independent t-test, $t = -3.656, p < 0.005$, Figure 2.2.2B) in the dry period (average 0.18 ± 0.04) than in the wet period (average 0.15 ± 0.03). OM content was significantly higher in IF compared to the other stages in the wet (Kruskal-Wallis, $H = 28.125, p < 0.0001$, Figure 2.2.2C) and the dry period (Kruskal-Wallis, $H = 17.843, p < 0.0001$, Figure 2.2.2C). For each forest stage, average OM content showed temporal variation in OF and YF, with higher values in the dry period (Mann-Whitney U, $U = 132.000, p < 0.0001$ and $U = 108.00, p < 0.05$ for OF and YF, respectively) while OM in IF was similar across periods ($p = 0.843$). Finally, in the wet period, SR in YF was significantly lower than in other stages (Kruskal-Wallis, $H = 10.572, p = 0.005$). In the dry period, SR in YF did not differ from the older stages but SR in OF was significantly lower than that in IF (one-way ANOVA, $F = 5.053, p = 0.012$, Figure 2.2.2D). SR was significantly higher in the wet period than in the dry period in all stages (Mann-Whitney U, $U = 245.000, p < 0.0001$, Figure 2.2.2D). Overall, SR and its driving factors varied differently across forest stages and periods of data collection.

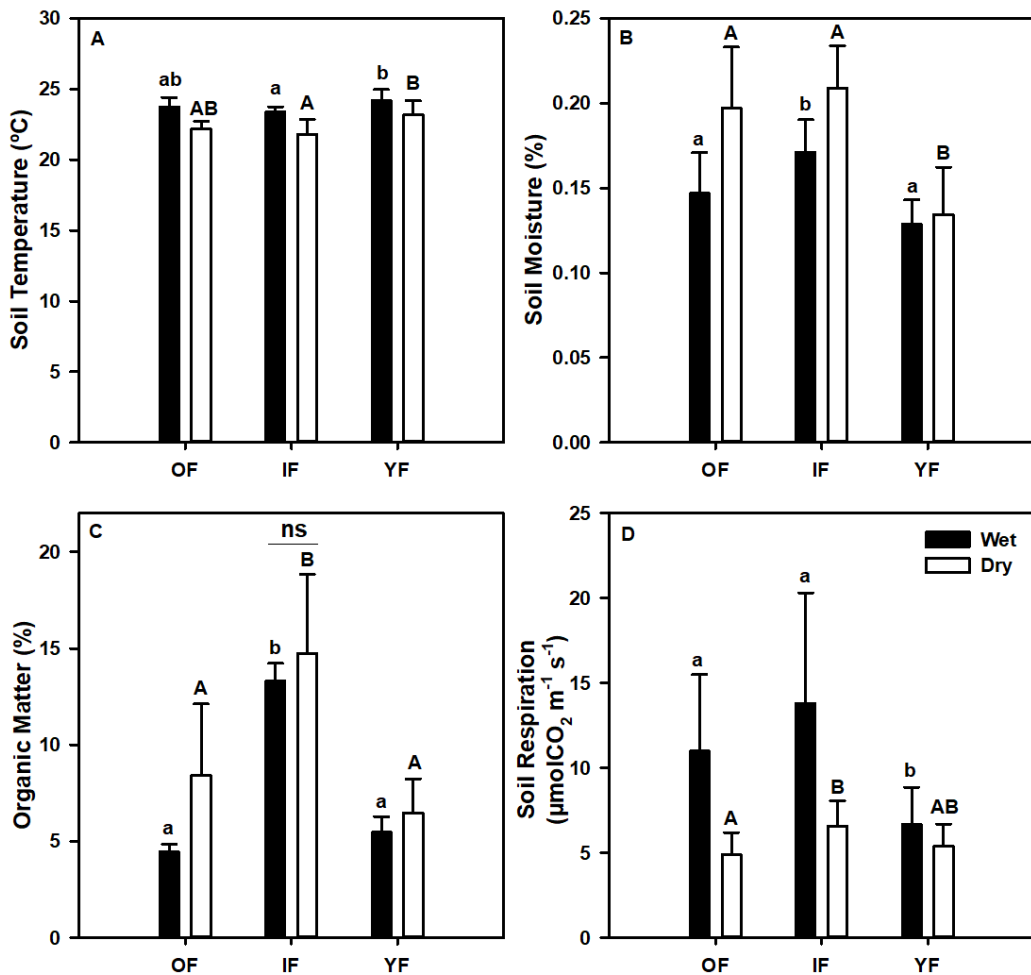


Figure 2.2.2 Mean values of the study variables including (A) soil temperature (°C), (B) soil moisture, (C) soil organic matter (%) and (D) soil respiration ($\mu\text{molCO}_2 \text{ m}^{-2} \text{ s}^{-1}$) measured in the wet (filled bars) and the dry (open bars) periods in the old-growth (OF), intermediate (IF) and young (YF) forest. Error bars indicate one standard deviation. Different small (capital) letters denote statistical differences among sites during the wet (dry) period at 5% significance level from Tukey post hoc test or pairwise comparisons. All values significantly differed between periods, except the organic matter content in IF as indicated by ‘ns’ or ‘not significant’ in (C).

Next, we analyzed the relationships between SR and its driving factors including ST, SM and OM. Considering each successional stage with data from both periods, SR in OF exponentially increased with ST ($p = 0.0007$, Figure 2.2.3A) whereas SR in IF and YF did not respond to changes in ST ($p \geq 0.05$, Figure 2.2.3B, C). Regardless of forest stages, SR did not respond to ST ($p = 0.07$, Figure 2.2.3D).

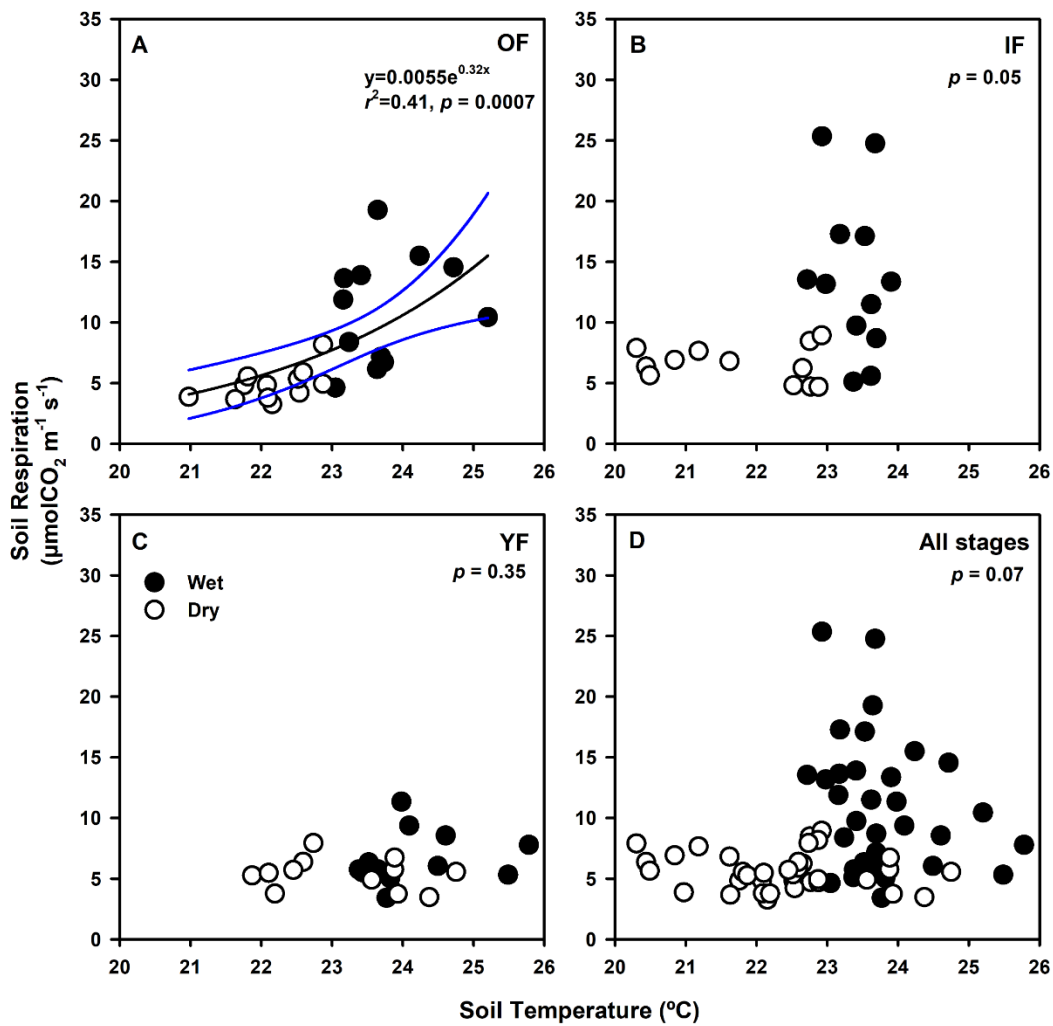


Figure 2.2.3 Relationships between soil respiration ($\mu\text{molCO}_2 \text{ m}^{-2} \text{ s}^{-1}$) and soil temperature ($^{\circ}\text{C}$) in the (A) old-growth (OF), (B) intermediate (IF), (C) young (YF) forest and (D) all forest stages. Closed (open) circles represent data from the wet (dry) period. Results from regression analysis for data combined across periods are shown accordingly. Black solid line indicates the significant regression result with 95% confidence intervals shown as blue lines. The significance level for the regression analysis was 0.05.

Considering the relationships between SR and SM separately for each forest stage and period, no patterns were observed ($p \geq 0.17$, Figure 2.2.4A–C). However, across forest stages, SR linearly increased with SM in the wet period ($p = 0.0023$), while no such response was observed in the dry period ($p = 0.87$, Figure 2.2.4D).

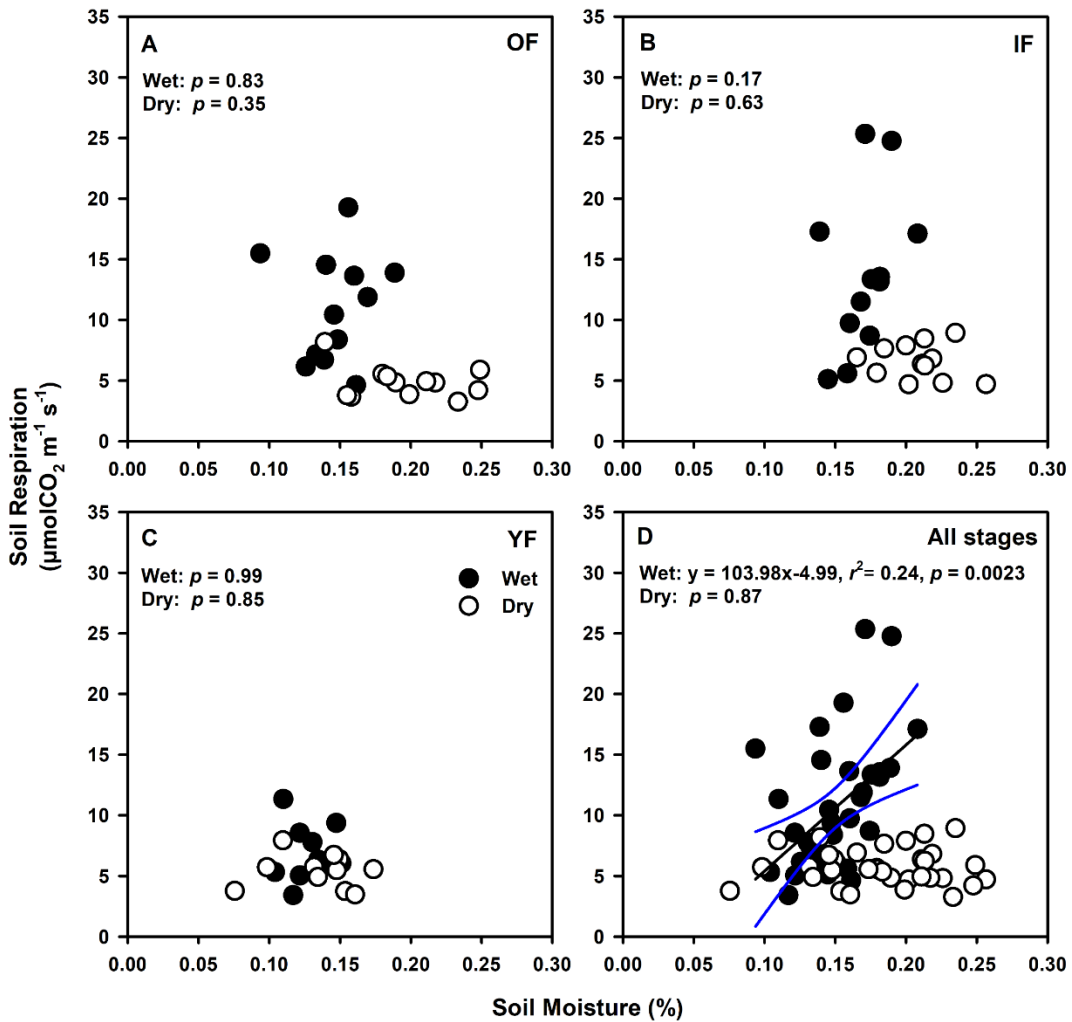


Figure 2.2.4 Relationships between soil respiration ($\mu\text{molCO}_2 \text{ m}^{-2} \text{ s}^{-1}$) and soil moisture in the (A) old-growth (OF), (B) intermediate (IF), (C) young (YF) forest and (D) all forest stages. Closed (open) circles represent data from the wet (dry) period. Results from regression analysis for data combined across periods are shown accordingly. Black solid line indicates a significant regression result with 95% confidence intervals shown as blue lines. The significance level for the regression analysis was 0.05.

Across all forest succession and periods, SR linearly increased with OM, with stronger increasing rate in the wet period ($p \leq 0.022$, Figure 5D). When analyzing the relationships separately by site, the response patterns were retained only in the dry period and in OF and IF ($p \leq 0.026$, Figure 5A, B) while no responses were observed in YF ($p \geq 0.60$, Figure 5C)

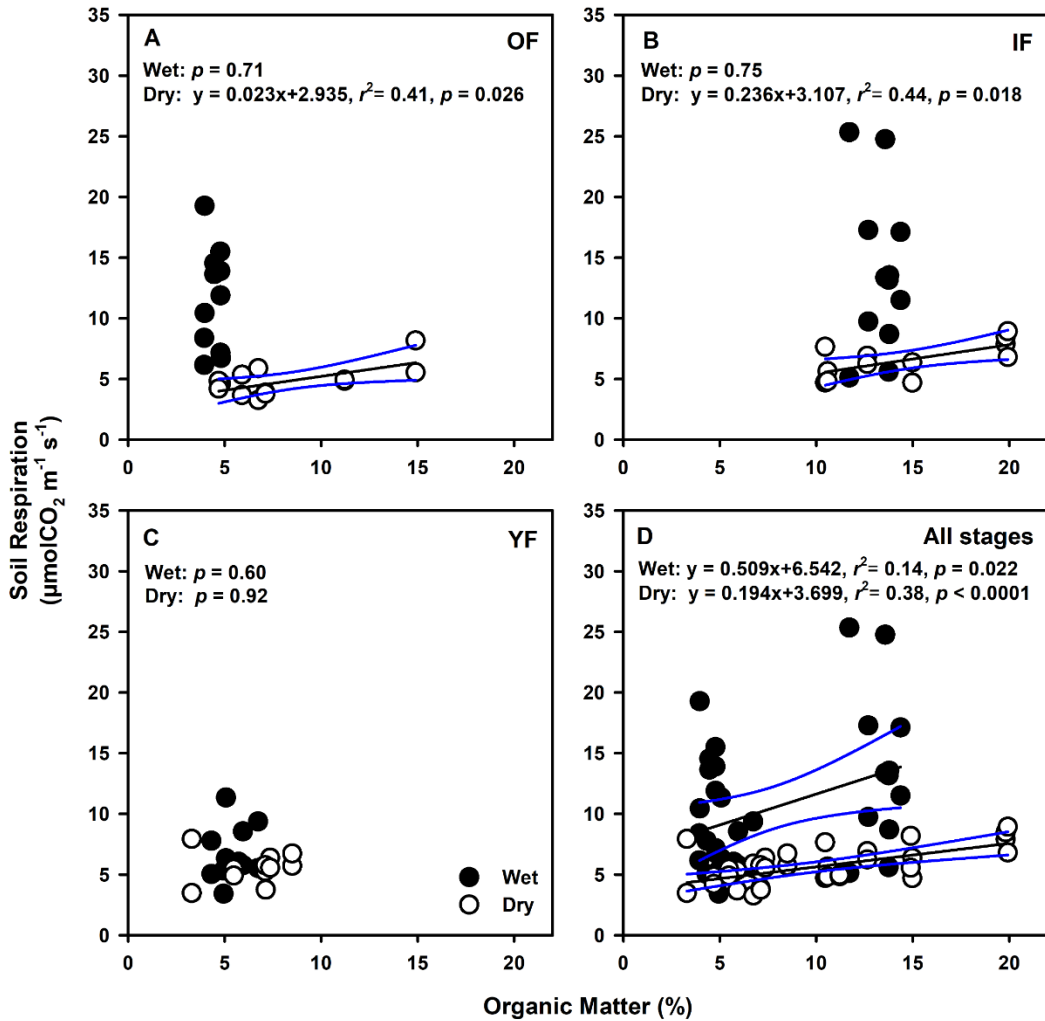


Figure 2.2.5 Relationships between soil respiration ($\mu\text{molCO}_2 \text{ m}^{-2} \text{ s}^{-1}$) and soil organic matter (%) in the (A) old-growth (OF), (B) intermediate (IF), (C) young (YF) forest and (D) all forest stages. Closed (open) circles represent data from the wet (dry) period. Results from regression analysis for data combined across periods are shown accordingly. Black solid line indicates the significant regression result with 95% confidence intervals shown as blue lines. The significance level for the regression analysis was 0.05.

2.2.4 Discussion

Comparison of SR from our study sites with reports from other forests in Southeast Asia

We summarized the SR values from previous studies in forests of Southeast Asia in Table 2.2.2. Our results could not be directly compared to any of these studies because it was unclear if any of these studies was conducted in similar seasonal evergreen forest. However, our SR values were within the ranges of those found in other Thai forests of various phenology, including dry evergreen forests (Adachi et al., 2009; Boonriam et al., 2021), dry dipterocarp forests (Hanpattanakit et al., 2015; Intanil et al., 2018), an evergreen forest (Hashimoto et al., 2004), a teak plantation (Kume et al., 2013), and a mixed deciduous forest (Takahashi et al., 2011). The SR values of our forests were also within the range of those from a lowland mixed dipterocarp forest in Malaysia (Ohashi et al., 2007; Katayama et al., 2009) while they were

generally higher than those from forests at Pasoh, peninsular Malaysia (Adachi et al., 2005; Kosugi et al., 2007). Overall, it is evident that SR rates in Southeast Asian forests are highly variable and site-specific.

Table 2.2.2 Literature survey of soil respiration in Southeast Asian tropical forests including this study. Values are shown as ranges. MAT and MAP stand for mean annual temperature in °C and mean annual precipitation in mm, respectively.

Location	Vegetation type	Dominant tree species	MAT (°C)	MAP (mm)	Soil respiration ($\mu\text{molCO}_2 \text{ m}^{-2} \text{ s}^{-1}$)	Reference
Pasoh area of Negeri Sembilan, Malaysia (2°5' N, 102°18' E, 75–150 m a.s.l.)	Primary and secondary mixed-dipterocarp forest	Dipterocarp species	27	1,788	Primary forest: 2.78–6.93 Secondary forest: 2.58–6.36	Adachi et al. (2005)
Pasoh Forest Reserve, Malaysia (2°59' N, 102°18' E, 75–150 m a.s.l.)	Lowland mixed-dipterocarp forest	<i>Shorea</i> and <i>Dipterocarpus</i> spp	25.4	1,800	2.5–6.5	Kosugi et al. (2007)
Lambir Hills National Park, Malaysia (4°20' N, 114°02' E, ~200 m a.s.l.)	Lowland mixed-dipterocarp forest	Dipterocarp species	27	2,700	1.3–22.9	Ohashi et al. (2007); Katayama et al. (2009)
Huai Kha Khaeng, Thailand (15°20' N, 99°27' E, 549–638 m a.s.l.)	Dry evergreen forest	Dipterocarp species	23.5	1,242	Wet season: 3.15–9.99 Dry season: 1.24–3.84	Adachi et al. (2009)
Sakaerat Environmental Research Station, Thailand (14°30' N, 101°56' E, ~500 m a.s.l.)	Dry evergreen forest	<i>Hopea ferrea</i> , and <i>Hopea odorata</i>	26.7	1,751	Wet season: 4.3–13.3 Dry season: 1.8–6.8	Boonriam et al. (2021)
Ratchaburi Province, Thailand	Dry dipterocarp forest	<i>Dipterocarpus intricatus</i> , <i>Dipterocarpus obtusifolius</i> ,	30.4	1,253	Wet season: 1.89–3.79 Dry season: 0.95–2.84	Hanpattanakit et al. (2015)

Location	Vegetation type	Dominant tree species	MAT (°C)	MAP (mm)	Soil respiration ($\mu\text{molCO}_2 \text{ m}^{-2} \text{ s}^{-1}$)	Reference
(35° 13.3' N, 99° 30' 3.9" E, 110 m a.s.l.)		<i>Dipterocarpus tuberculatus</i> , <i>Shorea obtusa</i> , and <i>Shorea siamensis</i>				
Kog-Ma Experimental Watershed of Kasetsart University, Thailand (18°48' N, 98°54' E, ~1,300 m a.s.l.)	Evergreen forest	<i>Castanopsis</i> , <i>Lithocarpus</i> , and <i>Quercus</i> spp	20	2,084	2.13–14.07	Hashimoto et al. (2004)
Phayao Province, Thailand (19°02'14.38" N, 99°54'10.96" E, 512 m a.s.l.)	Dry dipterocarp forest	<i>Dipterocarpus obtusifolius</i> , <i>Dipterocarpus tuberculatus</i> , <i>Shorea obtusa</i> , and <i>Shorea siamensis</i>	25.1	936	0.77–1.13	Intanil et al. (2018)
Teak stand in Mae Moh plantation, Lampang Province, Thailand (18°25' N, 99°43' E, 380 m a.s.l.)	Teak plantations	Teak	25.8	1,284	0.96–5.02	Kume et al. (2013)
Mae Klong Watershed Research Station, Kanchanaburi province, Thailand (14°35' N, 98°52' E, 100-900 m a.s.l.)	Mixed deciduous forest	<i>Shorea siamensis</i> , <i>Vitex peduncularis</i> , <i>Dillenia parviflora</i> var. <i>Keruui</i> , and <i>Xylia xylocarpa</i> var. <i>Keruui</i>	25	1,650	Wet season; ridge: 4.00–8.25 upper slope: 5.17–6.89 lower slope: 4.20–9.97 Dry season; ridge: 1.33–4.42 upper slope: 2.18–5.67 lower slope: 2.50–8.09	Takahashi et al. (2011)
Khao Yai National Park, Thailand (14°26' N, 101°22' E)	Primary and secondary seasonal evergreen forest	Old-growth forest <i>Dipterocarpus gracilis</i> , <i>Sloanea sigun</i> , <i>Ilex chevalieri</i> ,	22.4	2,100	Wet period; Old-growth forest: 6.51–15.49 Intermediate forest: 7.28–20.32	This study

Location	Vegetation type	Dominant tree species	MAT (°C)	MAP (mm)	Soil respiration ($\mu\text{molCO}_2 \text{ m}^{-2} \text{ s}^{-1}$)	Reference
700–800 m a.s.l.)		<p><i>Symplocos cochinchinensis</i>, <i>Schima wallichii</i></p> <p>Intermediate forest <i>Schima wallichii</i>, <i>Machilus gamblei</i>, <i>Eurya acuminata</i>, <i>Symplocos cochinchinensis</i>, <i>Syzygium nervosum</i></p> <p>Young forest <i>Cratoxylum cochinchinense</i>, <i>Syzygium antisepticum</i>, <i>Adinandra integrifolia</i>, <i>Syzygium nervosum</i>, <i>Symplocos cochinchinensis</i></p>			<p>Young forest: 4.50–8.86</p> <p>Dry period; Old-growth forest: 3.55–6.19</p> <p>Intermediate forest: 5.13–8.05</p> <p>Young forest: 4.09–6.69</p>	

Spatial variations in SR and the environmental factors across forest succession

Soil temperature showed spatial variation in both periods with higher values in the young forest than in the intermediate stage, although it was similar to that in the old-growth forest. The higher ST in the young forest may be associated with its sparse canopy compared to the more closed canopy in the intermediate forest as observed in our sites. The observations agreed with findings of higher ST in a Panamanian tropical forest with large forest gaps due to the direct heat from sunlight reaching the soil surface (Marthews et al., 2008). Our results showed that the differences in SM across forest stages varied temporally. In the dry period, soil moisture in YF was significantly lower than in the older stages. However, in the wet period, IF had higher SM than the other sites. Again, canopy development may contribute to such variation because the canopy of YF was very sparse while that of IF and OF was denser. Differing canopy density can affect the amount of light penetrating to the soil surface and litterfall input to the soil, influencing surface evaporation and thus soil moisture. Overall, organic matter in the intermediate forest, with its high canopy density, was consistently higher in both periods than in the other sites. This may be explained by the high litterfall production in IF compared to the other two forests in our study (averaging 1.65, 2.08, 1.04 $\text{g m}^{-2} \text{ day}^{-1}$ in OF, IF, and YF, respectively, across wet and dry seasons; unpublished data), although other factors, such as decomposition rate, need to be considered to verify this claim. While SR was generally similar in the older stages (OF and IF), it was significantly lowest in the young forest. This result agrees

with previous studies indicating increasing soil respiration with forest age (Yan 2006, 2009; Luo et al., 2012). Because soil carbon, which is highly correlated with soil organic matter, and soil moisture have been found to significantly explain variations in SR (La Scala et al., 2000; Stoyan et al., 2000), low materials for decomposition and consumption by the microbial community, and low soil moisture, may contribute to the low SR in YF. Additionally, variation of root biomass may affect the difference in SR across forest stages, as related to total below-ground carbon flux (TBCF; Litton and Giardina, 2008; Katayama et al., 2009). In fact, based on our preliminary measurements of fine root production in the older forests, we found that IF had higher fine root production than OF across both wet and dry periods ($0.57 \text{ g m}^{-2} \text{ day}^{-1}$ in IF versus $0.50 \text{ g m}^{-2} \text{ day}^{-1}$ in OF), which was consistent with the higher SR in IF than in OF (Figure 2.2.2D).

Temporal variations in SR and the environmental factors between the wet and the dry period

Regardless of forest stage, ST was lower, and SM was higher in the dry period than in the wet period, which may correspond to the cool dry season in this region. In addition, this may be attributed to low surface evaporation being blocked by the thick litter layer on the forest floor as observed through high monthly litterfall production in the dry season of the same study sites (averaged $2.07 \text{ and } 1.10 \text{ g m}^{-2} \text{ day}^{-1}$ in the dry and the wet season, respectively, unpublished data). The low surface evaporation may be consistent with lower evapotranspiration during the (cool) dry season than in the wet season over the Chi and Mun river basins, where our site is located, as estimated from a process-based model using satellite data from 2001 to 2015 (Zheng et al., 2019). Also, high litterfall production may have facilitated the retention of soil moisture because the increased volume of litter increased the time for soil drying or becoming saturated (Ogée and Brunet, 2002). Similarly, soil OM was generally higher in the dry period across forest succession, which may be associated with the higher litterfall in these sites during the dry season. In all forest stages, SR was significantly higher in the wet than in the dry period which is consistent with previous studies on soil respiration in various forests in Thailand (Hashimoto et al., 2004; Adachi et al., 2009; Takahashi et al., 2011; Kume et al., 2013; Boonriam et al., 2021).

The influence of environmental factors on SR

To gain insight into what factors play important roles in SR variation in these forests, we investigated the relationships between SR and the main drivers including ST, SM, and soil OM. Our results showed that ST and SM differently contributed to SR among forest stages and temporally, which was likely due to the inherent canopy and site characteristics of each stage. Overall, SR in our forests did not show a clear response to ST across both periods (Figure 3D). However, the general exponential relationship between SR and ST was significant only in the old-growth, undisturbed forest (Lang et al., 2017). Because canopy gaps were unequally dispersed in OF while those in IF and YF were more uniform, the range of ST was larger in OF across the wet and the dry period, possibly allowing high and significant variation of SR with ST (Figure 2.2.3A). In terms of soil moisture, SR of all forest stages increased with SM significantly only in the wet period (Figure 2.2.4D). This result indicated that low available soil moisture in the warm wet period constrained SR and thus was important for controlling microbial activity in these forests. In temperate and boreal forests, soil temperature has been identified as the major driver for soil respiration (Hursh et al., 2017). In fact, most models for

soil CO₂ efflux from these forests are empirical functions of soil temperature (Sugasti and Pinzón, 2020). In tropical regions, however, mixed results have been reported. Soil respiration of tropical forests is affected by both ST and SM in some sites (Sotta et al., 2006; Ohashi et al., 2008; Boonriam et al., 2021), only affected by ST in both primary and secondary sites of tropical montane forests in China (Zhou et al., 2013), and by only SM in various forests in Thailand (Hashimoto et al., 2004; Kosugi et al., 2007; Adachi et al., 2005, 2009; Takahashi et al., 2011). Another study has suggested that short-term variation in SR depends on ST, but SM had greater effects on long-term variation in SR in central Amazonian forests (Sotta et al., 2004). Therefore, the contribution of soil temperature and soil moisture to soil respiration rates in global forests varies greatly and is highly site-specific with no clear spatial or temporal variation.

Our data showed significant increases in SR of most forest stages with increasing soil OM, with greater response in the dry period than in the wet period (Figure 2.2.5). Thus, organic matter content in the soil was the main energy source for microbial activity that determined soil CO₂ efflux in the dry period of these forests. As previously mentioned, this period corresponded to high litter addition to the forest floor which may stimulate soil microbial activity as shown in greater soil CO₂ release (Bréchet et al., 2017; Sayer et al. 2019, 2020). Large variations in OM were observed across forest stages which may be explained by different quantity and quality of litter input (i.e., litterfall and roots) and different rates of litter decomposition in each stage. Note that the significant regression result for the wet period (Figure 2.2.5D) was mostly due to large differences in OM between IF and the other sites. Therefore, the observed significant pattern in the wet period may not represent the true response of SR to OM.

Overall, our results are still preliminary and suggest that different factors contribute to SR across spatial and temporal variation in our successional forests. In our forests, SM and OM were the limiting factors that significantly explained variation in SR in the wet and in the dry period, respectively, whereas ST might explain variation in SR of the old-growth forest with its non-uniform canopy compared to the younger forest stages. However, due to the limited data, further investigation including more sampling locations and higher frequency is needed to confirm these findings.

2.2.5 Conclusions

We investigated spatial and temporal variations in soil respiration (SR) and its driving factors including soil temperature (ST), soil moisture (SM), and organic matter content (OM), together with their relationships. Our analyses showed that SR was generally higher in the wet period and in older-stage forests (either primary or secondary). While ST has been identified as one of the main factors influencing SR in temperate and boreal forests, we found no significant relationships between SR and ST in our forests. However, in the old-growth forest where gaps are usually non-uniformly scattered, ST and OM determined SR, and there were variations in response patterns across forest stages and periods. Across the successional forests, SM was the determining factor of SR in the wet period while OM significantly explained SR variations in the dry period. Overall, the responses of SR to environmental factors were different across successional forests and data collection periods. Our results suggest the incorporation of

different responses in successional forests and site-specific information in modeling soil respiration of tropical forests. Nevertheless, detailed investigations involving long-term and high frequency measurements and sampling locations should be performed to confirm these results.

#####

Note: This work was published. Please refer to the publication in the Appendix.

2.3 Sap flow measurement

Sap flux density is the amount of water flow in tree's stem per unit sapwood area per time. It is the main parameter that we will use for scaling up to canopy water and carbon fluxes (i.e. canopy transpiration and canopy photosynthesis or GPP, respectively). We constructed sensors for sap flux measurement based on the thermal dissipation design (Granier 1987). We set up two systems of sap flux measurements in the old-growth (OF) and the young (YF) forest in Khao Yai National Park because these sites have the flux towers that can supply continuous electrical power to the datalogger used to collect sap flux data. For each site, we designed the sampling scheme for trees that will be used for the measurement as follows. Because the sap flux data will be used to scale up the entire forest canopy in the site, we need to consider the size distribution of each forest and sample trees covering the range of size distribution. Within each site, a plot of approximately 25 m radius around the respective tower is selected for sap flux measurement. The 25-m radius plot is based on the maximum acceptable distance between the measured trees and the datalogger for the sap flux measurements. In the 25 m plot, we select 2 trees from each size class to install sap flux sensors on. Data from these sap flux trees can be scaled up to the canopy scale using various scaling approaches, such as using basal area or leaf area index distribution of the forest, depending on the availability of canopy-scale data. In addition to collecting sap flux data, we installed some meteorological sensors, including air temperature and relative humidity, quantum sensor, wind speed and direction, and rain gauge above the canopy or where gaps are. All weather sensors, including those measuring sap flux, are connected to the same data logger which collects the 30-minute average values. Figure 2.3.1 shows the field campaign for the sap flux measurement set up during 12-13 September 2020. Currently, both systems have collected data since September 2020 for YF and since December 2020 for OF. The selected trees for sap flux measurements and corresponding sizes, expressed as diameter at breast height, are listed in Table 2.3.1.

Table 2.3.1 Selected tree species in the sap flux plots. DBH refers to diameter at breast height in cm.

Plot	Species	DBH (cm)
Mo Singto 1 (OF)	<i>Altingia excelsa</i>	21.2
	<i>Cinnamomum subavenium</i>	33
	<i>Eugenia syzygioides</i>	13, 47
	<i>Eugenia grata</i>	24.5
	<i>Nephelium melliferum</i>	32
	<i>Aquilaria crassna</i>	8, 11.1, 15, 53
Nong Khing (YF)	<i>Adinandra integerrima</i>	5.3, 6.5, 11, 11.3, 13.7
	<i>Cratoxylum cochinchinensis</i>	8.2
	<i>Eugenia grata</i>	17.8, 18.7, 22.4, 24.8
	<i>Eugenia cerasoides</i>	6, 11.9



Figure 2.3.1 A field campaign for installations of sap flux sensors during 12-13 September 2020 at the Mo Singto 1 and Nong Khing sites, the old-growth and the young forests, where a 50m and 20m tower was established in.

To scale up sap flux data to canopy transpiration, we need information about sapwood area which is the area in stem that transport water. This information is typically difficult to access because the most direct method to determine sapwood areas is to cut trees and it is usually not allowed. Therefore, we conducted a study to develop allometric equations for estimating sapwood area of the dominant species within each sap flux site. First, we focus on dominant species within each site based on the basal area ranking and the availability of trees outside the study plots. We took some tree core samples from the trees outside the already established study plots and measured sapwood depth using chemical stains. This study culminated in a publication (Yaemphum et al., 2021, accepted). We will then apply the allometric equations to estimate the sapwood areas of the entire study plots and calculate canopy transpiration for each site, in combination with the sap flux data.

For this reporting period, we utilized the sap flux density data to explore the performance of a Bayesian modeling framework called State-Space Canopy Conductance (StaCC) model (Bell et al., 2015). The StaCC model was developed to overcome limitations for scaling up the point measurements of sap flux density to tree and canopy level in some pine and broadleaved species in temperate forests. The limitations include lacking the considerations of time constant of water flow in stems which may contribute to the nighttime transpiration and the gapfilling of data by simple interpolations. Because the StaCC model has never been parameterized with data from tropical species. We tested the model using the sap flux density data that were previously measured in potted trees of some tropical species,

including *Pterocarpus indicus*, *Lagerstroemia speciosa*, and *Swietenia macrophylla* across wet and dry seasons in 2017-2018. Specifically, we used the model to estimate whole-tree canopy conductance and transpiration. The modeled results were validated using the measured values, resulting in high R^2 (0.76-0.91). Overall, we successfully parameterized the model in tropical species and therefore are planning to use this model to estimate canopy conductance of our study sites where sap flux data are being monitored (OF and YF). The estimated canopy conductance represents the linkage between water loss and carbon dioxide absorption by forests and its variation with environmental factors would imply the responses of the forests to climate variability. Results from the parameterization of StaCC model in tropical species was published in January 2021 (Andriyas et al., 2021).

Here, we present some preliminary results of canopy conductance and transpiration estimated from the StaCC model using the sap flux density data from the OF and YF sites. Figure 2.3.2 shows temporal profiles of daily averaged canopy conductance and leaf transpiration (canopy transpiration per unit leaf area) for the old-growth (OF) and the young (YF) forest during parts of the dry and the wet season in 2020-2021. Note that YF had longer data that covered parts of the wet season in 2020. We also examined diurnal patterns of these parameters as shown in Figure 2.3.3. Overall, the results indicated that the young forest had higher canopy conductance and leaf transpiration throughout both seasons which may imply that the young forest is more active than the old-growth forest by allowing faster water and carbon transports through stomata. Further investigations on the responses to the environmental factors are being performed and will be summarized in a manuscript for publication in the future.

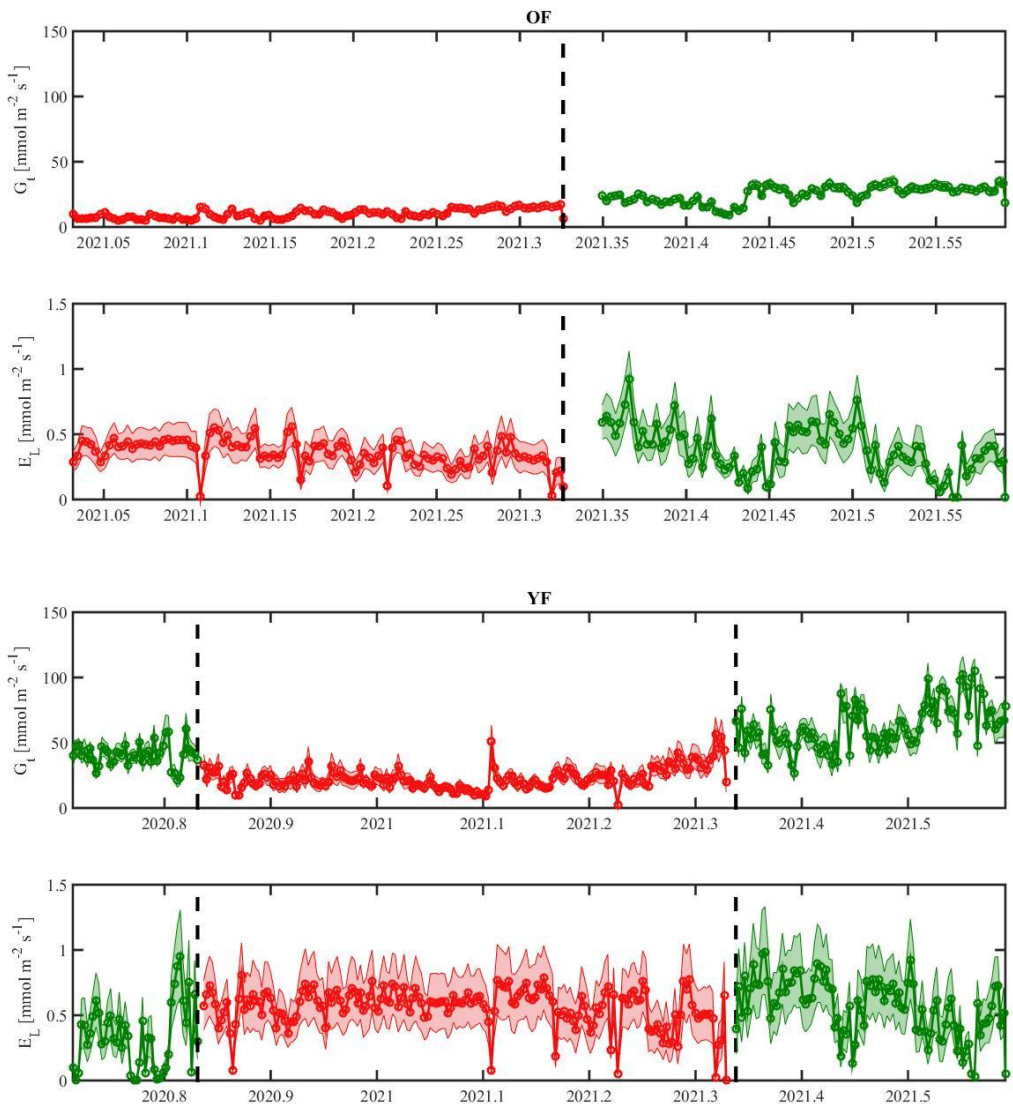


Figure 2.3.2 Estimated daily averaged canopy conductance and transpiration, G_t and E_L , for each forest type and for wet (green) and dry (red) season. The only vertical dash line in OF and the second vertical dash line in YF indicates the ending of the dry season (DOY 305 or 30th April 2021) while the first vertical dash line in YF ending of the first wet spell (31st October 2020). The shaded regions represent the 95% confidence intervals.

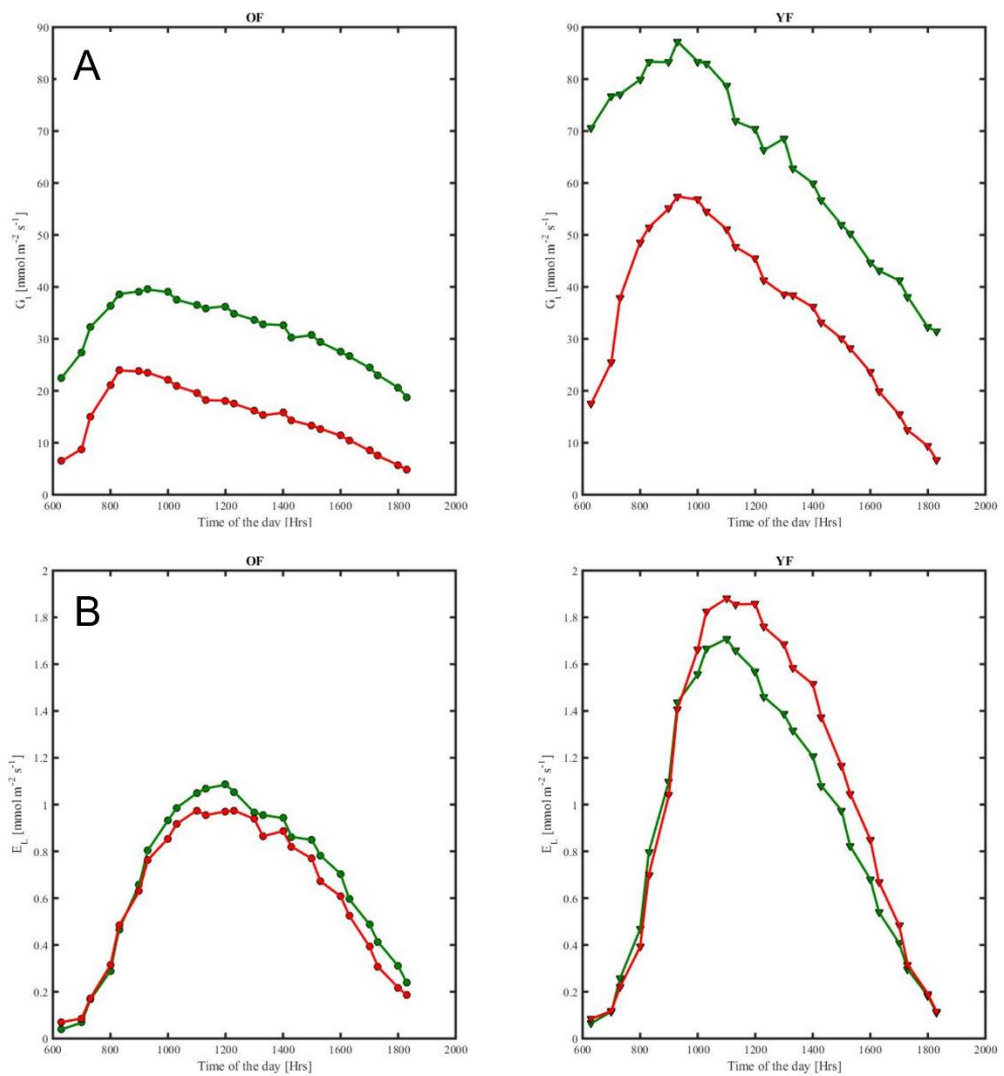


Figure 2.3.3 Variations in A) G_t , and B) E_L (averaged over 6 AM to 6 PM local time) during the dry and wet season with the columns corresponding to the two forest types and seasons plotted in green (wet) and red (dry).

2.4 Litterfall dynamics

Litterfall dynamics was investigated by using the litter trap method over two years (October 2019 – October 2021). Total 20 litter traps were installed at each study site which was classified into the different stages of forest development including the old-growth forest (OF), intermediate secondary forest (IF), and early stage of secondary forest (YF). The litterfall was collected once a month and oven-dried at 70 °C until having constant weight. Then the samples were weighed separately into the categories of leaf, branch, and reproductive parts.

2.4.1 Litterfall production

During 28-29 September 2019, we installed litter traps for litterfall collection to study the litterfall production in all three sites in Thailand (Figure 2.4.1). Then, we collected litterfall that is trapped by these litter traps once a month. For each collection, the litterfall is oven dried at 70 °C until constant weight is reached. Then, the dry samples are then separated into leaf, branch, and fruits/flowers, and are weighed accordingly as dry mass. We started the collection in October 2019 and continued for two full years.

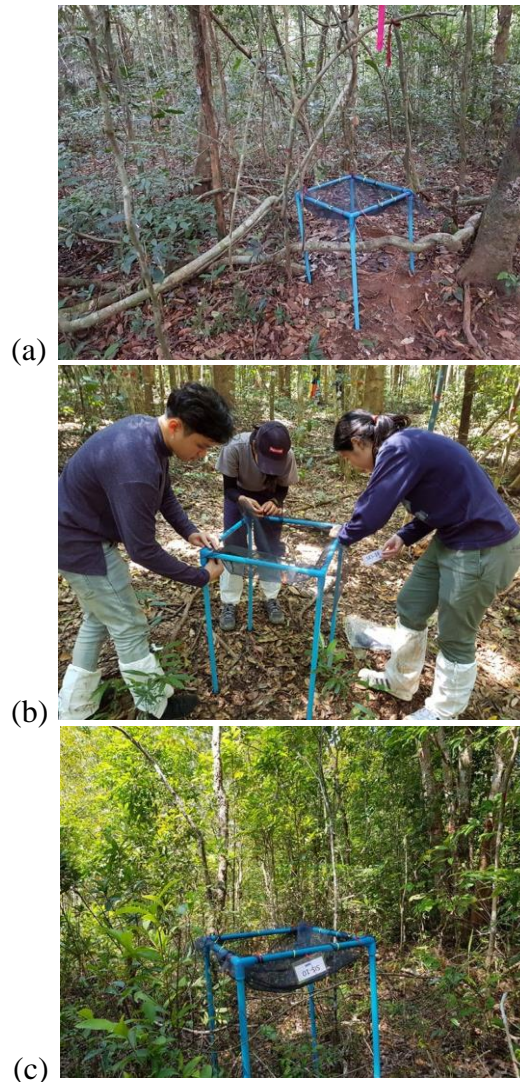


Figure 2.4.1 Installation of litter traps in the old-growth forest (OF) (a), intermediate forest (IF) (b) and young forest (YF) (c) sites.

Litter production rate during October 2019 to October 2021 showed a seasonal pattern that litterfall was higher in the dry season compared to those of the wet season (Independent samples t-test, $p < 0.05$, Table 2.4.1). In December 2019, litterfall reached a peak in every stage of forest development with the values of 3.58 , 4.70 , $2.36 \text{ g m}^{-2} \text{ day}^{-1}$ in the old-growth forest (OF), intermediate forest (IF), and young forest (YF), respectively. The low litter production followed the trend of low precipitation during the dry season. The rainfall in the late wet season was 3.74 mm/day in October 2019 then dramatically decreased to 0.18 mm/day in November 2019 and remained low in the dry season with the values of 0.03 and 0.00 mm/day in December 2019 and January 2020, respectively. Therefore, the changing pattern of precipitation under the global climate change might affect forest productivity at this study site, for example, lower productivity of litterfall in the drought year and shifting pattern of litterfall seasonality

Table 2.4.1 Average litter production rates in the wet and the dry seasons across different successional stages with statistical values tested by independent sample t-test.

Stages	Litter production ($\text{g/m}^2/\text{day}$) \pm SE		t-value	P
	Wet season	Dry season		
OF	1.56 ± 0.14	2.15 ± 0.18	-2.574	0.016
IF	1.27 ± 0.16	2.71 ± 0.27	-4.814	<0.001
YF	0.89 ± 0.11	1.72 ± 0.11	-5.361	<0.001

Regardless of the seasons, litter production significantly differed among the three successional stages (one-way ANOVA, $F = 5.027$, $p = 0.009$, Figure 2.4.2). The YF had significantly lower litter production than that of the OF and IF. However, litter production in the old-growth forest (OF) did not show the difference from that of the secondary forest in the intermediate stage (IF). This implies the importance of secondary forest in a global carbon cycle especially the stem exclusion stage or the intermediate stage that has high productivity, in terms of litterfall, which is almost similar to the old-growth forest.

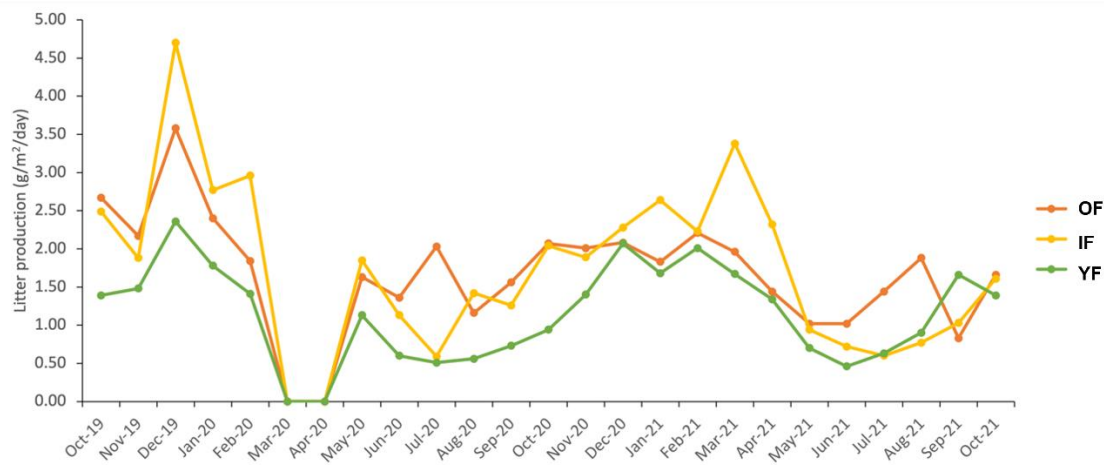


Figure 2.4.2 Rates of litter production in the three successional stages of tropical forests at Khao Yai National Park, the data was collected from October 2019 to October 2021 (the data of March and April 2020 was absent due to the park closure under the COVID-19 situation).

2.4.2 Leaf litter decomposition

The litter bags, which contain leaf litter from the study sites, were installed to determine decomposition rate of the litterfall during the wet and dry seasons (Figure 2.4.3). Five litter bags and one control bag, which contains filter papers, per site were installed. At 6, 14, 21, 28, 42 and 56 days after the installation (the wet season period covers 8 September – 3 November 2019 and the dry season period was from 8 December 2019 – 1 February 2020), we collected one litter bag and a control, cleaned all the soils from the bags and dry them in an oven at 70 °C until constant weight is reached. Then, we weighed the leaf litter that is left in the bag and use the values to determine the coefficient of decomposition (k) from the exponential function, written as

$$y = 100e^{-kx} \quad (2.4.1)$$

where y is the dry weight of leaf litter that is left in the bag, expressed as percentage of the initial weight, k is the coefficient of decomposition (day^{-1}) and x is time after the installation of litter bags (day).



Figure 2.4.3 Litter bags that were installed in the same sites as litterfall production study

The results indicate that, in the wet season, the dry mass of leaf litter in the bags in all sites continuously decreased after the installation (Figure 2.4.4). The k values in the wet season for the old-growth forest (OF), intermediate forest (IF) and young forest (YF) are 0.013, 0.016 and 0.022, respectively. The remaining mass of litter in the dry season reduced during the first five days of experiment and slightly decreased after ten days (Figure 2.4.4b). The k values in the dry season are lower compared to those of the wet season with the values of 0.003 (OF), 0.003 (IF) and 0.002 (YF). The different decomposition rates between the wet and dry seasons implied that the seasonality and climates play the important role determining the processes of carbon and nutrient fluxes via litter decomposition in this forest.

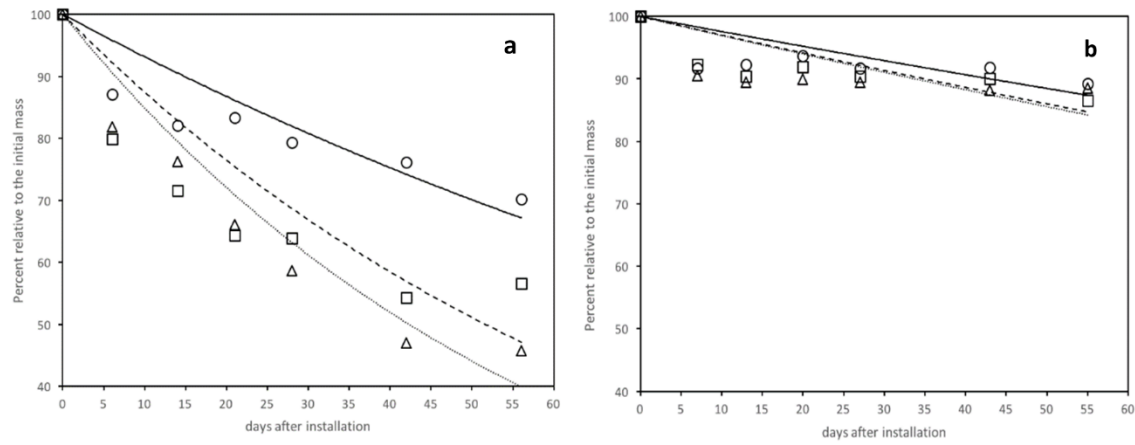


Figure 2.4.4 Average decomposition rate of litterfall in the Thai forests in the wet (a) and dry season (b). The wet season study period was from 8 September – 3 November 2019 and the dry season period was from 8 December 2019 – 1 February 2020. Symbols represent data points for OF (□), IF (△), and YF (○) while lines show the regression in the form of exponential function for OF (----), IF (···), and YF (—). OF, IF, and YF denote the old-growth forest, intermediate forest, and young forest, respectively.

2.5 Tree hydraulics

Midday leaf water potential (Ψ_{leaf}), which is one of the tree hydraulic parameters studied in this research, was measured using a pressure chamber (PMS instrument, Albany, OR). To minimize the variation of studied trees exposing to sunlight, the duration of measurement was set from 10.00-14.00 on rain-free days in both dry and wet seasons. This measurement was done on three mature and fully expanded sunlit leaves, which were randomly selected from the same trees used for gas exchange measurement. The differences in midday leaf water potential among different tree species in each plot and the species found in multiple sites were compared using one-way ANOVA analysis and T-test. All analyses were performed using R (version 3.5.2) and graphs were created from SigmaPlot (Systat Software, Inc., San Jose, California, USA).

Plant water status can be designated by Ψ_{leaf} , which always has a negative value. Trees with low Ψ_{leaf} values (more negative) could be implied that they are experiencing water stress from either insufficient soil water availability, or high atmospheric evaporative demand. Based on the preliminary results, Ψ_{leaf} was observed to be lower in drier environments. The species existing in drier environment had lower Ψ_{leaf} values in comparison to those occurred in wetter environment. From Figure 2.5.1, trees growing in YF had lower average Ψ_{leaf} values compared to trees in OF or IF ($P<0.0001$), probably because of its drier conditions. This difference was more obvious during dry season. Comparing Ψ_{leaf} for each study site, it was observed that Ψ_{leaf} was significantly lower in dry season than in wet season at all sites ($P<0.0001$).

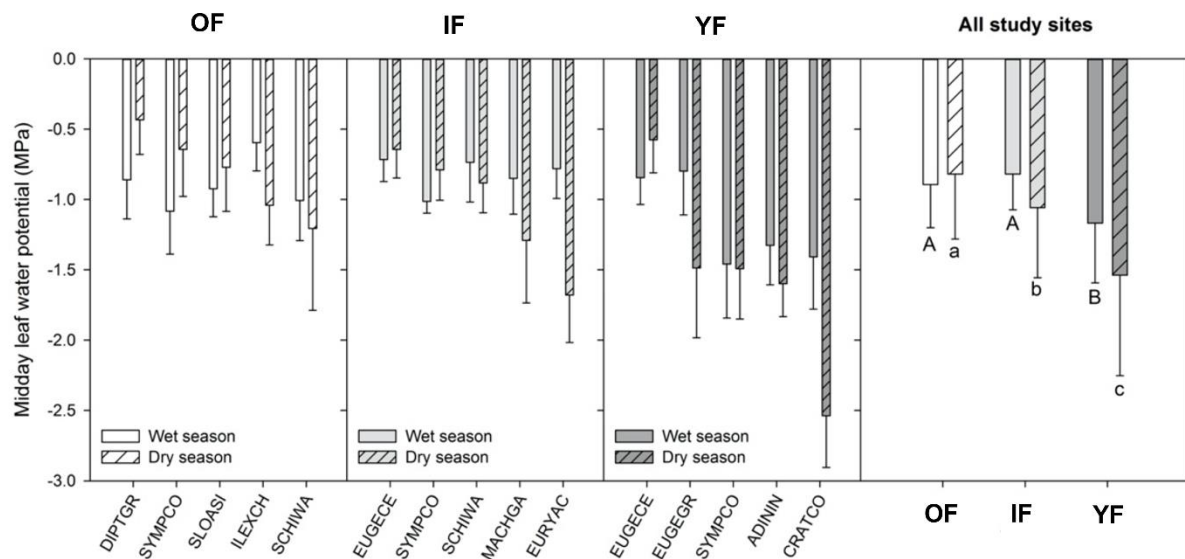


Figure 2.5.1 Midday leaf water potential of dominant tree species in Khao Yai National Park during dry and wet seasons. White, light grey, and dark grey bars represent the dominant tree species found in primary forest (OF), late-secondary forest (IF), and early secondary forest (YF), respectively. Error bars indicate one standard deviation and letters show results of post-hoc analysis with the Tukey's test at $P<0.05$.



Figure 2.5.1 Field measurement of midday leaf water potential at the old-growth forest.

For species found in multiple sites, the difference in Ψ_{leaf} was observed either between sites or between seasons. *S. cochinchinensis* had the lowest Ψ_{leaf} in YF, while this parameter was significantly similar in OF and IF. Comparing between the seasons, Ψ_{leaf} in OF and IF were observed to be significantly different for this species ($P<0.001$) (Figure 2.5.2A). For *S. wallichii*, lower Ψ_{leaf} was found in OF compared to that in IF in both seasons ($P<0.01$). Only in IF that Ψ_{leaf} was affected by seasonal change for this species ($P=0.023$) (Figure 2.5.2B). *E. cerasoides* had lower Ψ_{leaf} in YF during wet season ($P<0.01$); however, there was no difference during dry season in both IF and YF. Ψ_{leaf} of this species had affected by the seasonal variation in both study sites ($P<0.01$) (Figure 2.5.2C).

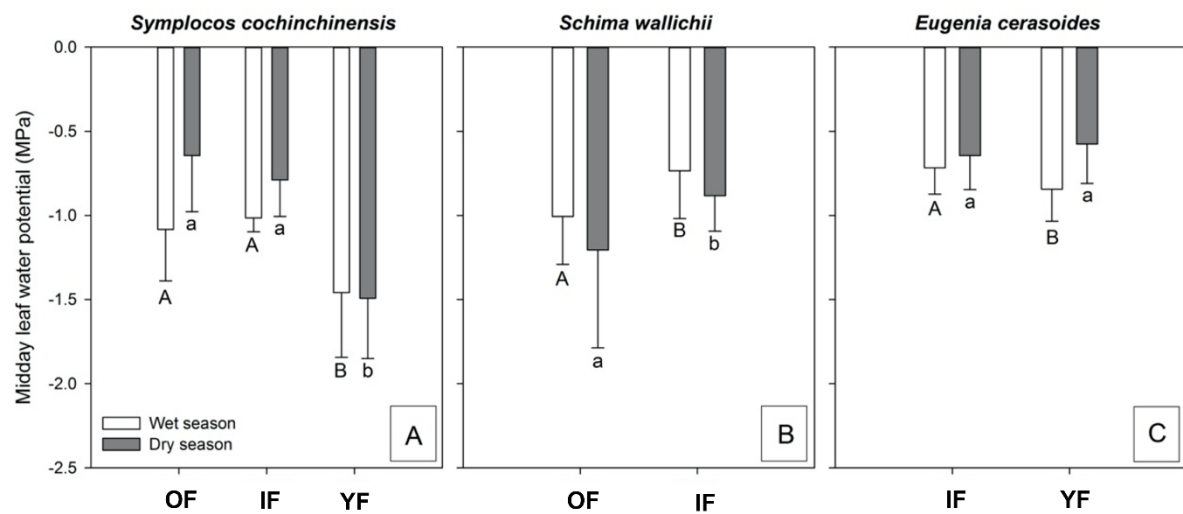


Figure 2.5.2 Midday leaf water potential of the species found in multiple sites in Khao Yai National Park for the dry (white bars) and the wet (dark grey bars) seasons. MST1, MST2 and SIS4 denote old-growth forest (OF), intermediate forest (IF) and young forest (YF), respectively. Error bars indicate one standard deviation and letters show results of (A) post-hoc analysis with the Tukey's test and (B) and (C) T-test at $P<0.05$.

The resistance of a species to cavitation can be described by a vulnerability curve, which shows the percentage loss of hydraulic conductivity (PLC) due to cavitation over a range of xylem pressure. To create a vulnerability curve, air-injection method was performed (Sperry and Saliendra, 1994) on 2-3 roots of dominant tree species collected from topsoil (10-25 cm) in early-secondary forest (YF). The principle of this method is to measure loss of conductivity in plant samples, while cavitation is manually induced by elevated air pressurization using a pressure chamber (PMS instrument, Albany, OR). In this study, the xylem pressure at which 50% conductivity is lost (P_{50}) was used to estimate xylem vulnerability to cavitation since it is a convenient representation of the range of cavitation pressures that has been widely used to compare cavitation resistance among and within species (Anderegg et al., 2016; Johnson et al., 2016; Pérez-Harguindeguy et al., 2016).

Xylem vulnerability to cavitation indicates the risk of hydraulic failure (a failure to transport water from root to tree crowns in plants) during water stress. A species that is

vulnerable to cavitation (having low P_{50}) should be more prone to hydraulic failure due to its lower ability to tolerate high xylem pressure. Considering all species within each forest stage, xylem vulnerability to embolism, represented by the xylem pressure inducing 50% loss of hydraulic conductivity (P_{50}), did not vary across forest successions (one-way ANOVA, $p = 0.123$). At the forest level, xylem vulnerability ranged from potentially more vulnerable in OF (-2.87 ± 0.30 MPa) to less vulnerable in IF (-3.04 ± 0.18 MPa) and in YF (-3.71 ± 0.39 MPa). Sensitivity to embolism was higher in OF (73.70 ± 21.60 % MPa $^{-1}$) than in IF (26.80 ± 1.25 % MPa $^{-1}$) and YF (23.40 ± 1.05 % MPa $^{-1}$). For the species occupying multiple forest stages, vulnerability to xylem embolism was generally comparable across forest successions. *S. cochinchinensis* exhibited similar P_{50} across successions (one-way ANOVA, $p = 0.687$), by having P_{50} of -3.27 ± 0.04 MPa in OF, -3.39 ± 0.03 MPa in IF, and -3.24 ± 0.21 MPa in YF. The same trend was also found in *S. nervosum* (independent sample t -test, $p = 0.762$), by having P_{50} of -2.30 ± 0.17 and -2.24 ± 0.03 MPa in IF and YF, respectively. In contrast, significant difference in P_{50} was found in *S. wallichii* between the two forest successions (independent sample t -test, $p < 0.05$), with 0.45 MPa lower in OF than in IF.

Within each forest successional stage, xylem vulnerability varied greatly among the dominant tree species (one-way ANOVA, $p < 0.05$, Figure 2.5.3). In OF, the lowest P_{50} was found in *I. chevalieri* (-4.17 ± 0.08 MPa, Figure 2.5.3C) whereas the highest P_{50} was found in *D. gracilis* (-0.89 ± 0.01 MPa, Figure 2.5.3A). Slopes of vulnerability curves were comparable across the dominant tree species in OF, except for *D. gracilis* that had the steepest slope than the others. PLC_{dry} differed substantially across species in OF, in which *I. chevalieri* experienced relatively lower impact during the dry season (1.02 %, Figure 2.5.3C) while a greater impact was observed in *S. sigun* (6.45%, Figure 2.5.3B) and *S. wallichii* (7.78%, Figure 2.5.3E). In IF, *E. acuminata* (Figure 2.5.3H) was the most while *S. nervosum* (Figure 2.5.3J) was the least resistant to xylem embolism (-4.01 ± 0.10 MPa and -2.30 ± 0.17 MPa, respectively) compared to other coexisting species. Sensitivity to xylem embolism was higher in *S. cochinchinensis* than the rest of the species in IF. *S. cochinchinensis* in IF also responded less to potentially dry conditions in the dry season by losing relatively small hydraulic conductivity at midday (2.79 %, Figure 2.5.3I) while *M. gamblei* in IF reacted more by further losing the hydraulic conductivity in the dry season (25.77 %, Figure 2.5.3G). In YF, *A. integerrima* (Figure 2.5.3M) displayed the lowest P_{50} value at -5.97 ± 0.06 MPa, with low response to dry conditions as observed from midday PLC_{dry} (1.40 %). *C. cochinchinense* (Figure 2.5.3K), however, had the highest P_{50} (-2.39 ± 0.25 MPa), with the greatest response from losing hydraulic conductivity in the dry season (52.77 %) compared to the other species. The steepest slope of vulnerability curve in YF was measured in *S. nervosum*.

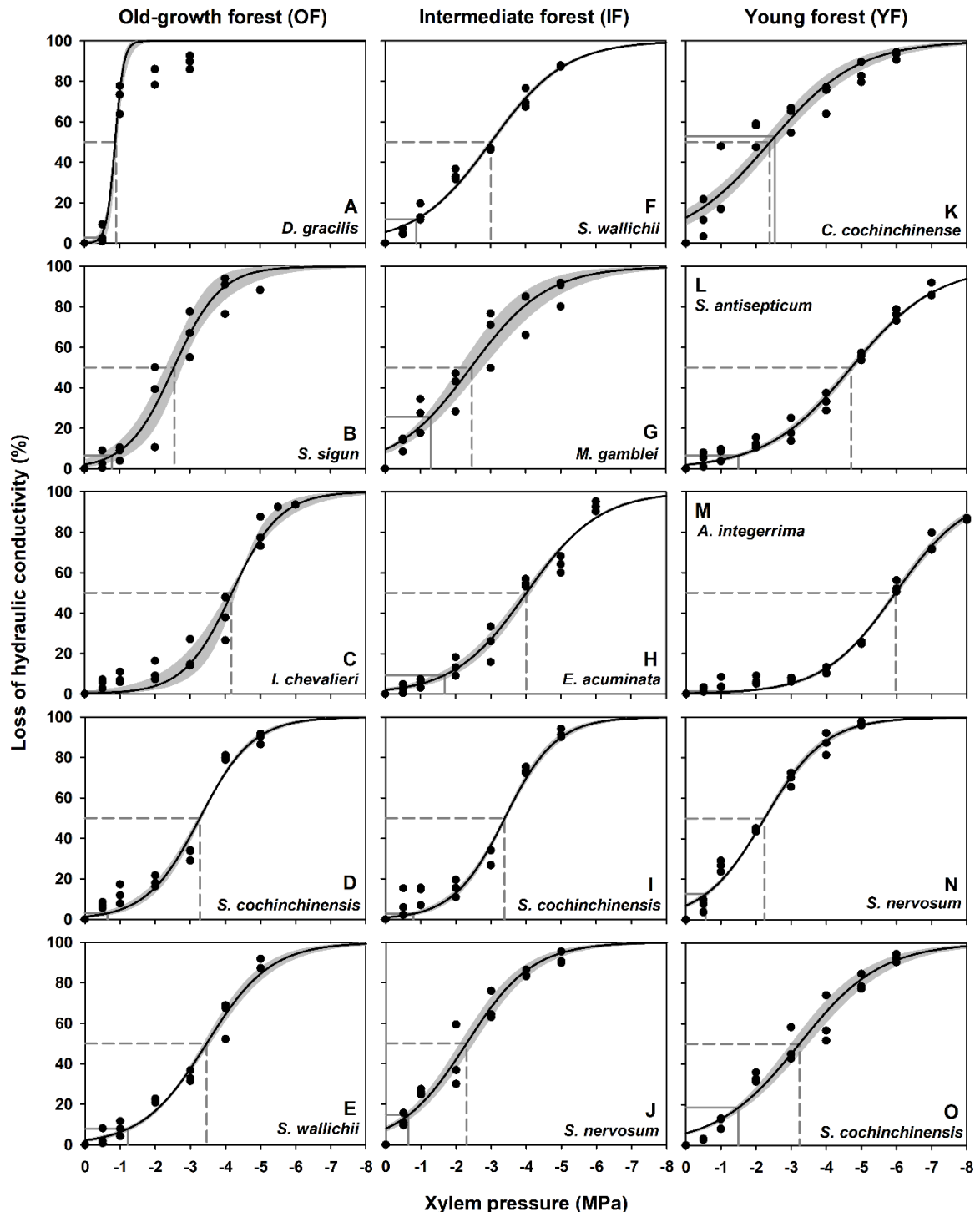


Figure 2.5.3 Vulnerability of xylem to embolism of branches from dominant tree species from different successions in Khao Yai National Park, Thailand. Mean vulnerability curves are presented with shaded bands representing one standard error from 3 branches for a given species. The gray dashed line indicates the xylem pressure at 50% loss of hydraulic conductivity (P₅₀).

#####

Note: The manuscript for this work is in preparation. Please see the draft in the Appendix.

Objective 3

The future impacts of climate change on forest biomass, productivity, and diversity.

We proposed to use a multilayered hydraulically driven soil–vegetation–atmosphere carbon and water transfer model (SPA, Williams et al. 2001) to estimate water balance and forest productivity of the forest ecosystems and analyze the variations of these parameters under different climate change scenarios. However, due to the difficulties in obtaining specific parameters for the models, we could not proceed with this plan. We therefore show an analysis of the vulnerability to xylem cavitation of tree species from different forests in Thailand and China, with implications for the drought tolerance of the forests. Because drought is predicted to increase and prolong in this region, we believe that it is useful to understand how different forests across climatic region are vulnerable to drought.

For the analysis, we used the xylem pressure inducing 50% loss of hydraulic conductivity (P_{50}) as a parameter that represents the vulnerability of a tree species to xylem cavitation. As previously explained, the lower P_{50} means the more tolerant to drought and thus more vulnerable to hydraulic failure. Previous studies showed that vulnerability to hydraulic failure predicts drought-induced mortality in tree species in temperate and tropical forests (Brodribb and Cochard, 2009; Barigah et al., 2013; Urli et al., 2013; Rowland et al., 2015). The distribution of plant species along environmental gradients can be significantly affected by their vulnerability to xylem cavitation (Pockman and Sperry, 2000). In fact, global meta-analyses have shown that P_{50} is related to climate variables such as mean annual precipitation (MAP) and mean annual temperature (MAT) (Choat et al., 2012; Maherli et al., 2004). The studies suggested that tropical evergreen species native to high rainfall areas are among the most vulnerable species. Here, we preliminarily investigated the relationship between P_{50} of dominant tree species in five forest sites in Thailand and China. Table 3.1 shows the information of these sites as available. Specifically, we considered site elevation, MAT, MAP, and mean canopy height as the independent variables. Figure 3.1 shows the result.

Table 3.1 Site information of the studied forests in China (Xishuangbanna and Yuanjiang) and successional forests in Thailand (old-growth forest (OF), intermediate forest (IF) and young forest (YF)). MAT and MAP are mean annual temperature and precipitation, respectively. LAI refers to leaf area index which is the leaf surface area per unit ground area.

Variables	Xishuangbanna (XSB)	Yuanjiang (YJ)	OF	IF	YF
Geographical location	21°55'39" N, 101°15'55" E	23°28'26" N, 102°10'39" E	14°26'31.33" N 101°21'52.1" E	14°26'31.33" N 101°21'52.10" E	14°25'11.3" N 101°22'30" E
Altitude (m)	780	480	750	750	750
MAT (°C)	21.0	23.05	22.4	22.4	22.4
MAP (mm)	1532	787	2073	2073	2073
Soil type	Latosol	n/a	Gray-Brown soil	Gray-Brown soil	Gray-Brown soil

Dominant species	<i>Terminalia myriocarpa</i> , <i>Barringtonia pendula</i> , <i>Saprosma ternatum</i> ,	n/a	<i>Dipterocarpus gracilis</i> , <i>Sloanea sigun</i> , <i>Symplocos cochinchinensis</i>	<i>Schima wallichii</i> , <i>Machilus gamblei</i> , <i>Eurya acuminata</i>	<i>Cratoxylum cochinchinensis</i> , <i>Eugenia grata</i> , <i>Adinandra integerrima</i>
Forest type	Seasonal evergreen forest	Savanna	Seasonal evergreen forest	Seasonal evergreen forest	Seasonal evergreen forest
Mean canopy height (m)	40	5	35	25	15
LAI (m² m⁻²)	~5	n/a	~5	~6	n/a

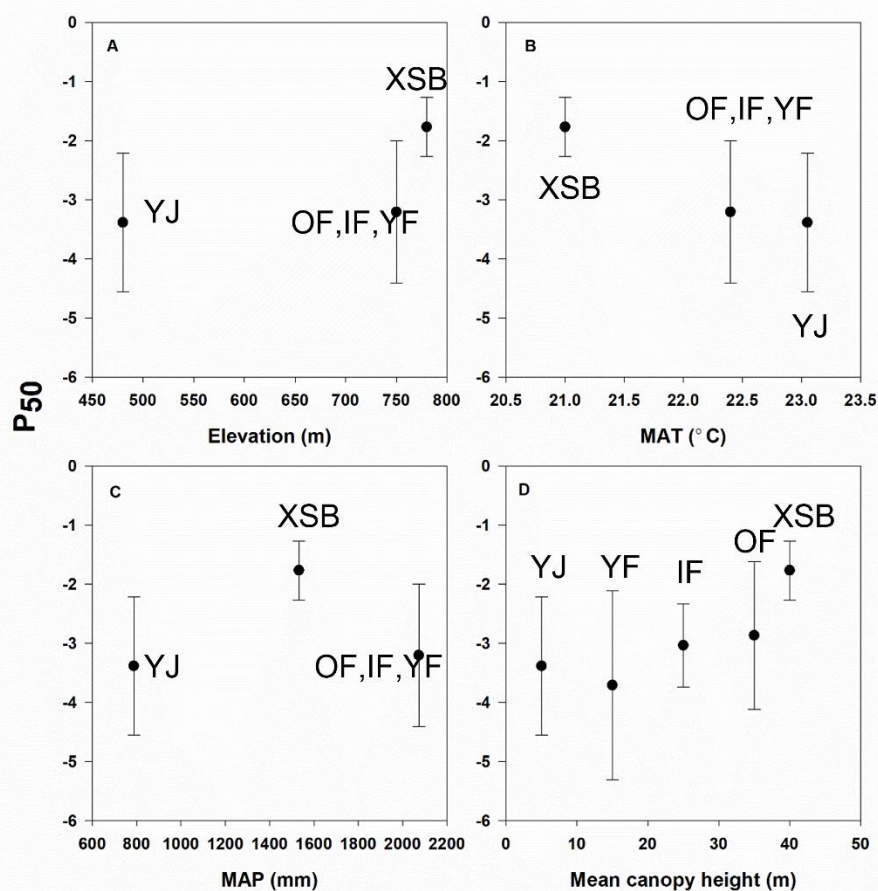


Figure 3.1 Scatter plots showing the association between P50 and parameters that represent site conditions including elevation, MAT, MAP and mean canopy height. Data are the averages with one standard deviation of the measure species within each site shown in Table 3.1.

Because of the small number of data points, we did not perform any statistical analysis on the data set. Rather, we will discuss these results based on the observed trends in the scatter plots. Generally, the results in Figure 3.1 agree with the findings presented in previous synthetic

studies. Species in high elevation site tends to be more vulnerable to drought with increasing P50 (Figure 3.1A), similar to observations in some rain forest species on a tropical island (Trueba et al., 2017). This trend coincides with the high vulnerability to drought in colder sites (Figure 3.1B) which was also found in previous studies (Maherali et al., 2014; Trueba et al., 2017). According to a global analysis, species growing in high rainfall region are more vulnerable to drought (Choat et al., 2012); however, such trend is not obvious in our result with relatively low P50 in the moist forest (Figure 3.1C). Finally, tall forests seem to be more vulnerable to drought (Figure 3.1D) which may be supported by the hydraulic limitation hypothesis. The hypothesis suggests that reduced growth in taller trees results from decreased hydraulic conductance due to the longer root-to-leaf pathway (Ryan et al., 2006). These results informed us about the risks of forest to future drought based on their current site conditions. For example, forests in wet climate may not survive droughts compared to those in the dry climate. Tall forests may be more prone to drought-induced mortality than the shorter ones. However, other local factors, such as nutrient and soil moisture conditions, may mediate such effects and change the results. Nevertheless, this preliminary synthetic analysis calls for more studies in forests across environmental gradients.

(Associate Professor Pantana Tor-ngern, Ph.D.)

Principal Investigator

Date:

References

Adachi, M., Bekku, Y. S., Konuma, A., Kadir, W. R., Okuda, T., Koizumi, H. 2005. Required sample size for estimating soil respiration rates in large areas of two tropical forests and of two types of plantation in Malaysia. *Forest Ecology and Management* 210(1-3), 455-459. <https://doi.org/10.1016/j.foreco.2005.02.011>.

Adachi, M., Ishida, A., Bunyavejchewin, S., Okuda, T., Koizumi, H., 2009. Spatial and temporal variation in soil respiration in a seasonally dry tropical forest, Thailand. *Journal of Tropical Ecology* 25, 531–539.

Adam HD, Luce CH, Breshears DD, Allen CD, Weiler M, Hale VC, Smith AMS, Huxman TE (2012) Ecohydrological consequences of drought- and infestation- triggered tree die-off: insights and hypotheses. *Ecohydrology* 5(2): 145 – 159.

Ainsworth EA, Rogers A (2007) The response of photosynthesis and stomatal conductance to rising [CO₂]: mechanisms and environmental interactions. *Plant Cell and Environment* 30(3): 258 – 270.

Allen CD, Macalady AK, Chenchouni H, Bachelet D, McDowell N, Vennetierf M, Kitzberger T, Rigling A, Breshears DD, Hogg EHT, Gonzalez P, Fensham R, Zhang Z, Castro J, Demidova N, Lim J-H, Allard G, Running SW, Semerci A, Cobb N (2010) A global overview of drought and heat-induced tree mortality reveals emerging climate change risks for forests. *Forest Ecol Manag*

Amoroso M, Daniels L, Baker P, Camarero J (2017) *Dendroecology Tree-Ring Analyses Applied to Ecological Studies: Tree-Ring Analyses Applied to Ecological Studies*.

Anderegg WRL, Kane JM, Anderegg LDL (2013) Consequences of widespread tree Mortality triggered by drought and temperature stress. *Nat Clim Change*. 3:30-36.

Anderegg WRL, Klein T, Barlett M, Sack L, Pellegrini AF, Choat B, Jansen S (2016) Meta-analysis reveals that hydraulic traits explain cross-species patterns of drought-induced tree mortality across the globe. *Proceedings of National Academy of Sciences of the United States of America* 113(8): 5024 – 5029.

Andriyas T, Leksungnoen N, Tor-ngern P. (2021) Comparison of water-use characteristics of tropical tree saplings with implications for forest restoration. *Sci. Rep.* 11: 1745.

Ashfaq M, Shi Y, Tung W, Trapp RJ, Gao X, Pal JS, Diffenbaugh NS (2009) Suppression of South Asian summer monsoon precipitation in the 21st century. *Geophys Res Lett.* 36: L01704.

Ball JT, Woodrow IT, Berry JA (1987) A model predicting stomatal conductance and its contribution to the control of photosynthesis under different environmental conditions. In: Biggins J. ed. *Progress in photosynthesis research*, Dordrecht, The Netherlands: Springer, 221 – 224.

Barigah TS, Charrier O, Douris M, Bonhomme M, Herbette S, Ameglio T, Cochard H (2013) Water stress-induced xylem hydraulic failure is a causal factor of tree mortality in beech and poplar. *Annals of Botany* 112, 1431-1437.

Bell DM, Ward EJ, Oishi AC, Oren R, Flikkema PG, Clark JS, Whitehead D. (2015) A state-space modeling approach to estimating canopy conductance and associated uncertainties from sap flux density data. *Tree Physiol.* 35: 792–802.

Betts RA, Boucher O, Collins M, et al. (2007) Projected increase in continental runoff due to plant responses to increasing carbon dioxide. *Nature* 448(7157): 1037 – U1035.

Bianco, R.L., Avellone, G., 2014. Diurnal regulation of leaf water status in high- and low-mannitol olive cultivars. *Plants* 3(2), 196-208.

Bonan GB (2008) Forests and climate change: forcings, feedbacks, and the climate benefits of forests. *Science* 320: 1444 – 1449.

Bond-Lamberty, B., Thomson, A., 2010. Temperature-associated increases in the global soil respiration record. *Nature* 464, 579–582.

Boonriam, W., Suwanwaree, P., Hasin, S., Archawakom, T., Chanonmuang, P., Yamada, A. 2021. Seasonal changes in spatial variation of soil respiration in dry evergreen forest, Sakaerat Biosphere Reserve, Thailand. *Scienceasia* 47, 112-119. <https://doi.org/10.2306/scienceasia1513-1874.2021.S009>.

Bondeau A, Smith PC, Zaehle S, Schaphoff S, Lucht W, Cramer W, Gerten D, Lotze-Campen H, Muller C, Reichstein M et al. (2007) Modelling the role of agriculture for the 20th century global terrestrial carbon balance. *Global Change Biol.* 13: 679-706.

Bradley R. (1999) Paleoclimatology: Reconstructing Climates of the Quaternary. Arctic, Antarctic, and Alpine Research 1, doi:10.2307/1552264.

Bréchet, L., Le Dantec, V., Ponton, S., Goret, J., Sayer, E., Bonal, D., Freycon, V., Roy, J., Epron, D., 2017. Short- and long-term influence of litter quality and quantity on simulated heterotrophic soil respiration in a lowland tropical forest. *Ecosystems* 20, 1190–1204.

Brienen R., Schöngart J., Zuidema P. (2016) Tree Rings in the Tropics: Insights into the Ecology and Climate Sensitivity of Tropical Trees. Volume 6.

Brockelman WY., Nathalang A., Maxwell JF. (2011) *The Mo Singto Forest Dynamics Plot, Khao Yai National Park, Thailand*; National Science and Technology Development Agency.

Brockelman, W.Y., Nathalang, A., Maxwell, J.F., 2017. Mo Singto Plot: Flora and Ecology. National Science and Technology Development Agency and Department of National Parks, Wildlife and Plant Conservation, Bangkok.

Brodribb T.J., Cochard H. (2009) Hydraulic failure defines the recovery and point of death in water-stressed conifers. *Plant Physiology* 149, 575-584.

Brodribb, T.J., Holbrook, N.M., 2004. Diurnal depression of leaf hydraulic conductance in a tropical tree species. *Plant Cell Environ.* 27(7), 820-827.

Brovkin V, Raddatz T, Reick CH, Claussen M, Gayler V (2009) Global biogeophysical interactions between forest and climate. *Geophys. Res. Lett.* 36: L07405.

Bunker, D.E., et al., 2005. Species loss and aboveground carbon storage in a tropical forest. *Science* 310, 1029–1031.

Bunn A. (2010) Statistical and visual crossdating in R using the dplR library. *Dendrochronologia* 28, 251-258, doi:10.1016/j.dendro.2009.12.001.

Carrer M., Urbinati C (2006) Long-term change in the sensitivity of tree-ring growth to climate forcing in *Larix decidua*. *New phytologist* 170, 861-871, doi:10.1111/j.1469-8137.2006.01703.x.

Chanthorn W., Brockelman W. (2008) Seed dispersal and seedling recruitment in the light-demanding tree *Choerospondias axillaris* in old-growth forest in Thailand. *ScienceAsia* 34, doi:10.2306/scienceasia1513-1874.2008.34.129.

Chanthorn, W., Ratanapongsai, Y., Brockelman, W.Y., Allen, M.A., Favier, C., Dubois, M.A., 2016. Viewing tropical forest succession as a three-dimensional dynamical system. *Theor. Ecol.* 9, 163-172.

Chanthorn, W., Hartig, F., Brockelman, W.Y., 2017. Structure and community composition in a tropical forest suggest a change of ecological processes during stand development. *For. Ecol. Manage.* 404, 100-107.

Chazdon, R.L., Pearcy, R.W., Lee, D.W., Fetcher, N. 1996. Photosynthetic responses of tropical forest plants to contrasting light environments. In *Tropical Plant Ecophysiology*. Eds. S. Mulkey, R.L. Chazdon and A.P. Smith. Chapman and Hall, New York, pp. 5-55.

Chazdon, R.L., 2014. *Second Growth: The Promise of Tropical Forest Regeneration in an Age of Deforestation*. University of Chicago Press, Chicago.

Chen, Y.J., Schnitzer, S.A., Zhang, Y.J., Fan, Z.X., Goldstein G., Tomlinson, K.W., Lin, H., Zhang, J.L., Cao, K.F., 2016. Physiological regulation and efficient xylem water transport regulate diurnal water and carbon balances of tropical lianas. *Funct. Ecol.* 31(2), 306-317.

Choat B, Jansen S, Brodribb TJ, Cochard H, Delzon S, Bhaskar R, Bucci SJ, Gleason SM, Hacke UG, Jacobsen AL, Lens F, Maherali H, Martinez-Vilalta J, Mayr S, Mencuccini M, Mitchell PJ, Nardini A, Pitermann J, Pratt RB, Sperry JS, Westoby M, Wright IJ, Zanne AE (2012) Global convergence in the vulnerability of forests to drought. *Nature*. 491:752.

Cobb RC, Eviner VT, Rizzo DM (2013) Mortality and community changes drive sudden oak death impacts on litterfall and soil nitrogen cycling. *New Phytol.* 200:422-431.

Condit, R. 1998. Tropical Forest Census Plots: Methods and Results from Barro Colorado Island, Panama and a Comparison with Other Plots. Springer-Verlag, Berlin, Heidelberg.

Cook ER., Kariukstis LA. (1990) Methods of Dendrochronology: Applications in the Environmental Sciences. Methods of dendrochronology: applications in the environmental sciences.

Corlett RT (2011) Impacts of warming on tropical lowland rainforests. *Trends Ecol Evol.* 26:606-13.

Coste, S., Roggy, J.-C., Imbert, P., Born, C., Bonal, D., Dreyer, E. 2005. Leaf photosynthetic traits of 14 tropical rain forest species in relation to leaf nitrogen concentration and shade tolerance. *Tree Physiol.* 25, 1127-1137.

Coste, S., Baraloto, C., Leroy, C., Marcon, E., Renaud, A., Richardson, A.D., Roggy, J.C., Schimass, H., Uddling, J., Héault, B., 2010. Assessing foliar chlorophyll contents with the SPAD-502 chlorophyll meter: a calibration test with thirteen tree species of tropical rainforest in French Guiana. *Ann. For. Sci.* 67, 607.

Cramer W, Bondeau A, Woodward FI, Prentice IC, Betts RA, Brovkin V, Cox PM, Fisher V, Foley JA, Friend AD et al. (2001) Global response of terrestrial ecosystem structure and function to CO₂ and climate change: results from six dynamic global vegetation models. *Global Change Biol.* 7:357-373.

Culf, A.D., Esteves, J.L., Marques Filho A.O., da Rocha, H.R., 1996. Radiation, temperature and humidity over forest and pasture in Amazonia. In: J.H.C., Gash, C.A., Nobre, J.M., Roberts, R.L., Victoria, (Eds.). *Amazonian Deforestation and Climate*. John Wiley & Sons, London, pp. 175-191.

Cunningham, S., 2004. Stomatal sensitivity to vapour pressure deficit of temperate and tropical evergreen rainforest trees of Australia. *Trees* 18, 399-407.

Curtis, P.G., Slay, C.M., Harris, N.L., Tyukavina, A., Hansen, M.C., 2018. Classifying drivers of global forest loss. *Science* 361(6407), 1108-1111. <https://doi.org/10.1126/science.aau3445>.

Dang, Q.L., Margolis, H.A., Coyea, M.R., Sy, M., Collatz, G.J., 1997. Regulation of branch-level gas exchange of boreal trees: roles of shoot water potential and vapor pressure difference. *Tree Physiol.* 17(8-9), 521–535. <https://doi.org/10.1093/treephys/17.8-9.521>.

Davidson, E.A., Janssens, I.A., Luo, Y.Q., 2006. On the variability of respiration in terrestrial ecosystems: moving beyond Q₁₀. *Global Change Biology* 12, 154–164.

Davies, et al., 2021. ForestGEO: Understanding forest diversity and dynamics through a global observatory network. *Biological Conservation* 253, 108907.

De Kovel, C.F., Wilms, Y.J.O., Berendse, F., 2000. Carbon and nitrogen in soil and vegetation at sites differing in successional age. *Plant Ecology* 149, 43–50.

Dietze MC, Moorcroft PR (2011) Tree mortality in the eastern and central United States: patterns and drivers. *Global Change Biol.* 17:3312-3326.

Dong Z., Baas P. (1993) Wood Anatomy of Trees and Shrubs from China. V. Anacardiaceae. IAWA Journal 14, 87-102, doi:10.1163/22941932-90000580.

Douville H, Planton S, Royer JF, Stephenson DB, Tyteca S, Kergoat L, Lafont S, Betts RA (2000) Importance of vegetation feedbacks in doubled-CO₂ climate experiments. *Journal of Geophysical Research-Atmospheres* 105(D11): 14841 – 14861.

Dye, P.J., Olbrich, B.W., 1993. Estimating transpiration from 6-year-old *Eucalyptus grandis* trees: development of a canopy conductance model and comparison with independent sap flux measurements. *Plant Cell Environ.* 16, 45-53.

Ellsworth, D.S., Reich, P.B., 1996. Photosynthesis and leaf nitrogen in five Amazonian tree species during early secondary succession. *Ecology* 77(2), 581-594.

Evans, J.R., 1989. Photosynthesis and nitrogen relationships in leaves of C3 plants. *Oecologia* 78, 9-19.

Fan, D.Y., Jie, S.-L., Liu, C.-C., Zhang, X.-Y., Xu, X.-W., Zhang, S.-R., Xie, Z.-Q., 2011. The trade-off between safety and efficiency in hydraulic architecture in 31 woody species in a karst area. *Tree Physiol.* 31, 865-877.

FAO and UNEP, 2020. The State of the World's Forests 2020. Forests, biodiversity and people. Rome. <https://doi.org/10.4060/ca8642en>.

Feeley K.J., Wright J., Nur Supardi M.N., Kassim A.R., Davies S.J. (2007) Decelerating growth in tropical forest trees. *Ecology Letters* 10, 461-469, doi:<https://doi.org/10.1111/j.1461-0248.2007.01033.x>.

Fekete, I., et al., 2014. Alterations in forest detritus inputs influence soil carbon concentration and soil respiration in a Central-European deciduous forest. *Soil Biology and Biochemistry* 74, 106–114.

Fichtler E. (2016) Dendroclimatology using tropical broad-leaved tree species – A review. *Erdkunde* 71, doi:10.3112/erdkunde.2017.01.01.

Field, C., Mooney, H.A., 1986. The photosynthesis-nitrogen relationship in wild plants. Cambridge University Press: 25-55.

Fisch, G., Tota, J., Machado, L.A.T., Silva Dias, M.A.F., Lyra, R.F.F., Nobre, C.A., Dolman, A.J., Gash, J.H.C., 2004. The convective boundary layer over pasture and forest in Amazonia. *Theor. Appl. Climatol.* 78, 47-59.

Flora of China. Choerospondias axillaris. Available online: (accessed on Fritts H (1976) Tree Rings and Climate. *SERBIULA (sistema Librum 2.0)*).

Gales, M. Jr., Julian, E., Kroner, R., 1966. Method for quantitative determination of total phosphorus in water. *J. Am. Water Works Ass.* 58(10), 1363.

Gao, F., Cui, X., Sang, Y., Song, J., 2020. Changes in soil organic carbon and total nitrogen as affected by primary forest conversion. *Forest Ecology and Management* 463, 118013.

Gerardin, T., Douthe, C., Flexas, J., Brendel, O. 2018. Shade and drought growth conditions strongly impact dynamic responses of stomata to variations in irradiance in *Nicotiana tabacum*. *Environ. Exp. Bot.* 153, 188-197.

Giardina, C.P., Binkley, D., Ryan, M.G., Fownes, J.H., Senock, R.S., 2004. Belowground carbon cycling in a humid tropical forest decreases with fertilization. *Oecologia* 139, 545–550.

Good, S.P., Noone, D., Bowen, G., 2015. Hydrologic connectivity constrains partitioning of global terrestrial water fluxes. *Science* 349(6244), 175-177.

Grace, J., 2004. Understanding and managing the global carbon cycle. *Journal of Ecology* 92(2), 189–202.

Granier A (1987) Evaluation of transpiration in a Douglas-fir stand by means of sap flow measurements. *Tree Physiology* 3: 309 – 319.

Granier, A., Ceschia, E., Damesin, C., et al., 2000. The carbon balance of a young Beech forest. *Functional Ecology* 14, 312–325.

Guada G., Camarero J., Sanchez-Salguero R., Navarro Cerrillo R. (2016) Limited Growth Recovery after Drought-Induced Forest Dieback in Very Defoliated Trees of Two Pine Species. *Frontiers in Plant Science* 7, doi:10.3389/fpls.2016.00418.

Gulías, J., Flexas, J., Mus, M., Cifre, J., Lefi, E., Medrano, H., 2003. Relationship between maximum leaf photosynthesis, nitrogen content and specific leaf area in Balearic endemic and non-endemic Mediterranean species. *Ann. Bot.* 92(2), 215-222.

Han, T., Huang, W., Liu, J., Zhou, G., Xiao, Y., 2015. Different soil respiration responses to litter manipulation in three subtropical successional forests. *Scientific Reports* 5, 18166.

Hanpattanakit, P., Leclerc, M. Y., Mcmillan, A. M. S., Limtong, P., Maeght, J. L., Panuthai, S., Inubushi, K., Chidhaisong, A. 2015. Multiple timescale variations and controls of soil respiration in a tropical dry dipterocarp forest, western Thailand. *Plant and Soil* 390(1-2), 167-181. <https://doi.org/10.1007/s11104-015-2386-8>.

Hardwick, S.R., Toumi, R., Pfeifer, M., Turner, E.C., Nilus, R., Ewers, R.M., 2015. The relationship between leaf area index and microclimate in tropical forest and oil palm plantation: Forest disturbance drives changes in microclimate. *Agr. Forest Meteorol.* 201, 187-195.

Harper, A., Baker, I.T., Denning, S., Randall, D.A., Dazlich, D., Branson, M., 2013. Impact of evapotranspiration on dry season climate in the Amazon forest. *J. Clim.* 27, 574-591.

Hartman H, Adams HD, Anderegg WR, Jansen S, Zeppel MJ (2015) Research frontiers in drought-induced tree mortality: crossing scales and disciplines. *New Phytologist* 205(3): 965 – 969.

Hashimoto, S., Carvalhais, N., Ito, A., et al., 2015. Global spatiotemporal distribution of soil respiration modeled using a global database. *Biogeosciences* 12, 4331–4364.

Hashimoto, S., Tanaka, N., Suzuki, M., Inoue, A., Takizawa, H., Kosaka, I., Tanaka, K., Tantasirin, C., Tangtham, N. 2004. Soil respiration and soil CO₂ concentration in a tropical forest, Thailand. *Journal of Forest Research* 9(1), 75-79. <https://doi.org/10.1007/s10310-003-0046-y>.

He G.P., Chen Y.T., Yu Y.H., Liu H.T., Cai, H.M., Chen Y.Z. (2004) Study on early growth characteristics of *Choerospondias axillaris* plantation and effect of *Choerospondias axillaris* and *Cunninghamia lanceolata* mixed stand. *Forest Research* 17, 206-212.

Hikada, A., Kitayama, K., 2009. Divergent patterns of photosynthetic phosphorus use efficiency versus nitrogen use efficiency of tree leaves along nutrient availability gradients. *J. Ecol.* 97: 984-991.

Hogan, K.P., Smith, A.P., Samaniego, M., 1995. Gas exchange in six tropical semi-deciduous forest canopy tree species during the wet and dry seasons. *Biotropica* 27(3), 324-333.

Hölscher, D., Leuschner, C., Bohman, K., Hagemeier, M., Juhrbandt, J., Tjitronegoro, S., 2006. Leaf gas exchange of trees in old-growth and young secondary forest stands in Sulawesi, Indonesia. *Trees* 20, 278-285.

Hu L., Fan Z. (2016) Stem radial growth in response to microclimate in an Asian tropical dry karst forest. *Acta Ecologica Sinica* 36, 401-409.

Huang, W., Han, T., Liu, J., Wang, G., Zhou, G., 2016. Change in soil respiration components and their specific respiration along three successional forests in the subtropics. *Functional Ecology* 30, 1466–1474.

Hubau, W., Lewis, S.L., Phillips, O.L., et al., 2020. Asynchronous carbon sink saturation in African and Amazonian tropical forests. *Nature* 579, 80-87.

Hughes AC. (2017) Understanding the drivers of Southeast Asian biodiversity loss. *Ecosphere* 8, e01624, doi:<https://doi.org/10.1002/ecs2.1624>.

Hursh, A., Ballantyne, A., Cooper, L., Maneta, M., Kimball, J., Watts, J., 2017. The sensitivity of soil respiration to soil temperature, moisture, and carbon supply at the global scale. *Global Change Biology* 23, 2090–2103.

Intanil, P., Boonpoke, A., Sanwangsri, M., Hanpattanakit, P. 2018. Contribution of Root Respiration to Soil Respiration during Rainy Season in Dry Dipterocarp Forest, Northern Thailand. *Applied Environmental Research* 40(3), 19–27. <https://doi.org/10.35762/AER.2018.40.3.3>.

Jasechko, S., Sharp, Z.D., Gibson, J.J., Birks, S.J., Yi, Y., Fawcett, P.J., 2013. Terrestrial water fluxes dominated by transpiration. *Nature* 496, 347-351. <https://doi.org/10.1038/nature11983>.

Jenkinson, D.S., Adams, D.E., Wild, A., 1991. Model estimates of CO₂ emission from soil in response to global warming. *Nature* 351, 304–306.

Jha, N., Tripathi, N.K., Chanthorn, W., et al., 2020. Forest aboveground biomass stock and resilience in a tropical landscape of Thailand. *Biogeosciences* 17, 121-134.

Jia, G.M., Cao, J., Wang, C.Y., Wang, G., 2005. Microbial biomass and nutrients in soil at the different stages of secondary forest succession in Ziwulin, northwest China. *Forest Ecology and Management* 217, 117–125.

Jiang XY, Rauscher SA, Ringler TD, Lawrence DM, Williams AP, Allen CD, Steiner AL, Cai DM, McDowell NG (2013) Projected future changes in vegetation in western North America in the twenty-first century. *Journal of Climate* 26(11): 3671 – 3687.

Johnson D.M., Wortemann R., McCulloh K.A., Jordan-Meille L., Ward E., Warren J.M., et al. (2016). A test of the hydraulic vulnerability segmentation hypothesis in angiosperm and conifer tree species. *Tree Physiology* 36(8): 983-993.

Jucker, T., Hardwick, S.R., Both, S., Elias, D.M.O., Ewers, R.M., Milodowski, D.T., Swinfield, T., Coomes, D.A., 2018. Canopy structure and topography jointly constrain the microclimate of human-modified tropical landscapes. *Global Change Biol.* 24, 5243-5258.

Kammerer, P.A., Rodel, M.G., Hughes, R.A., Lee, G.F., 1967. Low level Kjeldahl nitrogen determination on the Technicon Autoanalyzer. *Environ. Sci. Technol.* 1, 340.

Katayama, A., Kume, T., Komatsu, H., Ohashi, M., Nakagawa, M., Yamashita, M., Otsuki, K., Suzuki, M., Kumagai, T. 2009. Effect of forest structure on the spatial variation in soil respiration in a Bornean tropical rainforest. *Agricultural and Forest Meteorology* 149(10), 1666-1673. <https://doi.org/10.1016/j.agrformet.2009.05.007>.

Kimura, K., Ishida, A., Uemura, A., Matsumoto, Y., Terashima, C. 1998. Effects of current-year and previous-year PPFDs on shoot gross morphology and leaf properties in *Fagus japonica*. *Tree Physiol.* 18, 459-466.

Knops J., Koenig W., Carmen W. (2007) Negative correlation does not imply a tradeoff between growth and reproduction in California oaks. *Proceedings of the National Academy of Sciences of the United States of America* 104, 16982-16985, doi:10.1073/pnas.0704251104.

Kosugi, Y., Mitani, T., Ltoh, M., Noguchi, S., Tani, M., Matsuo, N., Takanashi, S., Ohkubo, S., Nik, A. R. 2007. Spatial and temporal variation in soil respiration in a Southeast Asian tropical rainforest. *Agricultural and Forest Meteorology* 147(1-2), 35-47. <https://doi.org/10.1016/j.agrformet.2007.06.005>

Kröber, W., Plath, I., Heklau, H., Bruelheide, H., 2015. Relating stomatal conductance to leaf functional traits. *J. Vis. Exp.* 104, 52738. <https://doi.org/10.3791/52738>.

Kull, O., Niinemets, Ü., 1998. Distribution of leaf photosynthetic properties in tree canopies: comparison of species with different shade tolerance. *Funct. Ecol.* 12, 472-479.

Kume, T., Tanaka, N., Yoshifuji, N., Chatchai, T., Igarashi, Y., Suzuki, M., Hashimoto, S. 2013. Soil respiration in response to year-to-year variations in rainfall in a tropical

seasonal forest in northern Thailand. *Ecohydrology* 6(1), 134-141. <https://doi.org/10.1002/eco.1253>.

Kurz WA, Dymond CC, Stinson G, Rampley GJ, Neilson ET, Carroll AL, Ebata T, Safranyik L (2008) Mountain pine beetle and forest carbon feedback to climate change. *Nature* 452: 987 – 990.

Lamont, B.B., Groom, P.K., Cowling, R.M., 2002. High leaf mass per area of related species assemblages may reflect low rainfall and carbon isotope discrimination rather than low phosphorus and nitrogen concentrations. *Funct. Ecol.* 16: 403-412.

Lang, R., Blagodatsky, S., Xu, J., Cadisch, G., 2017. Seasonal differences in soil respiration and methane uptake in rubber plantation and rainforest. *Agriculture, Ecosystems and environment* 240, 314–328.

La Scala, Jr., N., Marques, Jr., J., Pereita, G.T., 2000. Short-term temporal changes in the spatial variability model of CO₂ emission from a Brazilian bare soil. *Soil Biology and Biochemistry* 32, 1459–1462.

Lebrija-Trejos, E., Perez-Garcia, E.A., Meave, J.A., Bongers, F., Poorter, L., 2010. Functional traits and environmental filtering drive community assembly in a species-rich tropical system. *Ecology* 91, 386-398.

Lebrija-Trejos, E., Perez-Garcia, E.A., Meave, J.A., Poorter, L., Bongers, F., 2011. Environmental changes during secondary succession in a tropical dry forest in Mexico. *J. Trop. Ecol.* 27, 477–489.

Li, Y., Yang, F., Ou, Y., Zhang, D., Liu, J., Chu, G., et al., 2013. Changes in forest soil properties in different successional stages in lower tropical China. *PLoS ONE* 8, e81359.

Litton, C. M., Giardina, C. P. 2008. Below-ground carbon flux and partitioning: global patterns and response to temperature. *Functional Ecology* 22(6), 941-954. <https://doi.org/10.1111/j.1365-2435.2008.01479.x>.

Lewis SL, Brando PM, Phillips OL, van der Heijden GMF, Nepstad D (2011) The 2010 Amazon Drought. *Science*. 331:554-554.

Lohbeck, M., et al., 2013. Successional changes in functional composition contrast for dry and wet tropical forest. *Ecology* 94, 1211-1216.

Lohbeck, M., et al., 2015. Functional trait strategies of trees in dry and wet tropical forests are similar but differ in their consequences for succession. *Plos One* 10, e0123741.

Loo YY, Billa L, Singh A (2015) Effect of climate change on seasonal monsoon in Asia and its impact on the variability of monsoon rainfall in Southeast Asia. *Geoscience Frontiers* 6(6): 817 – 823.

Luo, J., Chen, Y., Wu, Y., Shi, P., She, J., Zhou, P., 2012. Temporal-spatial variation and controls of soil respiration in different primary succession stages on glacier forehead in Gongga mountain, China. *PLoS ONE* 7, e42354.

Maherali H., Pockman W.T., Jackson R.B. (2004) Adaptive variation in the vulnerability of woody plants to xylem cavitation. *Ecology* 85, 2184-2199.

Maness H, Kushner PJ, Fung I (2013) Summertime climate response to mountain pine beetle disturbance in British Columbia. *Nature Geoscience* 6(1): 65 – 70.

Marenco, R.A., Goncalves, J.F.D.C., Vieira, G., 2001. Leaf gas exchange and carbohydrates in tropical trees differing in successional status in two light environments in central Amazonia. *Tree Physiol.* 21, 1311-1318.

Markesteijn, L., Poorter, L., Bongers, F., Paz, H., Sack, L., 2011. Hydraulic and life history of tropical dry forest tree species: coordination of species' drought and shade tolerance. *New Phytol.* 191, 480-495.

Marthews, T.R., Burslem, D.F.R.P., Paton, S.R., Yangüez, F., Mullins, C.E., 2008. Soil drying in a tropical forest: Three distinct environments controlled by gap size. *Ecological Modelling* 216, 369–384.

McCaughey, J.H., Iacobelli, A., 1994. Modelling stomatal conductance in a northern deciduous forest, Chalk River, Ontario. *Can. J. For. Res.* 24, 904-910.

McDowell NG, Beerling DJ, Breshears DD, Fisher RA, Raffa KF, Stitt M (2011) The interdependence of mechanisms underlying climate-driven vegetation mortality. *Trends in Ecology & Evolution* 26(10): 523 – 532.

McDowell NG, Williams AP, Xu C, et al. (2015) Multi-scale predictions of massive conifer mortality due to chronic temperature rise. *Nature Climate Change* 6(3): 295 – 300.

Medlyn BE, Barton CVM, Broadmeadow MSJ, et al. (2001) Stomatal conductance of forest species after long-term exposure to elevated CO₂ concentration: a synthesis. *New Phytologist* 149(2): 247 – 264.

Medlyn, B.E., Duursma, R.A., Eamus, D., Ellsworth, D.S., Prentice, I.C., Barton, C.V.M., et al., 2011. Reconciling the optimal and empirical approaches to modelling stomatal conductance. *Glob. Change Biol.* 17(6), 2134-2144.

Mielke, M.S., de Almeida, A.F., Gomes, F.P., 2005. Photosynthetic traits of five neotropical rainforest tree species: interactions between light response curves and leaf-to-air vapor pressure deficit. *Braz. Arch. Biol. Technol.* 48(5), 815-824.

Miralles, D.G., De Jeu, R.A.M., Gash, J.H., Holmes, T.R.H., Dolman, A.J., 2011. Magnitude and variability of land evaporation and its components at the global scale. *Hydrol. Earth Syst. Sc.* 15(3), 967-981.

Motzner, T., Munz, N., Küppers, M., Schmitt, D., Anhuf, D., 2005. Stomatal conductance, transpiration and sap flow of tropical montane rain forest trees in the southern Ecuadorian Andes. *Tree Physiol.* 25, 1283-1293.

Mujawamariya, M., Manishimwe, A., Ntirugulirwa, B., Zibera, E., Ganszky, D., Bahati, E.N., Nyirambangutse, B., Nsabimana, D., Wallin, G., Uddling, J., 2018. Climate sensitivity of tropical trees along an elevation gradient in Rwanda. *Forests* 9, 647.

Mund M., Herbst M., Knohl A., Matthäus B., Schumacher J., Schall P., Siebicke L., Tamrakar R., Ammer C. (2020) It is not just a ‘trade-off’ – indications for sink- and source-limitation to vegetative and regenerative growth in an old-growth beech forest. *New Phytologist* 226, doi:10.1111/nph.16408.

Niinemets, Ü., 2001. Global-scale climatic controls of leaf dry mass per area, density, and thickness in trees and shrubs. *Ecology* 82, 453-469.

Ogée, J., Brunet, Y. 2002. A forest floor model for heat and moisture including litter layer. *Journal of Hydrology* 255, 212–233.

Ohashi, M., Kumagai, T., Kume, T., Gyokusen, K., Saitoh, T., Suzuki, M. 2008. Characteristics of soil CO₂ efflux variability in an aseasonal tropical rainforest in Borneo Island. *Biogeochemistry* 90(3), 275-289. <https://doi.org/10.1007/s10533-008-9253-0>.

Oren, R., Sperry, J.S., Katul, G.G., Pataki, D.E., Ewers, B.E., Phillips, N., Schäfer, K.V.R., 1999. Survey and synthesis of intra- and interspecific variation in stomatal sensitivity to vapour pressure deficit. *Plant Cell Environ.* 22, 1515-1526.

Pan YD, Birdsey RA, Fang JY, Houghton R, Kauppi PE, Kurz WA, Phillips OL, Shvidenko A, Lewis SL, Canadell JG et al. (2011) A large and persistent carbon sink in the world's forests. *Science* 323: 988 – 993.

Peng, F., You, Q.G., Xu, M.H., Zhou, X.H., Wang, T., Guo, J., Xue, X., 2015. Effects of experimental warming on soil respiration and its components in an alpine meadow in the permafrost region of the Qinghai-Tibet Plateau. *European Journal of Soil Science* 66, 145–154.

Pérez-Harguindeguy N., Díaz S., Garnier E., et al. (2016). New handbook for standardized measurement of plant functional traits worldwide. *Australian Journal of Botany* 64: 715-716.

Phillips OL, van der Heijden G, Lewis SL, Lopez-Gonzalez G, Aragao LEOC, Lloyd J, Malhi Y, Monteagudo A, Almeida S, Davila EA, Amaral I, Andelman S, Andrade A, Arroyo L, Aymard G, Baker TR, Blanc L, Bonal D, de Oliveira ACA, Chao KJ, Cardozo ND, da Costa L, Feldpausch TR, Fisher JB, Fyllas NM, Freitas MA, Galbraith D, Gloor E, Higuchi N, Honorio E, Jimenez E, Keeling H, Killeen TJ, Lovett JC, Meir P, Mendoza C, Morel A, Vargas PN, Patino S, Peh KSH, Cruz AP, Prieto A, Quesada CA, Ramirez F, Ramirez H, Rudas A, Salamao R, Schwarz M, Silva J, Silveira M, Slik JWF, Sonke B, Thomas AS, Stropp J, Taplin JRD, Vasquez R, Vilanova E (2010) Drought-mortality relationships for tropical forests. *New Phytol.* 187:631-646.

Pockman E.T., Sperry J.S. (2000) Vulnerability to xylem cavitation and the distribution of Sonoran Desert vegetation. *American Journal of Botany* 87, 1287-1299.

Poorter, H., Niinemets, Ü., Poorter, L., Wright, I.J., Villar, R., 2009. Causes and consequences of variation in leaf mass per area (LMA): a meta-analysis. *New Phytol.* 182, 565–588.

Powers, J.S., Marín-Spiotta, E., 2017. Ecosystem processes and biogeochemical cycles in secondary tropical forest succession. *Annu. Rev. Ecol. Evol. Syst.* 48(1), 497-519.

Prentice IC, Bondeau A, Cramer W, Harrison SP, Hickler T, Lucht W, Sitch S, Smith B, Sykes M (2007) Dynamic Global Vegetation Modeling: quantifying terrestrial ecosystem responses to large-scale environmental change. In: Canadell JG, Pataki DE, Pitelka LF, eds. *Terrestrial ecosystems in a changing world*. Berlin, Germany: Springer, 175-192.

Pumijumnong N. (2013) *Tree-Ring and Applications in Thailand*; Amarin Printing & Publishing Public Company Limited.: Bangkok.

Pumijumnong N., Buajan S. (2012) Seasonal cambial activity of five tropical tree species in central Thailand. *Trees* 27, doi:10.1007/s00468-012-0794-4.

Quero, J.L., Villar, R., Marañon, T., Zamora, R., 2006. Interactions of drought and shade effects on seedlings of four *Quercus* species: physiological and structural leaf responses. *New Phytol.* 170, 819-834.

Urli M., Porte A.J., Cochard H., Guegant Y., Burlett R., Delzon S. (2013) Xylem embolism threshold for catastrophic hydraulic failure in angiosperm trees. *Tree Physiology* 33, 672-683.

R Core Team. R: A Language and Environment for Statistical Computing. Vienna, Austria: R Foundation for Statistical Computing

Raddatz TJ, Reick CH, Knorr W, Kattge J, Roeckner E, Schnur R, Schnitzler KG, Wetzel P, Jungclaus J (2007) Will the tropical land biosphere dominate the climate-carbon cycle feedback during the twenty-first century? *Climate Dynamics* 29: 565 – 574.

Rahman M., Islam M., Wernicke J. (2018) Changes in Sensitivity of Tree-Ring Widths to Climate in a Tropical Moist Forest Tree in Bangladesh. *Forests* 9, 761, doi:10.3390/f9120761.

Raich, J.W., Tufekcioglu, A., 2000. Vegetation and soil respiration: correlations and controls. *Biogeochemistry* 48, 71–90.

Rakthai S., Fu P., Fan Z.-X., Gaire N., Pumijumnong N., Eiadthong W., Tangmitcharoen S. (2020) Increased Drought Sensitivity Results in a Declining Tree Growth of *Pinus latteri* in Northeastern Thailand. *Forests* 11, 361, doi:10.3390/f11030361.

Rambo, T.R., North, M.P., 2009. Canopy microclimate response to pattern and density of thinning in a Sierra Nevada forest. *For. Ecol. Manage.* 25(2), 435-442.

Redmond MD, Barger NN (2013) Tree regeneration following drought- and insect-induced mortality in pinon-juniper woodlands. *New Phytol.* 200:402-412.

Reich, P.B., Walters, M.B., Ellsworth, D.S., Uhl, C., 1994. Photosynthesis-nitrogen relations in Amazonian tree species I. Patterns among species and communities. *Oecologia* 97, 62-72.

Reich, P.B., Walters, M.B., Ellsworth, D.S., 1997. From tropics to tundra: global convergence in plant functioning. *Proc. Natl. Acad. Sci. U. S. A.* 94, 13730-13734.

Reich, P.B., Ellsworth, D.S., Walters, M.B., Vose, J.M., Gresham, C., Volin, J.C., Bowman, W.D., 1999. Generality of leaf trait relationships: a test across six biomes. *Ecology* 80: 1955-1969.

Reich, P.B., 2014. The world-wide 'fast-slow' plant economics spectrum: a traits manifesto. *J. Ecol.* 102, 275-301.

Rogelj J, Knutti R (2016) Geosciences after Paris. *Nat Geosci.* 9: 187 – 189.

Rowland L., Da Costa A.C.L., Galbraith D.R., Oliveira R.S., Binks O.J., Oliveira A.A.R., Meir P (2015) Death from drought in tropical forests is triggered by hydraulics not carbon starvation. *Nature* 528, 119-122.

Rozendaal D., Zuidema P.A. (2010) Dendroecology in the tropics: A review. *Trees - Structure and Function* 25, 3-16.

Ryan M.G., Phillips N., Bond B.J. (2006) The hydraulic limitation hypothesis revisited. *Plant, Cell & Environment* 29, 367-381.

Santiago, L.S., Mulkey, S.S., 2003. A test of gas exchange measurements on excised canopy branches of ten tropical tree species. *Photosynthetica* 41(3), 343-347.

Sarutanon S., Boonchirdchoo S., Arrigo R., Watanasak M., Barbetti M., Buckley B. (1995) Dendrochronological Investigations in Thailand. *IAWA Journal* 16, 393-409, doi:10.1163/22941932-90001429.

Sayer, E.J., Baxendale, C., Birkett, A.J., Bréchet, L.M., Castro, B., Kerdraon-Byrne, D., Lopez-Sangil, L., Rodtassana, C., 2020. Altered litter inputs modify carbon and nitrogen storage in soil organic matter in a lowland tropical forest. *Biogeochemistry* <https://doi.org/10.1007/s10533-020-00747-7>.

Sayer, E.J., Lopez-Sangil, L., Crawford, J.A., Bréchet, L.M., Birkett, A.J., Baxendale, C., Castro, B., Rodtassana, C., Garnett, M.H., Weiss, L., Schmidt, M.W., 2019 Tropical forest soil carbon stocks do not increase despite 15 years of doubled litter inputs. *Scientific Reports* 9, 18030.

Schewe J, Levermann A (2012) A statistically predictive model for future monsoon failure in India. *Environ Res Lett.* 7: 1 – 9.

Schlesinger, W.H., Andrews, J., 2000. Soil respiration and the global carbon cycle. *Biogeochemistry* 48, 7–20.

Schneider, C.A., Rasband, W.S., Eliceiri, K.W., 2012. NIH Image to ImageJ: 25 years of image analysis. *Nature Methods* 9, 671-675.

Sellers PJ, Bounoua L, Collatz GJ, et al. (1996) Comparison of radiative and physiological effects of doubled atmospheric CO₂ on climate. *Science* 271(5254): 1402 – 1406.

Sheil, D., 2001. Long-term observations of rain forest succession, tree diversity and responses to disturbance. *Plant Ecology* 155, 183–199.

Shrestha N. (2020) An Analysis of Production and Sales of *Choerospondias Axillaris*. *International journal of Horticulture, Agriculture and Food science* 4, doi:10.22161/ijhaf.4.1.2.

Slik JWF, Paoli G, McGuire K, et al. (2013) Large trees drive forest aboveground biomass variation in moist lowland forests across the tropics. *Global Ecology and Biogeography* 22(12): 1261 – 1271.

Slik JWF, Arroyo-Rodriguez V, Aiba S, et al. (2015) An estimate of the number of tropical tree species. *Proceedings of the National Academy of Sciences of the United States of America* 112(24): 7472 – 7477.

Smith NG, Dukes JS (2013) Plant respiration and photosynthesis in global-scale models: incorporating acclimation to temperature and CO₂. *Global Change Biology* 19(1): 45 – 63.

Snyder RL., Moratiel R., Zhenwei S., Swelam A., Jomaa I., Shapland T. (2011) Evapotranspiration response to climatic change; pp. 91-98.

Sperry J.S., and Saliendra N.Z. (1994). Intra- and inter-plant variation in xylem cavitation in *Betula occidentalis*. *Plant, Cell and Environment* 16:279-287.

Somogyi Z. (2008) Recent Trends of Tree Growth in Relation to Climate Change in Hungary. *Acta Silvatica & Lignaria Hungarica*, 4.

Sotta, E.D., Meir, P., Malhi, Y., Nober, A.D., Hodnet, M., Grace, J., 2004. Soil CO₂ efflux in a tropical forest in the central Amazon. *Global Change Biology* 10, 601–617.

Sotta, E.D., Veldkamp, E, Gumaraes, B.R., Paixao, P.K., Ruivo, M.I.P., Almeida, S.S., 2006. Landscape and climatic controls on spatial and temporal variation in soil CO₂ efflux in an Eastern Amazonian rainforest, Caxiuaná, Brazil. *Forest Ecology and Management* 237, 57–64.

Speer J. (2012) *The Fundamentals of Tree-Ring Research*.

Stoyan, H., De-Polli, H., Bohm, S., Robertson, G.P., Paul, E.A., 2000. Spatial heterogeneity of soil respiration and related properties at the plant scale. *Plant Soil* 222, 203–214.

Sugasti, L., Pinzón, R., 2020. First Approach of Abiotic Drivers of Soil CO₂ Efflux in Barro Colorado Island, Panama. *Air, Soil and Water Research* 13, 1–10.

Takahashi, M., Hirai, K., Limtong, P., Leaungvutivirog, C., Panuthai, S., Suksawang, S., Anusontpornperm, S., Marod, D. 2011. Topographic variation in heterotrophic and autotrophic soil respiration in a tropical seasonal forest in Thailand. *Soil Science and Plant Nutrition* 57(3), 452-465. <https://doi.org/10.1080/00380768.2011.589363>.

Takashima, T., Hikosaka, K., Hirose, T., 2004. Photosynthesis or persistence: nitrogen allocation in leaves of evergreen and deciduous *Quercus* species. *Plant, Cell & Environment* 27: 1047-1054.

Tenzin, K., Dukpa D. (2017) *Dendrochronological Manual*.

Tolosa, F.J.X., Vester, H.F.M., Marcial, N.R., Albores, J.C., Lawrence, D., 2003. Leaf litter decomposition of tree species in three successional phases of tropical dry secondary forest in Campeche, Mexico. *Forest Ecology and Management* 174, 401–412.

Tor-ngern P, Oren R, Ward EJ, Palmroth S, McCarthy HR, Domec JC (2015) Increases in atmospheric CO₂ have little influence on transpiration of a temperate forest canopy. *New Phytologist* 205(2): 518 – 525.

Tor-ngern P, Chart-asa C, Chanthorn W, Rodtassana C, Yampum S, Unawong W, Nathalang A, Brockelman W, Srinoppawan K, Chen YJ, Hasselquist NJ. (2021) Variation of leaf-level gas exchange rates and leaf functional traits of dominant trees across three successional stages in a Southeast Asian tropical forest. *For. Ecol. Manag.* 489: 119101.

Tsuji, S., Nakashizuka, T., Kuraji, K., Kume, A., Hanba, Y.T. 2020. Sensitivity of stomatal conductance to vapor pressure deficit and its dependence on leaf water relations and wood anatomy in nine canopy tree species in a Malaysian wet tropical rainforest. *Trees* 34, 1299-1311.

Trueba S., Pouteau R., Lens F., Feild T., Isnard S., Olson M.E., Delzon S. (2017) Vulnerability to xylem embolism as a major correlate of the environmental distribution of rain forest species on a tropical island. *Plant, Cell & Environment* 40, 277-289.

Urban, O., Klem, K., Holisová, P., et al., 2014. Impact of elevated CO₂ concentration on dynamics of leaf photosynthesis in *Fagus sylvatica* is modulated by sky conditions. *Environ. Pollut.* 185, 271-280.

Van der Sleen P., Groenendijk P., Vlam M., Anten N.P.R., Boom A., Bongers F., Pons T.L., Terburg G., Zuidema P.A. (2015) No growth stimulation of tropical trees by 150 years of CO₂ fertilization but water-use efficiency increased. *Nature Geoscience* 8, 24-28.

Van Mantgem PJ, Stephenson NL (2007) Apparent climatically induced increase of tree mortality rates in a temperate forest. *Ecol Lett.* 10: 909 – 916.

Vargas, G.G., Cordero, S.A., 2013. Photosynthetic responses to temperature of two tropical rainforest tree species from Costa Rica. *Trees* 27, 1261-1270.

Villar, R., Merino, J.A., 2001. Comparison of leaf construction cost in woody species with differing leaf life spans in contrasting ecosystems. *New Phytol.* 151, 213-226.

Vlam M., Baker P., Bunyavejchewin S., Zuidema P. (2013) Temperature and rainfall strongly drive temporal growth variation in Asian tropical forest trees. *Oecologia*, doi:10.1007/s00442-013-2846-x.

Von Arx, G., Pannatier, E.G., Thimonier, A., Rebetez, M. 2013. Microclimate in forests with varying leaf area index and soil moisture: potential implications for seedling establishment in a changing climate. *J. Ecol.* 101, 1201-1213.

Wang, C., Ma, Y., Trogisch, S., Huang, Y., Geng, Y., Scherer-Lorenzen, M., He, J., 2017. Soil respiration is driven by fine root biomass along a forest chronosequence in subtropical China. *Journal of Plant Ecology* 10(1), 36–46.

Wang-Erlandsson, L., van der Ent, R.J., Gordon, L.J., Savenije, H.H.G., 2014. Contrasting roles of interception and transpiration in the hydrological cycle – Part 1: Temporal characteristics over land. *Earth Syst. Dyn.* 5(2), 441-469.

Williams M, Law BE, Anthoni PM, Unsworth MH (2001) Use of simulation model and ecosystem flux data to examine carbon-water interactions in ponderosa pine. *Tree Physiol.* 21: 287-298.

Williams AP, Allen CD, Macalady AK, Griffin D, Woodhouse CA, Meko DM, Swetnam TW, Rauscher SA, Seager R, Grissino-Mayer HD, Dean JS, Cook ER, Gangodagamage C, Cai M, McDowell NG (2013) Temperature as a potent driver of regional forest drought stress and tree mortality. *Nat Clim Change.* 3:292-297.

Woodruff, D.R., Meinzer, F.C., McCulloh, K.A. 2009. Height-related trends in stomatal sensitivity to leaf-to-air vapour pressure deficit in a tall conifer. *J. Exp. Bot.* 61(1), 203-210.

Worbes M. (2002) One hundred years of tree-ring research in the tropics - A brief history and an outlook to future challenges. *Dendrochronologia* 20, 217-231, doi:10.1078/1125-7865-00018.

Wright, I.J., Reich, P.B., Westoby, M., Ackerly, D.D., Baruch, Z., Bongers, F., et al., 2004. The worldwide leaf economics spectrum. *Nature* 428, 821-827.

Wu, G., Liu, H., Hua, L., Luo, Q., Lin, Y., He, P., Feng, S., Liu, J., Ye, Q., 2018. Differential responses of stomata and photosynthesis to elevated temperature in two co-occurring subtropical forest tree species. *Frontiers in Plant Science* 9: 467.

Wu, J., Serbin, S.P., Ely, K.S., Wolfe, B.T., Dickman, L.T., Grossiord, C., Michaletz, S.T., Collins, A.D., Dettlo, M., McDowell, N.G., Wright, S.J., Rogers, A., 2019. The response of stomatal conductance to seasonal drought in tropical forests. *Glob. Change. Biol.* 26, 823-839.

Wullschleger SD, Gunderson CA, Hanson PJ, Wilson KB, Norby RJ (2002) Sensitivity of stomatal and canopy conductance to elevated CO₂ concentration – interacting variables and perspectives of scale. *New Phytologist* 153(3): 485 – 496.

Yan, J., Wang, Y., Zhou, G., Zhang, D., 2006. Estimates of soil respiration and net primary production of three forests at different succession stages in South China. *Global Change Biology* 12, 810–821.

Yan, J., Zhang, D., Zhou, G., Liu, J., 2009. Soil respiration associated with forest succession in subtropical forests in Dinghushan Biosphere Reserve. *Soil Biology and Biochemistry* 41, 991–999.

Yang, M., Liu, M., Lu, J., Yang, H. 2019. Effects of shading on the growth and leaf photosynthetic characteristics of three forages in an apple orchard on the Loess Plateau of eastern Gansu, China. *PeerJ* 7:e7594.

Zang C., Biondi, F. (2015) Treeclim: An R package for the numerical calibration of proxy-climate relationships. *Ecography* 38, 431–436, doi:10.1111/ecog.01335.

Zaw Z., Fan Z.-X., Liu W., Gaire N., Than K., Panthi S. (2021) Monsoon precipitation variations in Myanmar since AD 1770: linkage to tropical ocean-atmospheric circulations. *Climate Dynamics* 56, doi:10.1007/s00382-021-05645-8.

Zeng, Z., Estes, L., Ziegler, A.D., Chen, A., Searchinger, T., Hua, F., Guan, K., Jintrawet, A., Wood, E.F., 2018. Highland cropland expansion and forest loss in Southeast Asia in the twenty-first century. *Nat. Geosci.* 11, 556-562.

Zhang Z (2015) Tree-rings, a key ecological indicator of environment and climate change. *Ecological Indicators* 51, 107-116, doi:10.1016/j.ecolind.2014.07.042.

Zheng, C., Jia, L., Hu, G., Lu, J. 2019. Earth observations-based evapotranspiration in Northeastern Thailand. *Remote Sensing* 11, 138. doi:10.3390/rs11020138.

Zhou, Z., Jiang, L., Du, E., Hu, H., Li, Y., Chen, D., Fang, J. 2013. Temperature and substrate availability regulate soil respiration in the tropical mountain rainforests, Hainan Island, China. *Journal of Plant Ecology* 6, 325–334.

Zhou, X., Wan, S., Luo, Y., 2007. Source components and interannual variability of soil CO₂ efflux under experimental warming and clipping in a grassland ecosystem. *Global Change Biology* 13, 761–775.

Zuidema PA, Baker PJ, Groenendijk P, Schippers P, van der Sleen P, Vlam M, Sterck F (2013) Tropical forests and global change: filling knowledge gaps. *Trends in Plant Science* 18(8): 413 – 419.

Appendix

Article

Growth-Climate Relationships and Long-Term Growth Trends of the Tropical Forest Tree *Choerospondias axillaris* (Anacardiaceae) in East-Central Thailand

Wisawakorn Surayothee ^{1,2,3}, Supaporn Buajan ³ , Peili Fu ^{1,4,*}, Nathsuda Pumijumnong ^{3,*} , Zixin Fan ^{1,4,5} , Shankar Panthi ^{1,4} , Patrick M. Finnegan ⁶ , Yongjiang Zhang ⁷ , Yajun Chen ^{1,5}, Pantana Tor-ngern ^{8,9,10} , Wirong Chanthorn ¹¹, Anuttara Nathalang ¹² and Warren Y. Brockelman ^{12,13}

¹ CAS Key Laboratory of Tropical Forest Ecology, Xishuangbanna Tropical Botanical Garden, Chinese Academy of Sciences, Xishuangbanna 666303, China; wisawakorn1151@hotmail.com (W.S.); fanzixin@xtbg.org.cn (Z.F.); shankar.panthi@xtbg.ac.cn (S.P.); chenjy@xtbg.org.cn (Y.C.)

² University of the Chinese Academy of Sciences, Beijing 100049, China

³ Faculty of Environment and Resource Studies, Mahidol University, Salaya, Phutthamonthon, Nakhon Pathom 73170, Thailand; buajan_s@hotmail.com

⁴ Ailaoshan Station of Subtropical Forest Ecosystem Studies, Xishuangbanna Tropical Botanical Garden, Chinese Academy of Sciences, Pu'er 676209, China

⁵ Center for Plant Ecology, Core Botanical Gardens, Chinese Academy of Sciences, Xishuangbanna 666303, China

⁶ School of Biological Sciences, University of Western Australia, 35 Stirling Highway, Perth, WA 6009, Australia; patrick.finnegan@uwa.edu.au

⁷ School of Biology and Ecology, University of Maine, Orono, ME 04469, USA; yongjiang.zhang@maine.edu

⁸ Department of Environmental Science, Faculty of Science, Chulalongkorn University, Bangkok 10330, Thailand; pantana.t@chula.ac.th

⁹ Water Science and Technology and Sustainable Environment Research Group, Chulalongkorn University, Bangkok 10330, Thailand

¹⁰ Environment, Health and Social Data Analytics Research Group, Chulalongkorn University, Bangkok 10330, Thailand

¹¹ Department of Environmental Technology and Management, Faculty of Environment, Kasetsart University, Bangkok 10900, Thailand; wirong.c@ku.th.com

¹² National Biobank of Thailand, National Science and Technology Development Agency, Pathum Thani 12120, Thailand; anut@biotec.or.th (A.N.); wybrock@cscoms.com (W.Y.B.)

¹³ Institute of Molecular Biosciences, Mahidol University, Phutthamonthon 4 Road, Salaya, Nakhon Pathom 73170, Thailand

* Correspondence: fpl@xtbg.org.cn (P.F.); nathsuda@gmail.com (N.P.); Tel.: +86-158-8760-3507 (P.F.); +66-89-077-8837 (N.P.)



Citation: Surayothee, W.; Buajan, S.; Fu, P.; Pumijumnong, N.; Fan, Z.; Panthi, S.; Finnegan, P.M.; Zhang, Y.; Chen, Y.; Tor-ngern, P.; et al. Growth-Climate Relationships and Long-Term Growth Trends of the Tropical Forest Tree *Choerospondias axillaris* (Anacardiaceae) in East-Central Thailand. *Forests* **2021**, *12*, 1655. <https://doi.org/10.3390/f12121655>

Academic Editor: Brad Seely

Received: 25 October 2021

Accepted: 25 November 2021

Published: 29 November 2021

Publisher's Note: MDPI stays neutral with regard to jurisdictional claims in published maps and institutional affiliations.



Copyright: © 2021 by the authors. Licensee MDPI, Basel, Switzerland. This article is an open access article distributed under the terms and conditions of the Creative Commons Attribution (CC BY) license (<https://creativecommons.org/licenses/by/4.0/>).

Abstract: Tropical forests play important roles in global carbon cycling. Tree-ring analysis can provide important information for understanding long-term trends in carbon-fixation capacity under climate change. However, tree-ring studies in tropical regions are limited. We carried out a tree-ring analysis to investigate the dendrochronological potential of the tropical forest tree *Choerospondias axillaris* (Anacardiaceae) in east-central Thailand. Our study focused on growth-climate relationships and long-term growth trends. A chronology was constructed covering the period from 1932 to 2019. The tree-ring width index of *C. axillaris* was positively correlated with precipitation in June, July, and October. Furthermore, growth of *C. axillaris* was positively correlated with the Standardized Precipitation-Evapotranspiration Index (SPEI) from July to October, indicating that growth of *C. axillaris* is mainly limited by moisture availability in the late monsoon season. Moving correlation analysis further revealed the consistency and temporal stability of the relationship of tree growth with monsoon season precipitation and SPEI during the period under study. There was a significant increasing trend in long-term growth from 1932 to 2002 (slope = 0.017, $p < 0.001$); however, long-term growth decreased from 2003 to 2019 (slope = -0.014 , $p < 0.001$). Our study provides important insight into the growth-climate correlations of a broad-leaved tree species in a dry evergreen forest in tropical Asia.

Keywords: *Choerospondias axillaris*; growth-climate response; long-term growth pattern; Mo Singto Forest dynamic plot; Thailand; tree rings; tropical broad-leaved forests

1. Introduction

Climate change has major impacts on natural ecosystems worldwide. The most significant evidence for climate change is rising temperatures and the increasing frequency of extreme events, such as extreme drought, violent storms, and severe flooding [1]. Climate change and related increases in climate extremes have affected tree growth and forest productivity globally [2,3], including in tropical regions [4,5], the Himalayas [6,7] and Europe [8,9]. Tree-ring analysis can provide important information on climate change [10]. Tree rings provide a long-term record of past climates, and record environmental signals over the entire lifespan of a tree, both directly and indirectly [11]. The physiological mechanisms underlying variation in tree radial growth are complex, and are affected by climatic factors (e.g., precipitation and temperature), mean site conditions, and species characteristics [5,7]. The sensitivity of tree growth to climate may change over time, depending on the severity of climate change [8]. Positive and negative effects of climatic factors can be read from the relative width of the rings [12,13].

Tropical forests are known biodiversity hotspots. They have an important role in the global carbon cycle and are important for natural solutions to mitigate climate change [14,15]. The main factors that influence tropical tree growth in addition to climatic factors are soil factors (texture, structure, moisture, and nutrients) and topographic factors (elevation, slope, and aspect) [12,13]. Dendrochronology is the scientific method of the dating of trees and investigating tree growth-climate relationships [16]. There are no strong limiting climatic factors for tree growth in tropical regions, so cross-dating is a challenge for tropical trees. Several techniques can be used to study the responses of tropical tree species to climate variation, including analysis of tree-ring width, cambial activity, wood anatomy, and stable isotopes (^{13}C and ^{18}O) [17].

Increasing numbers of tree species in tropical regions have been found to form clear ring boundaries and have dendrochronological potential [11,13,18–20]. The growth of tropical tree species is positively correlated with precipitation and negatively correlated with temperature [2]. Climate change was not found to stimulate growth in tropical tree species across Cameroon, Bolivia, and Thailand [3]. However, most studies have thus far focused on conifer species; it is important to expand our knowledge in tropical broad-leaved species, as these species tend to play more important roles in tropical ecosystems.

Choerospondias axillaris (Anacardiaceae) is a deciduous tree with semi-ring porous wood [21]. It is widely distributed in tropical Asia [22] and is economically important in Southeast Asian countries [23]. Tree-ring boundaries in *C. axillaris* are very distinct (Figure S1). This trait forms the basis for this first dendroclimatic study on *C. axillaris*, which focused on the Mo Singto ForestGEO plot in Khao Yai National Park, east-central Thailand. The aim of this study was to use tree-ring width measurement to: (1) establish a tree-ring width chronology for *C. axillaris*, (2) determine the relationships between tree-ring width and climatic factors, and (3) reveal the long-term growth patterns of this tree species. We hypothesized that low moisture availability during growing season is the main climatic factor controlling the radial growth of *C. axillaris*, and increased year-to-year variability and rapid climate change will have negative impacts on tree-growth trend in recent decades.

2. Materials and Methods

2.1. Study Area and Climate

The study was conducted in the Mo Singto ForestGEO plot in Khao Yai National Park, east-central Thailand (latitude 101°22' E, longitude 14°26' N, elevation 725 to 815 m above sea level). The plot is located in broad-leaved, seasonal evergreen forest in which some species are briefly deciduous (Figure 1) [24]. The annual mean temperature and

total annual precipitation of the study area for the period of 1994 to 2019 were 22.5 °C and 2002 mm, respectively. The mean monthly temperature of the warmest month was 23.9 °C (May), and of the coldest month was 19.8 °C (January). The monsoon season was from the middle of May to the middle of November. September was the month with highest precipitation (approx. 350 mm). Since only a relatively short period of climate data (1994 to 2019) were available from the Mo Singto (Khao Yai National Park) station, we supplemented it with gridded monthly precipitation, temperature (maximum, mean, and minimum), and Standardized Precipitation-Evapotranspiration Index (SPEI) derived from the Climate Research Unit Time Series (CRU TS4.04; <https://crudata.uea.ac.uk/cru/data/>), accessed on 21 November 2021) [25]. We extracted data for the period 1932 to 2018 at latitude 14°26' N to 14°27' N and longitude 101°21' E to 101°22' E. The mean annual temperature and total annual precipitation for the CRU TS data were 27.3 °C and 1702 mm, respectively. The mean monthly maximum temperature of the warmest month (September) was 35.4 °C and the minimum temperature of the coldest month (December) was 18.4 °C. The long-term trends for climate in the CRU TS data and the Mo Singto area had similar patterns (Figures 2 and S2). However, the Mo Singto climate data were more variable than the CRU TS climate data. Precipitation in Mo Singto was higher and the mean annual temperature was lower than in the CRU TS data (Figure S2). These differences were likely due to the fact that the official provincial weather stations that the CRU TS data rely on are located in the lowlands (<400 m msl) that surround the mountain that Khao Yai National Park encompasses.

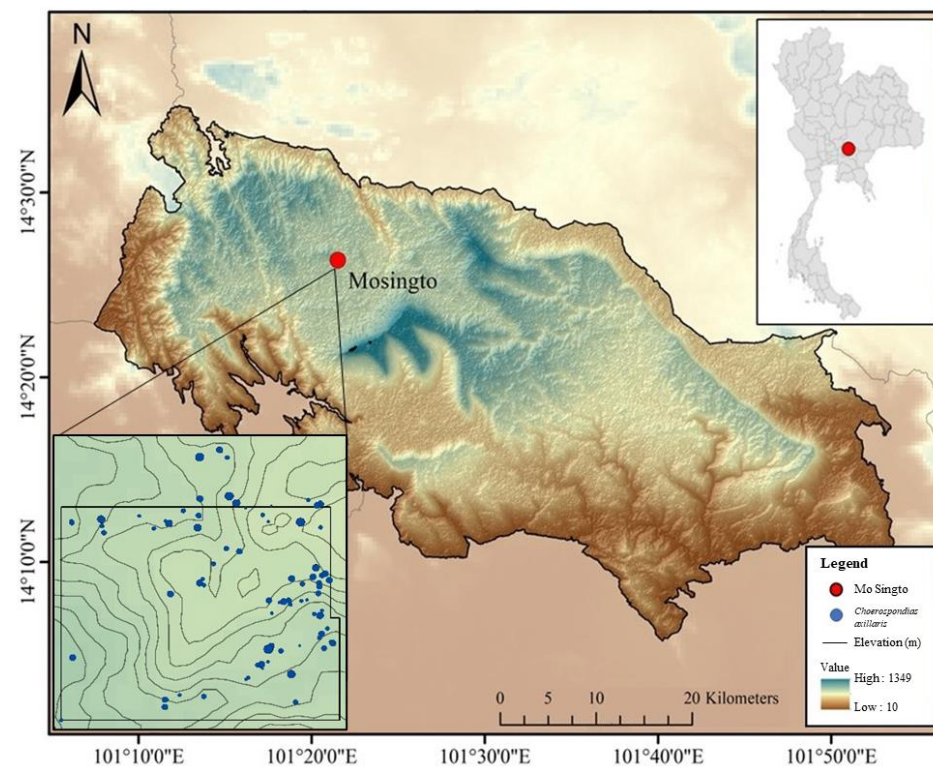


Figure 1. Map of the study area showing topography and the sampling location of *Choerospondias axillaris* trees (blue circles) in Mo Singto ForestGEO, Khao Yai National Park, Thailand. The distance between the contour lines is 10 m.

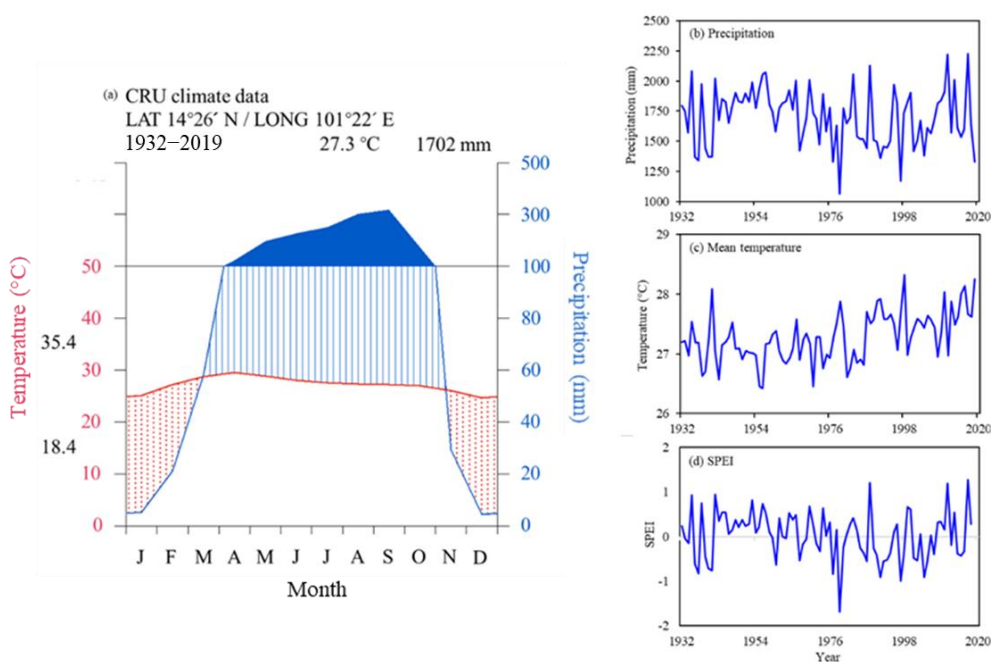


Figure 2. Climatic Research Unit Time Series (CRU TS) gridded climate data for the study area. (a) Walter and Lieth CRU climograph showing monthly temperature (red line) and precipitation (blue line). Red dots, vertical blue lines, and dark blue shape indicate dry period, humid period, and wet period, respectively. At the top are the mean annual temperature and mean annual precipitation. Mean monthly maximum temperature of the warmest month (September) and mean minimum temperature of the coldest month (December) are shown in black on the left. Blue lines show long-term climate trends for (b) precipitation, (c) mean temperature, and (d) Standardized Precipitation-Evapotranspiration Index (SPEI) covering the analysis period 1932 to 2019.

2.2. Study Species

Choerospondias axillaris (Roxb.) Burtt & Hill (Anacardiaceae), commonly known as Nepali Hog Plum, is widely distributed in tropical and subtropical Asia, mainly in China, Nepal, India, Japan, and the Indochina peninsula region [26]. It is a common canopy species in the Mo Singto plot with a density of about 5.6 trees ha^{-1} for trees at least 10 cm in diameter at breast height (DBH) [24]. The main canopy species at Mo Singto are *Illex chevalieri*, *Sloanea Sigun*, and *Dipterocarpus gracilis*, which together comprise 17.7% of the individuals in the plot. The basal area of *C. axillaris* is ranked third in the plot. Live, standing *C. axillaris* at the Mo Singto plot can reach 112 cm DBH, and 30 m height [24]. It is a fast-growing deciduous tree species in secondary forest, and usually grows on heavy clay or sandy clay soils [27]. The flowering period of *C. axillaris* in Mo Singto is January to March, while fruiting is June to November [28]. The cambium of *C. axillaris* is most active during the transition from dry to wet season (March) [29]. *Choerospondias axillaris* is a shade-intolerant, successional species that is used in forest restoration projects [30]. The species has a unimodal size distribution on the Mo Singto plot and is not regenerating in the old-growth forest of the plot (Figure S4). The fruit of *C. axillaris* is an important food for gibbon in the Mo Sinto plot.

2.3. Sampling, Sample Preparation, Tree Ring-Width Measurement and Cross-Dating

We collected 258 cores from 133 trees, with one to three cores per tree at breast height (1.30 m above the ground), using an increment borer (Haglöf Sweden). Samples were collected in January 2020. Samples were dried at ambient temperature in the laboratory and then mounted into wooden core frames. The dried cores were polished using progressively finer grades of sandpapers until the ring boundaries were clearly visible, following standard dendrochronological techniques [31]. Tree-ring width was measured at a precision of 0.001 mm under a stereomicroscope connected to a digital positioning table (LINTAB™

6, Rinntech, Heidelberg, Germany). Cores of *C. axillaris* showed distinct ring boundaries with ring-porous to semi ring-porous anatomical features. The early wood had larger vessels, compared to smaller vessels in late wood (Figure S1). The cross-dating of tree-ring width to calendar year of formation was done by visual growth pattern matching and statistical tests (sign test, *t*-test, and cross-date index) using TSAP-Win software (Rinn, 2003). The quality of cross-dating was further assessed with COFECHA software [32]. We removed cores with indistinct ring boundaries and cores that only covered a short period of time. Finally, 100 cores from 56 *C. axillaris* trees were successfully cross-dated and used for further analyses.

Raw tree-ring width data were standardized using cubic smoothing splines with a 50% frequency cut-off equal to two-thirds of the series length [33] using the “dplR” package [34] in R software [35]. We averaged all of the de-trended series into a mean standard chronology by computing the bi-weight robust mean. Average radial growth rate (AGR, mm year^{-1}) was calculated for the raw ring-width series, while mean sensitivity (MS) was calculated for the standard chronology. Mean sensitivity, ranging from 0 to 1, indicates year-to-year variation in tree-ring width. Mean sensitivity would approach 0 as tree rings became more similar in width, while mean sensitivity would approach 1 as rings became absent [11,36]. The inter-series correlation (Rbar) and the expressed population signal (EPS) were calculated with 30-year moving windows and 15-year overlaps. Rbar indicates the common signal strength (i.e., the growth synchrony) across the chronology, while EPS is an arbitrary threshold of shared population variance among the individual tree-ring series used to assess the quality of the derived chronology. A value of 0.85 is often used as an appropriate threshold for dendroclimatological purposes [37,38].

2.4. Growth-Climate Relationships

Growth-climate analyses were done using residual chronologies, since residual chronologies excluding tree-level autocorrelation are likely to contain more climate information [12]. Growth-climate relationships were analyzed by computing Pearson’s correlation coefficients between ring-width residual chronologies for *C. axillaris* and the extracted monthly CRU TS climate data using SPSS [39]. A 17-month window from the previous August to the current December was used for each year over the period 1932 to 2019. We did moving correlation analysis (30-year moving windows) to determine the temporal stability of growth-climate relationships using the package “treeclim” [40] in R [35].

2.5. Long-Term Growth Trends

Basal area increment (BAI) was calculated from the raw measurements of ring width using the “bai.out” function in the “dplR” package [41], assuming each ring was uniform and represented a circular cross-section of the tree. The BAI was calculated according to the following equation [42]:

$$\text{BAI} = \pi (R^2_t - R^2_{t-1}) \quad (1)$$

where R is the tree radius at breast height and t is the year of tree ring formation.

Changes in long-term growth trends of *C. axillaris* were identified by analyzing the break points in BAI for each individual tree using the “segmented” package in R [43]. The year 2003 had the highest frequency of break points according to the density distribution for break points (Figure S5). Therefore, we split the BAI into two sub-periods (1932 to 2002 and 2003 to 2019), and the growth trend for each of these sub-periods was analyzed separately. The trends in BAI were analyzed using linear mixed-effect models by using “Year” as the fixed effect and “TreeID” as the random effect in the “lme4” package in R [44].

$$\text{BAI} = \text{Year} + (1 | \text{Year} / \text{TreeID}) \quad (2)$$

3. Results

3.1. Characteristics Tree-Ring Chronology for *Choerospondias axillaris* at Mo Singto

The tree-ring width chronology of *C. axillaris* at Mo Singto spanned the period 1932 to 2019 (88 years). The AGR was $3.79 \text{ mm year}^{-1}$ (Table 1). Mean sensitivity was 0.412, and Rbar was 0.297. The EPS value (0.968) for the chronology surpassed the recommended criteria of 0.85 for the period 1932 to 2019, indicating that the entire 88-year chronology was acceptable for dendroclimatic analysis (Figure 3).

Table 1. Sampling site characteristics and chronology statistics for *Choerospondias axillaris* at Mo Singto, Khao Yai National Park, east-central Thailand.

Latitude (°N)	Longitude (°E)	Elevation (m asl)	Cores/ Trees	Time Span	AGR (mm year ⁻¹)	MSL (yr)	MS	Rbar	EPS
14.26	101.22	725–815	100/56	1932–2019	3.79	65	0.412	0.297	0.968

Note: AGR, Average growth rate; MSL, Mean segment length; MS, Mean sensitivity, Rbar, Inter-series correlation; EPS, Express population signal. AGR was calculated from the raw series, while MS, Rbar, and EPS were calculated after de-trending.

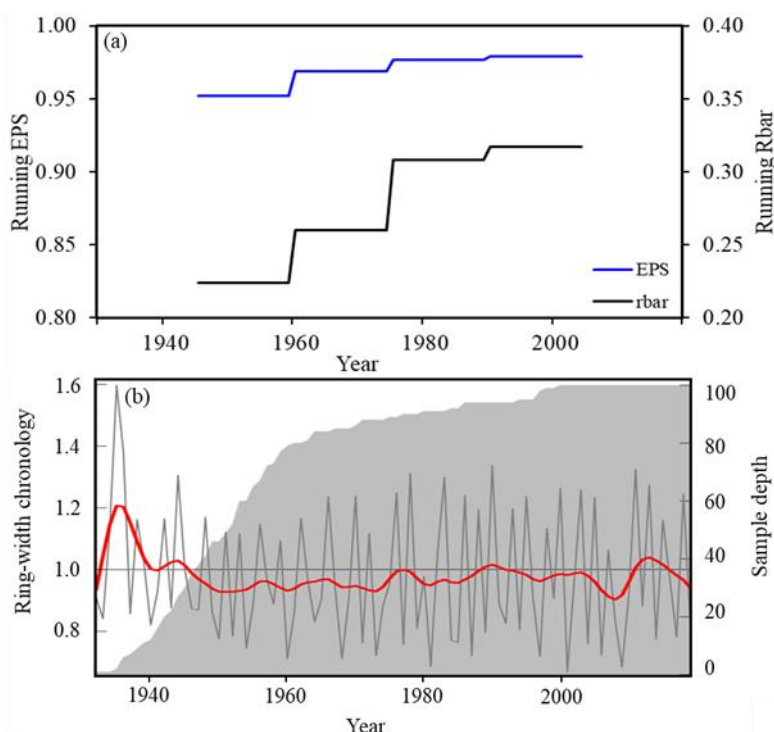


Figure 3. The residual chronology of *Choerospondias axillaris* at Mo Singto, Khao Yai National Park, east-central Thailand. (a) Running Expressed Population Signal (EPS) and running inter-series correlation (Rbar), and (b) *C. axillaris* residual chronology (grey line) with 10-year low pass filter (red line) and sample depth (grey area).

3.2. Growth-Climate Relationships

The tree-ring width index for *C. axillaris* was significantly and positively correlated with precipitation in June, July, and October. Similarly, tree-ring width index positively responded to SPEI during the monsoon season (July to October). However, there were no significant correlations between the tree-ring width index and mean temperature throughout the year (Figure 4). Moving correlation analysis revealed the consistency and temporal stability of tree growth with precipitation and SPEI during the study period. There were significant and positive correlations between tree-ring width index and precipitation in the late monsoon season (July to October) over the analysis period (1932 to 2019); the correlation was weaker during the earlier part of the analysis period, and gradually strengthened

over more recent decades. Conversely, the correlation between tree-ring width index and precipitation in June was significant during the early period, but became non-significant in more recent decades. The tree-ring index of *C. axillaris* was significantly and negatively correlated with SPEI during the second half of the year (July to December), and this correlation became stronger in the recent decades (Figure 5). However, correlations between mean temperature and tree growth were not stable throughout the analysis period.

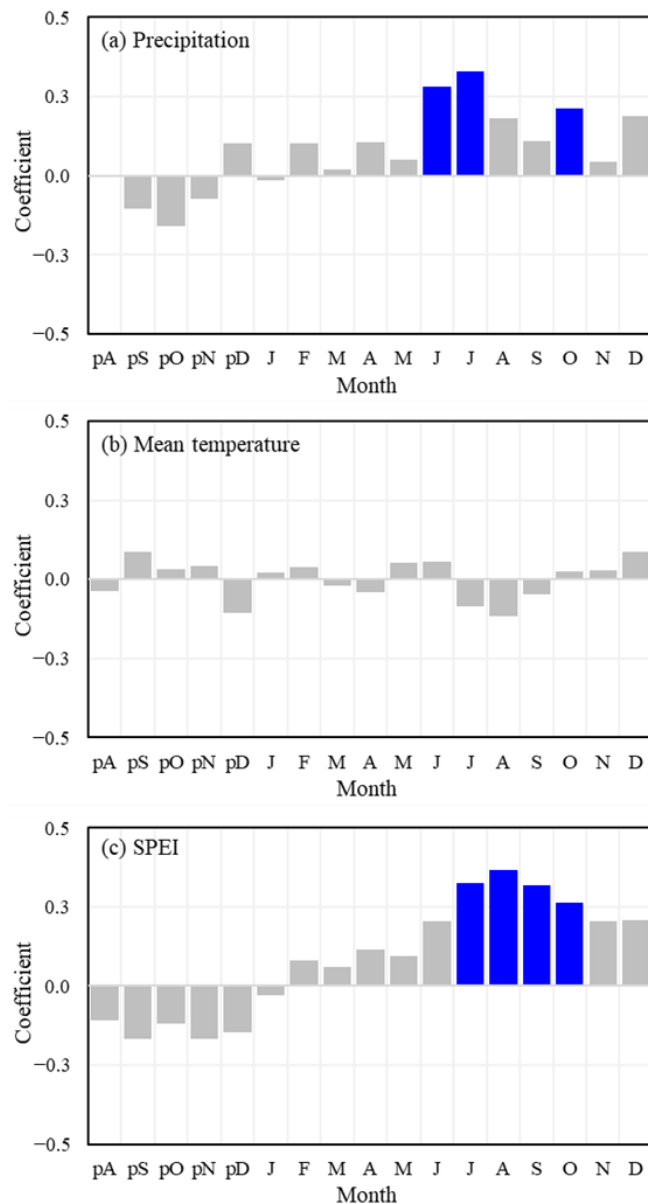


Figure 4. Correlation coefficients for *Choerospondias axillaris* tree-ring width index with monthly mean climate data. (a) Precipitation, (b) mean temperature, and (c) Standardized Precipitation–Evapotranspiration Index (SPEI). Blue and grey bars indicate statistically significant ($p < 0.05$) and non-significant ($p > 0.05$) correlations, respectively. p , month in the previous year.

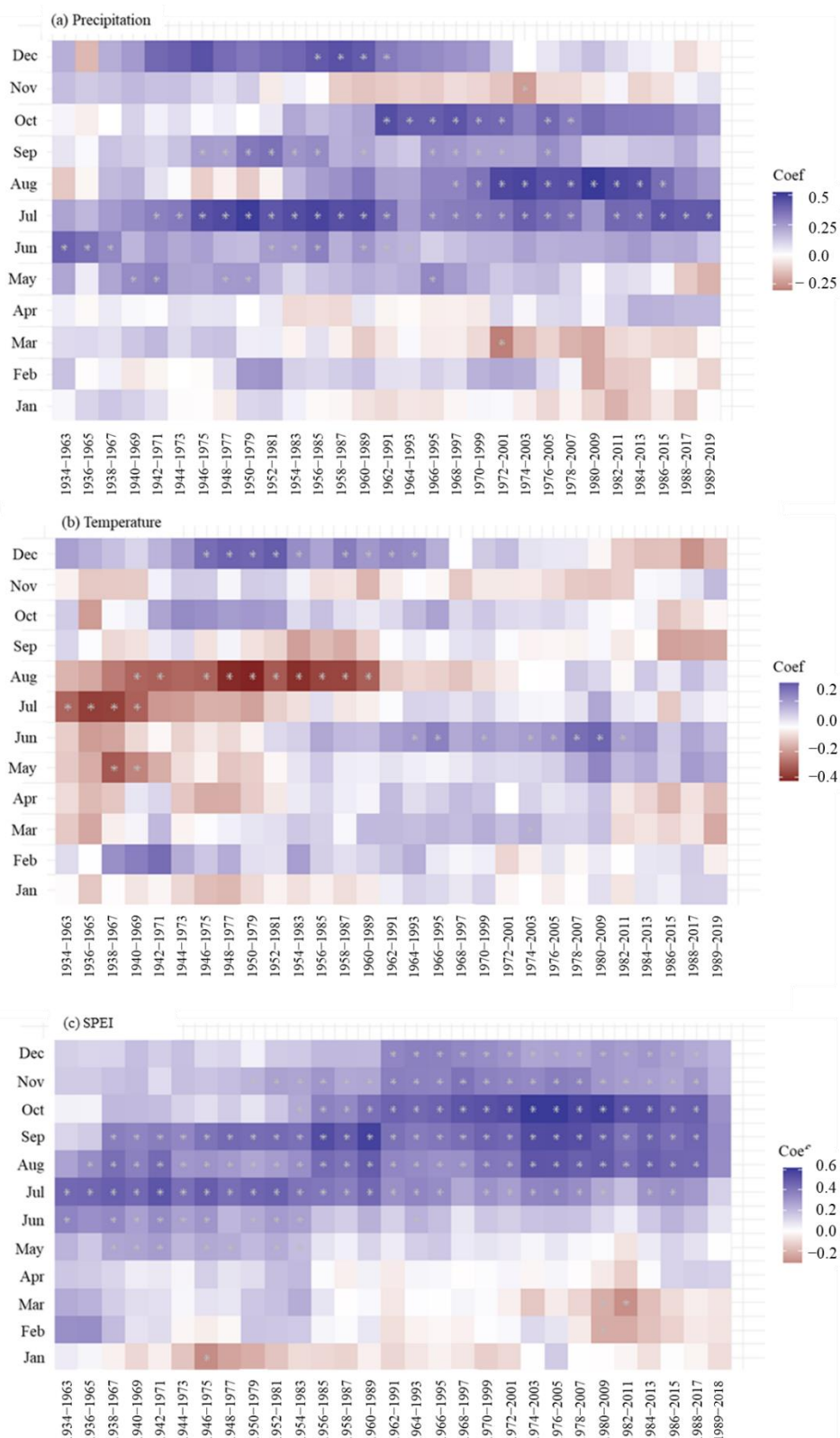


Figure 5. Moving correlation analysis of tree-ring width index for *Choerospondias axillaris* with (a) precipitation, (b) mean temperature, and (c) Standardized Precipitation-Evapotranspiration Index (SPEI). The correlation coefficients were computed from CRU TS climate data during the period of 1934 to 2019 for 30-year moving windows with a two-year offset. Color represents the scale of correlation coefficients ranging from positive (purple) to negative (brown). Significant correlation coefficients at 95% confidence level are indicated by white asterisks.

3.3. Long-Term Growth Trend and Climate Responses

The long-term growth of *C. axillaris* had a continually increasing trend from 1932 to 2002 (slope = 0.017, $p < 0.001$). However, growth had a significantly declining trend from 2003 to 2019 (slope = -0.014 , $p < 0.001$) (Figure 6).

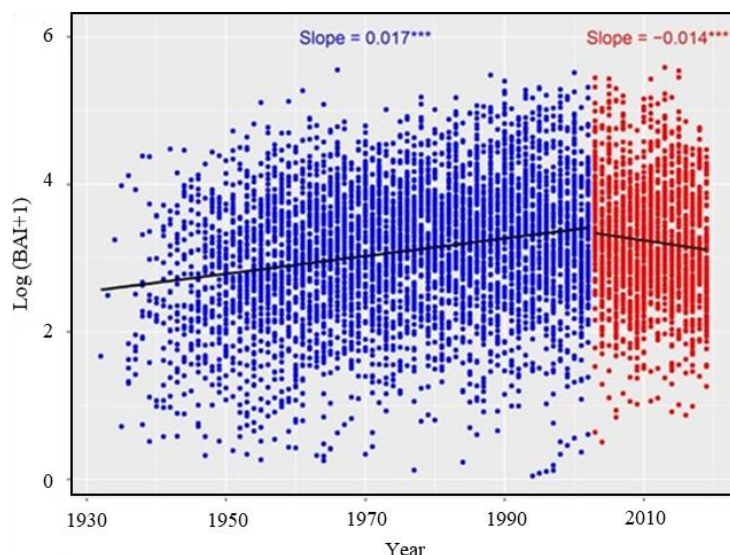


Figure 6. Long-term trends for basal area increment in *Choerospondias axillaris* at Mo Singto during the period 1932 to 2002 (blue) and 2003 to 2019 (red). Black lines represent growth trends modeled using linear mixed-effects models with “Year” as fixed factor, and “treeID” as a random factor. The slope of the fixed effect “Year” and the significance level from 1932 to 2002 and from 2003 to 2019 are given at the top (***, $p < 0.001$).

4. Discussion

4.1. *Choerospondias axillaris* Chronology Characteristics

Our study established a new tree-ring chronology for *C. axillaris* spanning from 1932 to 2019. Since only a few broad-leaved tree species have been studied in tropical regions, our study provided important information about the growth-climate relationships of tropical trees. Mean sensitivity (MS = 0.412) of this species was comparable to existing dendroclimatic studies for broad-leaved species from the tropics of Southeast Asia [45–48], indicating that growth of *C. axillaris* was highly responsive to year-to-year climatic variation. The Rbar was higher after 1985, indicating that the environmental influence on growth became stronger during recent decades. The EPS (0.968) of this chronology indicated that this species was reliable for dendroclimatic analysis [11].

We found that the tree-ring width chronology of *C. axillaris* had a rather high short-term variation, which may relate to the impact of fruit production. There is usually an inverse relationship between radial growth and fruit production [49,50]. Chanthorn and Brockelman (2008) observed that fruit production in the year 2004 was high (with abundant seeds in the field), whereas fruit production in the year 2005 was low (with fewer seeds in the field) [28]. High fruit production in 2004 corresponded to a narrower ring width index (0.76), whereas low fruit production in 2005 corresponded to a wider ring-width index (1.23). However, since long-term fruit production data were lacking, the relationship between radial growth and fruit production requires further study.

4.2. Growth–Climate Relationships

Our study found that the growth of *C. axillaris* was mainly limited by moisture availability in the monsoon season. Monsoon precipitation was found to limit the growth of teak (*Tectona grandis*) in Myanmar [45]. However, moisture availability during the dry season, or dry-to-wet season transition, was found to be the main limiting factor for tree

growth in tropical regions [48]. Pumijumnong and Buajan found that precipitation during March was the main factor influencing cambial activity of *C. axillaris* at the Mo Singto plot [29]. Although the cambial activity of tree species is related to climate in the transition season, maximum radial growth of tropical tree species occurs mainly in the late monsoon season (July to October) [51]. Our study found that the growth of *C. axillaris* was positively correlated with SPEI from July to October, which further confirmed that growth was limited by moisture availability in the late monsoon season.

Previous studies found that radial growth of tropical tree species was negatively correlated with temperature in the dry season and dry-to-wet transition in seasonally dry forests [48,52]. A higher temperature in the dry season increased evapotranspiration and induced water deficit [53], which further limits tree growth. However, we did not find a significant correlation between the radial growth of *C. axillaris* and temperature. It is possible that the mean temperature at this site was sufficiently low that evapotranspiration had not induced water deficit. The correlation between tree growth and July-to-October precipitation became stronger in recent years, which was similar to studies on *Pinus lamerri* in Northeastern Thailand [54] and *Pinus sylvestris* in Poland [55].

Individual genetic variation and topographic variables (slope, aspect, and elevation) will also impact tree growth-climate relations [13]. The relationships between fruit production and wood radial growth may also impact the growth-climate relationships for *C. axillaris*. Mund et al. (2020) [49] found that fruit production was negatively correlated with May precipitation, whereas wood growth was positively correlated with May precipitation. A precise understanding of climate-growth correlations needs to include long-term monitoring of fruiting.

4.3. Long-Term Growth Trends of *Choerospondias axillaris*

Our study revealed that the growth of *C. axillaris* in the Mo Singto plot had a continually increasing trend early in the analysis period, but that growth rate declined in recent decades, especially after the year 2003. These results were consistent with a previous study in which the growth trend of *P. lamerri* in Thailand had an increasing trend from 1951 to 1984, but a decreasing trend from 1985 to 2017 [54,56]. Growth over time also decreased for four broad-leaved tree species in Thailand [57]. The decreasing growth trend for *C. axillaris* in recent years could be related to increasing temperature and/or the decreasing trend in precipitation at the study site. Changes in temperature and precipitation may have affected tree growth in the last decades more widely [58]. Battipaglia et al. (2015) showed that decreasing growth for three tropical tree species from Central Africa was related to the increase in local temperature [59]. Van Der Sleen et al. (2015) found that there was no growth stimulation with the increase of water-use efficiency across three tropical forests worldwide [5]. The decrease in growth for *C. axillaris* in recent decades may also be related to the aging of the individual plants. The population of *C. axillaris* at Mo Singto was dominated by a cohort of aging individuals that were seeded around 90 years ago, and this species showed poor regeneration (i.e., recruitment failure) over time. Such recruitment failure over time alters the tree demography of the *C. axillaris* population, which has the potential to induce spurious negative growth trends in recent decades [60]. Therefore, multiple methods to detect growth trends and more robust analyses should be used to better understand the drivers of long-term trends in tree growth.

5. Conclusions

This study provided a new tree-ring chronology (spanning 1932 to 2019) for a tropical broad-leaved species, *Choerospondias axillaris*, from the Mo Singto Forest dynamic plot, Khao Yai National Park, east-central Thailand. The growth of *C. axillaris* was mainly limited by moisture availability in the late monsoon season during July to October. The long-term growth of *C. axillaris* had an increasing trend early in the chronology that transitioned into a decreasing growth trend during the two most-recent decades. Our study thus contributes a new broad-leaved species for dendrological studies in the tropics, where the number

of species targeted for tree-ring analysis needs to be increased to better understand and quantify the ecosystem services provided by tropical trees.

Supplementary Materials: The following are available online at <https://www.mdpi.com/article/10.3390/f12121655/s1>, Figure S1: Scanned image (a) and microscopic images from different sides, (b) cross section, (c) tangential section and (d) radial section of a wood core sample from *Choerospondias axillaris*. Black triangles indicate ring boundaries, while the year indicates calendar year of ring formation. The microscopic image taken from inside wood; Figure S2: Climate diagram according to Walter & Lieth for Mo Singto for the period from 1994 to 2019; Figure S3: Comparison of temporal pattern in annual climate between CRU TS data (blue line, 1932–2019) and Mo Singto station data (black line, 1994–2019) for (a) Precipitation, (b) Maximum temperature, (c) Mean temperature, and (d) Minimum temperature. ‘r’ indicates the correlation between CRU TS data and Mo Singto climate data for the period 1994 to 2019; Figure S4: Number of sampled trees classified according to DBH class. Figure S5: Density plot of break points for all individual trees of *Choerospondias axillaris*, calculated by the package ‘segmented’ in R. Dashed line indicates the highest frequency of break points, which was in the year 2003.

Author Contributions: P.F., N.P. and W.Y.B. conceived and designed the research; W.Y.B., Y.C., W.C., P.T.-n. and A.N. coordinated the permission for doing this study in the Khao Yai National Park; W.S. and S.B. performed the experiments; W.S., P.F. and S.P. analyzed the data; W.S., P.F. and N.P. wrote the draft; S.B., Z.F., P.M.F. and Y.Z. revised the draft. All the authors appraised the research, reviewed and edited the draft. All authors have read and agreed to the published version of the manuscript.

Funding: This work was supported by the National Natural Science Foundation of China (41861144016, 31870591, 3186113307), Thailand Science Research and Innovation (TSRI, RDG6230006), National Science and Technology Development Agency (NSTDA, P-18-51395), and Chinese Academy of Sciences President’s International Fellowship Initiative (No. 2018VBB0008 to P.M.F.).

Acknowledgments: We thank Arisa Kaewmano, Phisamai Maenpuen, Rampai Saenprasert and Xiaoxue Mo for their assistance in field sampling.

Conflicts of Interest: The authors declare no competing financial and any other potential conflict of interests.

References

1. IPCC. The physical science basis. In *Contribution of Working Group I to the Sixth Assessment Report of the Intergovernmental Panel on Climate Change*; Masson-Delmotte, V., Zhai, A.P., Pirani, S.L., Connors, C., Péan, S., Berger, N., Caud, Y., Chen, L., Goldfarb, M.I., Gomis, M., et al., Eds.; Cambridge University: Cambridge, UK, 2021.
2. Bonan, G.B. Forests and climate change: Forcings, feedbacks, and the climate benefits of forests. *Science* **2008**, *320*, 1444–1449. [\[CrossRef\]](#) [\[PubMed\]](#)
3. Allen, C.D.; Macalady, A.K.; Chenchoune, H.; Bachelet, D.; McDowell, N.; Vennetier, M.; Kitzberger, T.; Rigling, A.; Breshears, D.D.; Hogg, E.H.; et al. A global overview of drought and heat-induced tree mortality reveals emerging climate change risks for forests. *For. Ecol. Manag.* **2010**, *259*, 660–684. [\[CrossRef\]](#)
4. Zuidema, P.; Groenendijk, P.; Trouet, V.; Babst, F. Sensitivity of tropical tree growth to climatic variation: A global meta-analysis of tree-ring data. In *EGU General Assembly Conference Abstracts*; EGU: Munich, Germany, 2020; p. 7770.
5. Van Der Sleen, P.; Groenendijk, P.; Vlam, M.; Anten, N.P.R.; Boom, A.; Bongers, F.J.J.M.; Pons, T.L.; Terburg, G.; Zuidema, P. No growth stimulation of tropical trees by 150 years of CO₂ fertilization but water-use efficiency increased. *Nat. Geosci.* **2015**, *8*, 24–28. [\[CrossRef\]](#)
6. Panthi, S.; Bräuning, A.; Zhou, Z.-K.; Fan, Z.-X. Tree rings reveal recent intensified spring drought in the central Himalaya, Nepal. *Glob. Planet. Chang.* **2017**, *157*, 26–34. [\[CrossRef\]](#)
7. Panthi, S.; Fan, Z.; Van Der Sleen, P.; Zuidema, P.A. Long-term physiological and growth responses of Himalayan fir to environmental change are mediated by mean climate. *Glob. Chang. Biol.* **2019**, *26*, 1778–1794. [\[CrossRef\]](#) [\[PubMed\]](#)
8. Carrer, M.; Urbinati, C. Long-term change in the sensitivity of tree-ring growth to climate forcing in *Larix decidua*. *New Phytol.* **2006**, *170*, 861–872. [\[CrossRef\]](#)
9. Debel, A.; Meier, W.J.-H.; Bräuning, A. Climate signals for growth variations of *F. sylvatica*, *P. abies*, and *P. sylvestris* in Southeast Germany over the past 50 years. *Forests* **2021**, *12*, 1433. [\[CrossRef\]](#)
10. Elias, S.A.; Bradley, R.S.; Oakes, J.; Ogilvie, A.E.J.; Van Woert, M.L. Paleoclimatology: Reconstructing climates of the quaternary. *Arctic Antarct. Alp. Res.* **1999**, *31*, 329. [\[CrossRef\]](#)
11. Speer, J. *The Fundamentals of Tree-Ring Research*; The University of Arizona Press: Tucson, Arizona, 2012.

12. Brienen, R.J.W.; Schöngart, J.; Zuidema, P.A. Tree rings in the tropics: Insights into the ecology and climate sensitivity of tropical trees. In *Tree Physiology*; Springer: Singapore, 2016; Volume 6, pp. 439–461.

13. Pumijumnong, N. *Tree-Ring and Applications in Thailand*; Amarin Printing & Publishing Public Company Limited: Bangkok, Thailand, 2013.

14. Hughes, A.C. Understanding the drivers of Southeast Asian biodiversity loss. *Ecosphere* **2017**, *8*, e01624. [\[CrossRef\]](#)

15. Simonsen, D. The Importance of Tropical Forests: Why We Should Conserve Them and How They Affect the Rest of the World. Available online: <https://www.oxfordstudent.com/2018/10/16/the-importance-of-tropical-forests-why-we-should-conserve-them-and-how-they-affect-the-rest-of-the-world/> (accessed on 21 September 2021).

16. Tansley, A.G.; Douglass, A.E. Climatic cycles and tree-growth: A study of the annual rings of trees in relation to climate and solar activity. *J. Ecol.* **1920**, *8*, 62. [\[CrossRef\]](#)

17. Rozendaal, D.M.A.; Zuidema, P. Dendroecology in the tropics: A review. *Trees* **2010**, *25*, 3–16. [\[CrossRef\]](#)

18. Sarutanon, S.; Boonchirdchoo, S.; Arrigo, R.; Watanasak, M.; Barbetti, M.; Buckley, B. Dendrochronological investigations in Thailand. *IAWA J.* **1995**, *16*, 393–409.

19. Worbes, M. One hundred years of tree-ring research in the tropics—a brief history and an outlook to future challenges. *Dendrochronologia* **2002**, *20*, 217–231. [\[CrossRef\]](#)

20. Fichtler, E. Dendroclimatology using tropical broad-leaved tree species—a review. *Erdkunde* **2017**, *71*, 5–22. [\[CrossRef\]](#)

21. Dong, Z.; Baas, P. Wood anatomy of trees and shrubs from China. V. Anacardiaceae. *IAWA J.* **1993**, *14*, 87–102. [\[CrossRef\]](#)

22. Min, T.-L.; Barford, A. *Choerospondias axillaris*. Flora of China. Missouri Botanical Garden, St. Louis, MO & Harvard University Herbaria, Cambridge, MA, USA. Available online: http://www.efloras.org/florataxon.aspx?flora_id=2&taxon_id=200012681 (accessed on 25 November 2021).

23. Shrestha, N. An analysis of production and sales of *Choerospondias axillaris*. *Int. J. Hortic. Agric. Food Sci.* **2020**, *4*, 10–13.

24. McConkey, K.R.; Brockelman, W.Y.; Saralamba, C.; Nathalang, A.; Appendix, A. Percentage of *Garcinia benthamii* trees ($n = 10$) with fruit from 2003 to 2010 on the Mo Singto Forest Dynamics Plot, Khao Yai National Park, Thailand. In *2007 All Adult G. Benthamii Trees (n = 54) on the Plot Were Checked for Fruit and 45% Were Fruiting; Hence, Figures from 10 Trees May not Be Representative of Overall Fruit Availability*; Figshare: London, UK, 2016.

25. Harris, I.; Osborn, T.J.; Jones, P.; Lister, D. Version 4 of the CRU TS monthly high-resolution gridded multivariate climate dataset. *Sci. Data* **2020**, *7*, 1–18. [\[CrossRef\]](#)

26. Chayamarit, K. Preliminary Checklist of the Family Anacardiaceae in Thailand. *Thai For. Bull. Bot.* **1994**, *22*, 1–25.

27. Van Sam, H.; Nanthavong, K.; Kessler, P. Trees of Laos and Vietnam: A Field Guide to 100 Economically or Ecologically Important Species. *Blumea-Biodivers. Evol. Biogeogr. Plants* **2004**, *49*, 201–349. [\[CrossRef\]](#)

28. Chanthorn, W.; Brockelman, W. Seed dispersal and seedling recruitment in the light-demanding tree *Choerospondias axillaris* in old-growth forest in Thailand. *Sci. Asia* **2008**, *34*, 129–135. [\[CrossRef\]](#)

29. Pumijumnong, N.; Buajan, S. Seasonal cambial activity of five tropical tree species in central Thailand. *Trees* **2013**, *27*, 409–417. [\[CrossRef\]](#)

30. Elliott, S.; Navakitbumrung, P.; Kuarak, C.; Zangkum, S.; Anusarnsunthorn, V.; Blakesley, D. Selecting framework tree species for restoring seasonally dry tropical forests in northern Thailand based on field performance. *For. Ecol. Manag.* **2003**, *184*, 177–191. [\[CrossRef\]](#)

31. Cook, E.R.; Kariukstis, L.A. *Methods of Dendrochronology: Applications in the Environmental Sciences*; Springer: Dordrecht, The Netherlands, 1990; p. 394.

32. Holmes, R.L. Computer-Assisted quality control in Tree-Ring dating and measurement. *Tree-Ring Bull.* **1983**, *44*, 69–75.

33. Cook, E.R.; Peters, K. Calculating unbiased tree-ring indices for the study of climatic and environmental change. *Holocene* **1997**, *7*, 361–370. [\[CrossRef\]](#)

34. Bunn, A. A dendrochronology program library in R (dplR). *Dendrochronologia* **2008**, *26*, 115–124. [\[CrossRef\]](#)

35. R Core Team. *R: A Language and Environment for Statistical Computing*; R Foundation for Statistical Computing: Vienna, Austria, 2020. Available online: <https://www.R-project.org/> (accessed on 26 May 2021).

36. Fritts, H. *Tree Rings and Climate*; Serbiula (Sistema Librum 2.0); Elsevier: Amsterdam, The Netherlands, 1976.

37. Wigley, T.M.L.; Briffa, K.R.; Jones, P.D. On the average value of correlated time series, with applications in dendroclimatology and hydrometeorology. *J. Clim. Appl. Meteorol.* **1984**, *23*, 201–213. [\[CrossRef\]](#)

38. Briffa, K.R. Interpreting High-Resolution proxy climate data—The example of dendroclimatology. In *Analysis of Climate Variability: Applications of Statistical Techniques*; von Storch, H., Navarra, A., Eds.; Springer: Berlin/Heidelberg, Germany, 1995; pp. 77–94.

39. IBM Corp. IBM SPSS Statistics for Windows, 25.0. Available online: <https://www.ibm.com/analytics/spss-statistics-software> (accessed on 21 November 2021).

40. Zang, C.; Biondi, F. Treeclim: An R package for the numerical calibration of proxy-climate relationships. *Ecography* **2015**, *38*, 431–436. [\[CrossRef\]](#)

41. Bunn, A. Statistical and visual crossdating in R using the dplR library. *Dendrochronologia* **2010**, *28*, 251–258. [\[CrossRef\]](#)

42. Guada, G.; Camarero, J.; Sanchez-Salguero, R.; Navarro Cerrillo, R. Limited growth recovery after drought-induced forest dieback in very defoliated trees of two pine species. *Front. Plant Sci.* **2016**, *7*, 418. [\[CrossRef\]](#)

43. Muggeo, V.M. Interval estimation for the breakpoint in segmented regression: A smoothed score-based approach. *Aust. N. Z. J. Stat.* **2017**, *59*, 311–322. [\[CrossRef\]](#)

44. Bates, D.; Mächler, M.; Bolker, B.; Walker, S. Fitting linear mixed-effects models using lme4. *arXiv* **2015**, arXiv:1406.5823.

45. Zaw, Z.; Fan, Z.-X.; Bräuning, A.; Liu, W.; Gaire, N.P.; Than, K.Z.; Panthi, S. Monsoon precipitation variations in Myanmar since AD 1770: Linkage to tropical ocean-atmospheric circulations. *Clim. Dyn.* **2021**, *56*, 3337–3352. [\[CrossRef\]](#)

46. Rahman, M.; Islam, R.; Islam, M. Long-term growth decline in *Toona ciliata* in a moist tropical forest in Bangladesh: Impact of global warming. *Acta Oecol.* **2017**, *80*, 8–17. [\[CrossRef\]](#)

47. Pumijumnong, N. Teak tree ring widths: Ecology and climatology research in Northwest Thailand. *Sci. Tech. Dev.* **2012**, *31*, 165–174.

48. Vlam, M.V.; Baker, P.; Bunyavejchewin, S.; Zuidema, P. Temperature and rainfall strongly drive temporal growth variation in Asian tropical forest trees. *Oecologia* **2014**, *174*, 1449–1461. [\[CrossRef\]](#)

49. Mund, M.; Herbst, M.; Knohl, A.; Matthäus, B.; Schumacher, J.; Schall, P.; Siebicke, L.; Tamrakar, R.; Ammer, C. It is not just a ‘trade-off’ indications for sink and source limitation to vegetative and regenerative growth in an old growth beech forest. *New Phytol.* **2020**, *226*, 111–125. [\[CrossRef\]](#)

50. Knops, J.M.H.; Koenig, W.; Carmen, W.J. Negative correlation does not imply a tradeoff between growth and reproduction in California oaks. *Proc. Natl. Acad. Sci. USA* **2007**, *104*, 16982–16985. [\[CrossRef\]](#)

51. Hu, L.; Fan, Z. Stem radial growth in response to microclimate in an Asian tropical dry karst forest. *Acta Ecol. Sin.* **2016**, *36*, 401–409. [\[CrossRef\]](#)

52. Rahman, M.; Islam, M.; Wernicke, J.; Bräuning, A. Changes in sensitivity of Tree-Ring widths to climate in a tropical moist forest tree in Bangladesh. *Forests* **2018**, *9*, 761. [\[CrossRef\]](#)

53. Snyder, R.L.; Moratiel, R.; Zhenwei, S.; Swelam, A.; Jomaa, I.; Shapland, T. Evapotranspiraiton response to climate change. *Acta Hortic* **2011**, *922*, 91–98. [\[CrossRef\]](#)

54. Rakthai, S.; Fu, P.-L.; Fan, Z.-X.; Gaire, N.; Pumijumnong, N.; Eiadthong, W.; Tangmitcharoen, S. Increased drought sensitivity results in a declining tree growth of *Pinus latheri* in Northeastern Thailand. *Forest* **2020**, *11*, 361. [\[CrossRef\]](#)

55. Sensuła, B.; Wilczyński, S.; Opała, M. Tree growth and climate relationship: Dynamics of scots pine (*Pinus Sylvestris* L.) growing in the near-source region of the combined heat and power plant during the development of the pro-ecological strategy in Poland. *Water Air Soil Pollut.* **2015**, *226*, 1–17. [\[CrossRef\]](#) [\[PubMed\]](#)

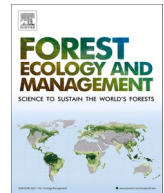
56. He, G.P.; Chen, Y.T.; Yu, Y.H.; Liu, H.T.; Cai, H.M.; Chen, Y.Z. Study on early growth characteristics of *Choerospondias axillaris* plantation and effect of *Choerospondias axillaris* and Cunninghamia lanceolata mixed stand. *For. Res.* **2004**, *17*, 206–212.

57. Groenendijk, P. Long-Term Trends in Tropical Tree Growth: A Pantropical Study. Ph.D. Thesis, Wageningen University, Wageningen, The Netherlands, 2015.

58. Somogyi, Z. Recent trends of tree growth in relation to climate change in Hungary. *Acta Silv. Lignaria Hung.* **2008**, *4*, 17–27.

59. Battipaglia, G.; Zalloni, E.; Castaldi, S.; Marzaioli, F.; Gatti, R.C.; Lasserre, B.; Tognetti, R.; Marchetti, M.; Valentini, R. Long Tree-Ring chronologies provide evidence of recent tree growth decrease in a central african tropical forest. *PLoS ONE* **2015**, *10*, e0120962. [\[CrossRef\]](#)

60. Brienen, R.J.W.; Gloor, E.; Zuidema, P.A. Detecting evidence for CO₂ fertilization from tree ring studies: The potential role of sampling biases. *Glob. Biogeochem. Cycles* **2012**, *26*, 26. [\[CrossRef\]](#)



Variation of leaf-level gas exchange rates and leaf functional traits of dominant trees across three successional stages in a Southeast Asian tropical forest



Pantana Tor-ngern ^{a,b,c,*}, Chidsanuphong Chart-as^{a,b}, Wirong Chanthorn ^{d,e}, Chadtip Rodtassana ^f, Siriphong Yampum ^g, Weerapong Unawong ^h, Anuttara Nathalang ⁱ, Warren Brockelman ⁱ, Kanchit Srinoppawan ^j, Yajun Chen ^k, Niles J. Hasselquist ^l

^a Department of Environmental Science, Faculty of Science, Chulalongkorn University, Bangkok 10330, Thailand

^b Environment, Health and Social Data Analytics Research Group, Chulalongkorn University, Bangkok 10330, Thailand

^c Water Science and Technology for Sustainable Environment Research Group, Chulalongkorn University, Bangkok 10330, Thailand

^d Department of Environmental Technology and Management, Faculty of Environment, Kasetsart University, Bangkok 10900, Thailand

^e Department of Ecological Modelling, Helmholtz Centre for Environmental Research UFZ, 04318, Leipzig, Germany

^f Department of Botany, Faculty of Science, Chulalongkorn University, Bangkok 10330, Thailand

^g Graduate School, Chulalongkorn University, Bangkok 10330, Thailand

^h Center of Excellence on Hazardous Substance Management, Chulalongkorn University Bangkok 10330, Thailand

ⁱ National Biobank of Thailand, National Science and Technology Development Agency, Pathum Thani 12120, Thailand

^j Department of National Parks, Wildlife and Plant Conservation, Bangkok 10900, Thailand

^k Key Laboratory of Tropical Forest Ecology, Xishuangbanna Tropical Botanical Garden, Chinese Academy of Sciences, Mengla, Yunnan 666303, China

^l Department of Forest Ecology and Management, Swedish University of Agricultural Sciences, Umeå 90183, Sweden

ARTICLE INFO

ABSTRACT

Keywords:

Forest succession

Functional traits

Photosynthesis

Stomatal conductance

Tropical forests

Deforestation has created heterogeneous patches of old-growth and secondary forests throughout Southeast Asia, posing challenges for understanding the hydrological and carbon cycles. In addition to changes in species composition, environmental conditions differ across successional stages which in turn can influence forest water use and productivity. Here, we investigated leaf-level area-based photosynthesis (A_{area}) and stomatal conductance (g_s) of 11 tree species dominating an old-growth (OF; >200 years), an intermediate (IF; ~44 years), and a young forest (YF; ~4 years) in Thailand during both the wet and dry season. Specifically, we compared A_{area} and g_s and assessed the sensitivity of g_s to vapor pressure deficit (VPD). We also examined relationships between gas exchange parameters and key functional leaf traits, including leaf mass per area (LMA), nitrogen (N), phosphorus (P), and chlorophyll concentration. All three forests showed comparable A_{area} and g_s in the wet season, whereas significantly lower values were observed in IF during the dry season. All forest stages displayed similar sensitivity of g_s to VPD. Among the leaf functional traits considered, LMA, N and P were significantly higher in YF compared to the other two successional stages. Our results suggested that forest succession may not influence gas exchange, rather, canopy development associated with forest stage produced the main effect. Furthermore, the young forest was the most active in resource acquisition with its high LMA and leaf nutrient concentrations, which could result in high photosynthetic rates. However, low soil water availability in YF possibly limit the gas exchange rates thereby making them similar to those in the old-growth forest. These findings highlight the potential effects of canopy characteristics inherent in successional forests on water and carbon exchanges between trees and the atmosphere and their sensitivity to atmospheric drought. These results call for the need for further studies to identify the main factors influencing forest productivity during secondary succession in the tropics, particularly in the Southeast Asian region where such information is lacking.

* Corresponding author at: Department of Environmental Science, Faculty of Science, Chulalongkorn University, Bangkok 10330, Thailand.

E-mail address: Pantana.t@chula.ac.th (P. Tor-ngern).

1. Introduction

Tropical forests play an important role in the biosphere, especially in global water and carbon cycles. Transpiration represents *ca.* 40–90% of the total amount of water emitted to the atmosphere (e.g., Miralles et al., 2011; Jasechko et al., 2013; Wang-Erlundsson et al., 2014; Good et al., 2015) and thus strongly influences hydrology and energy partitioning in terrestrial ecosystems (Bonan, 2008). Tropical forests sequester *ca.* 0.28–1.26 Pg C each year (Hubau et al., 2020) and thus play a critical role in mitigating rising atmospheric carbon dioxide and related climate change impacts. However, widespread deforestation and land use change are rapidly transforming these ecosystems, with over 80 million hectares of natural, old-growth tropical forests being lost since 1990 (FAO and UNEP, 2020). Deforestation and land use change is especially pervasive across Southeast Asia (Zeng et al., 2018; FAO and UNEP, 2020), where large-scale agricultural production and commercial tree plantations have been the main drivers of forest loss (Curtis et al., 2018). However, many of these large-scale operations have been abandoned because of unsustainable practices, leading to the regeneration of secondary forests either through natural or aided processes. Consequently, forests in Southeast Asia are characterized by a patchy mosaic of primary, old-growth forests, and forests at different stages of secondary succession.

Structural attributes, such as canopy height and tree density, vary considerably among forests which in turn can strongly influence the microclimate (Rambo and North, 2009; Jucker et al., 2018) as well as the carbon and water balance in old growth, primary forests, and forests at different stages of secondary succession (Powers and Marín-Spiotta, 2017). Old-growth forests usually contain larger trees and heterogeneous canopy layers, and lower stem density, compared to secondary forests (Chazdon, 2014; Chanthorn et al., 2016, 2017; Jucker et al., 2018). Conversely, the intermediate successional stage, namely the “stem exclusion” stage, has a relatively homogeneous canopy and high stem density (Chazdon, 2014; Chanthorn et al., 2016, 2017). Variation in canopy height can lead to differences in the convective boundary layer which is responsible for transport of energy and gases from plant surfaces to the atmosphere. Smaller convective boundary layers over early successional forest (stand initiation stage), which are characterized by low canopy height, result in a hotter and drier microclimate, especially during the dry season (Fisch et al., 2004). Additionally, early successional forests have greater variability in their physical environments, including water and light conditions, compared to later successional and old growth forests (Culf et al., 1996). Consequently, species acclimated to early-successional stages tend to have higher gas exchange rates, and higher stomatal conductance and photosynthesis (Hölscher et al., 2006; Vargas and Cordero, 2013; Mujawamariya et al., 2018). In contrast, the canopy is more homogeneous and shaded in the intermediate, stem exclusion stage (Chazdon, 2014; Chanthorn et al., 2016, 2017), which constrains gas exchange, especially leaf transpiration (Hardwick et al., 2015).

Environmental gradients during secondary succession can impact the strategies trees use to acquire resources and ultimately lead to differences in tree species richness and composition among different successional forests (Zhang et al., 2012; Chazdon, 2014; Chanthorn et al., 2016, 2017). Previous studies in humid tropical forests have shown that decreasing light penetration during secondary succession results in changes of leaf traits (Lohbeck et al., 2013, 2015). Most trees in early successional forests are fast-growing species and, according to the leaf economic spectrum (Wright et al., 2004), have leaf traits promoting quick returns on investment in nutrients and carbon (i.e., high specific leaf area and nutrient levels, short lifespan and high metabolic rates). In contrast, trees in old growth forests tend to exhibit conservative strategies (Lohbeck et al., 2013, 2015) with high investments in leaf carbon structures (i.e., high leaf dry matter content). However, in dry tropical forests, the light gradient during succession is less pronounced and these forests are often more water-limited and have higher temperatures

which may be stronger factors driving changes in plant communities (Lebrero-Trejos et al., 2010, 2011). In general, trees growing in more xeric conditions tend to exhibit leaf traits with slow returns on resource investment, i.e., have conservative strategies (Reich, 2014). Yet, we still know little about how leaf traits vary during secondary succession in dry tropical forests and how variation in leaf traits and microclimate conditions affect leaf gas exchange measurements (i.e., photosynthesis and transpiration) and ultimately, the growth and productivity of these forests.

In this study, we measured leaf-level gas exchange and plant functional traits of the dominant tree species in a seasonal evergreen forest in Thailand. Measurements were made during both the wet (May–October) and dry (November–April) season as well as within forests representing different stages of succession: a young forest (YF, \sim 4 years), an intermediate forest (IF, \sim 44 years) and an old-growth forest (OF, >200 years). Specifically, our study addressed the following questions: (Q1) Does leaf-level gas exchange (photosynthesis and stomatal conductance) differ across successional forests and between seasons? (Q2) Does the sensitivity of stomatal conductance to changes in atmospheric demand vary across different stages of forest succession? (Q3) How do different leaf functional traits relate to leaf gas exchange parameters, and do these relationships change depending on forest stage? Results from this study will improve our understanding of the underlying mechanisms governing water and carbon fluxes in different successional forests as well as assessing how these forests may respond to a hotter, drier future.

2. Materials and methods

2.1. Site description

The study was carried out in Khao Yai National Park (KYNP), a seasonal evergreen forest in Nakhon Ratchasima Province, Thailand ($14^{\circ}26'31''$ N, $101^{\circ}22'55''$ E, 700–800 m asl; Fig. 1). Based on 1994–2018 data, mean annual temperature and precipitation at the site are about 22.4°C and 2100 mm, respectively. The wet season usually covers the months from May to October while the dry season ranges from November to April, when monthly precipitation is less than 100 mm (Brockelman et al., 2017). KYNP contains a mosaic of different forest types including old-growth (primary) forests and secondary forests of different ages that have regenerated from old fields within the past 42 years (Jha et al., 2020). In this study, we selected three plots representing different successional stages. The first plot was within the 30-ha Mo Singto forest dynamic plot (Brockelman et al., 2017), a ForestGEO plot in the network of the Centre for Tropical Forest Science (CTFS), Smithsonian Tropical Research Institute. These plots were established using a uniform methodology (Condit, 1998) in which every woody stem ≥ 1 cm DBH is identified, mapped, and measured every five years. This plot represented an old-growth stage (hereafter OF), with the age of at least *ca.* 200 years. The OF's main canopy height was 20–30 m with some emergent trees being higher than 50 m, a leaf area index (LAI) of 5 and stem density of 1112 trees ha^{-1} (Chanthorn et al., 2016; Brockelman et al., 2017). Adjacent to the northern edge of this plot, a 1-ha plot in a secondary forest was established in 2003, using the same CTFS methods. This plot (hereafter IF) was in an intermediate successional stage at about 44 years of age and classified as stem exclusion stage. The forest canopy of IF was more homogenous and denser compared to that of OF and had a mean canopy height of 25 m, an LAI of 6, and stem density of 2052 trees ha^{-1} (Chanthorn et al., 2016). Approximately 3 km away from the OF plot, we established a 2-ha plot in a 4-year-old, early successional forest (hereafter YF). Its mean canopy height was 15 m and stem density of 1226 trees ha^{-1} . Despite the lack of LAI data, the YF canopy was distinctly sparse compared to the other stages based on visual observation. The IF and YF were classified as “stem exclusion” and “stand initiation” stages, respectively (Chazdon, 2014; Chanthorn et al., 2016, 2017). The soil type of these forests was gray, brown ultisol, but the soils under the IF and YF were degraded by

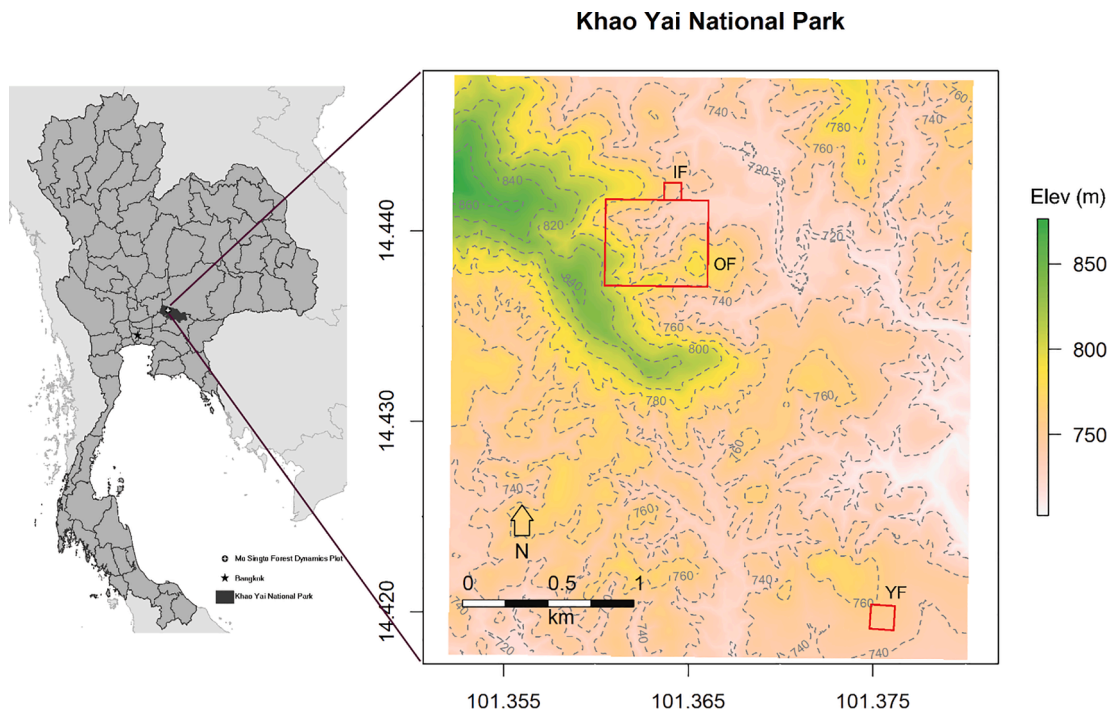


Fig. 1. Study sites include a young (YF), an intermediate (IF) and an old growth (OF) forest in Khao Yai National Park, Thailand.

shifting agriculture and burning prior to regeneration (Chanthorn et al., 2016, 2017).

2.2. Plant materials and measurements

In each plot, we selected five dominant tree species, based on basal area ranking within the site. The selection resulted in 11 species in total with three species occurring in more than one forest stage: *Syzygium nervosum* in IF and YF, *Schima wallichii* in OF and IF, and *Symplocos cochinchinensis* in all stages. Table 1 summarizes the selected dominant species in each study site.

For each species, five trees of similar stem size (diameter at breast height averaged 13.83 ± 2.74 cm (standard deviation); Table S1 in *Supplementary Information*) were randomly selected for gas exchange measurements and leaf sample collection. For each tree, we randomly chose three mature and fully expanded leaves with good exposure to sunlight from the lower and outside branches (Kröber et al., 2015). For sampling in the intermediate and old-growth forests, we particularly selected leaves that were always present in light gaps within each canopy to ensure that the leaves received full or substantial sunlight (Fan et al., 2011; Markesteijn et al., 2011; Zhu et al., 2013). Since the canopy could not be accessed directly due to the unavailability of towers or canopy cranes, we had to perform the measurements on cut branches containing the sun-exposed leaves with the stems submerged in a container filled with water. Prior to gas exchange measurements, the stems of individual branches were recut underwater to allow the restoration of the xylem water column (Dang et al., 1997). Within 5 min

after re-cutting, we placed a leaf in the cuvette for gas exchange measurement to minimize excision-induced effects (Santiago and Mulkey, 2003). Then, we waited for at least 2–3 min to allow the leaf to reach small changes in gas exchange over time before logging the data after observing stable gas exchange parameters. Leaf gas exchange measurements were made using a portable photosynthesis system (TARGAS-1, PP Systems, Amesbury, MA, USA). All leaves covered the entire window area of the cuvette which was equal to 4.5 cm^2 . Area-based photosynthetic rate (A_{area} ; $\mu\text{mol m}^{-2} \text{s}^{-1}$) and stomatal conductance (g_s ; $\text{mmol m}^{-2} \text{s}^{-1}$) were recorded for each leaf and reported per unit area. All measurements were conducted between 0900 and 1600 h (Mareno et al., 2001). We realized that the measurement period was longer than that often used for gas exchange measurement to avoid stomatal closure which is usually 1–2 h before and after midday (Brodribb and Holbrook, 2004; Bianco and Avelone, 2014; Urban et al., 2014). However, because of logistical issues, we utilized sunny conditions between the periods for gas exchange measurements. Nevertheless, we compared both A_{area} and g_s values that were recorded after 1400 h with those recorded during midday (1000–1400 h) on the same day and found no statistical differences (Fig. S1; $p \geq 0.064$). The flow rate was set to 250 ml min^{-1} (TARGAS-1 Portable Photosynthesis System Operation Manual Version 1.04 2018). Photosynthetically active radiation (PAR; $\mu\text{mol m}^{-2} \text{s}^{-1}$) inside the cuvette was set to $1700 \mu\text{mol m}^{-2} \text{s}^{-1}$, which corresponded to the light saturation point (data not shown; Hölscher et al., 2006; Zhu et al., 2013). Temperature, relative humidity and CO_2 concentration were not controlled and thus tracking ambient conditions. Because no previous publications reporting gas exchange measurements from this model of portable photosynthesis system were found, we compared our measured values to others made in tropical forests (Table S2) by plotting photosynthesis against stomatal conductance (Fig. S2). Although our values are mostly concentrated in the low ranges of photosynthesis and stomatal conductance, they fall within the ranges of values measured by other techniques. We realized that this comparison may not fully justify our measurements, but our main goal was to study the variations among forest stages rather than attempting to quantify absolute gas exchange rates.

Leaf-to-air vapor pressure deficit (VPD; kPa) was recorded for each measurement and used in the sensitivity analysis. Leaf-level gas ex-

Table 1
Dominant tree species selected for measurements in each forest stage in Khao Yai National Park, Thailand.

Old growth (OF)	Intermediate (IF)	Young (YF)
<i>Dipterocarpus gracilis</i>	<i>Syzygium nervosum</i>	<i>Adinandra integerrima</i>
<i>Ilex chevalieri</i>	<i>Eurya acuminata</i>	<i>Cratoxylum cochinchinensis</i>
<i>Schima wallichii</i>	<i>Machilus gamblei</i>	<i>Syzygium nervosum</i>
<i>Sloanea sigu</i>	<i>Schima wallichii</i>	<i>Syzygium antisepticum</i>
<i>Symplocos cochinchinensis</i>	<i>Symplocos cochinchinensis</i>	<i>Symplocos cochinchinensis</i>

change measurements were performed in both the dry (March 2019, total monthly precipitation = 0.8 mm) and the wet (July 2019, total monthly precipitation = 141.7 mm) seasons. During the wet season campaign, we also collected the leaves on which gas exchange measurements were made to measure leaf functional traits. Leaf functional traits used in this study included leaf mass per area (LMA; g m^{-2}), area-based nitrogen (N; g cm^{-2}) and phosphorus (P; g cm^{-2}) concentration, and chlorophyll concentration (Chl; $\mu\text{g cm}^{-2}$). LMA was calculated as the ratio of leaf dry mass and leaf area (Poorter et al., 2009), measured by ImageJ (Schneider et al., 2012). For chemical analyses of total N and P concentrations, three leaves from each tree were pooled to obtain enough samples (at least 0.1 g) for laboratory analyses. Total N was determined using the Kjeldahl method (Kammerer et al., 1967) and the colorimetric method was used to determine total P (Gales et al., 1966). Chlorophyll concentration was estimated from SPAD values (range 34.3–75.8) which were measured using the SPAD-502 chlorophyll meter (Konica Minolta, Tokyo, Japan). We converted SPAD into Chl using the relationship derived from 13 Neotropical species ($\text{Chl} = \frac{117.1 \times \text{SPAD}}{148.84 - \text{SPAD}}$, $r^2 = 0.89$, SPAD value ≤ 80 ; Coste et al., 2010).

2.3. Statistical analyses

To test for significant differences in A_{area} and g_s among forest stages and seasons (Q1), we used a General Linear Mixed Model with forest stage and season as fixed factors and species as a random factor. A Tukey's test was applied for post hoc analysis. We conducted regression analyses using exponential decay and logarithmic functions to analyze the sensitivity of g_s to VPD. To compare the sensitivity across forest stages (Q2), we performed the analysis with pooled data from all species within each stage and then analyze the data from species that existed in multiple stages (i.e., *Syzygium nervosum* (IF, YF), *Schima wallichii* (OF, IF) and *Symplocos cochinchinensis* (all stages)). We applied an F-test to compare the regression curves among stages. In these analyses, the sample size was 15 per species, resulting in 75 samples for each stage. We performed a one-way Analysis of Variance (ANOVA) to compare leaf traits, which were only measured in the wet season, across forest stages. We did regression analysis to evaluate the relationships between A_{area} and g_s and the leaf traits and used an Analysis of Covariance (ANCOVA) to assess variations of significant relationships across forest stages. All analyses of comparisons were done in SPSS (IBM Corp. Released 2013. IBM SPSS Statistics for Windows, Version 22.0. Armonk, NY, USA) and regression analyses were performed in SigmaPlot (version 12.0, Systat Software, Inc., San Jose, CA, USA). In all statistical analyses, we used the significance level of 0.01.

3. Results

3.1. Does leaf-level gas exchange differ across successional forests and between seasons?

In general, species in all forest stages had higher A_{area} and g_s in the wet than in the dry season ($p \leq 0.0001$). When combining data from both the wet and dry season, there was no significant difference in A_{area} and g_s among successional forest stages ($p \geq 0.184$). However, when comparing dry-season measurements, there were significant differences in A_{area} and g_s among the forest stages ($p \leq 0.0006$; Fig. 2 brown bars), whereas there were no differences in the wet season ($p \geq 0.03$; Fig. 2 yellow bars). In the dry season, trees in OF and YF had comparable A_{area} and g_s but higher values than trees in IF (Fig. 2).

For *Schima wallichii* and *Symplocos cochinchinensis*, tree species found in multiple sites, there was no significant difference in A_{area} and g_s among forest stages during the wet season ($p \geq 0.659$; Fig. 3A, B, D, E; yellow bars). However, during the dry season these two species had significantly higher gas exchange rates in OF compared to the younger sites ($p \leq 0.004$, 3A, B, D, E; brown bars). For *Syzygium nervosum*, which was found in the intermediate and early successional forests, A_{area} and g_s were similar across stages regardless of season (Fig. 3C, F; $p \geq 0.631$).

3.2. Does the sensitivity of stomatal conductance to changes in atmospheric demand vary across forest succession?

We tested the relationship between g_s and VPD in all tree species using data from both seasons. Various equations have been proposed to explain such relationship, including linear (McCaughay and Iacobelli, 1994), exponential (Dye and Olbrich, 1993) and logarithmic (Oren et al., 1999). We employed these equations in our regression analysis for each species in each stage and found significant results with exponential ($y = a \times \exp(-bx) + c$) and logarithmic ($y = b \times \ln(x) + c$) forms in 10 out of 11 species, which is consistent with previous studies of various tree species (Oren et al., 1999; Mielke et al., 2005; Motzer et al., 2005). No equation could explain the relationship in *Machilus gamblei*. First, we examined the relationship between g_s

and VPD in all dominant species within each site. We found that g_s exponentially decreased with VPD in all forests ($p < 0.0001$, $r^2 \geq 0.66$) with no difference among successional stages (Fig. 4A, $F_{2,447} = 1.25$, $p = 0.287$). Next, we further considered the species that occurred in multiple forest stages. A logarithmic decline was the best fit between g_s and VPD for *Syzygium antisepticum*, whereas for *Schima wallichii* and *Symplocos cochinchinensis*, an exponentially decaying function was the best fit (Fig. 4B-D; $p \leq 0.01$). When compared among sites, the relationships between g_s and VPD for these species were similar across forest stages ($p \geq 0.136$). Summary statistics for regression and comparative analyses are shown in Table S3.

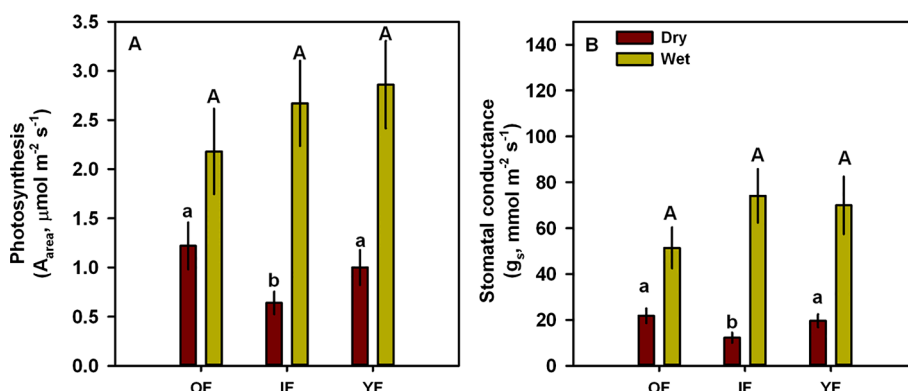


Fig. 2. Overall mean ($\pm 1 \text{ SE}$) leaf-level (A) photosynthesis (A_{area} ; $\mu\text{mol m}^{-2} \text{s}^{-1}$) and (B) stomatal conductance (g_s ; $\text{mmol m}^{-2} \text{s}^{-1}$) in young (YF), intermediate (IF) and old-growth forests (OF) within Khao Yai National Park, Thailand. Measurements were taken in the dry (brown bars) and the wet (yellow bars) season. Different lowercase (uppercase) letters indicate significant difference among forest stages during the dry (wet) season. (For interpretation of the references to colour in this figure legend, the reader is referred to the web version of this article.)

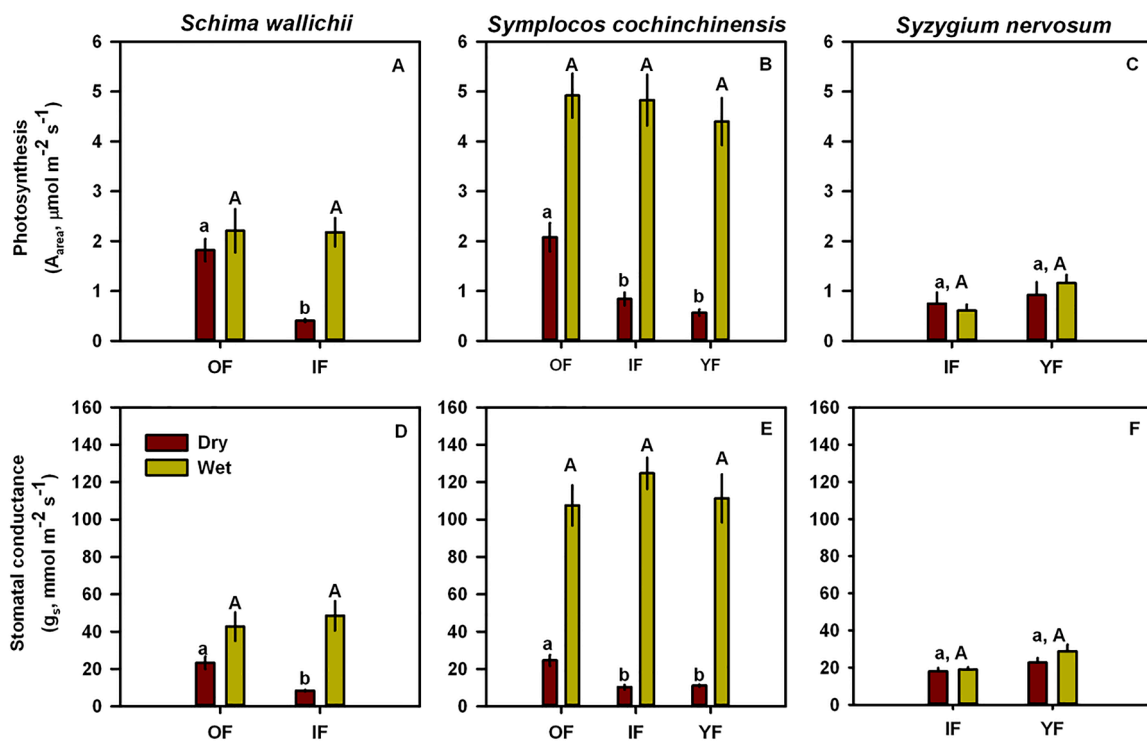


Fig. 3. Mean (± 1 SE) leaf-level (A–C) photosynthesis (A_{area} ; $\mu\text{mol m}^{-2} \text{s}^{-1}$) and (D–F) stomatal conductance (g_s ; $\text{mmol m}^{-2} \text{s}^{-1}$) of species that occurred in multiple forest stages in Khao Yai National Park. Measurements were made during the dry (brown bars) and wet (yellow bars) season. Different lowercase (uppercase) letters indicate significant difference among forest stages during the dry (wet) season. (For interpretation of the references to colour in this figure legend, the reader is referred to the web version of this article.)

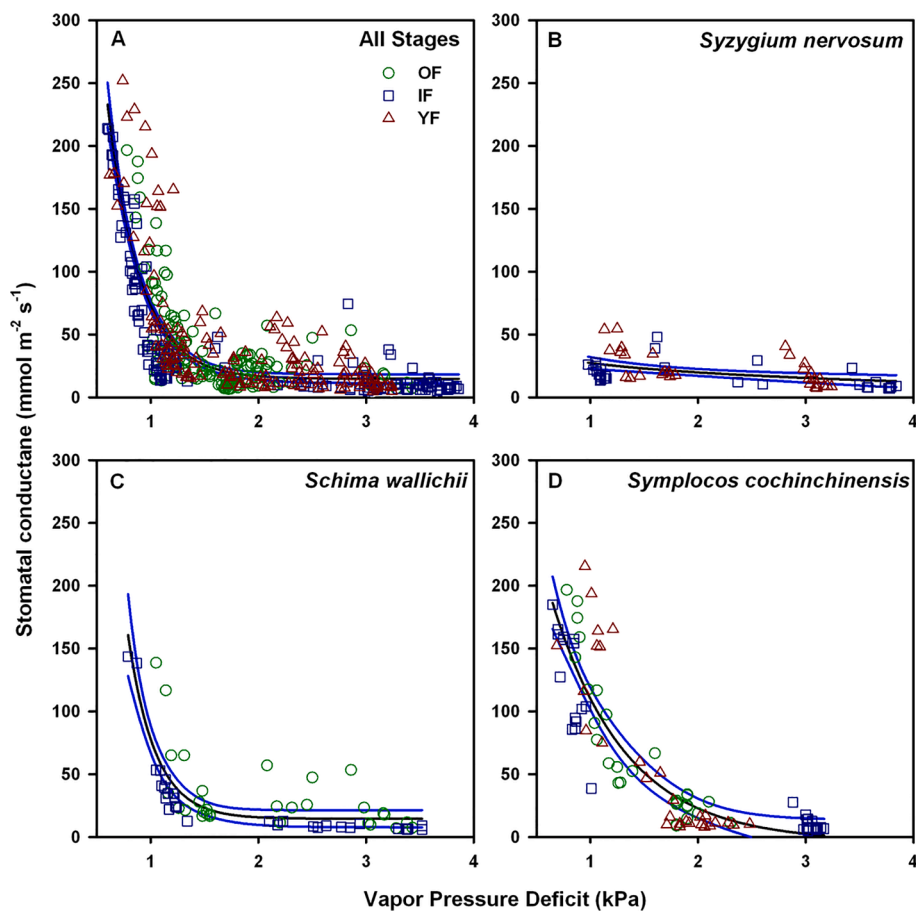


Fig. 4. Relationships between leaf-level stomatal conductance (g_s ; $\text{mmol m}^{-2} \text{s}^{-1}$) and leaf-to-air vapor pressure deficit (VPD; kPa) for (A) all forest stages (B) *Syzygium nervosum*, (C) *Schima wallichii*, and (D) *Symplocos cochinchinensis*. Measurements were made in an old-growth forest (OF, green circles), an intermediate forest (IF, blue squares), and a young forest (YF, red triangles). Black solid lines show the best fits with 95% confidence intervals (blue lines) for pooled data after finding no difference among different stages. Regression statistics are presented in Table S3. (For interpretation of the references to colour in this figure legend, the reader is referred to the web version of this article.)

3.3. How do different leaf functional traits relate to leaf gas exchange parameters and do these relationships change depending on forest stage?

For this research question, we focused on the wet season only due to the availability of data. Across the three forest stages, average LMA, P and N values were higher in YF compared to the two older forests (Fig. 5A–C; $p < 0.0001$). In contrast, there was no significant difference in Chl among the successional forests (Fig. 5D; $p = 0.067$). Next, we explored the relationships between gas exchange parameters and the leaf traits. Of all considered traits, only LMA and N were significantly related with A_{area} and g_s in IF and OF ($p \leq 0.01$). We further compared the relationships between both gas exchange parameters and LMA and N in OF and IF and found no difference between the stages ($p \geq 0.024$). Fig. 6 shows the significant relationships for the pooled data from both OF and IF (black solid lines; regression statistics are listed in Table S3).

4. Discussion

Seasonal variations in both gas exchange parameters were observed at the forest level and at species level. Generally, both A_{area} and g_s were higher in the wet than in the dry season. For all studied species, lower A_{area} and g_s in the dry season corresponded to higher VPD (Table S1) which is consistent with plants closing their stomata in response to increasing atmospheric drought (Cunningham, 2004; Chen et al., 2016). These results suggested that productivity of these successional stages may differ, especially during the dry season when both atmospheric and soil humidity are usually limiting (Harper et al., 2013). However, we found no significant difference in the gas exchange parameters across our successional forests during the wet season. Instead, a significant decrease in the parameters was observed in the intermediate forest (IF) with the highest stem density (2052 trees ha^{-1} vs. 1112 trees ha^{-1} and 1226 trees ha^{-1} in OF and YF, respectively), in the dry season. Such high density induces shading in the canopy with lower variability in LAI (Chazdon, 2014; Chanthorn et al., 2016, 2017) and may limit the gas exchange as previously observed in shade-acclimated trees (Chazdon et al., 1996; Gerardin et al., 2018; Yang et al., 2019). Based on

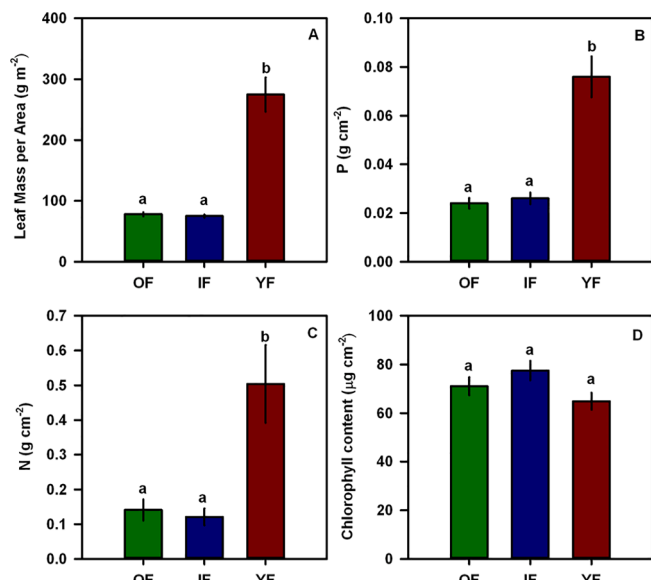


Fig. 5. Mean (\pm SE) (A) leaf mass per area (LMA; $g m^{-2}$), (B) phosphorus concentration (P; $g cm^{-2}$), (C) total nitrogen concentration (N; $g cm^{-2}$) and (D) chlorophyll concentration (Chl; $\mu g cm^{-2}$) among the old-growth (OF; green bars), intermediate (IF, blue bars), and young (YF, red bars) forest stages. Lower case letters indicate significant differences among forest stages. (For interpretation of the references to colour in this figure legend, the reader is referred to the web version of this article.)

observations, the indifference of gas exchange parameters across stages in the wet season may result from the higher canopy leaves in OF and YF compared to those in the dry season. In other words, the shaded canopy in IF maintained throughout seasons while the canopy in OF and YF varied seasonally, with the greatest difference between seasons in YF. Further measurements of canopy leaf areas should be performed to confirm this point. Overall, our results suggest that the gas exchange rates did not differ across forest succession but were affected by different microclimates induced by different canopy density. Nevertheless, previous reports on gas exchange measurements in various tropical tree species have shown inconclusive evidence on the effects of forest succession on leaf gas exchange rates (Hogan et al., 1995; Coste et al., 2005; Hölscher et al., 2006).

Next, we examined species that grew in multiple successional stages to further investigate the effect of forest succession on gas exchange rates. There were no differences in gas exchange for *Syzygium nervosum* among the forest stages regardless of season. In contrast, *Schima wallichii* and *Symplocos cochinchinensis* exhibited higher gas exchange rates in the old growth forest compared to the two young successional forests during the dry season. The lack of difference in the gas exchange rates of *Syzygium nervosum* may be supported by similar stomatal density ($p = 0.22$, data not shown) across seasons, showing unchanged number of sites available for gas exchange per unit leaf area (Wu et al., 2018). Compared to the rates in the primary forest, lower rates of *Schima wallichii* and *Symplocos cochinchinensis* in the intermediate forest agreed with site-level results of limited gas exchange under shaded canopy while lower rates in the young forest may be attributed to its drier soil (average soil moisture = $23.85 \pm 5.34\%$ in YF vs. $44.54 \pm 8.46\%$ and $38.11 \pm 6.73\%$ in OF and IF, respectively). Nevertheless, further investigations on physiological responses such as tree hydraulic conductivity and architecture should be performed to confirm these results.

Sensitivity of g_s to VPD provides insight into how trees respond to increasing atmospheric drought (i.e., higher temperature combined with low humidity). Trees with greater sensitivity of g_s to VPD, closing stomata more rapidly when air dries, acclimate better to increasing atmospheric drought compared to those with lower sensitivity. Nevertheless, trees in our successional forests did not show distinct sensitivity of g_s to VPD when considering both the forest level and species level. Most studies investigating the sensitivity of stomatal conductance to VPD in tree species found differences in the relationships across various factors besides species, such as crown height and wood anatomy (Woodruff et al., 2009; Tsuji et al., 2020). However, our data showed similar sensitivities of stomatal conductance to changing vapor pressure deficit across our successional forests, suggesting similar responses of the dominant trees to varying atmospheric humidity throughout the year. This finding may support the observed similarity in the gas exchange rates between the two contrasting forest stages (OF and YF), despite the widely reported results that early successional species usually have greater maximum gas change rates than late-successional ones (Hölscher et al., 2006; Zhu et al., 2013). Regarding the response of stomatal conductance to atmospheric conditions, we further examined the slope parameter in the unified stomatal optimization model (USO; Medlyn et al., 2011; Fig. S3, S4) which represents a measure of intrinsic plant water-use efficiency. Wu et al. (2019) showed that the slope parameter significantly varied with leaf mass per area in tropical forests. However, we tested this finding with our data and found an insignificant result ($p = 0.998$, Fig. S5), suggesting similar intrinsic water-use efficiency among the dominant trees regardless of LMA. Furthermore, we found no difference in slope parameters across successional forests in the case of species existing in multiple sites (Fig. S4, $p \geq 0.66$). Nevertheless, further studies on canopy fluxes should be conducted to confirm such findings because results from leaf-level measurements can obscure those from the canopy level (Tor-ngern et al., 2015).

While similar chlorophyll concentration was observed across all forest stages, LMA, leaf N and P were significantly higher in YF compared to other forest stages. Previous studies indicated that nutrient-

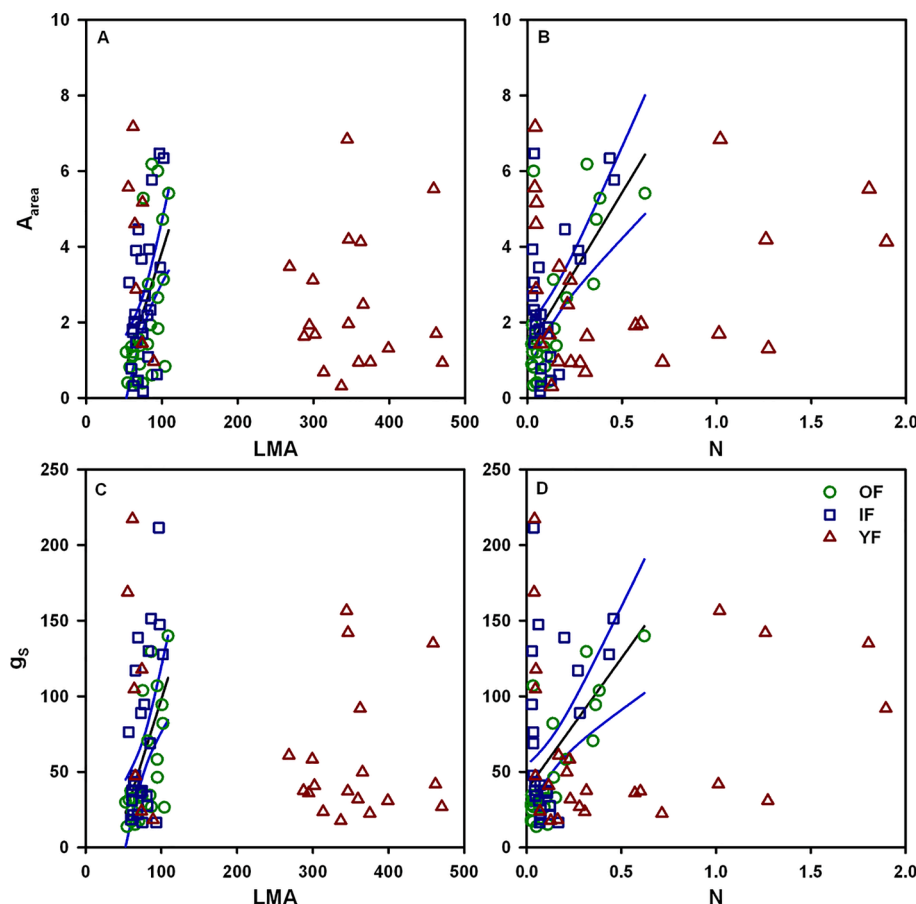


Fig. 6. Linear relationships between photosynthesis (A_{area} ; $\mu\text{mol m}^{-2} \text{s}^{-1}$) and stomatal conductance (g_s ; $\text{mmol m}^{-2} \text{s}^{-1}$) and leaf mass per area (LMA; g m^{-2}) and total nitrogen concentration (N; g cm^{-2}). Measurements were made in an old-growth forest (OF, green circles), an intermediate forest (IF, blue squares), and a young forest (YF, red triangles). Black solid lines show the best fits with 95% confidence intervals (blue lines) for pooled data of OF and IF after finding no difference among the stages. Note that no significant relationships were found in YF. Regression statistics are presented in Table S3. (For interpretation of the references to colour in this figure legend, the reader is referred to the web version of this article.)

poor soils may induce larger allocation of leaf nitrogen into cell walls, increasing LMA but decreasing maximum photosynthesis (Takashima et al., 2004; Hikada and Kitayama, 2009). However, we found no significant difference in soil N and P among the forest stages ($p \geq 0.21$; data not shown), suggesting that the soil condition in YF was not nutrient poor compared to the others. Other studies have shown that species with high LMA usually occur in areas with low rainfall and high light and temperature (Niiinemets, 2001; Villar and Merino, 2001; Lamont et al., 2002; Wright et al., 2004). This supports our result because trees in YF experience more xeric conditions and higher radiation due to their sparse canopy cover. Higher LMA may be associated with greater accumulation of nutrients in leaves (Kimura et al., 1998) as observed in our data, allowing high photosynthesis under adverse growing conditions, such as low soil moisture as often observed in sparse canopy forests with low leaf area indices (Von Arx et al., 2013). Nevertheless, our results did not show such high photosynthesis in YF which may be limited by the low soil water availability of this site compared to the others.

To gain insight into which leaf traits were linked to tree growth, we explored the relationships between leaf functional traits and gas exchange parameters (A_{area} and g_s) within the different successional forests. Maximum net photosynthesis is usually affected by various leaf traits, such as LMA (Field and Mooney, 1986; Reich et al., 1999; Poorter et al., 2009), and leaf nutrient concentrations (Evans, 1989; Reich et al., 1999; Wright et al., 2004). Several studies have reported significantly positive correlations between maximum photosynthesis rate and LMA (Reich et al., 1997; Wright et al., 2004; Quero et al., 2006), leaf N (Reich et al., 1994; Ellsworth and Reich, 1996; Kull and Niiinemets, 1998; Gulás et al., 2003; Hölscher et al., 2006) and P (Hölscher et al., 2006; Zhang et al., 2018). Our results showed that LMA and leaf N were significantly related to the gas exchange rates in IF and OF, although we

found no relationships between the rates and leaf P. Comparing the linear dependence of A_{area} and g_s on LMA and N between OF and IF, we found no differences between the trends, which is in contrast to a recent study that showed a lower slope between A_{area} and N in climax species (Zhang et al., 2018). However, the study argued that such difference was relevant to different soil phosphorus concentrations between successional stages, which was not the case for our sites. Interestingly, we observed no significant relationships between maximum gas exchange parameters and any leaf traits in YF. High variations of species-specific data may contribute to the insignificant relationship as seen in clearly separated clusters of data, corresponding to different species within YF. This finding suggests that trees in the young forest (YF) may be more active in resource acquisition, as shown by the large variation in leaf nutrients, and in morphological acclimation through the increased LMA for greater nutrient accumulation. Such acclimation should facilitate high gas exchange rates; however, the different soil water availability may have limited the rates in the young forest. Nevertheless, findings from this study warrant further investigations from different perspectives, including other physiological parameters, such as tree hydraulics and canopy-level measurements, to arrive at firm conclusions.

5. Conclusions

Varying environmental conditions among different successional forests present a challenge for estimating forest water use and productivity in tropical forests. Such heterogeneity in environmental conditions can strongly influence water and carbon exchanges between the forest canopy and the atmosphere. Our results show that, in general, gas exchange rates between the tree canopy and the atmosphere did not vary across forest stages yet differed among them in the dry season, as a result of changes in canopy density during secondary succession. The similar

rates were further supported by similar sensitivity of stomatal conductance to changing atmospheric humidity across forest stages. Our data also suggest that the young forest was highly active in acquiring resources, but such high resource acquisition did not allow high gas exchange rates because of limiting soil water availability. These findings highlight the potential effects of inherent canopy characteristics of successional forests on water and carbon exchanges between trees and the atmosphere. Nevertheless, further studies on canopy level are needed to confirm such findings.

CRediT authorship contribution statement

Pantana Tor-ngern: Conceptualization, Methodology, Formal analysis, Writing - original draft, Writing - review & editing, Visualization, Project administration, Funding acquisition. **Chidsanuphong Chart-asu:** Formal analysis. **Wirong Chanthorn:** Writing - review & editing. **Chadtip Rodtassana:** Writing - review & editing. **Siriphong Yampum:** Project administration. **Weerapong Unawong:** Visualization, Project administration. **Anuttara Nathalang:** Project administration. **Warren Brockelman:** Writing - review & editing. **Kanchit Srinoppawan:** Resources. **Yajun Chen:** Writing - review & editing. **Niles J. Hasselquist:** Writing - review & editing, Funding acquisition.

Declaration of Competing Interest

The authors declare that they have no known competing financial interests or personal relationships that could have appeared to influence the work reported in this paper.

Acknowledgements

This work was financially supported by the National Science and Technology Development Agency (NSTDA, P-18-51395) and the Thailand Science Research and Innovation (TSRI, RDG6230006). We would like to thank the Department of Environmental Science, Faculty of Science, Chulalongkorn University, for laboratory facilities. NJ Hasselquist would like to thank the Knut and Alice Wallenberg Foundation (Branchpoint; #2015.0047) and the Swedish Research Council (VR, 2015-04791; FORMAS, 2018-00030) for financial support. W Chanthorn was supported by the Alexander von Humboldt Foundation. We thank Noppawan Lomwong, Thunyatanit Khemrugga and Jittiwat Phalodom for field assistance for collecting soil samples that were used in the additional analysis for the discussion.

Appendix A. Supplementary material

Supplementary data to this article can be found online at <https://doi.org/10.1016/j.foreco.2021.119101>.

References

Bianco, R.L., Avellone, G., 2014. Diurnal regulation of leaf water status in high- and low-mannitol olive cultivars. *Plants* 3 (2), 196–208.

Bonan, G.B., 2008. Forests and climate change: forcings, feedbacks, and the climate benefits of forests. *Science* 320, 1444–1449.

Brockelman, W.Y., Nathalang, A., Maxwell, J.F., 2017. Mo Singto Plot: Flora and Ecology. National Science and Technology Development Agency and Department of National Parks, Wildlife and Plant Conservation, Bangkok.

Brodrribb, T.J., Holbrook, N.M., 2004. Diurnal depression of leaf hydraulic conductance in a tropical tree species. *Plant Cell Environ.* 27 (7), 820–827.

Chanthorn, W., Ratanapongsai, Y., Brockelman, W.Y., Allen, M.A., Favier, C., Dubois, M.A., 2016. Viewing tropical forest succession as a three-dimensional dynamical system. *Theor. Ecol.* 9, 163–172.

Chanthorn, W., Hartig, F., Brockelman, W.Y., 2017. Structure and community composition in a tropical forest suggest a change of ecological processes during stand development. *For. Ecol. Manage.* 404, 100–107.

Chazdon, R.L., Pearcy, R.W., Lee, D.W., Fletcher, N., 1996. Photosynthetic responses of tropical forest plants to contrasting light environments. In: Mulkey, S., Chazdon, R.L., Smith, A.P. (Eds.), *Tropical Plant Ecophysiology*. Chapman and Hall, New York, pp. 5–55.

Chazdon, R.L., 2014. Second Growth: The Promise of Tropical Forest Regeneration in an Age of Deforestation. University of Chicago Press, Chicago.

Chen, Y.J., Schnitzer, S.A., Zhang, Y.J., Fan, Z.X., Goldstein, G., Tomlinson, K.W., Lin, H., Zhang, J.L., Cao, K.F., 2016. Physiological regulation and efficient xylem water transport regulate diurnal water and carbon balances of tropical lianas. *Funct. Ecol.* 31 (2), 306–317.

Condit, R., 1998. Tropical Forest Census Plots: Methods and Results from Barro Colorado Island, Panama and a Comparison with Other Plots. Springer-Verlag, Berlin, Heidelberg.

Coste, S., Roggy, J.-C., Imbert, P., Born, C., Bonal, D., Dreyer, E., 2005. Leaf photosynthetic traits of 14 tropical rain forest species in relation to leaf nitrogen concentration and shade tolerance. *Tree Physiol.* 25, 1127–1137.

Coste, S., Baraloto, C., Leroy, C., Marcon, E., Renaud, A., Richardson, A.D., Roggy, J.C., Schimass, H., Uddling, J., Héault, B., 2010. Assessing foliar chlorophyll contents with the SPAD-502 chlorophyll meter: a calibration test with thirteen tree species of tropical rainforest in French Guiana. *Ann. For. Sci.* 67, 607.

Culf, A.D., Esteves, J.L., Marques Filho A.O., da Rocha, H.R., 1996. Radiation, temperature and humidity over forest and pasture in Amazonia. In: J.H.C., Gash, C.A., Nobre, J.M., Roberts, R.L., Victoria, (Eds.), *Amazonian Deforestation and Climate*. John Wiley & Sons, London, pp. 175–191.

Cunningham, S., 2004. Stomatal sensitivity to vapour pressure deficit of temperate and tropical evergreen rainforest trees of Australia. *Trees* 18, 399–407.

Curtis, P.G., Slay, C.M., Harris, N.L., Tyukavina, A., Hansen, M.C., 2018. Classifying drivers of global forest loss. *Science* 361 (6407), 1108–1111. <https://doi.org/10.1126/science.aau3445>.

Dang, Q.L., Margolis, H.A., Coyea, M.R., Sy, M., Collatz, G.J., 1997. Regulation of branch-level gas exchange of boreal trees: roles of shoot water potential and vapor pressure difference. *Tree Physiol.* 17 (8–9), 521–535. <https://doi.org/10.1093/treephys/17.8.9.521>.

Dye, P.J., Olbrich, B.W., 1993. Estimating transpiration from 6-year-old *Eucalyptus grandis* trees: development of a canopy conductance model and comparison with independent sap flux measurements. *Plant Cell Environ.* 16, 45–53.

Ellsworth, D.S., Reich, P.B., 1996. Photosynthesis and leaf nitrogen in five Amazonian tree species during early secondary succession. *Ecology* 77 (2), 581–594.

Evans, J.R., 1989. Photosynthesis and nitrogen relationships in leaves of C3 plants. *Oecologia* 78, 9–19.

Fan, D.Y., Jie, S.-L., Liu, C.-C., Zhang, X.-Y., Xu, X.-W., Zhang, S.-R., Xie, Z.-Q., 2011. The trade-off between safety and efficiency in hydraulic architecture in 31 woody species in a karst area. *Tree Physiol.* 31, 865–877.

FAO and UNEP, 2020. The State of the World's Forests 2020. Forests, biodiversity and people. Rome. <https://doi.org/10.4060/ca8642en>.

Field, C., Mooney, H.A., 1986. *The Photosynthesis-Nitrogen Relationship in Wild Plants*. Cambridge University Press, pp. 25–55.

Fisch, G., Tota, J., Machado, L.A.T., Silva Dias, M.A.F., Lyra, R.F.F., Nobre, C.A., Dolman, A.J., Gash, J.H.C., 2004. The convective boundary layer over pasture and forest in Amazonia. *Theor. Appl. Climatol.* 78, 47–59.

Gales Jr., M., Julian, E., Kroner, R., 1966. Method for quantitative determination of total phosphorus in water. *J. Am. Water Works Ass.* 58 (10), 1363.

Gerardin, T., Douthet, C., Flexas, J., Brendel, O., 2018. Shade and drought growth conditions strongly impact dynamic responses of stomata to variations in irradiance in Nicotiana tabacum. *Environ. Exp. Bot.* 153, 188–197.

Good, S.P., Noone, D., Bowen, G., 2015. Hydrologic connectivity constrains partitioning of global terrestrial water fluxes. *Science* 349 (6244), 175–177.

Gulfas, J., Flexas, J., Mus, M., Cifre, J., Lefi, E., Medrano, H., 2003. Relationship between maximum leaf photosynthesis, nitrogen content and specific leaf area in Balearic endemic and non-endemic Mediterranean species. *Ann. Bot.* 92 (2), 215–222.

Hardwick, S.R., Toumi, R., Pfeifer, M., Turner, E.C., Nilus, R., Ewers, R.M., 2015. The relationship between leaf area index and microclimate in tropical forest and oil palm plantation: Forest disturbance drives changes in microclimate. *Agr. Forest Meteorol.* 201, 187–195.

Harper, A., Baker, I.T., Denning, S., Randall, D.A., Dazlich, D., Branson, M., 2013. Impact of evapotranspiration on dry season climate in the Amazon forest. *J. Clim.* 27, 574–591.

Hikida, A., Kitayama, K., 2009. Divergent patterns of photosynthetic phosphorus use efficiency versus nitrogen use efficiency of tree leaves along nutrient availability gradients. *J. Ecol.* 97, 984–991.

Hogan, K.P., Smith, A.P., Samaniego, M., 1995. Gas exchange in six tropical semi-deciduous forest canopy tree species during the wet and dry seasons. *Biotropica* 27 (3), 324–333.

Hölscher, D., Leuschner, C., Bohman, K., Hagemeier, M., Juhrbandt, J., Tjirosemito, S., 2006. Leaf gas exchange of trees in old-growth and young secondary forest stands in Sulawesi, Indonesia. *Trees* 20, 278–285.

Hubau, W., Lewis, S.L., Phillips, O.L., et al., 2020. Asynchronous carbon sink saturation in African and Amazonian tropical forests. *Nature* 579, 80–87.

Jasechko, S., Sharp, Z.D., Gibson, J.J., Birks, S.J., Yi, Y., Fawcett, P.J., 2013. Terrestrial water fluxes dominated by transpiration. *Nature* 496, 347–351. <https://doi.org/10.1038/nature11983>.

Jha, N., Tripathi, N.K., Chanthorn, W., et al., 2020. Forest aboveground biomass stock and resilience in a tropical landscape of Thailand. *Biogeosciences* 17, 121–134.

Jucker, T., Hardwick, S.R., Both, S., Elias, D.M.O., Ewers, R.M., Mlodowski, D.T., Swinfield, T., Coomes, D.A., 2018. Canopy structure and topography jointly constrain the microclimate of human-modified tropical landscapes. *Global Change Biol.* 24, 5243–5258.

Kammerer, P.A., Rodel, M.G., Hughes, R.A., Lee, G.F., 1967. Low level Kjeldahl nitrogen determination on the Technicon Autoanalyzer. *Environ. Sci. Technol.* 1, 340.

Kimura, K., Ishida, A., Uemura, A., Matsumoto, Y., Terashima, C., 1998. Effects of current-year and previous-year PPFDs on shoot gross morphology and leaf properties in *Fagus japonica*. *Tree Physiol.* 18, 459–466.

Kröber, W., Plath, I., Heklau, H., Brüelheide, H., 2015. Relating stomatal conductance to leaf functional traits. *J. Vis. Exp.* 104, 52738. <https://doi.org/10.3791/52738>.

Kull, O., Niinemets, Ü., 1998. Distribution of leaf photosynthetic properties in tree canopies: comparison of species with different shade tolerance. *Funct. Ecol.* 12, 472–479.

Lamont, B.B., Groom, P.K., Cowling, R.M., 2002. High leaf mass per area of related species assemblages may reflect low rainfall and carbon isotope discrimination rather than low phosphorus and nitrogen concentrations. *Funct. Ecol.* 16, 403–412.

Lebría-Trejos, E., Pérez-García, E.A., Meave, J.A., Bongers, F., Poorter, L., 2010. Functional traits and environmental filtering drive community assembly in a species-rich tropical system. *Ecology* 91, 386–398.

Lebría-Trejos, E., Pérez-García, E.A., Meave, J.A., Poorter, L., Bongers, F., 2011. Environmental changes during secondary succession in a tropical dry forest in Mexico. *J. Trop. Ecol.* 27, 477–489.

Lohbeck, M., et al., 2013. Successional changes in functional composition contrast for dry and wet tropical forest. *Ecology* 94, 1211–1216.

Lohbeck, M., et al., 2015. Functional trait strategies of trees in dry and wet tropical forests are similar but differ in their consequences for succession. *Plos One* 10, e0123741.

Marenco, R.A., Gonçalves, J.F.D.C., Vieira, G., 2001. Leaf gas exchange and carbohydrate in tropical trees differing in successional status in two light environments in central Amazonia. *Tree Physiol.* 21, 1311–1318.

Markesteijn, L., Poorter, L., Bongers, F., Paz, H., Sack, L., 2011. Hydraulic and life history of tropical dry forest tree species: coordination of species' drought and shade tolerance. *New Phytol.* 191, 480–495.

McCaughay, J.H., Iacobelli, A., 1994. Modelling stomatal conductance in a northern deciduous forest, Chalk River, Ontario. *Can. J. For. Res.* 24, 904–910.

Medlyn, B.E., Duursma, R.A., Eamus, D., Ellsworth, D.S., Prentice, I.C., Barton, C.V.M., et al., 2011. Reconciling the optimal and empirical approaches to modelling stomatal conductance. *Glob. Change Biol.* 17 (6), 2134–2144.

Mielke, M.S., de Almeida, A.F., Gomes, F.P., 2005. Photosynthetic traits of five neotropical rainforest tree species: interactions between light response curves and leaf-to-air vapor pressure deficit. *Braz. Arch. Biol. Technol.* 48 (5), 815–824.

Miralles, D.G., De Jeu, R.A.M., Gash, J.H., Holmes, T.R.H., Dolman, A.J., 2011. Magnitude and variability of land evaporation and its components at the global scale. *Hydrol. Earth Syst. Sc.* 15 (3), 967–981.

Motzter, T., Munz, N., Küppers, M., Schmitt, D., Anhuf, D., 2005. Stomatal conductance, transpiration and sap flow of tropical montane rain forest trees in the southern Ecuadorian Andes. *Tree Physiol.* 25, 1283–1293.

Mujawamariya, M., Manishimwe, A., Ntirugulirwa, B., Zibera, E., Ganszky, D., Bahati, E. N., Nyirambangutse, B., Nsabimana, D., Wallin, G., Uddling, J., 2018. Climate sensitivity of tropical trees along an elevation gradient in Rwanda. *Forests* 9, 647.

Niinemets, Ü., 2001. Global-scale climatic controls of leaf dry mass per area, density, and thickness in trees and shrubs. *Ecology* 82, 453–469.

Oren, R., Sperry, J.S., Katul, G.G., Pataki, D.E., Ewers, B.E., Phillips, N., Schäfer, K.V.R., 1999. Survey and synthesis of intra- and interspecific variation in stomatal sensitivity to vapour pressure deficit. *Plant Cell Environ.* 22, 1515–1526.

Poorter, H., Niinemets, Ü., Poorter, L., Wright, I.J., Villar, R., 2009. Causes and consequences of variation in leaf mass per area (LMA): a meta-analysis. *New Phytol.* 182, 565–588.

Powers, J.S., Marín-Spiotta, E., 2017. Ecosystem processes and biogeochemical cycles in secondary tropical forest succession. *Annu. Rev. Ecol. Evol. Syst.* 48 (1), 497–519.

Quero, J.L., Villar, R., Marañón, T., Zamora, R., 2006. Interactions of drought and shade effects on seedlings of four *Quercus* species: physiological and structural leaf responses. *New Phytol.* 170, 819–834.

Rambo, T.R., North, M.P., 2009. Canopy microclimate response to pattern and density of thinning in a Sierra Nevada forest. *For. Ecol. Manage.* 25 (2), 435–442.

Reich, P.B., Walters, M.B., Ellsworth, D.S., Uhl, C., 1994. Photosynthesis-nitrogen relations in Amazonian tree species I. Patterns among species and communities. *Oecologia* 97, 62–72.

Reich, P.B., Walters, M.B., Ellsworth, D.S., 1997. From tropics to tundra: global convergence in plant functioning. *Proc. Natl. Acad. Sci. USA* 94, 13730–13734.

Reich, P.B., Ellsworth, D.S., Walters, M.B., Vose, J.M., Gresham, C., Volin, J.C., Bowman, W.D., 1999. Generality of leaf trait relationships: a test across six biomes. *Ecology* 80, 1955–1969.

Reich, P.B., 2014. The world-wide 'fast-slow' plant economics spectrum: a traits manifesto. *J. Ecol.* 102, 275–301.

Santiago, L.S., Mulkey, S.S., 2003. A test of gas exchange measurements on excised canopy branches of ten tropical tree species. *Photosynthetica* 41 (3), 343–347.

Schneider, C.A., Rasband, W.S., Eliceiri, K.W., 2012. NIH Image to ImageJ: 25 years of image analysis. *Nature Methods* 9, 671–675.

Takashima, T., Hikosaka, K., Hirose, T., 2004. Photosynthesis or persistence: nitrogen allocation in leaves of evergreen and deciduous *Quercus* species. *Plant, Cell & Environment* 27, 1047–1054.

Tor-ngern, P., Oren, R., Ward, E.J., Palmroth, S., McCarthy, H.R., Domec, J.-C., 2015. Increases in atmospheric CO₂ have little influence on transpiration of a temperate forest canopy. *New Phytologist* 205, 518–525.

Tsuji, S., Nakashizuka, T., Kuraji, K., Kume, A., Hanba, Y.T., 2020. Sensitivity of stomatal conductance to vapor pressure deficit and its dependence on leaf water relations and wood anatomy in nine canopy tree species in a Malaysian wet tropical rainforest. *Trees* 34, 1299–1311.

Urban, O., Klem, K., Holisová, P., et al., 2014. Impact of elevated CO₂ concentration on dynamics of leaf photosynthesis in *Fagus sylvatica* is modulated by sky conditions. *Environ. Pollut.* 185, 271–280.

Vargas, G.G., Cordero, S.A., 2013. Photosynthetic responses to temperature of two tropical rainforest tree species from Costa Rica. *Trees* 27, 1261–1270.

Villar, R., Merino, J.A., 2001. Comparison of leaf construction cost in woody species with differing leaf life-spans in contrasting ecosystems. *New Phytol.* 151, 213–226.

Von Arx, G., Pannatier, E.G., Thimonier, A., Rebetez, M., 2013. Microclimate in forests with varying leaf area index and soil moisture: potential implications for seedling establishment in a changing climate. *J. Ecol.* 101, 1201–1213.

Wang-Erlandsson, L., van der Ent, R.J., Gordon, L.J., Savenije, H.H.G., 2014. Contrasting roles of interception and transpiration in the hydrological cycle – Part 1: Temporal characteristics over land. *Earth Syst. Dyn.* 5 (2), 441–469.

Woodruff, D.R., Meinzer, F.C., McCulloh, K.A., 2009. Height-related trends in stomatal sensitivity to leaf-to-air vapour pressure deficit in a tall conifer. *J. Exp. Bot.* 61 (1), 203–210.

Wright, I.J., Reich, P.B., Westoby, M., Ackerly, S.D., Baruch, Z., Bongers, F., et al., 2004. The worldwide leaf economics spectrum. *Nature* 428, 821–827.

Wu, G., Liu, H., Hua, L., Luo, Q., Lin, Y., He, P., Feng, S., Liu, J., Ye, Q., 2018. Differential responses of stomata and photosynthesis to elevated temperature in two co-occurring subtropical forest tree species. *Front. Plant Sci.* 9, 467.

Wu, J., Serbin, S.P., Ely, K.S., Wolfe, B.T., Dickman, L.T., Grossiord, C., Michaletz, S.T., Collins, A.D., Dett, M., McDowell, N.G., Wright, S.J., Rogers, A., 2019. The response of stomatal conductance to seasonal drought in tropical forests. *Glob. Change Biol.* 26, 823–839.

Yang, M., Liu, M., Lu, J., Yang, H., 2019. Effects of shading on the growth and leaf photosynthetic characteristics of three forages in an apple orchard on the Loess Plateau of eastern Gansu, China. *PeerJ* 7, e7594.

Zeng, Z., Estes, L., Ziegler, A.D., Chen, A., Searchinger, T., Hua, F., Guan, K., Jintrawet, A., Wood, E.F., 2018. Highland cropland expansion and forest loss in Southeast Asia in the twenty-first century. *Nat. Geosci.* 11, 556–562.

Zhang, H., John, R., Peng, Z., Yuan, J., Chu, C., Du, G., Zhou, S., 2012. The relationship between species richness and evenness in plant communities along a successional gradient: a study from sub-alpine meadows of the eastern Qinghai-Tibetan plateau, China. *PLOS One* 7 (11), e49024.

Zhang, G., Zhang, L., Wen, D., 2018. Photosynthesis of subtropical forest species from different successional status in relation to foliar nutrients and phosphorus fractions. *Sci. Rep.* 8, 10455.

Zhu, S.-D., Song, J.-J., Li, R.-H., Ye, Q., 2013. Plant hydraulics and photosynthesis of 34 woody species from different successional stages of subtropical forests. *Plant, Cell Environ.* 36, 879–891.

Different responses of soil respiration to environmental factors across forest stages in a Southeast Asian forest

Chadtip Rodtassana¹ | Weerapong Unawong² | Siriphong Yaemphum³ |
 Wirong Chanthorn^{4,5}  | Sakonvan Chawchai⁶  | Anuttara Nathalang⁷ |
 Warren Y. Brockelman^{7,8} | Pantana Tor-ngern^{9,10,11} 

¹Department of Botany, Faculty of Science, Chulalongkorn University, Bangkok, Thailand

²Center of Excellence on Hazardous Substance Management, Chulalongkorn University, Bangkok, Thailand

³Graduate School, Chulalongkorn University, Bangkok, Thailand

⁴Department of Environmental Technology and Management, Faculty of Environment, Kasetsart University, Bangkok, Thailand

⁵Department of Ecological Modelling, Helmholtz Centre for Environmental Research UFZ, Leipzig, Germany

⁶Department of Geology, Faculty of Science, Chulalongkorn University, Bangkok, Thailand

⁷National Biobank of Thailand, National Science and Technology Development Agency, Pathum Thani, Thailand

⁸Institute of Molecular Biosciences, Mahidol University, Nakhon Pathom, Thailand

⁹Department of Environmental Science, Faculty of Science, Chulalongkorn University, Bangkok, Thailand

¹⁰Water Science and Technology for Sustainable Environment Research Group, Chulalongkorn University, Bangkok, Thailand

¹¹Environment, Health and Social Data Analytics Research Group, Chulalongkorn University, Bangkok, Thailand

Correspondence

Pantana Tor-ngern, Department of Environmental Science, Chulalongkorn University 254 Payathai Rd, Wang Mai, Pathumwan, Bangkok 10330, Thailand.
Email: pantana.t@chula.ac.th

Funding information

National Science and Technology Development Agency, Grant/Award Number: P-18-51395; Thailand Science Research and Innovation, Grant/Award Number: RDG6230006

Abstract

Soil respiration (SR) in forests contributes significant carbon dioxide emissions from terrestrial ecosystems and is highly sensitive to environmental changes, including soil temperature, soil moisture, microbial community, surface litter, and vegetation type. Indeed, a small change in SR may have large impacts on the global carbon balance, further influencing feedbacks to climate change. Thus, detailed characterization of SR responses to changes in environmental conditions is needed to accurately estimate carbon dioxide emissions from forest ecosystems. However, data for such analyses are still limited, especially in tropical forests of Southeast Asia where various stages of forest succession exist due to previous land-use changes. In this study, we measured SR and some environmental factors including soil temperature (ST), soil moisture (SM), and organic matter content (OM) in three successional tropical forests in both wet and dry periods. We also analyzed the relationships between SR and these environmental variables. Results showed that SR was higher in the wet period and in older forests. Although no response of SR to ST was found in younger forest stages, SR of the old-growth forest significantly responded to ST, plausibly due to the nonuniform forest structure, including gaps, that resulted in a wide range of ST. Across forest stages, SM was the limiting factor for SR in the wet period, whereas SR

significantly varied with OM in the dry period. Overall, our results indicated that the responses of SR to environmental factors varied temporally and across forest succession. Nevertheless, these findings are still preliminary and call for detailed investigations on SR and its variations with environmental factors in Southeast Asian tropical forests where patches of successional stages dominate.

KEY WORDS

forest succession, soil moisture, soil organic matter, soil respiration, soil temperature, tropical forests

1 | INTRODUCTION

The role of climate change in the functioning of forests has been increasingly recognized by the global community. Forests cover about 30% of the global land surface and store ~45% of terrestrial carbon (Bonan, 2008). Global forests sequester and store carbon in above- and below-ground parts (Bunker et al., 2005; Giardina et al., 2004), and they release carbon dioxide (CO_2) back into the atmosphere through respiration by plants and soil. Soil respiration (SR) is an important component of the global carbon cycle, contributing 78–95 Pg of carbon back into the atmosphere annually (Bond-Lamberty & Thomson, 2010; Hashimoto et al., 2015). Specifically, SR in forests represents 40–90% of total CO_2 emissions from terrestrial ecosystems (Granier et al., 2000; Schlesinger & Andrews, 2000).

Soil respiration is highly sensitive to environmental change because it is influenced by many factors including soil temperature, soil moisture, the microbial community, surface litter, and vegetation type (Davidson et al., 2006; Fekete et al., 2014; Grace, 2004; Jenkinson et al., 1991; Yan et al., 2006). In fact, even small changes in SR can incur profound impacts on the global carbon balance, further affecting feedbacks to climate change (Davidson et al., 2006). Despite several studies on SR and its drivers in forests in boreal and temperate regions, such investigations remain elusive in tropical systems, especially in Southeast Asia. Deforestation and land-use change are particularly pervasive across Southeast Asia (FAO & UNEP, 2020; Zeng et al., 2018), where large-scale agricultural production and commercial tree plantations are the main drivers of forest loss (Curtis et al., 2018). However, due to unsustainable practices, such large-scale operations have often been abandoned, leading to the regeneration of secondary forests naturally or artificially. Consequently, forests in Southeast Asia are mostly characterized by patches of primary, old-growth forest and forests at different stages of secondary succession. Such variations in forests may exert different impacts on SR through modifications of environmental factors associated with successional gradients.

Forest succession often modifies microclimatic conditions and biogeochemical cycles (De Kovel et al., 2000; Lebrija-Trejos et al., 2011; Li et al., 2013) and varies with species composition and abundance (Sheil, 2001). Therefore, the driving factors for SR are affected by the forest succession (Raich & Tufekcioglu, 2000). For instance,

soil organic carbon, total nitrogen, and microbial biomass increase rapidly with secondary forest succession (Jia et al., 2005). The rate of surface litter decomposition has been found to be higher in older successional stages of tropical dry secondary forests (Tolosa et al., 2003). Although several studies have investigated SR and its driving factors in association with forest succession (Gao et al., 2020; Han et al., 2015; Huang et al., 2016; Luo et al., 2012; Wang et al., 2017; Yan et al., 2006, 2009), none of these studies were conducted in tropical forests of Southeast Asia.

To help fill this knowledge gap, we measured SR of three successional forest plots in a seasonal evergreen forest in Thailand. We performed the measurements in the wet (June and September 2020) and the dry (February and March 2021) periods within plots of different stages of succession: young forest (YF, ~5 years), intermediate forest (IF, ~45 years), and old-growth forest (OF, >200 years). The main research questions included the following: (1) Does SR differ across successional forests and among periods of data collection? and (2) Does SR respond to environmental factors including soil organic matter (OM), soil temperature (ST), and soil moisture (SM) and whether these relationships (if any) differ across forest stages? Note that we did not intend to estimate total carbon dioxide efflux from these forests, but rather aimed to investigate the dynamical changes of SR in response to various environmental factors across forest succession.

2 | MATERIALS AND METHODS

2.1 | Site description

The study was conducted in seasonal evergreen forest at 700–800 m asl in Khao Yai National Park (KYNP), Nakhon Ratchasima Province, Thailand (14°26'31"N, 101°22'55"E; Figure 1a). According to data spanning 1994–2018, mean annual temperature and precipitation at the site are 22.4 °C and 2,100 mm, respectively (Department of National Parks, Wildlife and Plant Conservation; 25-year means). The wet season lasts from May to October and the dry season from about late October to April, when monthly precipitation is less than 100 mm (Brockelman et al., 2017). During the study, precipitation peaked in September, which accounted for 21% (2019)

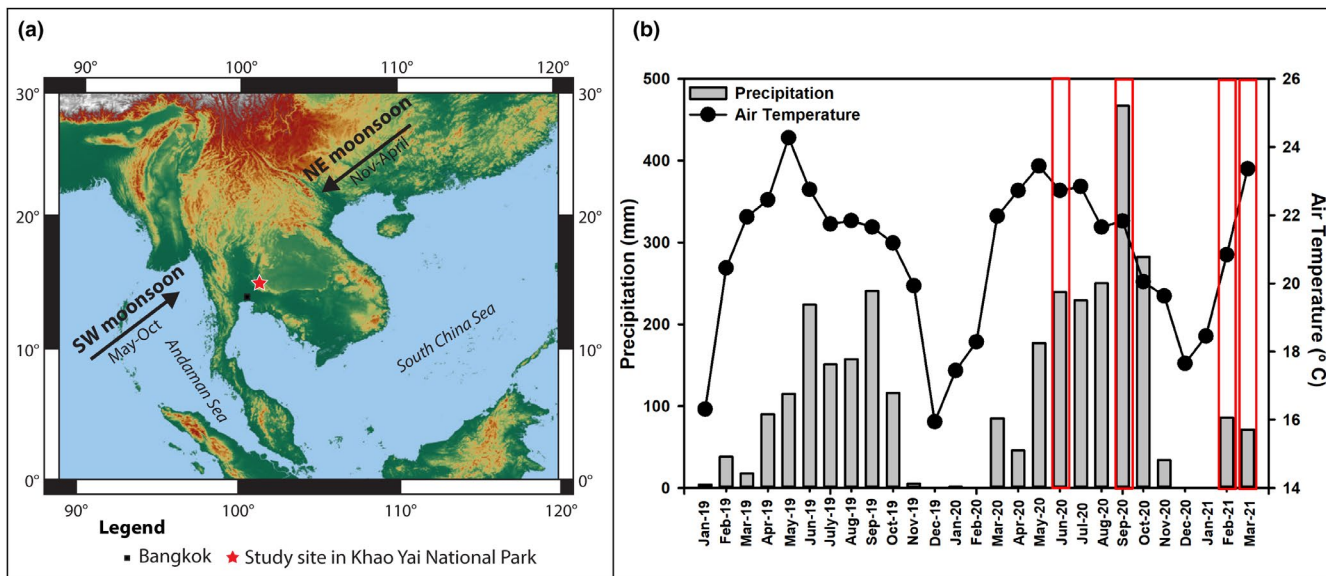


FIGURE 1 (a) Location of Khao Yai National Park in Thailand where the study was performed. (b) Monthly total precipitation (mm; bars) and average air temperature (°C; circles) profiles in Khao Yai National Park. Data from January 2019 to December 2020 were obtained from a local station near the old-growth forest (OF), whereas those from January to March 2021 were from the weather station near the young forest (YF). Red boxes indicate the months in which our measurements were made

and 26% (2020) of total precipitation in the wet season (data from a rain logger near the study site). Monthly precipitation was 239.2 mm (June 2020), 466.9 mm (September 2020), 33.6 mm (February 2021), and 1.4 mm (March 2021), as shown in Figure 1b. Using the same criteria as in Brockelman et al. (2017), we identified two data collection periods: the wet period in June through September 2020, when monthly precipitation exceeded 100 mm, and the dry period in February and March 2021.

KYNP contains mostly old-growth (primary) forest with scattered patches of secondary forest at various stages, which have regenerated from old fields within the past 50 years (Jha et al., 2020). For this study, we selected three plots representing different stages. The first plot was within the 30-ha Mo Singto forest dynamic plot (Brockelman et al., 2017), a ForestGEO plot in the global network of the Center for Tropical Forest Science (CTFS), Smithsonian Tropical Research Institute (Davies et al., 2021). CTFS plots are established using a uniform methodology (Condit, 1998) in which every woody stem ≥ 1 cm DBH is identified, mapped, and measured every 5 years. This plot represented an old-growth stage (hereafter OF), with the age of at least ca. 200 years. The OF's mean canopy height was 30 m with some emergent trees higher than 50 m, a leaf area index (LAI) of 5, and stem density of 1,112 trees ha^{-1} (Brockelman et al., 2017; Chanthorn et al., 2016). Adjacent to the northern edge of this plot, a 1-ha plot in a secondary forest was established in 2003, using the same CTFS methods. This plot (hereafter IF) was at an intermediate successional stage about 45 years of age, classified as the stem exclusion stage. The forest canopy of IF was more uniform and denser than that of and had a mean canopy height of 25 m, an LAI of 6, and stem density of 2,052 trees ha^{-1} (Chanthorn et al., 2016). About 3 km away from the OF plot, we established a 2-ha plot in a 5-year-old, initial stage forest (hereafter YF). Its mean canopy height was 15 m,

and stem density was 1,226 trees ha^{-1} . Despite the lack of LAI data, the YF canopy was distinctly sparse compared with the other stages based on visual observation. The soil type of these forests was gray, brown ultisol, but the soils under the IF and YF were degraded by shifting agriculture and burning prior to regeneration (Chanthorn et al., 2016, 2017). Based on the preliminary measurement at the sites, bulk density of the soil in IF (averaged 0.93 g cm^{-3}) was lower than that in OF and YF (1.26 and 1.24 g cm^{-3} , respectively). The soil texture at the study plots, measured at 10 cm depth, was classified as sandy clay-loam and clay loam with the highest sand contents in YF plots measured in September 2020 and February 2021 as $64.4 \pm 3.06\%$ and $56.4 \pm 5.03\%$, respectively (Appendix A, Table A1). All study sites (OF, IF, and YF) are similar with respect to geology and slope (Appendix A, Figure A1).

2.2 | Measurements of the study variables

We performed the study in two different periods of contrasting rainfall, which we will refer to as “wet” and “dry” periods in the results. In each period, we conducted the measurements twice, each separated by at least a month (Figure 1b, red frames). In each forest stage, we established a 1-ha plot and divided it into 20-m \times 20-m subplots, as shown in Figure A2. Then, we randomly selected six sampling points within the 1-ha plot and measured all study variables concurrently at each point during 1000–1500 h on sunny days. For SR, we used a portable photosynthesis system (TARGAS-1, PP Systems) connected to a soil respiration chamber (SRC-2 Soil Respiration Chamber, PP Systems). In this process, the SR rate, measured in $\text{g CO}_2 \text{ m}^{-2} \text{ h}^{-1}$, was calculated by measuring the rate of increase in CO_2 concentration in the chamber over a period, which was set to 60 s. Before taking

measurements, we installed a soil collar with a cross-sectional area of 78 cm², on each selected sampling point at 5-cm depth in the soil, leaving it for at least 1 h prior to SR measurement. Before putting the soil respiration chamber on the soil collar, we removed small living plants and coarse litter from the soil surface within the collar to avoid measuring their respiration (Peng et al., 2015; Zhou et al., 2007). Simultaneously, ST was measured using a probe (STP-2 soil temperature probe, PP Systems) at 10 cm depth near the soil collar. Soil moisture was measured at 5 cm depth from the soil surface using a probe (SM150T, DeltaT Devices). For each sampling point, all measurements of SR, ST and SM were repeated three times and then averaged to represent each sampling point. In addition, the unit of SR was converted to $\mu\text{molCO}_2 \text{ m}^{-2} \text{ s}^{-1}$ to facilitate the comparisons with other studies which mostly present the SR rate in this unit. For the soil analyses, we collected three 3.2-cm diameter soil core samples from each study plot at 10-cm soil depth in the wet season (September 2020) and the dry season (February 2021). We used a total organic carbon analyzer (Multi N/C 3100, Analytik Jena) to obtain OM values.

2.3 | Statistical analysis

To answer the research questions, we analyzed differences in the measured variables across forest stages and between both periods. Before performing the data analysis, we used the Shapiro-Wilk test and Levene's test to check for normality and homogeneity of variance, respectively. For the comparison between two collection periods (wet and dry), we employed an independent *t* test for the data with normal distribution and the Mann-Whitney *U* test for nonnormal data. Then, for each period, we compared the SR, ST, SM, and OM across forest stages by using one-way ANOVA with a Tukey's post hoc analysis for normally distributed data and the Kruskal-Wallis test with pairwise comparisons for nonparametric data. All statistical tests were performed in SPSS (IBM Corp. Released 2013. IBM SPSS Statistics for Windows, version 22.0). For the relationships among the variables, we performed regression analyses in SigmaPlot (version 12.0, Systat Software, Inc.) with SR as the dependent variable and ST, SM, and OM as the independent variables. In all statistical analyses, we used the significance level of 0.05.

3 | RESULTS

Figure 2 shows data of all measured variables, including soil temperature (ST), soil moisture (SM), soil organic matter (OM), and soil respiration (SR) during both collection periods. In both periods, ST in YF was significantly higher than in IF (Kruskal-Wallis, $H = 8.074$, $p < .05$ and $H = 7.803$, $p < .05$ for wet and dry periods, respectively), although it was not significantly different from that in OF. Soil temperature in all forest stages was significantly lower in the dry period in February and March 2021 (Mann-Whitney *U*, $U = 164.000$, $p < .0001$, Figure 2a), with an average of $22.4 \pm 1.1^\circ\text{C}$ (one standard

deviation) than in the wet period in June and September 2020, with an average of $23.7 \pm 0.7^\circ\text{C}$. Variations in SM across successional stages was observed across periods. During the dry period, SM in OF and IF was significantly higher than that in YF (one-way ANOVA, $F = 21.25$, $p < .0001$), whereas in the wet period, SM in IF was the highest (one-way ANOVA, $F = 14.31$, $p < .0001$). Overall, SM was significantly higher (independent *t* test, $t = -3.656$, $p < .005$, Figure 2b) in the dry period (average 0.18 ± 0.04) than that in the wet period (average 0.15 ± 0.03). The OM content was significantly higher in IF than in the other stages in the wet (Kruskal-Wallis, $H = 28.125$, $p < .0001$, Figure 2c) and the dry period (Kruskal-Wallis, $H = 17.843$, $p < .0001$, Figure 2c). For each forest stage, the average OM content showed temporal variation in OF and YF, with higher values in the dry period (Mann-Whitney *U*, $U = 132.000$, $p < .0001$ and $U = 108.00$, $p < .05$ for OF and YF, respectively), whereas OM in IF was similar across periods ($p = .843$). Finally, in the wet period, SR in YF was significantly lower than that in other stages (Kruskal-Wallis, $H = 10.572$, $p = .005$). In the dry period, SR in YF did not differ from the older stages, but SR in OF was significantly lower than that in IF (one-way ANOVA, $F = 5.053$, $p = .012$, Figure 2d). SR was significantly higher in the wet period than in the dry period in all stages (Mann-Whitney *U*, $U = 245.000$, $p < .0001$, Figure 2d). Overall, SR and its driving factors varied differently across forest stages and periods of data collection.

Next, we analyzed the relationships between SR and its driving factors including ST, SM, and OM. Considering each successional stage with data from both periods, SR in OF exponentially increased with ST ($p = .0007$, Figure 3a), whereas SR in IF and YF did not respond to changes in ST ($p \geq .05$, Figure 3b,c). Regardless of forest stages, SR did not respond to ST ($p = .07$, Figure 3d).

Considering the relationships between SR and SM separately for each forest stage and period, no patterns were observed ($p \geq .17$, Figure 4a-c). However, across forest stages, SR linearly increased with SM in the wet period ($p = .0023$), whereas no such response was observed in the dry period ($p = .87$, Figure 4d).

Across all forest succession and periods, SR linearly increased with OM, with stronger increasing rate in the wet period ($p \leq .022$, Figure 5d). When analyzing the relationships separately by site, the response patterns were retained only in the dry period and in OF and IF ($p \leq .026$, Figure 5a,b), whereas no responses were observed in YF ($p \geq .60$, Figure 5c).

4 | DISCUSSION

4.1 | Comparison of SR from our study sites with reports from other forests in Southeast Asia

We summarized the SR values from previous studies in forests of Southeast Asia in Table A2. Our results could not be directly compared with any of these studies because it was unclear if any of these studies was conducted in similar seasonal evergreen forest. However, our SR values were within the ranges of those found in

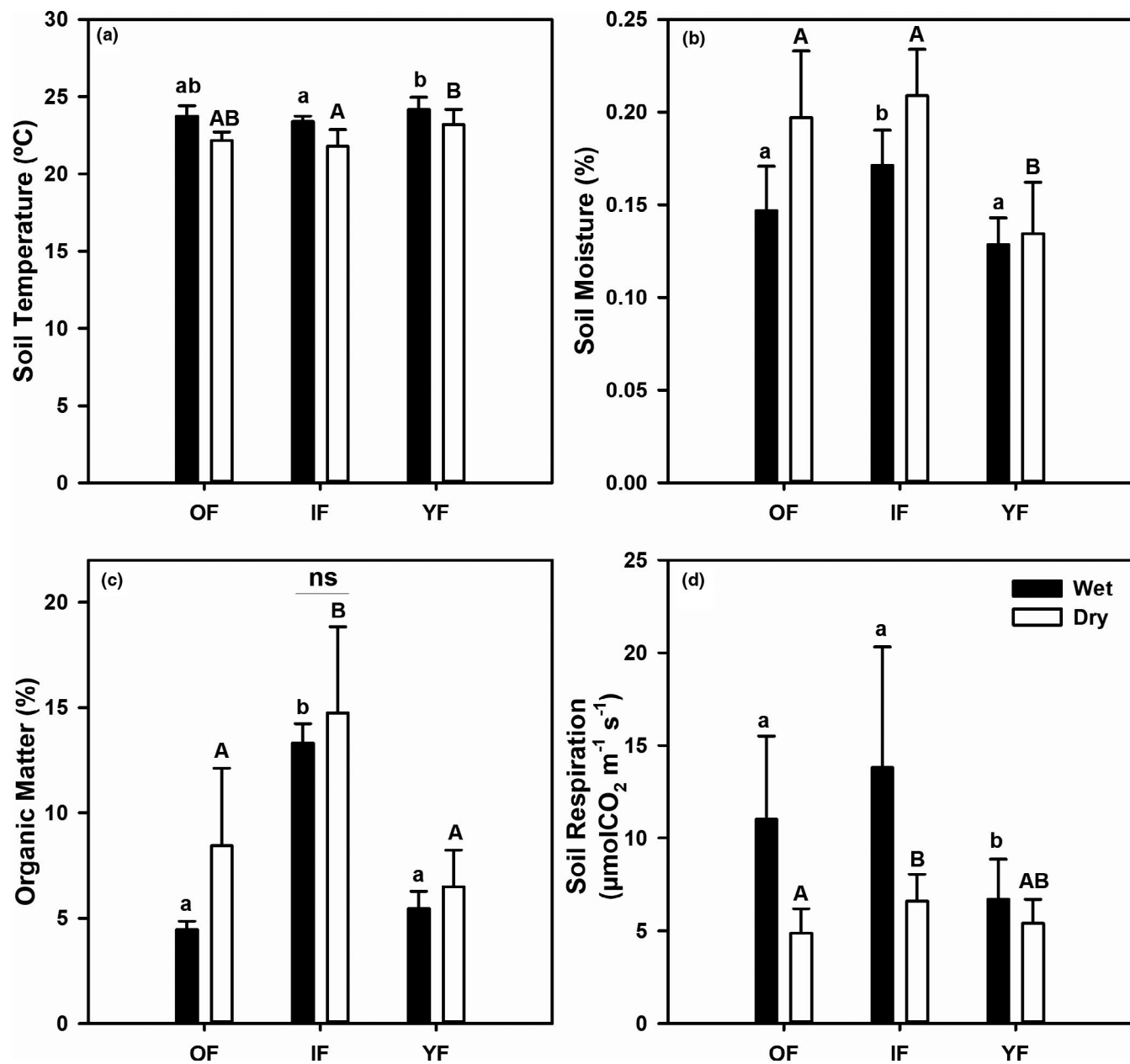


FIGURE 2 Mean values of the study variables including (a) soil temperature (°C), (b) soil moisture, (c) soil organic matter (%), and (d) soil respiration ($\mu\text{molCO}_2 \text{ m}^{-2} \text{ s}^{-1}$) measured in the wet (filled bars) and the dry (open bars) periods in the old-growth (OF), intermediate (IF) and young (YF) forest. Error bars indicate one standard deviation. Different small (capital) letters denote statistical differences among sites during the wet (dry) period at 5% significance level from the Tukey post hoc test or pairwise comparisons. All values significantly differed between periods, except the organic matter content in IF as indicated by "ns" or "not significant" in (c)

other Thai forests of various phenology, including dry evergreen forests (Adachi et al., 2009; Boonriam et al., 2021), dry dipterocarp forests (Hanpattanakit et al., 2015; Intanil et al., 2018), an evergreen forest (Hashimoto et al., 2004), a teak plantation (Kume et al., 2013), and a mixed deciduous forest (Takahashi et al., 2011). The SR values of our forests were also within the range of those from a lowland mixed dipterocarp forest in Malaysia (Katayama et al., 2009; Ohashi et al., 2008), whereas they were generally higher than those from forests at Pasoh, peninsular Malaysia (Adachi et al., 2005; Kosugi et al., 2007). Overall, it is evident

that SR rates in Southeast Asian forests are highly variable and site-specific.

4.2 | Spatial variations in SR and the environmental factors across forest succession

Soil temperature showed spatial variation in both periods with higher values in the young forest than in the intermediate stage, although it was similar to that in the old-growth forest. The higher

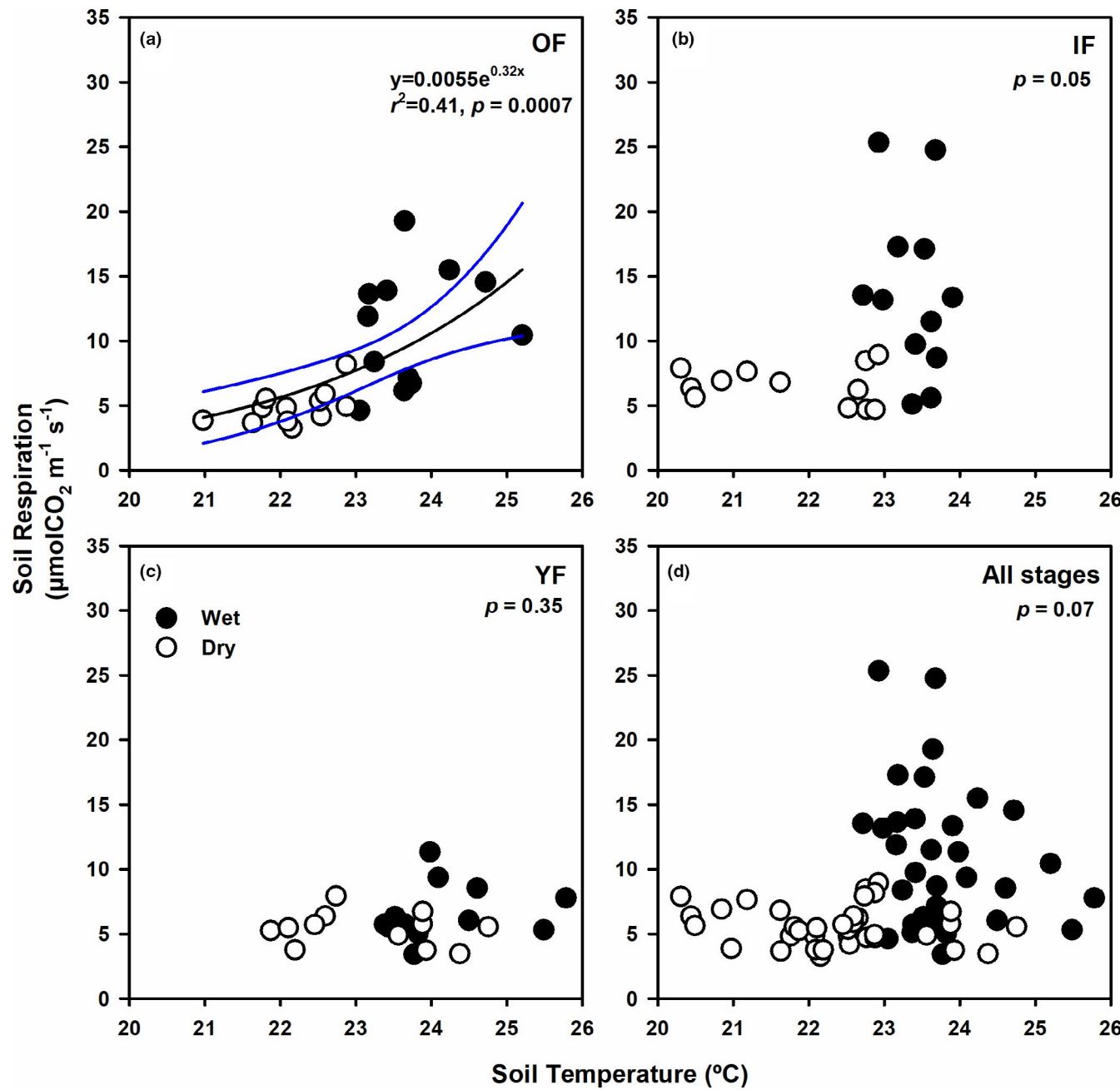


FIGURE 3 Relationships between soil respiration ($\mu\text{molCO}_2 \text{ m}^{-2} \text{ s}^{-1}$) and soil temperature ($^{\circ}\text{C}$) in the (a) old-growth (OF), (b) intermediate (IF), (c) young (YF) forest, and (d) all forest stages. Closed (open) circles represent data from the wet (dry) period. Results from regression analysis for data combined across periods are shown accordingly. Black solid line indicates the significant regression result with 95% confidence intervals shown as blue lines. The significance level for the regression analysis was 0.05

ST in the young forest may be associated with its sparse canopy compared with the more closed canopy in the intermediate forest, as observed in our sites. The observations agreed with findings of higher ST in a Panamanian tropical forest with large forest gaps due to the direct heat from sunlight reaching the soil surface (Marthens et al., 2008). Our results showed that the differences in SM across forest stages varied temporally. In the dry period, soil moisture in YF was significantly lower than that in the older stages. However, in the wet period, IF had higher SM than that in the other sites. Again, canopy development may contribute to such variation because the canopy of YF was very sparse, whereas that of IF and OF was denser.

Differing canopy density can affect the amount of light penetrating the soil surface and litterfall input to the soil, influencing surface evaporation and thus soil moisture. Overall, organic matter in the intermediate forest, with its high canopy density, was consistently higher in both periods than in that in the other sites. This may be explained by the high litterfall production in IF compared with the other two forests in our study (averaging 1.65, 2.08, 1.04 $\text{g m}^{-2} \text{ day}^{-1}$ in OF, IF, and YF, respectively, across wet and dry seasons; unpublished data), although other factors such as decomposition rate need to be considered to verify this claim. Although SR was generally similar in the older stages (OF and IF), it was significantly lowest in

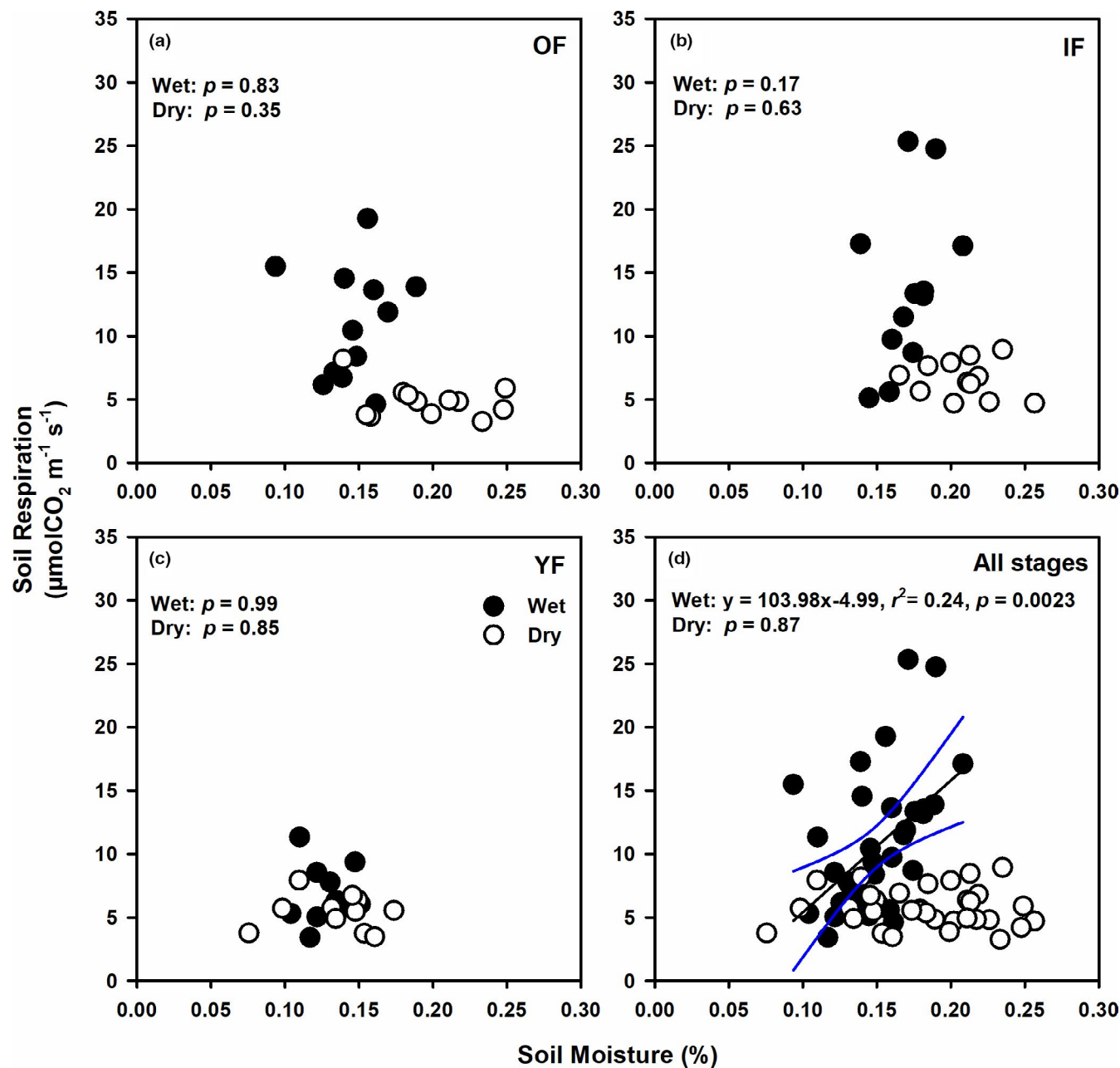


FIGURE 4 Relationships between soil respiration ($\mu\text{molCO}_2 \text{ m}^{-2} \text{ s}^{-1}$) and soil moisture in the (a) old-growth (OF), (b) intermediate (IF), (c) young (YF) forest, and (d) all forest stages. Closed (open) circles represent data from the wet (dry) period. Results from regression analysis for data combined across periods are shown accordingly. Black solid line indicates a significant regression result with 95% confidence intervals shown as blue lines. The significance level for the regression analysis was 0.05

the young forest. This result agrees with previous studies indicating increasing soil respiration with forest age (Luo et al., 2012; Yan et al., 2006, 2009). Because soil carbon, which is highly correlated with soil organic matter, and soil moisture have been found to significantly explain variations in SR (La Scala et al., 2000; Stoyan et al., 2000), low materials for decomposition and consumption by the microbial community, and low soil moisture may contribute to the low SR in YF. Additionally, variation of root biomass may affect the difference in SR across forest stages, as related to total below-ground carbon flux (TBCF; Katayama et al., 2009; Litton & Giardina, 2008). In fact, based on our preliminary measurements of fine root production in the older forests, we found that IF had higher fine root production

than OF across both wet and dry periods ($0.57 \text{ g m}^{-2} \text{ day}^{-1}$ in IF versus $0.50 \text{ g m}^{-2} \text{ day}^{-1}$ in OF), which was consistent with the higher SR in IF than in OF (Figure 2d).

4.3 | Temporal variations in SR and the environmental factors between the wet and the dry period

Regardless of forest stage, ST was lower and SM was higher in the dry period than in the wet period, which may correspond to the cool dry season in this region. In addition, this may be attributed to

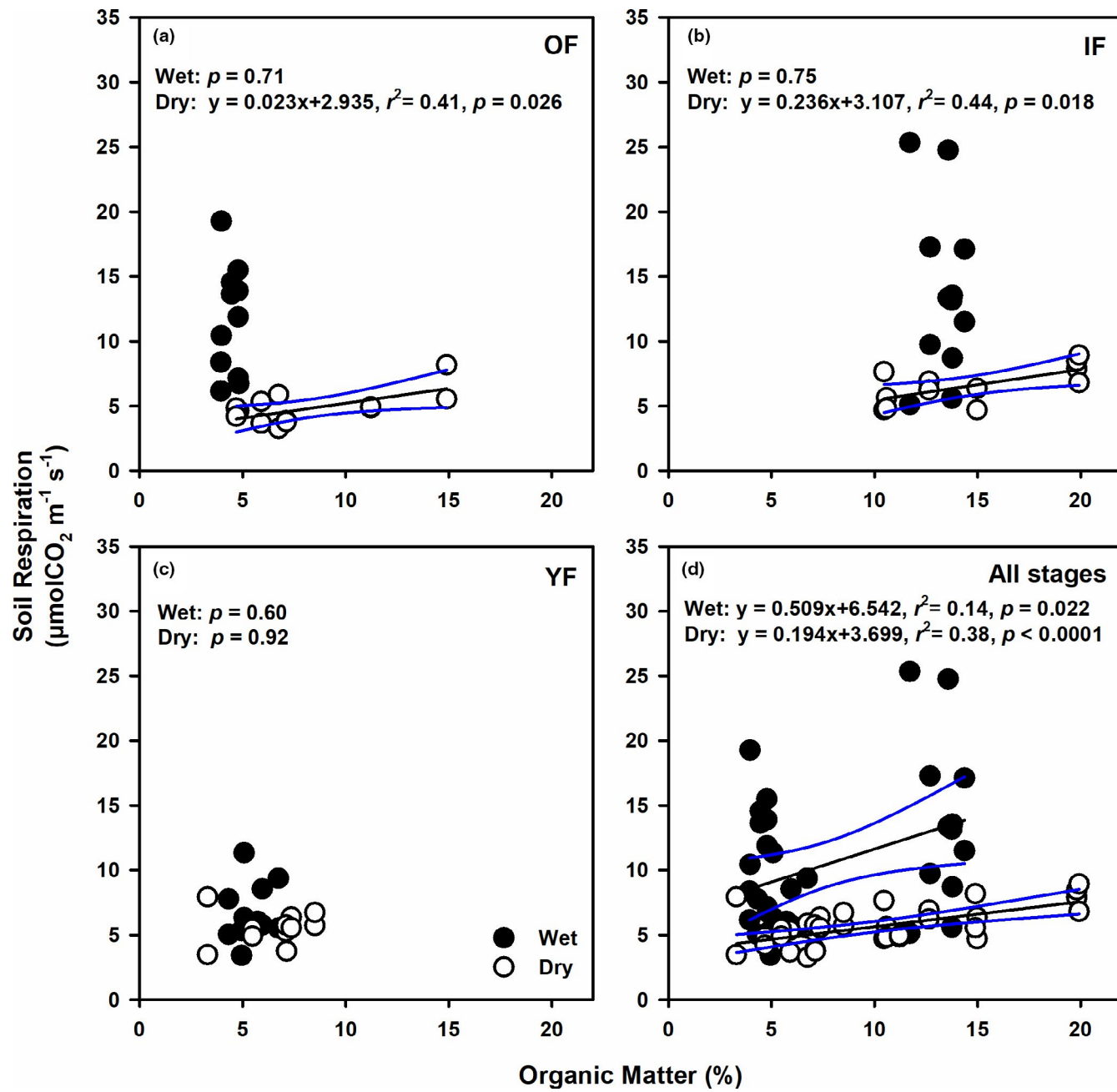


FIGURE 5 Relationships between soil respiration ($\mu\text{molCO}_2 \text{ m}^{-2} \text{ s}^{-1}$) and soil organic matter (%) in the (a) old-growth (OF), (b) intermediate (IF), (c) young (YF) forest, and (d) all forest stages. Closed (open) circles represent data from the wet (dry) period. Results from regression analysis for data combined across periods are shown accordingly. The black solid line indicates the significant regression result, with 95% confidence intervals shown as blue lines. The significance level for the regression analysis was 0.05

low surface evaporation being blocked by the thick litter layer on the forest floor as observed through high monthly litterfall production in the dry season of the same study sites (averaged 2.07 and $1.10 \text{ g m}^{-2} \text{ day}^{-1}$ in the dry and the wet season, respectively, unpublished data). The low surface evaporation may be consistent with lower evapotranspiration during the (cool) dry season than in the wet season over the Chi and Mun river basins, where our site is located, as estimated from a process-based model using satellite data from 2001 to 2015 (Zheng et al., 2019). Also, high litterfall production may

have facilitated the retention of soil moisture because the increased volume of litter increased the time for soil drying or becoming saturated (Ogée & Brunet, 2002). Similarly, soil OM was generally higher in the dry period across forest succession, which may be associated with the higher litterfall in these sites during the dry season. In all forest stages, SR was significantly higher in the wet than in the dry period, which is consistent with previous studies on soil respiration in various forests in Thailand (Adachi et al., 2009; Booniam et al., 2021; Hashimoto et al., 2004; Kume et al., 2013; Takahashi et al., 2011).

4.4 | The influence of environmental factors on SR

To gain insights into the factors that play important roles in SR variation in these forests, we investigated the relationships between SR and the main drivers including ST, SM, and soil OM. Our results showed that ST and SM differently contributed to SR among forest stages and temporally, which was likely due to the inherent canopy and site characteristics of each stage. Overall, SR in our forests did not show a clear response to ST across both periods (Figure 3d). However, the general exponential relationship between SR and ST was significant only in the old-growth, undisturbed forest (Lang et al., 2017). Because canopy gaps were unequally dispersed in OF, whereas those in IF and YF were more uniform, the range of ST was larger in OF across the wet and the dry period, possibly allowing high and significant variation of SR with ST (Figure 3a). In terms of soil moisture, SR of all forest stages increased with SM significantly only in the wet period (Figure 4d). This result indicated that low available soil moisture in the warm wet period constrained SR and thus was important for controlling microbial activity in these forests. In temperate and boreal forests, soil temperature has been identified as the major driver for soil respiration (Hursh et al., 2017). In fact, most models for soil CO_2 efflux from these forests are empirical functions of soil temperature (Sugasti & Pinzón, 2020). In tropical regions, however, mixed results have been reported. Soil respiration of tropical forests is affected by both ST and SM in some sites (Boonriam et al., 2021; Ohashi et al., 2008; Sotta et al., 2006), only affected by ST in both primary and secondary sites of tropical montane forests in China (Zhou et al., 2013), and by only SM in various forests in Thailand (Adachi et al., 2005, 2009; Hashimoto et al., 2004; Kosugi et al., 2007; Takahashi et al., 2011). Another study has suggested that short-term variation in SR depends on ST, but SM had greater effects on long-term variation in SR in central Amazonian forests (Sotta et al., 2004). Therefore, the contribution of soil temperature and soil moisture to soil respiration rates in global forests varies greatly and is highly site-specific with no clear spatial or temporal variation.

Our data showed significant increases in SR of most forest stages with increasing soil OM, with greater response in the dry period than in the wet period (Figure 5). Thus, the organic matter content in the soil was the main energy source for microbial activity that determined soil CO_2 efflux in the dry period of these forests. As previously mentioned, this period corresponded to high litter addition to the forest floor, which may stimulate soil microbial activity as shown in greater soil CO_2 release (Bréchet et al., 2017; Sayer et al., 2019, 2020). Large variations in OM were observed across forest stages, which may be explained by different quantity and quality of litter input (i.e., litterfall and roots) and different rates of litter decomposition in each stage. Note that the significant regression result for the wet period (Figure 5d) was mostly due to large differences in OM between IF and the other sites. Therefore, the observed significant pattern in the wet period may not represent the true response of SR to OM.

Overall, our results are still preliminary and suggest that different factors contribute to SR across spatial and temporal variation in

our successional forests. In our forests, SM and OM were the limiting factors that significantly explained variation in SR in the wet and the dry period, respectively, whereas ST might explain variation in SR of the old-growth forest with its nonuniform canopy compared with the younger forest stages. However, due to the limited data, further investigation including more sampling locations and higher frequency is needed to confirm these findings.

5 | CONCLUSIONS

We investigated spatial and temporal variations in soil respiration (SR) and its driving factors including soil temperature (ST), soil moisture (SM), and organic matter content (OM), together with their relationships. Our analyses showed that SR was generally higher in the wet period and in older-stage forests (either primary or secondary). Although ST has been identified as one of the main factors influencing SR in temperate and boreal forests, we found no significant relationships between SR and ST in our forests. However, in the old-growth forest where gaps are usually nonuniformly scattered, ST and OM determined SR, and there were variations in response patterns across forest stages and periods. Across the successional forests, SM was the determining factor of SR in the wet period, whereas OM significantly explained SR variations in the dry period. Overall, the responses of SR to environmental factors were different across successional forests and data collection periods. Our results suggest the incorporation of different responses in successional forests and site-specific information in modeling soil respiration of tropical forests. Nevertheless, detailed investigations involving long-term and high-frequency measurements and sampling locations should be performed to confirm these results.

ACKNOWLEDGEMENTS

This work was financially supported by the National Science and Technology Development Agency (NSTDA, P-18-51395) and the Thailand Science Research and Innovation (TSRI, RDG6230006). WC was supported by the Alexander von Humboldt Foundation. We thank Kansuda Termpornlert and Jittiwat Phalodom for field assistance.

CONFLICT OF INTEREST

None declared.

AUTHOR CONTRIBUTIONS

Chadtip Rodtassana: Conceptualization (equal); formal analysis (equal); funding acquisition (supporting); methodology (equal); writing-original draft (equal); writing-review and editing (equal).

Weerapong Unawong: Methodology (supporting).

Siriphong Yaemphum: Methodology (supporting).

Wirong Chanthorn: Funding acquisition (supporting); methodology (supporting); project administration (equal); resources (equal); writing-review and editing (supporting).

Sakonvan Chawchai: Funding acquisition (supporting); visualization (equal); writing-review and editing (supporting).

Anuttara Nathalang: Funding acquisition (supporting); project administration (equal); resources (equal). **Warren Y. Brockelman:** Funding acquisition (supporting); project administration (equal); resources (equal); writing-review and editing (supporting). **Pantana Tor-ngern:** Conceptualization (equal); formal analysis (equal); funding acquisition (lead); methodology (equal); writing-original draft (equal); writing-review and editing (equal).

DATA AVAILABILITY STATEMENT

The raw data used in this study are publicly available in the Dryad repository at <https://doi.org/10.5061/dryad.t4b8gtj2p>

ORCID

Wirong Chanthorn  <https://orcid.org/0000-0002-9854-2179>
 Sakonvan Chawchai  <https://orcid.org/0000-0003-0527-9381>
 Pantana Tor-ngern  <https://orcid.org/0000-0001-7363-4926>

REFERENCES

Adachi, M., Bekku, Y. S., Konuma, A., Kadir, W. R., Okuda, T., & Koizumi, H. (2005). Required sample size for estimating soil respiration rates in large areas of two tropical forests and of two types of plantation in Malaysia. *Forest Ecology and Management*, 210(1-3), 455–459. <https://doi.org/10.1016/j.foreco.2005.02.011>

Adachi, M., Ishida, A., Bunyavejchewin, S., Okuda, T., & Koizumi, H. (2009). Spatial and temporal variation in soil respiration in a seasonally dry tropical forest, Thailand. *Journal of Tropical Ecology*, 25, 531–539. <https://doi.org/10.1017/S026646740999006X>

Bonan, G. B. (2008). Forests and climate change: Forcings, feedbacks, and the climate benefits of forests. *Science*, 320, 1444–1449. <https://doi.org/10.1126/science.1155121>

Bond-Lamberty, B., & Thomson, A. (2010). Temperature-associated increases in the global soil respiration record. *Nature*, 464, 579–582. <https://doi.org/10.1038/nature08930>

Boonriam, W., Suwanwaree, P., Hasin, S., Archawakom, T., Chanonmuang, P., & Yamada, A. (2021). Seasonal changes in spatial variation of soil respiration in dry evergreen forest, Sakaerat Biosphere Reserve, Thailand. *Scienceasia*, 47, 112–119. <https://doi.org/10.2306/sciencessia1513-1874.2021.S009>

Bréchet, L., Le Dantec, V., Ponton, S., Goret, J., Sayer, E., Bonal, D., Freycon, V., Roy, J., & Epron, D. (2017). Short- and long-term influence of litter quality and quantity on simulated heterotrophic soil respiration in a lowland tropical forest. *Ecosystems*, 20, 1190–1204. <https://doi.org/10.1007/s10021-016-0104-x>

Brockelman, W. Y., Nathalang, A., & Maxwell, J. F. (2017). *Mo singto plot: Flora and ecology*. National Science and Technology Development Agency and Department of National Parks, Wildlife and Plant Conservation.

Bunker, D. E., DeClerck, F., Bradford, J. C., Colwell, R. K., Perfecto, I., Phillips, O. L., Sankaran, M., & Naeem, S. (2005). Species loss and aboveground carbon storage in a tropical forest. *Science*, 310, 1029–1031. <https://doi.org/10.1126/science.1117682>

Chanthorn, W., Hartig, F., & Brockelman, W. Y. (2017). Structure and community composition in a tropical forest suggest a change of ecological processes during stand development. *Forest Ecology and Management*, 404, 100–107. <https://doi.org/10.1016/j.foreco.2017.08.001>

Chanthorn, W., Ratanapongsai, Y., Brockelman, W. Y., Allen, M. A., Favier, C., & Dubois, M. A. (2016). Viewing tropical forest succession as a three-dimensional dynamical system. *Theoretical Ecology*, 9, 163–172. <https://doi.org/10.1007/s12080-015-0278-4>

Condit, R. (1998). *Tropical forest census plots: Methods and results from Barro Colorado Island, Panama and a comparison with other plots*. Springer-Verlag.

Curtis, P. G., Slay, C. M., Harris, N. L., Tyukavina, A., & Hansen, M. C. (2018). Classifying drivers of global forest loss. *Science*, 361(6407), 1108–1111. <https://doi.org/10.1126/science.aau3445>

Davidson, E. A., Janssens, I. A., & Luo, Y. Q. (2006). On the variability of respiration in terrestrial ecosystems: Moving beyond Q_{10} . *Global Change Biology*, 12, 154–164.

Davies, S., Abiem, I., Salim, K. A., Aguilar, S., Allen, D., Alonso, A., Anderson-Teixeira, K., Andrade, A., Arellano, G., Ashton, P. S., Baker, P., Baker, M. E., Baltzer, J. L., Basset, Y., Bissiengo, P., Bohlman, S., Bourg, N. A., Brockelman, W. Y., Bunyavejchewin, S., ... Zuleta, D. (2021). ForestGEO: Understanding forest diversity and dynamics through a global observatory network. *Biological Conservation*, 253, 108907.

De Kovel, C. F., Wilms, Y. J. O., & Berendse, F. (2000). Carbon and nitrogen in soil and vegetation at sites differing in successional age. *Plant Ecology*, 149, 43–50.

FAO and UNEP (2020). *The State of the World's Forests 2020. Forests, biodiversity and people*. Rome. <https://doi.org/10.4060/ca8642en>

Fekete, I., Kotrocóz, Z., Varga, C., Nagy, P. T., Várbiró, G., Bowden, R. D., Tóth, J. A., & Lajtha, K. (2014). Alterations in forest detritus inputs influence soil carbon concentration and soil respiration in a Central-European deciduous forest. *Soil Biology and Biochemistry*, 74, 106–114. <https://doi.org/10.1016/j.soilbio.2014.03.006>

Gao, F., Cui, X., Sang, Y., & Song, J. (2020). Changes in soil organic carbon and total nitrogen as affected by primary forest conversion. *Forest Ecology and Management*, 463, 118013. <https://doi.org/10.1016/j.foreco.2020.118013>

Giardina, C. P., Binkley, D., Ryan, M. G., Fownes, J. H., & Senock, R. S. (2004). Belowground carbon cycling in a humid tropical forest decreases with fertilization. *Oecologia*, 139, 545–550. <https://doi.org/10.1007/s00442-004-1552-0>

Grace, J. (2004). Understanding and managing the global carbon cycle. *Journal of Ecology*, 92(2), 189–202. <https://doi.org/10.1111/j.0022-0477.2004.00874.x>

Granier, A., Ceschia, E., Damesin, C., Dufrêne, E., Epron, D., Gross, P., Lebaube, S., Le Dantec, V., Le Goff, N., Lemoine, D., Lucot, E., Ottorini, J. M., Pontailler, J. Y., & Saugier, B. (2000). The carbon balance of a young Beech forest. *Functional Ecology*, 14, 312–325. <https://doi.org/10.1046/j.1365-2435.2000.00434.x>

Han, T., Huang, W., Liu, J., Zhou, G., & Xiao, Y. (2015). Different soil respiration responses to litter manipulation in three subtropical successional forests. *Scientific Reports*, 5, 18166. <https://doi.org/10.1038/srep18166>

Hanpattanakit, P., Leclerc, M. Y., Mcmillan, A. M. S., Limtong, P., Maeght, J. L., Panuthai, S., Inubushi, K., & Chidthaisong, A. (2015). Multiple timescale variations and controls of soil respiration in a tropical dry dipterocarp forest, western Thailand. *Plant and Soil*, 390(1-2), 167–181. <https://doi.org/10.1007/s11104-015-2386-8>

Hashimoto, S., Carvalhais, N., Ito, A., Migliavacca, M., Nishina, K., & Reichstein, M. (2015). Global spatiotemporal distribution of soil respiration modeled using a global database. *Biogeosciences*, 12, 4331–4364.

Hashimoto, S., Tanaka, N., Suzuki, M., Inoue, A., Takizawa, H., Kosaka, I., Tanaka, K., Tantasirin, C., & Tangtham, N. (2004). Soil respiration and soil CO₂ concentration in a tropical forest, Thailand. *Journal of Forest Research*, 9(1), 75–79. <https://doi.org/10.1007/s10310-003-0046-y>

Huang, W., Han, T., Liu, J., Wang, G., & Zhou, G. (2016). Change in soil respiration components and their specific respiration along three successional forests in the subtropics. *Functional Ecology*, 30, 1466–1474.

Hursh, A., Ballantyne, A., Cooper, L., Maneta, M., Kimball, J., & Watts, J. (2017). The sensitivity of soil respiration to soil temperature, moisture, and carbon supply at the global scale. *Global Change Biology*, 23, 2090–2103. <https://doi.org/10.1111/gcb.13489>

Intanil, P., Boonpoke, A., Sanwangsri, M., & Hanpattanakit, P. (2018). Contribution of root respiration to soil respiration during rainy season in dry dipterocarp forest, Northern Thailand. *Applied Environmental Research*, 40(3), 19–27. <https://doi.org/10.35762/AER.2018.40.3.3>

Jenkinson, D. S., Adams, D. E., & Wild, A. (1991). Model estimates of CO₂ emission from soil in response to global warming. *Nature*, 351, 304–306.

Jha, N., Tripathi, N. K., Chanthorn, W., Brockelman, W., Nathalang, A., Pélissier, R., Pimmasarn, S., Ploton, P., Sasaki, N., Virdis, S. G. P., & Réjou-Méchain, M. (2020). Forest aboveground biomass stock and resilience in a tropical landscape of Thailand. *Biogeosciences*, 17, 121–134. <https://doi.org/10.5194/bg-17-121-2020>

Jia, G. M., Cao, J., Wang, C. Y., & Wang, G. (2005). Microbial biomass and nutrients in soil at the different stages of secondary forest succession in Ziwulin, northwest China. *Forest Ecology and Management*, 217, 117–125. <https://doi.org/10.1016/j.foreco.2005.05.055>

Katayama, A., Kume, T., Komatsu, H., Ohashi, M., Nakagawa, M., Yamashita, M., Otsuki, K., Suzuki, M., & Kumagai, T. (2009). Effect of forest structure on the spatial variation in soil respiration in a Bornean tropical rainforest. *Agricultural and Forest Meteorology*, 149(10), 1666–1673. <https://doi.org/10.1016/j.agrmet.2009.05.007>

Kosugi, Y., Mitani, T., Ltoh, M., Noguchi, S., Tani, M., Matsuo, N., Takanashi, S., Ohkubo, S., & Nik, A. R. (2007). Spatial and temporal variation in soil respiration in a Southeast Asian tropical rainforest. *Agricultural and Forest Meteorology*, 147(1–2), 35–47. <https://doi.org/10.1016/j.agrmet.2007.06.005>

Kume, T., Tanaka, N., Yoshifuji, N., Chatchai, T., Igarashi, Y., Suzuki, M., & Hashimoto, S. (2013). Soil respiration in response to year-to-year variations in rainfall in a tropical seasonal forest in northern Thailand. *Ecohydrology*, 6(1), 134–141. <https://doi.org/10.1002/eco.1253>

Lang, R., Blagodatsky, S., Xu, J., & Cadisch, G. (2017). Seasonal differences in soil respiration and methane uptake in rubber plantation and rainforest. *Agriculture, Ecosystems and Environment*, 240, 314–328. <https://doi.org/10.1016/j.agee.2017.02.032>

Lebrja-Trejos, E., Perez-Garcia, E. A., Meave, J. A., Poorter, L., & Bongers, F. (2011). Environmental changes during secondary succession in a tropical dry forest in Mexico. *Journal of Tropical Ecology*, 27, 477–489. <https://doi.org/10.1017/S0266467411000253>

Li, Y., Yang, F., Ou, Y., Zhang, D., Liu, J., Chu, G., Zhang, Y., Otieno, D., & Zhou, G. (2013). Changes in forest soil properties in different successional stages in lower tropical China. *PLoS One*, 8, e81359. <https://doi.org/10.1371/journal.pone.0081359>

Litton, C. M., & Giardina, C. P. (2008). Below-ground carbon flux and partitioning: global patterns and response to temperature. *Functional Ecology*, 22(6), 941–954. <https://doi.org/10.1111/j.1365-2435.2008.01479.x>

Luo, J., Chen, Y., Wu, Y., Shi, P., She, J., & Zhou, P. (2012). Temporal-spatial variation and controls of soil respiration in different primary succession stages on glacier forehead in Gongga mountain, China. *PLoS One*, 7, e42354. <https://doi.org/10.1371/journal.pone.0042354>

Marthews, T. R., Burslem, D. F. R. P., Paton, S. R., Yangüez, F., & Mullins, C. E. (2008). Soil drying in a tropical forest: Three distinct environments controlled by gap size. *Ecological Modelling*, 216, 369–384. <https://doi.org/10.1016/j.ecolmodel.2008.05.011>

Ohé, J., & Brunet, Y. (2002). A forest floor model for heat and moisture including litter layer. *Journal of Hydrology*, 255, 212–233.

Ohashi, M., Kumagai, T., Kume, T., Gyokusen, K., Saitoh, T., & Suzuki, M. (2008). Characteristics of soil CO₂ efflux variability in an aseasonal tropical rainforest in Borneo Island. *Biogeochemistry*, 90(3), 275–289. <https://doi.org/10.1007/s10533-008-9253-0>

Peng, F., You, Q. G., Xu, M. H., Zhou, X. H., Wang, T., Guo, J., & Xue, X. (2015). Effects of experimental warming on soil respiration and its components in an alpine meadow in the permafrost region of the Qinghai-Tibet Plateau. *European Journal of Soil Science*, 66, 145–154. <https://doi.org/10.1111/ejss.12187>

Raich, J. W., & Tufekcioglu, A. (2000). Vegetation and soil respiration: Correlations and controls. *Biogeochemistry*, 48, 71–90.

Sayer, E. J., Baxendale, C., Birkett, A. J., Bréchet, L. M., Castro, B., Kerdraon-Byrne, D., Lopez-Sangil, L., & Rodtassana, C. (2020). Altered litter inputs modify carbon and nitrogen storage in soil organic matter in a lowland tropical forest. *Biogeochemistry*, 156(1), 115–130. <https://doi.org/10.1007/s10533-020-00747-7>

Sayer, E. J., Lopez-Sangil, L., Crawford, J. A., Bréchet, L. M., Birkett, A. J., Baxendale, C., Castro, B., Rodtassana, C., Garnett, M. H., Weiss, L., & Schmidt, M. W. (2019). Tropical forest soil carbon stocks do not increase despite 15 years of doubled litter inputs. *Scientific Reports*, 9, 18030. <https://doi.org/10.1038/s41598-019-54487-2>

Scala, N. Jr., Marques, J. Jr., & Pereira, G. T. (2000). Short-term temporal changes in the spatial variability model of CO₂ emission from a Brazilian bare soil. *Soil Biology and Biochemistry*, 32, 1459–1462.

Schlesinger, W. H., & Andrews, J. (2000). Soil respiration and the global carbon cycle. *Biogeochemistry*, 48, 7–20.

Sheil, D. (2001). Long-term observations of rain forest succession, tree diversity and responses to disturbance. *Plant Ecology*, 155, 183–199.

Sotta, E. D., Meir, P., Malhi, Y., Naber, A. D., Hodnet, M., & Grace, J. (2004). Soil CO₂ efflux in a tropical forest in the central Amazon. *Global Change Biology*, 10, 601–617.

Sotta, E. D., Veldkamp, E., Gumaraes, B. R., Paixao, P. K., Ruivo, M. I. P., & Almeida, S. S. (2006). Landscape and climatic controls on spatial and temporal variation in soil CO₂ efflux in an Eastern Amazonian rainforest, Caxiuna, Brazil. *Forest Ecology and Management*, 237, 57–64.

Stoyan, H., De-Polli, H., Bohm, S., Robertson, G. P., & Paul, E. A. (2000). Spatial heterogeneity of soil respiration and related properties at the plant scale. *Plant and Soil*, 222, 203–214.

Sugasti, L., & Pinzón, R. (2020). First approach of abiotic drivers of soil CO₂ efflux in Barro Colorado Island, Panama. *Air, Soil and Water Research*, 13, 1–10.

Takahashi, M., Hirai, K., Limtong, P., Leaungvutivirog, C., Panuthai, S., Suksawang, S., Anusontpornperm, S., & Marod, D. (2011). Topographic variation in heterotrophic and autotrophic soil respiration in a tropical seasonal forest in Thailand. *Soil Science and Plant Nutrition*, 57(3), 452–465. <https://doi.org/10.1080/00380768.2011.589363>

Tolosa, F. J. X., Vester, H. F. M., Marcial, N. R., Albores, J. C., & Lawrence, D. (2003). Leaf litter decomposition of tree species in three successional phases of tropical dry secondary forest in Campeche, Mexico. *Forest Ecology and Management*, 174, 401–412. [https://doi.org/10.1016/S0378-1127\(02\)00059-2](https://doi.org/10.1016/S0378-1127(02)00059-2)

Wang, C., Ma, Y., Trogisch, S., Huang, Y., Geng, Y., Scherer-Lorenzen, M., & He, J. (2017). Soil respiration is driven by fine root biomass along a forest chronosequence in subtropical China. *Journal of Plant Ecology*, 10(1), 36–46. <https://doi.org/10.1093/jpe/rtw044>

Yan, J., Wang, Y., Zhou, G., & Zhang, D. (2006). Estimates of soil respiration and net primary production of three forests at different successional stages in South China. *Global Change Biology*, 12, 810–821. <https://doi.org/10.1111/j.1365-2486.2006.01141.x>

Yan, J., Zhang, D., Zhou, G., & Liu, J. (2009). Soil respiration associated with forest succession in subtropical forests in Dinghushan Biosphere Reserve. *Soil Biology and Biochemistry*, 41, 991–999. <https://doi.org/10.1016/j.soilbio.2008.12.018>

Zeng, Z., Estes, L., Ziegler, A. D., Chen, A., Searchinger, T., Hua, F., Guan, K., Jintrawet, A., & Wood, E. F. (2018). Highland cropland expansion and forest loss in Southeast Asia in the twenty-first century. *Nature Geoscience*, 11, 556–562. <https://doi.org/10.1038/s41561-018-0166-9>

Zheng, C., Jia, L., Hu, G., & Lu, J. (2019). Earth observations-based evapotranspiration in Northeastern Thailand. *Remote Sensing*, 11, 138. <https://doi.org/10.3390/rs11020138>

Zhou, X., Wan, S., & Luo, Y. (2007). Source components and interannual variability of soil CO_2 efflux under experimental warming and clipping in a grassland ecosystem. *Global Change Biology*, 13, 761–775.

Zhou, Z., Jiang, L., Du, E., Hu, H., Li, Y., Chen, D., & Fang, J. (2013). Temperature and substrate availability regulate soil respiration in

the tropical mountain rainforests, Hainan Island, China. *Journal of Plant Ecology*, 6, 325–334.

How to cite this article: Rodtassana, C., Unawong, W., Yaemphum, S., Chanthorn, W., Chawchai, S., Nathalang, A., Brockelman, W. Y., & Tor-ngern, P. (2021). Different responses of soil respiration to environmental factors across forest stages in a Southeast Asian forest. *Ecology and Evolution*, 00, 1–14. <https://doi.org/10.1002/ece3.8248>

APPENDIX A

TABLE A1 Soil particle distribution (mean \pm SD) and soil texture classification of three forest successional stages at Khao Yai National Park, Thailand

Soil particle	Wet season (Sep 2020)			Dry season (Feb 2021)		
	OF	IF	YF	OF	IF	YF
Sand	53.7 \pm 1.15 ^a	37.7 \pm 1.15 ^b	64.4 \pm 3.06 ^c	40.3 \pm 2.42 ^a	35.7 \pm 3.06 ^a	56.4 \pm 5.03 ^b
Silt	16.9 \pm 1.15 ^a	26.3 \pm 6.00 ^b	12.3 \pm 2.00 ^a	27.7 \pm 7.20 ^a	30.3 \pm 2.00 ^a	13.6 \pm 2.31 ^b
Clay	29.3 \pm 1.15 ^{ab}	36.0 \pm 5.03 ^a	23.3 \pm 1.15 ^b	32.0 \pm 7.57 ^a	34.0 \pm 1.15 ^a	30.0 \pm 3.06 ^a
Soil texture	Sandy clay loam	Clay loam	Sandy clay loam	Clay loam	Clay loam	Sandy clay loam

Note: Different letters denote statistical difference among sites during each season at 5% significant level. The proportions of sand and silt in the soils of all sites significantly differed between seasons ($p \leq .017$), but the percentage of clay in the soils did not vary between seasons ($p = .219$).

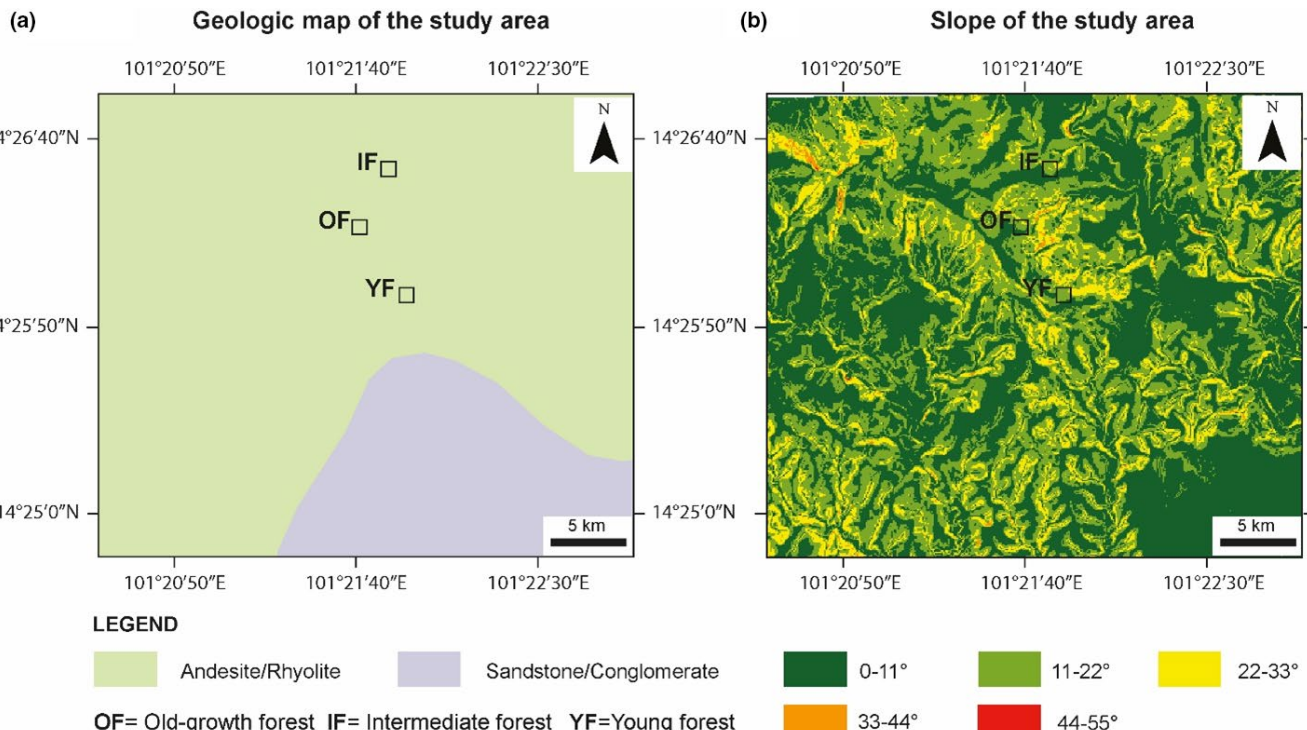


FIGURE A1 (a) Geologic map and (b) Slope of the study area and location of the study sites

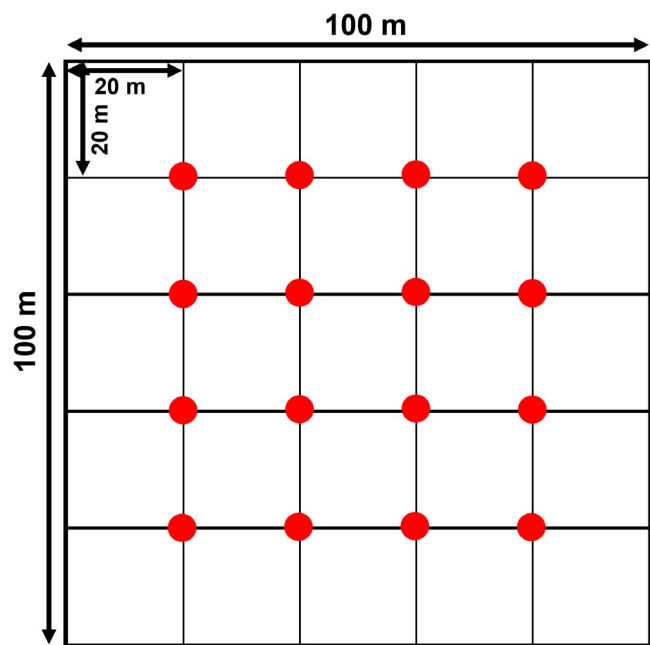


FIGURE A2 Diagram showing the grided study plot in each forest stage. Circles show the locations from which sampling points were randomly chosen for the measurements

TABLE A2 Literature survey of soil respiration in Southeast Asian tropical forests including this study

Location	Vegetation type	Dominant tree species	MAT (°C)	MAP (mm)	Soil respiration ($\mu\text{molCO}_2 \text{ m}^{-2} \text{ s}^{-1}$)	Reference
Pasoh area of Negeri Sembilan, Malaysia (2°5'N, 102°18'E, 75–150 m a.s.l.)	Primary and secondary mixed-dipterocarp forest	Dipterocarp species	27	1,788	Primary forest: 2.78–6.93 Secondary forest: 2.58–6.36	Adachi et al. (2005)
Pasoh Forest Reserve, Malaysia (2°59'N, 102°18'E, 75–150 m a.s.l.)	Lowland mixed-dipterocarp forest	<i>Shorea</i> and <i>Dipterocarpus</i> spp	25.4	1,800	2.5–6.5	Kosugi et al. (2007)
Lambir Hills National Park, Malaysia (4°20'N, 114°02'E, ~200 m a.s.l.)	Lowland mixed-dipterocarp forest	Dipterocarp species	27	2,700	1.3–22.9	Ohashi et al. (2008); Katayama et al. (2009)
Huai Kha Khaeng, Thailand (15°20'N, 99°27'E, 549–638 m a.s.l.)	Dry evergreen forest	Dipterocarp species	23.5	1,242	Wet season: 3.15–9.99 Dry season: 1.24–3.84	Adachi et al. (2009)
Sakaerat Environmental Research Station, Thailand (14°30' N, 101°56' E, ~500 m a.s.l.)	Dry evergreen forest	<i>Hopea ferrea</i> and <i>Hopea odorata</i>	26.7	1,751	Wet season: 4.3–13.3 Dry season: 1.8–6.8	Booniam et al. (2021)
Ratchaburi Province, Thailand (35°13.3'N, 99°30'3.9"E, 110 m a.s.l.)	Dry dipterocarp forest	<i>Dipterocarpus intricatus</i> , <i>Dipterocarpus obtusifolius</i> , <i>Dipterocarpus tuberculatus</i> , <i>Shorea obtusa</i> , and <i>Shorea siamensis</i>	30.4	1,253	Wet season: 1.89–3.79 Dry season: 0.95–2.84	Hanpattanakit et al. (2015)
Kog-Ma Experimental Watershed of Kasetsart University, Thailand (18°48'N, 98°54'E, ~1,300 m a.s.l.)	Evergreen forest	<i>Castanopsis</i> , <i>Lithocarpus</i> , and <i>Quercus</i> spp	20	2,084	2.13–14.07	Hashimoto et al. (2004)
Phrayao Province, Thailand (19°02'14.38"N, 99°54'10.96"E, 512 m a.s.l.)	Dry dipterocarp forest	<i>Dipterocarpus obtusifolius</i> , <i>Dipterocarpus tuberculatus</i> , <i>Shorea obtusa</i> , and <i>Shorea siamensis</i>	25.1	936	0.77–1.13	Intanil et al. (2018)
Teak stand in Mae Moh plantation, Lampang Province, Thailand (18°25'N, 99°43'E, 380 m a.s.l.)	Teak plantations	Teak	25.8	1,284	0.96–5.02	Kume et al. (2013)
Mae Klong Watershed Research Station, Kanchanaburi province, Thailand (14°35'N, 98°52'E, 100–900 m a.s.l.)	Mixed deciduous forest	<i>Shorea siamensis</i> , <i>Vitex peduncularis</i> , <i>Dillenia parviflora</i> var. <i>Keruui</i> , and <i>Xylia xylocarpa</i> var. <i>Keruui</i>	25	1,650	Wet season; ridge: 4.00–8.25 upper slope: 5.17–6.89 lower slope: 4.20–9.97	Takahashi et al. (2011)
Khao Yai National Park, Thailand (14°26'N, 101°22'E, 700–800 m a.s.l.)	Primary and secondary seasonal evergreen forest	Old-growth forest <i>Dipterocarpus gracilis</i> , <i>Sloanea sigun</i> , <i>Ilex chevalieri</i> , <i>Symplocos cochinchinensis</i> , <i>Schima wallachii</i> intermediate forest <i>Schima wallacii</i> , <i>Machilus gamblei</i> , <i>Eurya acuminata</i> , <i>Symplocos cochinchinensis</i> , <i>Syzygium nervosum</i> Young forest <i>Cratoxylum cochinchinense</i> , <i>Syzygium antisepicum</i> , <i>Adinandra integrifolia</i> , <i>Syzygium nervosum</i> , <i>Symplocos cochinchinensis</i>	22.4	2,100	Old-growth forest: 6.51–15.49 Intermediate forest: 7.28–20.32 Young forest: 4.50–8.86 Dry period; Old-growth forest: 3.55–6.19 Intermediate forest: 5.13–8.05 Young forest: 4.09–6.69	This study

Note: Values are shown as ranges. MAT and MAP stand for mean annual temperature in °C and mean annual precipitation in mm, respectively.

Sapwood area~DBH allometries for 14 common tree species in a successional tropical forest in Thailand

Siriphong Yaemphum¹, Weerapong Unawong² and Pantana Tor-ngern^{3,4}

¹Graduate School, Chulalongkorn University, 254 Payathai Rd, Wang Mai, Pathumwan, Bangkok 10330, Thailand

²Center of Excellence on Hazardous Substance Management, Chulalongkorn University, 254 Payathai Rd, Wang Mai, Pathumwan, Bangkok 10330, Thailand

³Department of Environmental Science, Faculty of Science, Chulalongkorn University, 254 Payathai Rd, Wang Mai, Pathumwan, Bangkok 10330, Thailand

⁴Water Science and Technology for Sustainable Environment Research Group, Chulalongkorn University, 254 Payathai Rd, Wang Mai, Pathumwan, Bangkok 10330, Thailand

*Corresponding author E-mail: Pantana.t@chula.ac.th

Received 8 August 2021

Sapwood area is an important parameter for estimating canopy transpiration in the forest water cycle. However, sapwood area highly varies across species and forest ecosystems and is difficult to measure directly. Therefore, species- and site-specific allometric equations are needed to estimate the sapwood area of all trees in a forest. Here, we conducted a comprehensive campaign to measure sapwood thickness and to estimate the sapwood area of 14 common tree species in a successional forest in Thailand. These data represent the first comprehensive measurements of sapwood area in south-east Asian successional forests growing under diverse environmental conditions in terms of soil moisture and canopy density. The results show that a power function can significantly explain the relationship between sapwood area and stem size, represented by diameter at breast height (DBH), in all species in both primary and secondary forests. Interestingly, a single equation could describe the sapwood area~DBH relationship in all species and forest stages, except for *Dipterocarpus gracilis*, an emergent, dominant species in the primary forest. The latter showed slower growth in sapwood area once the trees reached a DBH of ~30 cm. Overall, our results can benefit future studies that estimate canopy transpiration of tropical forests with similar conditions as in our study sites.

Introduction

Forests are an important part of the global water cycle. Specifically, transpiration from forests represents ~40–90 per cent of the total amount of water emitted to the atmosphere (Miralles *et al.*, 2011; Jasechko *et al.*, 2013; Wang-Erlansson *et al.*, 2014; Good *et al.*, 2015), thus significantly affecting the hydrological and energy partitioning processes in terrestrial ecosystems (Bonan, 2008). Among the global forests, tropical forests play an important role in mitigating rising atmospheric carbon (C) dioxide contents and thus related climate change impacts by sequestering ca. 0.28–1.26 Pg C annually (Hubau *et al.*, 2020). However, widespread deforestation and land use change in the tropics are rapidly transforming these ecosystems, with over 80 million ha of natural, old-growth tropical forests being lost since 1990 (FAO and UNEP, 2020). In south-east Asia, transformation of forests to large-scale agricultural production and commercial tree plantations has been identified as the main drivers of forest loss (Curtis *et al.*, 2018). In some areas, the abandonment of such large-scale agricultural operations due to unsustainable practices led to the regeneration of secondary

forests (SFs) through natural or artificial processes. As a result, forests in south-east Asia typically comprise a mosaic of primary, old-growth forests and forests at different stages of secondary succession.

Because tropical forests commonly contain various successional stages, it is challenging to estimate canopy transpiration, which is influenced by many factors, including canopy structure, microclimatic and soil conditions and species composition. Many studies have demonstrated that sap flow measurements are an effective but time-consuming and hence costly method to estimate tree water use and thus canopy transpiration. Most sap flow measurement methods rely on point measurements of sap flux density across the conductive sapwood (xylem) area. The whole tree water use is generally defined as the product of sap flux density and sapwood area. Previous studies showed that the variability of sap flux density among trees of different ages and sizes is relatively low (e.g. Kumagai *et al.*, 2007; Reyes-Acosta and Lubczynski, 2013, 2014; Jaskierniak *et al.*, 2016; Tor-Ngern *et al.*, 2017); therefore, the whole tree water use within a given forest should mostly depend on the sapwood area of the trees in the area.

Despite the importance of quantifying sapwood areas of trees, there is inadequate research on this topic. One of the major constraints in using sapwood area for estimating canopy transpiration is the potentially high variability of sapwood patterns among species, especially in tropical trees (Parolin *et al.*, 2008; Horna *et al.*, 2011). Another limitation is that cutting down trees for measuring sapwood area is often prohibited and it is hence challenging to collect corresponding data. An alternative approach is the extraction of wood cores using an increment borer to measure sapwood depth and then estimate the sapwood area. After being collected from trees, the increment cores are stained with a chemical solution to reveal the difference in chemical composition between the hydro-conductive sapwood and the non-conductive heartwood areas. Some examples of chemical solutions for staining wood cores include methyl orange, benzidine, sodium nitrite, safranin, astra and Eosin-B (Lubczynski *et al.*, 2017). The latter were proven to be successful in estimating sapwood areas in many studies (Pfautsch *et al.*, 2012). Once sapwood area is determined, the whole tree water use can be estimated in combination with the measured sap flux density (e.g. Granier *et al.*, 1996; Wullschleger *et al.*, 1998; Tor-Ngern *et al.*, 2017). At the forest scale, the canopy transpiration is calculated using the total sapwood area of all trees within the stand and the weighted average sap flux density data from sampled trees, depending on the site-specific scaling approach. Because it is difficult to determine sapwood area of all trees in the forest stand, species-specific allometric equations for estimating sapwood area from biometric parameters, such as diameter at breast height (DBH), basal area or crown area, are often used to obtain the total sapwood areas within a stand (Lubczynski *et al.*, 2017; Güney, 2018; Aparecido *et al.*, 2019).

Allometric equations for estimating sapwood area using biometric parameters of trees have been developed for various tree species and forest ecosystems (e.g. Cienciala *et al.*, 2000; Wullschleger *et al.*, 2002; Kumagai *et al.*, 2005; Parolin *et al.*, 2008; Lubczynski *et al.*, 2017; Güney, 2018; Aparecido *et al.*, 2019), but only a few of them exist in tropical regions, and studies for successional forests in South-east Asia are particularly rare. This study aims to develop species-specific allometric equations relating sapwood area with tree size, represented by DBH, for 14 common species in a south-east Asian forest harboring two successional stages. Additionally, one of the examined species existed in both primary and secondary successional stages with different canopy heights and soil moisture conditions. Because allometric relationships between sapwood area and tree size of the same species can vary across site conditions, such as elevation (Mitra *et al.*, 2020), we hence used the data of this species to explore whether different forest stages, with corresponding site conditions, affected the relationship between sapwood area and tree size. In this study, we did not intend to perform deep investigation on the physiological mechanism of sapwood growth. However, we aimed to develop allometric equations for estimating sapwood area of common species in successional forests, which will be used in combination with the ongoing monitored sap flux measurement in the forests to estimate canopy transpiration. The derived equations may be used for estimating tree and canopy transpiration in other successional forests of this region and may also facilitate the calculation of sapwood areas of trees in other tropical forests growing under similar environmental conditions.

Methods

Study site

The measurements were conducted in a seasonal evergreen forest in Khao Yai National Park (KYNP), Nakhon Ratchasima Province, Thailand (14°26'31" N, 101°22'55" E, 700–800 m asl). Mean annual temperature and rainfall at the site are 22.4°C and 2100 mm, respectively, based on 1994–2018 data (Department of National Parks, Wildlife and Plant Conservation; 25-year means). The wet season is usually from May to October, while the dry season lasts from late October to April, when the total monthly rainfall is <100 mm (Brockelman *et al.*, 2017). KYNP consists of old-growth (primary) forest with scattered regions of SFs at multiple successional stages, which have regenerated from old fields within the past 50 years (Jha *et al.*, 2020). In this study, we selected common tree species occurring in two permanent plots, one located in a primary and the other in a SF. The first plot was a 30-ha Mo Singto forest dynamic plot (Brockelman *et al.*, 2017), which is a ForestGEO plot in the global network of the Center for Tropical Forest Science, Smithsonian Tropical Research Institute (Davies *et al.*, 2021). This plot represents an old-growth, primary forest (hereafter PF), with an age of at least 200 years. The PF's mean canopy height was 30 m, with a leaf area index (LAI) of 5 and a stem density of 1112 trees ha⁻¹ (Chanthorn *et al.*, 2016; Brockelman *et al.*, 2017). Approximately, 3 km away from the PF plot, a 2-ha plot in a 4-year-old, initial-stage SF was established. Its mean canopy height was 15 m and stem density was 1226 trees ha⁻¹. For this plot, no LAI data were available but the SF canopy visually appeared to be distinctly sparse compared with the canopy of PF. The soil type of both forests was gray, brown ultisol (Brockelman *et al.*, 2017), with soil bulk densities of 1.26 and 1.24 g cm⁻³ in PF and SF, respectively. In a separate campaign for another study, soil moisture was measured at 25 locations in each plot during the onset of the dry season (February 2020). The measurements showed that soil moisture was significantly higher in PF (45.4 ± 8.72 per cent) than in SF (23.9 ± 5.34 per cent).

Tree sampling and measurements

We used information on occurring tree species and their size distribution, which were collected in the most recent census during which all trees with DBH > 1 cm were surveyed and measured for DBH. The corresponding measurements were conducted in 2016 for PF (Brockelman *et al.*, 2017) and in 2017 for SF (Chanthorn *et al.*, 2017). For each forest stage, we selected common species based on the ranking of relative basal area and by ensuring a sufficiently high number of trees that we could sample from around the permanent study plots. According to the ranking in PF, we selected species with relative basal area ranging from 3 to 11 per cent, whereas it was 12–31 per cent in SF. The seemingly low species-specific relative basal area values in PF were due to the high diversity in this site. The species with the highest measured relative basal area was *Dipterocarpus gracilis* with 11 per cent. After using the plot data to identify representative species, we sampled trees outside the permanent plots to collect tree cores to avoid disturbance of trees in the plots that are subject to ongoing studies. In total, we sampled 14 common species: 11 species were from PF (*D. gracilis*, *Choerospondias axillaris*,

Ilex chevalieri, *Symplocos cochinchinensis*, *Gironniera nervosa*, *Sloanea sigun*, *Cinnamomum subavenium*, *Machilus gamblei*, *Schima wallichii*, *Mastixia pentandra* and *Syzygium nervosum*) and 3 species were from SF (*Adinandra integririma*, *Syzygium antisepticum* and *Cratoxylum cochinchinensis*). Among the chosen species, only one of them, *S. nervosum*, existed in both successional stages and was used to explore whether the allometric equation differed between the two forest stages. For the tree sampling, we additionally considered the DBH distribution of each species based on the 2016 (PF) and 2017 (SF) measurement campaigns. We realized that the information of tree size that was used to determine sampling intervals did not match with the ages of trees during our measurement campaign, which should be older. However, such mismatch should not affect our main objective for developing the allometric equations. Furthermore, data from the 2016–2017 census were the only available information we had to determine the size distribution of trees. To ensure that our dataset for developing the allometries contained samples from the complete spectrum of DBH values occurring on the sites, we partitioned the range of the DBH data into intervals of 10 cm and sampled three trees from each interval for measurements. Only healthy trees with no apparent diseases, broken tops or hollowed stem were chosen.

The sample collection was done in July–September 2020 and in June 2021 which corresponded to the wet season. After measuring the DBH of each study tree, we debarked a small area on the tree and took a wood core sample from three equally spaced position along the azimuthal direction around the stem. We used an increment borer of 5.15 mm diameter (Haglöf, Sweden) to collect a wood core sample of at least half the DBH of each tree. The sample collection was done during 10:00 a.m.–15:00 p.m. when transpiration was high (Tor-ngern *et al.*, 2021). Then, we immediately stained each core sample with 0.1 per cent methyl orange which, after 15 min, distinguished regions of sapwood with light color compared with the dark region of heartwood (Forrester *et al.*, 2010; Burgess and Downey, 2014; Molina *et al.*, 2016; Macfarlane *et al.*, 2018). The sapwood thickness was then measured using a ruler. To avoid further damage to the sample trees, we randomly chose a tree from the sampled ones within each class size for measuring bark thickness. For each selected tree, we took three wood core samples of up to 5 cm depth from the outside bark and measured bark thickness using a vernier caliper. Then, we took the average of measured bark thickness values from the three samples and used it in our calculation. Next, we calculated sapwood area (A_s) of the trees using the following equation:

$$A_s = \pi \left((R - \bar{D}_{\text{bark}})^2 - (R - \bar{D}_{\text{bark}} - \bar{D}_{\text{sapwood}})^2 \right), \quad (1)$$

where R is stem radius, and \bar{D}_{bark} and \bar{D}_{sapwood} represent averaged bark thickness and sapwood thickness, respectively. All units are in cm. Because our data showed small azimuthal variation in sapwood thickness for each tree ($CV \leq 7$ per cent), our assumption of circular shape for calculating the sapwood area was confirmed.

Data analysis

We performed an exploratory data analysis and implemented regression analyses to derive allometric equations between A_s and DBH in SigmaPlot 12.0 (Systat Software, Inc., San Jose, CA, US). Although some previous studies also explored bark thickness and sapwood thickness as predictors (Güney, 2018), we did not use it in our analysis after finding no significant relationship in the former (Supplementary Figure S1). By contrast, the relationship between sapwood area and sapwood thickness was significant (Supplementary Figure S2). However, we chose DBH as the main predictor to make our allometries universally applicable for future analysis such as estimating the sapwood area of all trees in the forests for calculating canopy transpiration. In addition, using DBH is more suitable because it is a commonly measured metric and causes no damage to the trees. We first performed the analyses by species, then with pooled data for each study site and finally from all sites if no significant difference was found, using an F -test to analyze the difference between regression lines. We also compared the allometric equation of the only species growing in both sites (i.e. *S. nervosum*). Based on the exploratory data analysis, two types of equations were tested: an exponential growth function ($y = ae^{bx}$) and a power function ($y = ax^b$). Both equation forms had to go through the origin under the assumption that no sapwood area would be observed with zero DBH. The power function yielded lower standard error of the regression than the exponential growth form (Supplementary Table S1); thus, we employed the power function in our analysis. To validate the performance of the selected regression lines, we further assessed whether residuals of the regression varied with DBH. All statistical tests were based on the significance level of 5 per cent.

Finally, we considered different physiological characteristics, including wood type (i.e. hard- vs softwood) and leaf habit (deciduous vs evergreen), in the studied species as shown in Table 1. Hardwood species are often associated with slow growth and they tend to build more heartwood than sapwood, whereas the opposite is observed in softwood species (Gartner and Meinzer, 2005; Lachenbruch *et al.*, 2011). For leaf habit, deciduous species generally grow fast in the active season, resulting in larger variation in sapwood growth in the species compared with in evergreen species (Givnish, 2002). We therefore tested whether the allometric relationships for the group of these physiological traits differed.

Results

Table 1 summarizes the average values and range of bark and sapwood thickness and corresponding estimates of sapwood area of the selected species. Mean sapwood thickness of the species ranged between 7.6 and 24.8 cm, accounting for 35 per cent–99 per cent of the stem radius. *Dipterocarpus gracilis* showed distinctively low fraction of sapwood thickness, and therefore a large heartwood region, compared with the other species. Average sapwood area of each studied species ranged from 230 to 3258 cm², comprising 63 per cent–99 per cent of the tree basal area. Among the studied species, almost no heartwood was observed in four species, including *S. cochinchinensis*, *G. nervosa*, *I. chevalieri* and *M. pentandra*. Despite the relatively high

Table 1 Information of the selected tree species for developing allometric equations in the primary forest and secondary forests, along with mean \pm 1 SD in bold and the range of DBH (cm), bark and sapwood thickness (cm) and sapwood area (m^2) for each species. The sample size (n) is the number of trees used in the analysis. Leaf habit was identified as deciduous (D) or evergreen (E) according to Brockelman *et al.* (2017). The species were categorized into two wood types: moderately hard to hardwood (H) and softwood (S) according to the noted references.

Species	Leaf habit	Wood type	n	DBH (cm)	Bark thickness (cm)	Sapwood thickness (cm)	Sapwood area (m^2)
Primary forest							
<i>Dipeterocarpus gracilis</i>	D	H ^{1,2}	30	59.19 \pm 30.93 (10.4–127.0)	0.41 \pm 0.12 (0.27–0.62)	10.48 \pm 2.76 (4.94–15.33)	0.17 \pm 0.13 (0.01–0.43)
<i>Choerospondias axillaris</i>	D	H ³	30	60.43 \pm 28.74 (15.4–112.0)	0.47 \pm 0.05 (0.40–0.55)	24.81 \pm 10.17 (7.30–41.67)	0.33 \pm 0.26 (0.02–0.90)
<i>Ilex chevalieri</i>	E	S ⁴	12	25.32 \pm 11.68 (12.1–42.5)	0.06 \pm 0.02 (0.03–0.09)	13.78 \pm 5.32 (6.00–21.16)	0.07 \pm 0.05 (0.01–0.14)
<i>Symplocos cochinchinensis</i>	E	S ⁵	15	34.97 \pm 12.55 (16.0–52.3)	0.05 \pm 0.01 (0.04–0.07)	17.38 \pm 6.30 (7.96–26.09)	0.11 \pm 0.07 (0.02–0.21)
<i>Gironniera nervosa</i>	E	H ⁴	15	35.17 \pm 13.75 (15.5–57.4)	0.17 \pm 0.02 (0.14–0.19)	17.03 \pm 6.32 (7.61–26.91)	1.09 \pm 0.08 (0.02–0.25)
<i>Sloanea sigun</i>	E	S ⁶	15	33.57 \pm 13.99 (10.4–54.1)	0.56 \pm 0.14 (0.34–0.73)	15.34 \pm 6.34 (4.86–24.42)	0.10 \pm 0.07 (0.01–0.21)
<i>Cinnamomum subavenium</i>	E	S ⁷	15	35.4 \pm 14.06 (13.2–59.5)	0.10 \pm 0.06 (0.04–0.19)	14.63 \pm 5.70 (5.63–23.83)	1.08 \pm 0.08 (0.01–0.25)
<i>Machilus gamblei</i>	E	S ⁸	15	34.51 \pm 14.15 (13.5–58.0)	0.08 \pm 0.01 (0.06–0.10)	11.98 \pm 5.29 (5.60–23.50)	0.10 \pm 0.07 (0.01–0.22)
<i>Schima wallichii</i>	E	H ⁹	15	33.73 \pm 14.45 (13.7–55.0)	0.43 \pm 0.08 (0.34–0.56)	8.52 \pm 3.22 (4.33–14.17)	0.08 \pm 0.06 (0.01–0.17)
<i>Mastixia pentandra</i>	E	S ¹⁰	15	34.71 \pm 14.45 (13.7–56.3)	0.22 \pm 0.2 (0.20–0.26)	17.00 \pm 7.11 (6.64–27.93)	1.07 \pm 0.08 (0.01–0.25)
<i>Syzygium nervosum</i>	E	H ⁴	15	35.11 \pm 14.79 (11.4–59.2)	0.47 \pm 0.03 (0.44–0.52)	12.37 \pm 4.57 (5.18–19.33)	0.10 \pm 0.07 (0.01–0.23)
Secondary Forest							
<i>S. nervosum</i>	E	H ⁴	9	25.18 \pm 9.79 (11.0–39.5)	0.54 \pm 0.06 (0.49–0.61)	8.94 \pm 5.38 (3.60–17.00)	0.05 \pm 0.04 (0.01–0.11)
<i>Adinandra integerrima</i>	E	S ⁴	6	17.1 \pm 5.11 (11.1–30.0)	0.23 \pm 0.01 (0.22–0.23)	7.60 \pm 1.95 (5.33–10.23)	0.02 \pm 0.01 (0.01–0.04)
<i>Syzygium antisepticum</i>	E	H ⁴	9	22.94 \pm 8.78 (12.3–33.5)	0.31 \pm 0.03 (0.28–0.34)	10.36 \pm 4.02 (5.87–16.43)	0.04 \pm 0.03 (0.01–0.09)
<i>Cratoxylum cochinchinensis</i>	D	H ^{11,12}	9	24.19 \pm 10.94 (10.7–39.6)	0.44 \pm 0.14 (0.25–0.56)	9.62 \pm 3.46 (5.00–14.80)	0.05 \pm 0.04 (0.01–0.11)

¹Uphof (1959). ²Gamal (2014). ³Phongkrathung *et al.* (2016). ⁴De Guzman and Siemonsma (1999). ⁵Weerakoon *et al.* (2014). ⁶Priyadi *et al.* (2010).

⁷Wuu-Kuang (2011). ⁸Schultz (2005). ⁹Handayani and Hidayati (2020). ¹⁰Matthew (1976). ¹¹Wong (1995). ¹²Kritsanachandee and Sookchaloem (2006).

variation in the averages, the standard deviation (SD) of sapwood thickness and area were quite similar among the species.

Regression analysis between sapwood area and DBH showed significant results for all species (Figures 1–3). The residual analyses of the derived models showed no significant trends with changes in DBH in all species (Supplementary Figures S3–S5) and hence confirmed the validity of the allometries. Overall, the power function explained the relationships between DBH and sapwood area very well with r^2 values ranging from 0.97 to 1.00. Concerning the examined physiological characteristics (hard vs softwood and deciduous vs evergreen species) our results showed no significant difference among them. For *S. nervosum* which grew in both PF and SF, a single equation could

explain the DBH~sapwood relationship across both successional stages (Figure 3A). Considering pooled data, a power function significantly described the DBH~sapwood relationship for all species, regardless of successional stages, except for *D. gracilis* (Figure 4).

Discussion

Although many techniques are available for determining sapwood area of trees, all of them have their own advantages and disadvantages, which make the techniques more or less suitable for different purposes. For example, recent

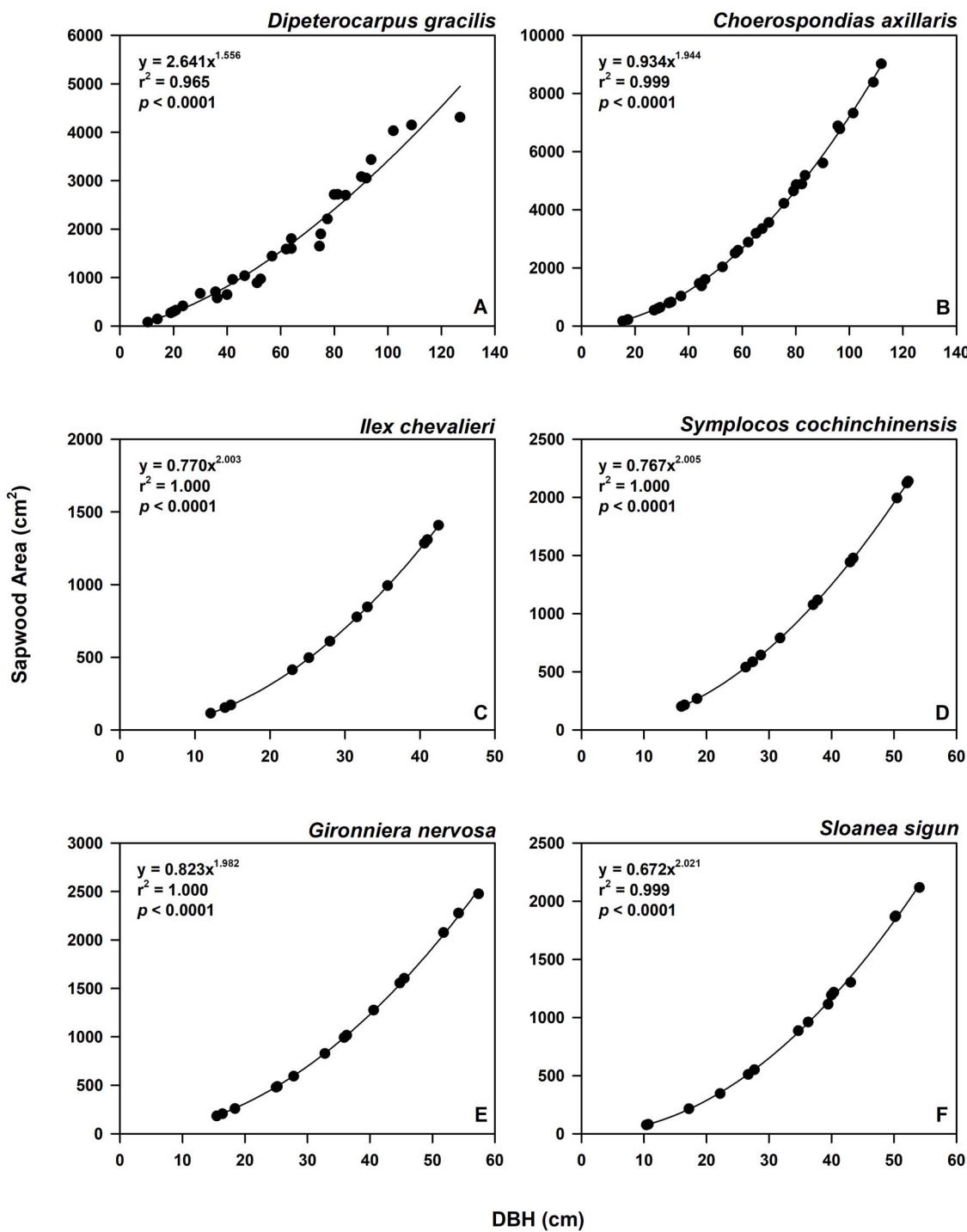


Figure 1 Regression results for the relationship between sapwood area (cm^2) and DBH (cm) of the species in primary forest in KYNP, Thailand, including (A) *Dipterocarpus gracilis* (B) *Choerospondias axillaris* (C) *Ilex chevalieri* (D) *Symplocos cochinchinensis* (E) *Gironniera nervosa* and (F) *Sloanea sigun*. Note that the scales are different.

studies recommended using computer tomography for accurate estimation of sapwood, but the technique is expensive and requires extensive data processing (Quinonez-Pinon and Valeo, 2017). The cut-and-dye technique is perhaps the most direct method for measuring sapwood area, but it is highly destructive

and hence often infeasible, particularly in protected areas. For this study, we chose the staining method which we applied to three bore-cores extracted from each sampled tree during periods of high transpiration. We believe that our method was suitable, given the challenging situation in the field and

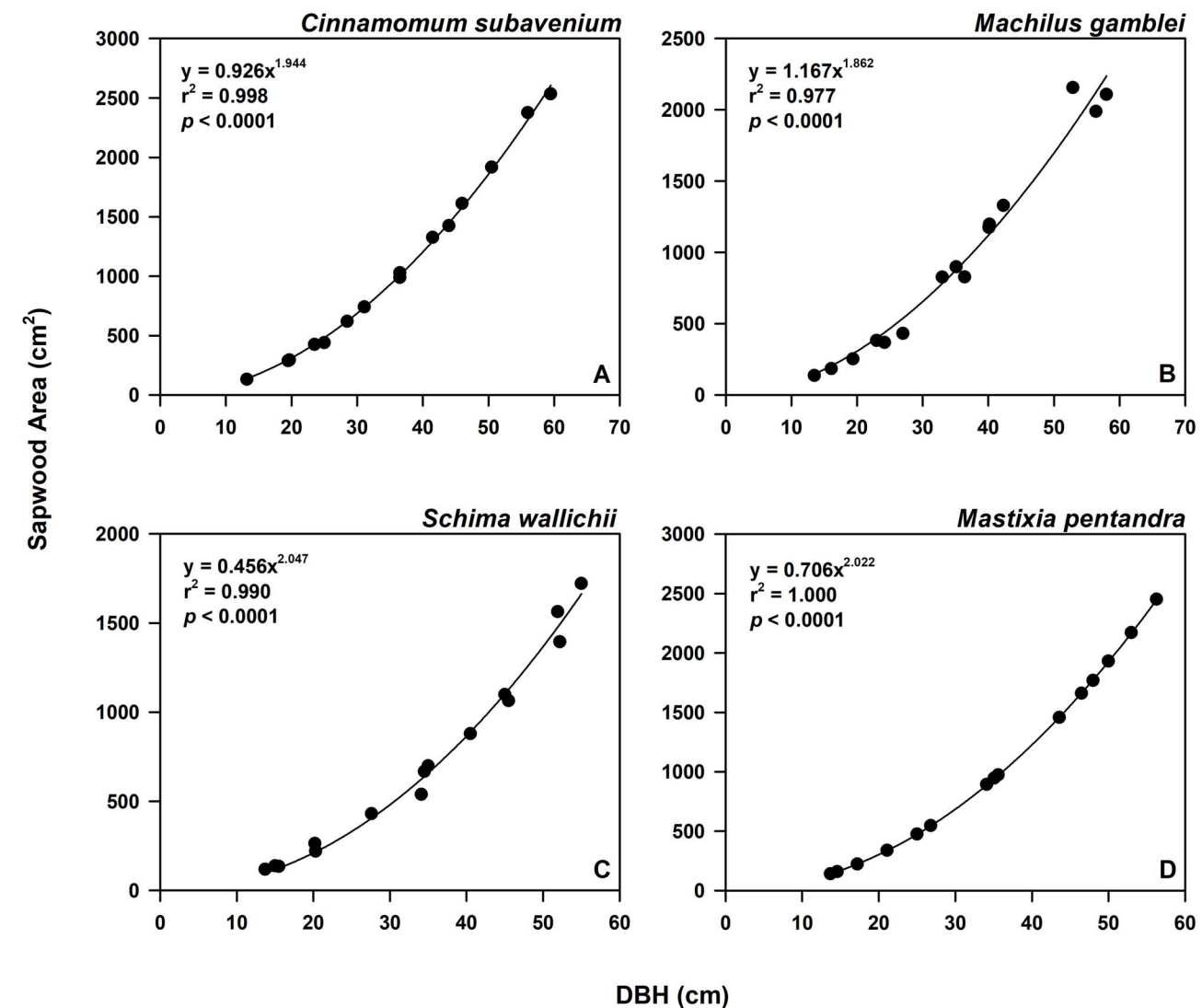


Figure 2 Regression results for the relationship between sapwood area (cm^2) and DBH (cm) of the species in primary forest in KYNP, Thailand, including (A) *Cinnamomum subavenium* (B) *Machilus gamblei* (C) *Schima wallichii* and (D) *Mastixia pentandra*. Note that the scales are different.

considering the conservation status of the study area. Nevertheless, future studies using other techniques may be performed to verify our approach in this area. One factor that may affect the measurement of sapwood thickness is the presence of hollow stems, which was found to account for up to 83 per cent of stems' cross sections in other tropical sites (Heineman *et al.*, 2015). However, none of our sample trees was hollow because we carefully selected healthy trees and excluded trees from the selection if we found large cavities in the cores. Furthermore, the relatively small to medium sizes of most sample trees may have contributed to the sparse number of hollow stems during our sampling procedure as hollow stems have been frequently observed in trees of DBH > 50 cm in tropical forests (Heineman *et al.*, 2015).

For all species, sapwood thickness did not vary circumferentially, validating the assumption of circular sapwood area. The invariant sapwood thickness around the tree also

implied that the trees were not influenced by environmental conditions, such as variations in light exposure and soil moisture around the tree. In some boreal species, sapwood thickness was significantly different between north-facing and south-facing sides of the trees which experienced different solar irradiation (Quinonez-Pinon and Valeo, 2017), resulting in smaller sapwood thickness in the side with longer sunlight exposure – an adaptation of the tree to avoid losing much water. Sapwood areas of the studied species (ranging from 230 to 3258 cm^2 for DBH ranges of 10.4–127 cm) were within the range of values reported for seven tree species in another tropical forest in south-east Asia (43–4395 cm^2 for DBH ranges of 10.4–95 cm; Horna *et al.*, 2011), but somewhat higher than those in other neotropical and montane forests (Granier *et al.*, 1996; Andrade *et al.*, 1998; Goldstein *et al.*, 1998; Anhuf *et al.*, 1999; Meinzer *et al.*, 1999; Motzer *et al.*, 2005; Parolin *et al.*, 2008; Aparecido *et al.*, 2016; Kunert *et al.*, 2017; Moore *et al.*, 2018).

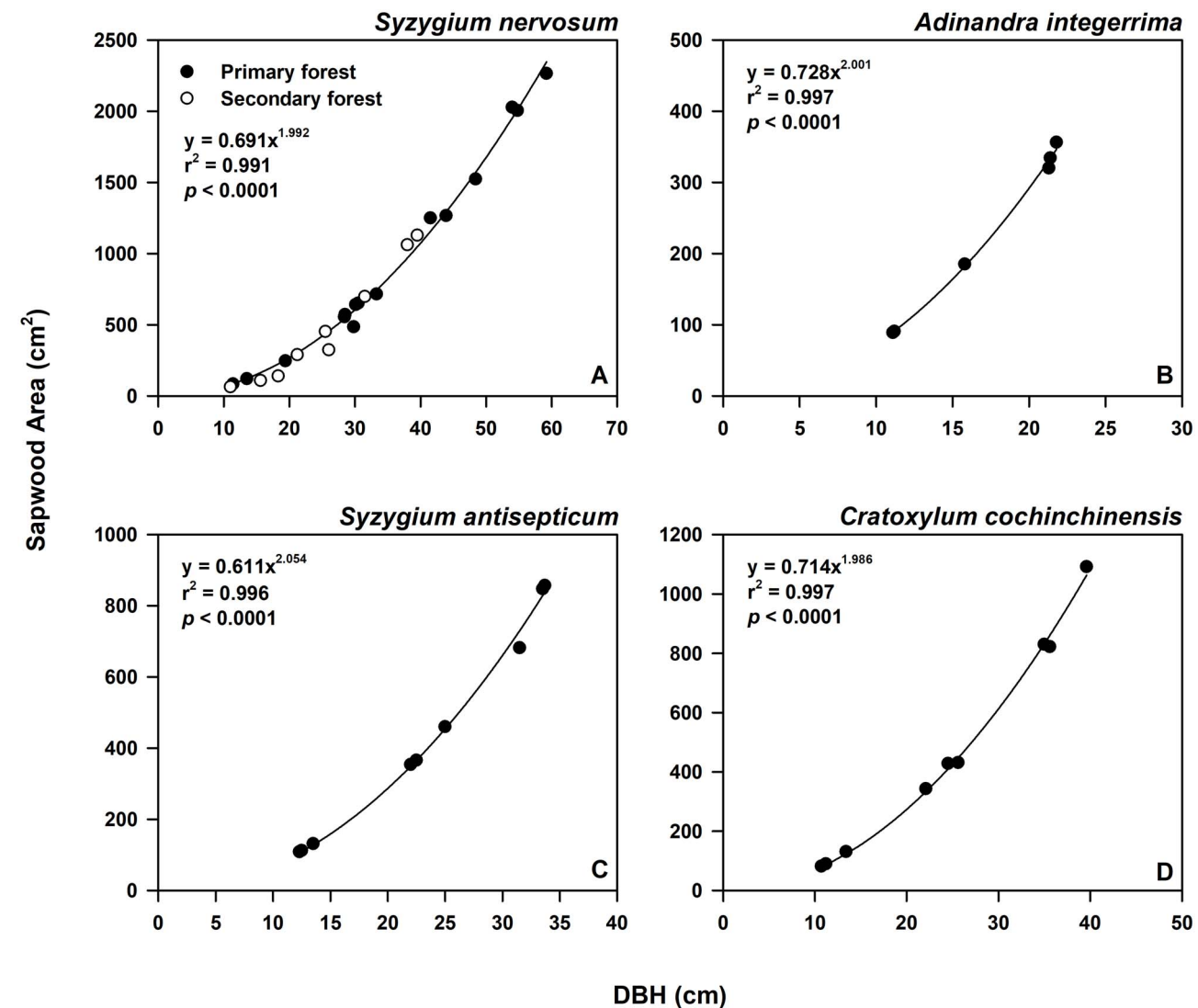


Figure 3 Regression results for the relationship between sapwood area (cm²) and DBH (cm) of the species in SF in KYNP, Thailand. Note that the result for *S. nervosum* (A) included data from both primary (closed circles) and secondary (open circles) forests and that the scales are different. (B) - (D) show results for *Adinandra integerrima*, *Syzygium antisepticum* and *Cratoxylum cochinchinensis*, respectively.

According to these studies, sapwood area in tropical tree species considerably varies across species and forest ecosystems. However, our result surprisingly showed that the allometric relationship between sapwood area and tree size was mostly consistent across tree species and the two examined successional stages with partly differing environmental conditions.

At the tree level, several biometric parameters have been explored to predict sapwood area. For example, in a montane Mediterranean conifer, Güney (2018) related sapwood area to DBH, tree basal area, sapwood thickness and stem radius without bark. The study found that stem radius without bark explained most of the variation in data. In our study, we also measured the bark thickness of the sample trees and found a generally small bark thickness (<4 per cent of stem radius) which related less well to sapwood area (Supplementary Figure S1). Additionally, previous studies often used DBH as the predictor for sapwood

area because it is the most common tree metric that is frequently measured in the field. Thus, we here focused on DBH as the main predictor of sapwood area. Tree height and crown area have also been used to predict sapwood area (Lubczynski et al., 2017; Güney, 2018; Aparecido et al., 2019), but it was difficult to perform measurements of both parameters in these forests with our available tools. Nevertheless, a further study including measurements of these parameters would potentially improve the allometric equations to extend their use to cover application with large-scale analysis, such as one involving remote-sensing data. The power function significantly described the relationships between sapwood area and DBH in all species, suggesting that these trees continued to develop sapwood area as they grow. Furthermore, a single equation could explain the DBH~sapwood area relationship for *S. nervosum* samples collected in both successional stages. Thus, different environmental conditions in both

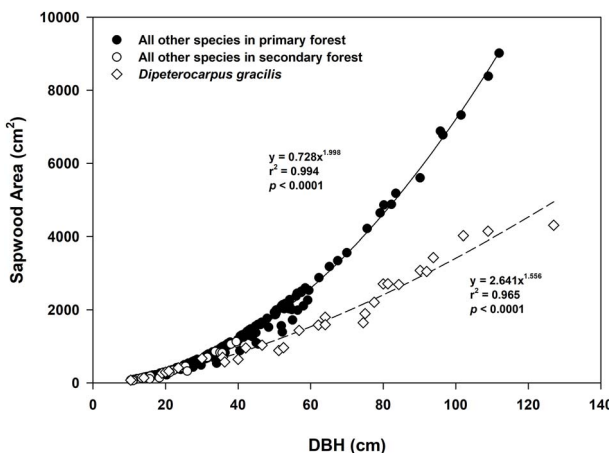


Figure 4 Regression results for the relationship between sapwood area (cm^2) and DBH (cm) of all study species in KYNP, Thailand. Circles represent data from all species except *D. gracilis* which is shown in diamonds. Closed (open) circles represent data from all species except *D. gracilis* in the primary (secondary) forest.

sites did not influence the relation between sapwood area and tree size in this particular species, supporting its presence in multiple forest stages.

Combining data from all species, a single power function significantly described the relationship between sapwood area and DBH, regardless of forest stages, except for *D. gracilis*. The equation for *D. gracilis* suggested that sapwood area of this species grows fast in small trees (i.e. $\text{DBH} < 30 \text{ cm}$) but is slow in large trees. In fact, sapwood area of *D. gracilis* individuals with $\text{DBH} < 30 \text{ cm}$ on average accounted for ~96.8 per cent of the basal area. However, for the larger trees with a $\text{DBH} \geq 30 \text{ cm}$, the average proportion of sapwood area to basal area was 33.8 per cent. This indicates that the small trees almost exclusively grow sapwood to rapidly acquire and transport resources to outcompete others; however, when the trees reach a certain size, they invest more in building heartwood for structural support (Gower *et al.*, 1993; Pruy *et al.*, 2003). A future study investigating whether detailed physiological and functional traits of the species affect the allometric equations between DBH and sapwood is desirable. The two traits examined in our study (hard vs softwood and deciduous vs evergreen species) did not show any effect on the DBH + sapwood relationship. The developed allometric equations for the pooled dataset can hence be used for calculating the sapwood area of most trees in these forests if their DBH is known. The resulting sapwood area estimates can be used for estimating canopy transpiration, which is a significant component of water cycles in forests (e.g. Tor-ngern *et al.*, 2017).

Conclusions

In this study, we performed measurements of sapwood thickness and estimated sapwood area of 14 common tree species in a successional forest in Thailand. These data represent the first comprehensive measurements of these parameters in tropical forests in south-east Asia growing in forests of two successional stages. The results show that a power function significantly explains the

relationship between sapwood area and stem size, represented by DBH, in all species in both primary and SFs. Interestingly, a single equation could describe the relationship in all species and sites, except for *D. gracilis*, an emergent, dominant species in the primary forest. The allometric equation for *D. gracilis* indicated that the sapwood area of this species grows slower than in other species in this forest once tree individuals have reached a DBH of ~30 cm. Our results will greatly benefit studies that aim to estimate the canopy transpiration of tropical forests growing under similar conditions as the forests in our study sites.

Supplementary data

Supplementary data are available at *Forestry* online.

Acknowledgements

We would like to thank Dr. Warren Brockelman, Dr. Wirong Chanthon and Ms. Anuttara Nathalang for information about tree species and size distribution of trees in permanent plots in the PFs and SFs. We appreciate comments and suggestions for improving the theoretical writing of the manuscript from the editors, the reviewers and Dr. Nisa Leksungnoen. We are grateful for field assistance from Rathasart Somnuk, Ratchanon Ampornpitak and Prangwilai Khobpee.

Conflict of interest statement

None declared.

Funding

National Science and Technology Development Agency (P-18-51395); Thailand Science Research and Innovation (RDG6230006).

Data availability

The raw data used in this study are publicly available in the Dryad repository at doi:10.5061/dryad.qz612jmgh.

References

- Andrade, J.L., Meinzer, F.C., Goldstein, G., Holbrook, N.M., Cavelier, J., Jackson, P. *et al.* 1998 Regulation of water flux through trunks, branches, and leaves in trees of a lowland tropical forest. *Oecologia* **115**, 463–471.
- Anhuf, D., Motzer, T., Rollenbeck, R., Xfc, Tger, Schr *et al.* 1999 Water budget of the Surumoni crane site (Venezuela). *Selbyana* **20**, 179–185.
- Aparecido, L.M.T., Miller, G.R., Cahill, A.T. and Moore, G.W. 2016 Comparison of tree transpiration under wet and dry canopy conditions in a Costa Rican premontane tropical forest. *Hydro. Process.* **30**, 5000–5011.
- Aparecido, L.M.T., dos Santos, J., Higuchi, N. and Kunert, N. 2019 Relevance of wood anatomy and size of Amazonian trees in the determination and allometry of sapwood area. *Acta Amazon.* **49**, 1–10.
- Bonan, G.B. 2008 Forests and climate change: forcings, feedbacks, and the climate benefits of forests. *Science* **320**, 1444–1449.
- Brockelman, W.Y., Nathalang, A. and Maxwell, J.F. 2017 *Mo Singto Forest Dynamics Plot: Flora and Ecology*. National Science and Technology Development Agency.

Burgess, S. and Downey, A. 2014 *SFM1 Sap Flow Meter Manual*. ICT International Pty. Ltd.

Chanthorn, W., Hartig, F. and Brockelman, W.Y. 2017 Structure and community composition in a tropical forest suggest a change of ecological processes during stand development. *For. Ecol. Manag.* **404**, 100–107.

Chanthorn, W., Ratanapongsai, Y., Brockelman, W., Allen, M., Favier, C. and Dubois, M.-A. 2016 Viewing tropical forest succession as a three-dimensional dynamical system. *Theor. Ecol.* **9**, 163–172.

Cienciala, E., Kucera, J. and Malmer, A. 2000 Tree sap flow and stand transpiration of two *Acacia mangium* plantations in Sabah. *Borneo. J. Hydrol.* **236**, 109–120.

Curtis, P.G., Slay, C.M., Harris, N.L., Tyukavina, A. and Hansen, M.C. 2018 Classifying drivers of global forest loss. *Science* **361**, 1108–1111.

Davies, S.J., Abiem, I., Abu Salim, K., Aguilar, S., Allen, D., Alonso, A. et al. 2021 ForestGEO: understanding forest diversity and dynamics through a global observatory network. *Biol. Conserv.* **253**, 108907.

De Guzman, C.C. and Siemonsma, J.S. 1999 *Plant Resources of South-East Asia No 13: Spices*. Backhuys Publishers, 400.

FAO and UNEP 2020 *The State of the World's Forests. Forests, Biodiversity and People*. FAO and UNEP. <https://doi.org/10.4060/ca8642en>.

Forrester, D.I., Collopy, J.J. and Morris, J.D. 2010 Transpiration along an age series of *Eucalyptus globulus* plantations in southeastern Australia. *For. Ecol. Manag.* **259**, 1754–1760.

Gamal, H.M.S. 2014 *Investigation of selected wood properties and the suitability for industrial utilization of Acacia seyal var. seyal Del and Balanites aegyptiaca (L.) Delile grown in different climatic zones of Sudan*. Ph.D. thesis, Technische Universität Dresden.

Gartner, B.L. and Meinzer, F.C. 2005 Structure-function relationships in sapwood water transport and storage. In *Vascular Transport in Plants*. N.M., Holbrook, M., Zwieniecki (eds.). Elsvier/Academic Press, pp. 307–331.

Givnish, T.J. 2002 Adaptive significance of evergreen vs. deciduous leaves: solving the triple paradox. *Silva Fennich* **36**, 1322–1343.

Goldstein, G., Andrade, J.L., Meinzer, F.C., Holbrook, N.M., Cavelier, J., Jackson, P. et al. 1998 Stem water storage and diurnal patterns of water use in tropical forest canopy trees. *Plant Cell Environ.* **21**, 397–406.

Good, S.P., Noone, D. and Bowen, G. 2015 Hydrologic connectivity constrains partitioning of global terrestrial water fluxes. *Science* **349**, 175–177.

Gower, S.T., Haynes, B.E., Fassnacht, K.S., Running, S.W. and Hunt, E.R. Jr. 1993 Influence of fertilization on the allometric relations for two pines in contrasting environments. *Can. J. For. Res.* **23**, 1704–1711.

Granier, A., Huc, R. and Barigah, S.T. 1996 Transpiration of natural rain forest and its dependence on climatic factors. *Agric. For. Meteorol.* **78**, 19–29.

Güney, A. 2018 Sapwood area related to tree size, tree age, and leaf area index in *Cedrus libani*. *Bilge. Sci.* **2**, 83–91.

Handayani, A. and Hidayati, S. 2020 *Schima wallichii* (DC.) Korth. Theaceae. In *Ethnobotany of the Mountain Regions of Southeast Asia*. F.M., Franco (ed.). Springer International Publishing, Cham, pp. 1–8.

Heineman, K.D., Russo, S.E., Baillie, I.C., Marnit, J.D., Chai, P.P.K., Chai, L. et al. 2015 Evaluation of stem rot in 339 Bornean tree species: implications of size, taxonomy, and soil-related variation for aboveground biomass estimates. *Biogeosciences* **12**, 5735–5751.

Horna, V., Schuldt, B., Brix, S. and Leuschner, C. 2011 Environment and tree size controlling stem sap flux in a perhumid tropical forest of Central Sulawesi. *Indonesia. Ann. Forest. Sci.* **68**, 1027–1038.

Hubau, W., Lewis, S.L., Phillips, O.L., Affum-Baffoe, K., Beeckman, H., Cuni-Sánchez, A. et al. 2020 Asynchronous carbon sink saturation in African and Amazonian tropical forests. *Nature* **579**, 80–87.

Jasechko, S., Sharp, Z.D., Gibson, J.J., Birks, S.J., Yi, Y. and Fawcett, P.J. 2013 Terrestrial water fluxes dominated by transpiration. *Nature* **496**, 347–350.

Jaskierniak, D., Kuczera, G., Benyon, R.G. and Lucieer, A. 2016 Estimating tree and stand sapwood area in spatially heterogeneous southeastern Australian forests. *J. Plant Ecol.* **9**, 272–284.

Jha, N., Tripathi, N.K., Chanthorn, W., Brockelman, W., Nathalang, A., Pelissier, R. et al. 2020 Forest aboveground biomass stock and resilience in a tropical landscape of Thailand. *Biogeosciences* **17**, 121–134.

Kritsanachandee, N. and Sookchaloem, D. 2006 Systematic studies of *Cra-toxylum Blume* and *Hypericum L.* (Guttiferae) in Thailand. In *Proceedings of 44th Kasetsart University Annual Conference : Engineering, Architecture, Natural Resources and Environmental Management*. Kasetsart University, Bangkok, Thailand, pp. 602–609.

Kumagai, T., Aoki, S., Shimizu, T. and Otsuki, K. 2007 Sap flow estimates of stand transpiration at two slope positions in a Japanese cedar forest watershed. *Tree Physiol.* **27**, 161–168.

Kumagai, T.O., Nagasawa, H., Mabuchi, T., Ohsaki, S., Kubota, K., Kogi, K. et al. 2005 Sources of error in estimating stand transpiration using allometric relationships between stem diameter and sapwood area for *Cryptomeria japonica* and *Chamaecyparis obtusa*. *For. Ecol. Manag.* **206**, 191–195.

Kunert, N., Aparecido, L.M.T., Wolff, S., Higuchi, N., dos Santos, J., de Araujo, A.C. et al. 2017 A revised hydrological model for the Central Amazon: the importance of emergent canopy trees in the forest water budget. *Agric. For. Meteorol.* **239**, 47–57.

Lachenbruch, B., Moore, J.R. and Evans, R. 2011 Radial variation in wood structure and function in woody plants, and hypotheses for its occurrence. In *Size- and Age-related Changes in Tree Structure and Function*. F.C., Meinzer, B., Lachenbruch, T.E., Dawson (eds.). Vol. **4**. Springer, pp. 121–164. *Tree Physiology*.

Luczynski, M.W., Chavarro-Rincon, D.C. and Rossiter, D.G. 2017 Conductive sapwood area prediction from stem and canopy areas-allometric equations of Kalahari trees. *Botswana. Ecohydrology* **10**, e1856.

Macfarlane, C., Grigg, A., McGregor, R., Ogden, G. and Silberstein, R. 2018 Overstorey evapotranspiration in a seasonally dry Mediterranean eucalypt forest: response to groundwater and mining. *Ecohydrology* **11**, e1971.

Matthew, K.M. 1976 A revision of the genus *Mastixia* (Cornaceae). *Blumea* **23**, 51–93.

Meinzer, F.C., Goldstein, G., Franco, A.C., Bustamante, M., Igler, E., Jackson, P. et al. 1999 Atmospheric and hydraulic limitations on transpiration in Brazilian cerrado woody species. *Funct. Ecol.* **13**, 273–282.

Miralles, D.G., De Jeu, R.A.M., Gash, J.H., Holmes, T.R.H. and Dolman, A.J. 2011 Magnitude and variability of land evaporation and its components at the global scale. *Hydrol. Earth Syst. Sc.* **15**, 967–981.

Mitra, B., Papuga, S.A., Alexander, M.R., Swetnam, T.L. and Abramson, N. 2020 Allometric relationships between primary size measures and sapwood area for six common tree species in snow-dependent ecosystems in the Southwest United States. *J. For. Res.* **31**, 2171–2180.

Molina, A.J., Aranda, X., Carta, G., Llorens, P., Romero, R., Save, R. et al. 2016 Effect of irrigation on sap flux density variability and water use estimate in cherry (*Prunus avium*) for timber production: azimuthal profile, radial profile and sapwood estimation. *Agr. Water Manage.* **164**, 118–126.

Moore, G.W., Orozco, G., Aparecido, L.M.T. and Miller, G.R. 2018 Upscaling transpiration in diverse forests: insights from a tropical premontane site. *Ecohydrology* **11**, e1920.

Motzer, T., Munz, N., Kuppers, M., Schmitt, D. and Anhuf, D. 2005 Stomatal conductance, transpiration and sap flow of tropical montane rain forest trees in the southern Ecuadorian Andes. *Tree Physiol.* **25**, 1283–1293.

Parolin, P., M Ller, E.K.H. and Junk, W.J. 2008 Sapwood area in seven common tree species of central amazon floodplains. *Pesqui. Bot.* **59**, 277–286.

Pfautsch, S., Macfarlane, C., Ebdon, N. and Meder, R. 2012 Assessing sapwood depth and wood properties in *Eucalyptus* and *Corymbia* spp. using visual methods and near infrared spectroscopy (NIR). *Trees* **26**, 963–974.

Phongkrathung, R., Vajrodaya, S. and Kermanee, P. 2016 Wood anatomy and properties of three species in the genus *Spondias* l. (Anacardiaceae) found in Thailand. *Agric. Nat. Resour.* **50**, 14–19.

Priyadi, H., Takao, G., Rahmawati, I., Supriyanto, B., Ikbal Nursal, W. and Rahman, I. 2010 *Five hundred plant species in Gunung Halimun Salak National Park, West Java: A checklist Including Sundanese Names, Distribution and Use.*, Center for International Forestry Research (CIFOR).

Pruyn, M.L., Harmon, M.E. and Gartner, B. 2003 Stem respiratory potential in six softwood and four hardwood tree species in the central cascades of Oregon. *Oecologia* **137**, 10–21.

Quinonez-Pinon, M.R. and Valeo, C. 2017 Allometry of sapwood depth in five boreal trees. *Forests* **8**, 457.

Reyes-Acosta, J.L. and Lubczynski, M.W. 2013 Mapping dry-season tree transpiration of an oak woodland at the catchment scale, using object-attributes derived from satellite imagery and sap flow measurements. *Agric. For. Meteorol.* **174**, 184–201.

Reyes-Acosta, J.L. and Lubczynski, M.W. 2014 Optimization of dry-season sap flow measurements in an oak semi-arid open woodland in Spain. *Ecohydrology* **7**, 258–277.

Schultz, J. 2005 *The Ecozones of the World*. 2nd edn. Springer, 252.

Tor-Ngern, P., Oren, R., Oishi, A.C., Uebelherr, J.M., Palmroth, S., Tarvainen, L. et al. 2017 Ecophysiological variation of transpiration of pine forests: synthesis of new and published results. *Ecol. Appl.* **27**, 118–133.

Tor-ngern, P., Chart-asa, C., Chanthorn, W., Rodtassana, C., Yampum, S., Unawong, W. et al. 2021 Variation of leaf-level gas exchange rates and leaf functional traits of dominant trees across three successional stages in a Southeast Asian tropical forest. *For. Ecol. Manag.* **489**, 119101.

Uphof, J.C.T. 1959 *Dictionary of Economic Plants*. (Bergstrasse) H. R. Engelmann; Hafner, 400.

Wang-Erlandsson, L., van der Ent, R.J., Gordon, L.J. and Savenije, H.H.G. 2014 Contrasting roles of interception and transpiration in the hydrological cycle - Part 1: temporal characteristics over land. *Earth Syst. Dynam.* **5**, 441–469.

Weerakoon, W.M.A.I., Damunupola, J.W. and Gunaratne, A.M.T.A. 2014 *Vegetative Propagation of Two Native Tree Species for the Restoration of Degraded Grasslands in Knuckles Forest Reserve*. University of Peradeniya, p. 592.

Wong, K.M. 1995 Hypericaceae. In *Tree Flora of Sabah and Sarawak*. E., Soepadmo, K.M., Wong (eds.). Sabah Forestry Department, Forest Research Institute Malaysia, Sarawak Forestry Department.

Wullschleger, S.D., Meinzer, F.C. and Vertessy, R.A. 1998 A review of whole-plant water use studies in trees. *Tree Physiol.* **18**, 499–512.

Wullschleger, S.D., Gunderson, C.A., Hanson, P.J., Wilson, K.B. and Norby, R.J. 2002 Sensitivity of stomatal and canopy conductance to elevated CO₂ concentration - interacting variables and perspectives of scale. *New Phytol.* **153**, 485–496.

Wuu-Kuang, S. 2011 Taxonomic revision of *Cinnamomum* (Lauraceae) in Borneo. *Blumea* **56**, 241–264.

1 **Journal:** Journal of Ecology

2 **Variations in leaf water status and drought tolerance of dominant tree species among**

3 **three successional forests in Southeast Asia**

4 Weerapong Unawong¹, Siriphong Yaemphum², Anuttara Nathalang³, Yajun Chen^{4,5}, Jean-

5 Christophe Domec^{6,7} Pantana Tor-ngern^{8,9*}

6 ¹Center of Excellence on Hazardous Substance Management, Chulalongkorn University

7 Bangkok 10330 Thailand

8 ²Graduate School, Chulalongkorn University, Bangkok 10330 Thailand

9 ³National Biobank of Thailand, National Science and Technology Development Agency,

10 Pathum Thani 12120 Thailand

11 ⁴Key Laboratory of Tropical Forest Ecology, Xishuangbanna Tropical Botanical Garden,

12 Chinese Academy of Sciences, Mengla, Yunnan 666303 China

13 ⁵Yuanjiang Savanna Ecosystem Research Station, Xishuangbanna Tropical Botanical Garden,

14 Chinese Academy of Sciences, Yuanjiang, Yunnan 666303 China

15 ⁶Bordeaux Sciences AGRO, UMR 1391 ISPA INRA, 1 Cours du général de Gaulle 33175,

16 Gradignan Cedex, France

17 ⁷Nicholas School of the Environment and Earth Sciences, Duke University, Durham, NC

18 27708, USA

19 ⁸Department of Environmental Science, Faculty of Science, Chulalongkorn University,

20 Bangkok 10330 Thailand

21 ⁹Water Science and Technology for Sustainable Environment Research Group,

22 Chulalongkorn University, Bangkok 10330 Thailand

23 *Corresponding author Email: Pantana.t@chula.ac.th

24 **Abstract (273/350 words)**

25 1. Due to large-scale abandoned agricultural areas in Southeast Asia, secondary tropical
26 forests commonly comprise various forest stages, resulting in multiple characteristics
27 and inherent environmental conditions. Such spatial heterogeneity challenges the
28 study of how these forests respond to environmental changes, especially under the
29 predicted increasing climatic water stress. Therefore, the information of trees'
30 response to changing environments is still lacking in tropical forests, especially in
31 Southeast Asia.

32 2. To fill the knowledge gap, we investigated seasonal variation in leaf water status and
33 drought tolerance of dominant tree species in three forests of different ages, ranging
34 from 5 to > 200 years old, in Thailand.

35 3. We found that trees growing in the driest site, associated with the young forest stage
36 with sparse canopy, demonstrated increased apparent water stress in leaf water status
37 and distinct seasonal differences. Moreover, a large variation in the capacity to
38 tolerate drought was observed among the study species even within one forest stage.
39 However, when focusing on a given tree species that grow in all three sites, it
40 exhibited similar drought tolerance across forest stages. Overall, the results suggested
41 that soil water availability may influence plant water status and drought tolerance of
42 trees. Nevertheless, species with high drought tolerance can remain active regardless
43 of various soil moisture conditions.

44 4. *Synthesis.* Our results suggest that the responses to water stress of tree species in
45 different forest ages greatly vary. Therefore, evaluating species' performance under
46 water stress should be carefully interpreted. Such information would be beneficial for
47 selecting ones that could be well adapted to specific environments, thus improving the
48 strategies for managing forests of different ages under a warmer future.

49 **Keywords:** tropical forest, forest succession, midday leaf water potential, xylem

50 vulnerability to embolism, forest management

Manuscript Draft

51 **1. Introduction**

52 Native tropical forests in Southeast Asia have been substantially converted to other forms of
53 land use. In the past few decades, the rate of forest clearance in this region has been ranked
54 among the highest in the tropics, with an average net loss of 1.6 million ha yr⁻¹ between 1990
55 and 2010 (Stibig et al., 2014). Such land conversion is mostly attributed to many human
56 activities, including commercial logging (Wilcove et al., 2013), intense cultivation (Zeng et
57 al., 2018), and food production (Imai et al., 2018). The remaining degraded areas are then
58 usually abandoned after several years of operation and transformed into secondary forests,
59 whether by natural succession or human plantation. Consequently, forested areas in Southeast
60 Asia consist of various stages of forest succession including primary forests and different
61 phases of secondary forests. Evidence showed that tropical forests have been severely
62 affected by extreme events from human-induced climate change, such as droughts, warmer
63 temperature including heat waves, and fires (Allen et al., 2010; McDowell et al., 2016).
64 Among these adverse impacts, droughts may have the greatest effect on forested areas
65 worldwide (Reichstein et al., 2013). In particular, the ongoing impacts from increases in
66 frequency, duration and intensity of droughts are threatening the productivity and survival of
67 forests (Barbeta et al., 2015). Thus, droughts have been identified as a major contributing
68 factor affecting forest physiological responses in many regions (Allen et al., 2010; Mueller et
69 al., 2005), potentially accelerating the rates of tree decline and forest mortality (Carnicer et
70 al., 2011; Shaw et al., 2005). Therefore, the combination of the impacts from anthropogenic
71 disturbances and severe droughts will certainly be exacerbated in Southeast Asian forests,
72 hence the need to improve the understanding of underlying mechanisms governing ecosystem
73 functions in these mosaic patches of forests.

74 Forest structure and species composition in different forest stages differ (Lebrija-
75 Trejos et al., 2011). Disparate vegetation structures, such as canopy height and density,

76 differentiate microclimate and soil properties among successional stages (Lee et al., 2006),
77 thus affecting location, duration, and distribution of regenerated tree species within each
78 stage (Lebrija-Trejos et al., 2010). Moreover, differences in canopy openness, tree density,
79 vertical stratification, and the amount of plant litter cause variations in atmospheric
80 temperature and humidity, and soil water availability along successional stages (Heithecker &
81 Halpern, 2007; Marthews et al., 2008). As a result, trees in secondary forests usually
82 experience warmer and drier environments, compared to those in primary forests (Pineda-
83 Garcia et al., 2013). Since trees establishing in different succession may respond differently
84 to droughts (Bretfeld et al., 2018), an interesting research question would be: how do trees in
85 successional forests respond to water stress, which is predicted to be intensified by future
86 droughts? Studies that attempt to understand physiological mechanisms across forest
87 succession have emerged in temperate and tropical ecosystems (Matheny et al., 2017; Pineda-
88 Garcia et al., 2016; Powell et al., 2017; Ruiz-Benito et al., 2017), but rarely in Southeast
89 Asia. This knowledge gap is a crucial limitation for the restoration of forests along
90 successional gradients, as commonly observed in Southeast Asian forests, providing
91 definitive recommendations for selecting tree species that are suitable for local environments.

92 Investigating responses of forests to changing environment relies on the
93 understanding of drought-induced physiological mechanisms of dominant trees at the species
94 level (Choat et al., 2018). Instead of carbon starvation from reduced photosynthesis, it has
95 been revealed that deterioration of the water transport system, also known as hydraulic
96 failure, could be the cause of plant mortality triggering tree death from drought in tropical
97 areas (Rowland et al., 2015). Since water is essential in many plant processes, its limitation
98 could lead to many dysfunctions in terrestrial plants. One method to study the response of
99 trees to drought-induced hydraulic failure is by quantifying their responses to water supply.
100 Leaf water potential is a direct indicator of tree water status and represents the overall plant

101 health (Taiz & Zeiger, 2003), providing a relative index of water stress that indicates how
102 different tree species comparatively respond to changes in their surroundings (McDowell et
103 al., 2008; Steppe, 2018). Low water availability during droughts reduces soil, and stem and
104 leaf water potentials, thus triggering cavitation-induced embolism in xylem conduits (Taiz &
105 Zeiger, 2003), eventually leading to tree death (Adams et al., 2017). Regarding such event,
106 xylem vulnerability to embolism is often used to distinguish the drought tolerance of tree
107 species (Skelton et al., 2015). It has been shown that the xylem vulnerability strongly relates
108 to the ability of woody trees to survive and recover from periods of prolonged drought
109 (Domec et al., 2015). This hydraulic trait varies among species and is largely determined by
110 differences in xylem structure (Maherali et al., 2004). Therefore, investigating the responses
111 of tree species to drought-induced hydraulic failure and their xylem vulnerabilities will
112 improve the knowledge of the limits of drought tolerance for woody tree species and
113 determining trends in drought-induced forest mortality of different successional forests.

114 With these regards, this study aimed (1) to evaluate seasonal variation of tree water
115 status through leaf water potential and (2) to assess xylem vulnerability to embolism of
116 dominant tree species from different forest successional stages located in Khao Yai National
117 Park in Thailand, which is part of a UNESCO world heritage site. The study sites covered
118 three forest stages: an old-growth forest (OF, >200 years), an intermediate forest (IF, ~45
119 years), and a young forest (YF, ~5 years). The outcome from this study will fulfill the
120 knowledge gap on species-specific hydraulic responses along the forest successional stages in
121 tropical forests which is needed for accurately modelling climate change impacts on forest
122 productivity. Additionally, insights from this study can benefit policy decisions on tropical
123 forest management, especially for selecting species to effectively restore forests in highly
124 deforested and degraded regions, such as in Southeast Asia.

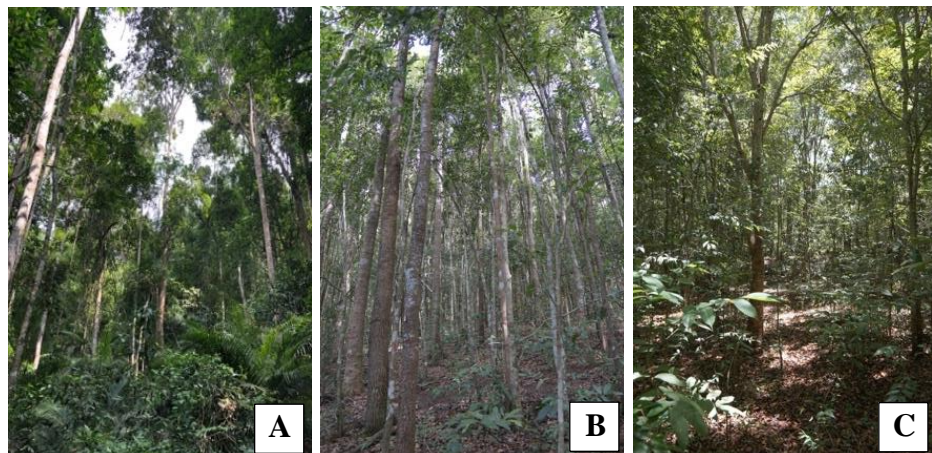
125 **2. Materials and Methods**

126 ***2.1 Study site***

127 The study site was done in different forest successional stages located in Khao Yai National
128 Park, Thailand (14°26'31" N, 101°22'55" E). The average elevation ranges 700–800 meters
129 above sea level. This region is dominated by monsoon climate, where the dry season usually
130 lasts from November to April and from May to October for the wet season (Brockelman et
131 al., 2017). Based on data during 1994 to 2014, the overall mean annual temperature was 22.4
132 °C, with monthly temperature ranging from 19.4 °C in December to 24.3 °C in April. The
133 mean annual rainfall was 2,073 mm. We used meteorological data from the weather station
134 located at Khao Yai National Park headquarter, which was about 3 km away from the study
135 sites. Khao Yai National Park comprises the mosaic fragments in different forest successional
136 stages, ranging from old-growth forests to different ages of secondary forests that naturally
137 regenerated from either natural disturbance (i.e., fires or fallen trees) or anthropogenic
138 impacts (i.e., deforestation or land conversion). In this study, three forest stands representing
139 different forest successional stages including an old-growth forest (OF), an intermediate
140 forest (IF) and a young forest (YF) were selected for the study sites. The OF (Figure 1A) was
141 in the 30-ha Mo Singto forest dynamics plot, one of the ForestGEO plots of the Centre for
142 Tropical Forest Science (CTFS) network (Davies et al., 2021), with the age over 200 years
143 (Brockelman et al., 2017). This forest has several tree layers, with the main canopy height of
144 about 20-30 m and a leaf area index (LAI) of 5 (Chanthorn et al., 2016). The IF (Figure 1B)
145 was located in the northern side of OF. This 45-year-old plot had an area of 1 ha, with an
146 average canopy height of 25 m and an LAI of 6 (Chanthorn et al., 2017). The YF (Figure 1C)
147 was located approximately 3 km away in the southeastern direction of OF. This forest had an
148 area of 2 ha and the age of ~5 years (Chanthorn et al., 2017). The YF's mean canopy height
149 was 15 m, with sparser vegetation coverage compared to the other successional forests. The

150 soil type and soil texture in these forests were classified as gray-brown ultisol and as sandy
151 clay-loam to clay loam, respectively (Rodtassana et al., 2021).

152



153

154 **Figure 1** The studied sites in Khao Yai National Park for (A) Old-growth forest (OF), (B)
155 Intermediate forest (IF), and (C) Young forest (YF)

156

157 **2.2 Species selection**

158 The dominant tree species in each forest stage were chosen based on their relative abundance,
159 which was calculated from the basal area of one species relative to total basal area of all
160 species within the site. Then, five dominant tree species and five individuals per species from
161 each of the three successional forests were selected for all measurements, resulting in a total
162 of 75 trees sampled and 11 different species, with some species existing in multiple sites
163 (Table 1), including *Schima wallichii* (OF and IF), *Syzygium nervosum* (IF and YF), and
164 *Symplocos cochinchinensis* (all sites). A summary of characteristics of dominant tree species
165 is shown in Table 1, and detailed information about the flora and characteristics of selected
166 species is described in Brockelman et al. (2017). According to Brockelman et al. (2017),
167 *Dipterocarpus gracilis* and *Cratoxylum cochinchinense* are deciduous by shedding their
168 leaves and stipules during February-March but are never completely leafless (field

169 observations during the measurements). The other sampled species are evergreen. A large
 170 canopy gap resulted from fallen trees was also observed around the sampled trees of *S.*
 171 *wallichii*, and some of the sampled trees of *S. cochinchinensis*. The sampled trees in IF
 172 existed in a hilly area, where its canopy coverage was more homogeneous and denser
 173 compared to that of OF and YF (Chanthorn et al., 2016). Overall, all sampled trees in YF
 174 experienced drier conditions and stronger radiation from more open canopy in contrast to OF
 175 and IF (Chanthorn et al., 2016; Tor-ngern et al., 2021).

176

177 **Table 1** Characteristics of dominant tree species from the study sites of different forest
 178 succession in Khao Yai National Park. Relative basal area refers to the percentage of total
 179 basal area of the species to total basal area of all trees within the plot. Leaf habit shows
 180 whether the species is deciduous (D) or evergreen (E). Diameter at breast height (DBH; cm),
 181 tree height (m) and sampling height (m), at which the sampled leaves were taken, are
 182 expressed in mean \pm SD values for the sampled trees for each species.

Species	Relative basal area (%)	Leaf habit	DBH (cm) of the sampled trees	Tree (sampling) height (m) of the sampled trees
Old-growth forest (OF)				
<i>Dipterocarpus gracilis</i>	10.54	D	13.78 \pm 3.27	17.16 \pm 1.44 (9.63 \pm 3.00)
<i>Sloanea sigun</i>	8.09	E	13.38 \pm 2.19	13.52 \pm 2.96 (6.70 \pm 0.98)
<i>Ilex chevalieri</i>	5.00	E	16.74 \pm 3.89	17.32 \pm 1.58 (6.90 \pm 0.95)
<i>Symplocos cochinchinensis</i>	3.40	E	16.00 \pm 2.51	12.68 \pm 3.54 (9.77 \pm 2.55)
<i>Schima wallichii</i>	1.58	E	13.00 \pm 1.98	12.04 \pm 1.64 (6.33 \pm 1.04)
Intermediate forest (IF)				
<i>Schima wallichii</i>	36.00 %	E	12.68 \pm 1.90	10.60 \pm 2.28 (7.83 \pm 2.31)
<i>Machilus gamblei</i>	36.00 %	E	14.50 \pm 3.76	21.14 \pm 7.88 (8.33 \pm 1.29)
<i>Eurya acuminata</i>	4.00 %	E	10.58 \pm 0.76	9.52 \pm 2.30 (5.20 \pm 0.75)
<i>Symplocos cochinchinensis</i>	3.00 %	E	12.80 \pm 2.09	11.82 \pm 3.68 (9.13 \pm 2.22)
<i>Syzygium nervosum</i>	2.00 %	E	13.34 \pm 2.41	14.50 \pm 5.82 (8.20 \pm 0.43)
Young forest (YF)				
<i>Cratoxylum cochinchinense</i>	30.75 %	D	14.36 \pm 2.67	9.30 \pm 2.37 (5.42 \pm 0.13)
<i>Syzygium antisepticum</i>	26.52 %	E	13.98 \pm 1.70	9.34 \pm 3.02 (6.40 \pm 1.25)
<i>Adinandra integerrima</i>	12.08 %	E	15.28 \pm 2.21	9.24 \pm 2.63 (4.61 \pm 0.13)
<i>Syzygium nervosum</i>	11.95 %	E	16.74 \pm 2.97	8.80 \pm 1.77 (4.00 \pm 1.73)
<i>Symplocos cochinchinensis</i>	3.24 %	E	16.58 \pm 3.26	9.98 \pm 1.50 (5.62 \pm 1.20)

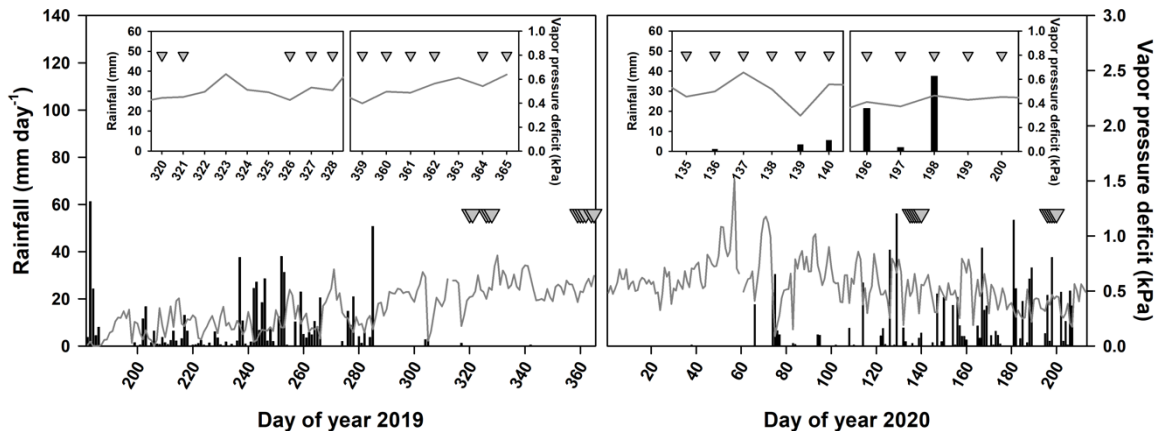
183

184 **2.3 Measurement of midday leaf water potential**

185 Midday leaf water potential (Ψ_{md}) was measured with a Scholander pressure chamber (Model
186 1505D-EXP, PMS instrument, Albany, OR, USA) on samples taken between 10:00 and
187 14:00h in all study sites. The measurement was conducted twice during each of the dry
188 (November to December of 2019) and the wet season (May to July of 2020) to characterize
189 seasonal variation in Ψ_{md} . For each tree species, five individuals with similar stem diameter
190 (10–20 cm DBH, Table 1) were chosen. For each individual tree, three healthy leaves fully
191 exposed to sunlight were randomly selected from the bottom and outermost branches. Each
192 leaf was cut with a razor blade and placed inside the pressure chamber with its cut end of the
193 leaf stalk protruding from the sealing port. The chamber was then gradually pressurized using
194 nitrogen gas (N_2) until a drop of water appeared at the cut surface of the stalk. The balancing
195 pressure inside the chamber, which is equivalent to Ψ_{md} , was then recorded. To avoid the
196 potential loss of water from the leaves, this measurement was conducted immediately after
197 the leaves were collected. Meteorological data concomitant to the measurements of Ψ_{md}
198 (Figure 2, inset figures) were obtained from the weather station located at Khao Yai National
199 Park headquarter, which was about 3 km away from the forest plots. During the measurement
200 periods, rainfall was not observed, except in the wet season during which rainfall occurred
201 mostly at night. The average daily vapor pressure deficit (VPD) from the sampling days
202 during the dry and wet seasons were similar (independent sample *t*-test, $p = 0.34$), averaging
203 0.50 ± 0.07 kPa and 0.46 ± 0.09 kPa, respectively. In addition, soil moisture was measured
204 using a soil moisture probe (SM150T, DeltaT Devices, London, UK) around the sampled
205 trees in each study site during the onset of the dry season (February 2020), which did not
206 coincide with our measurement campaigns, and compared across the three sites. The
207 differences in soil moisture among forest stages were significant (one-way ANOVA, $p <$

208 0.0001), in which OF had the highest mean soil moisture ($45.4 \pm 8.7\%$), followed by IF ($37.8 \pm 7.0\%$), and YF ($23.9 \pm 5.3\%$), respectively.

210



211

212 **Figure 2** Distribution in rainfall (black bars) and vapor pressure deficit (VPD, gray line) from
213 1st July 2019 (day of year 182 in 2019) to 30th July 2020 (day of year 213 in 2020) at Khao
214 Yai National Park, Thailand. Gray triangles indicate the sampling days for midday leaf water
215 potential (Ψ_{md}) measurements. Inset figures are the zoomed-in version of daily rainfall and
216 VPD patterns during the Ψ_{md} sampling periods.

217

218 **2.4 Measurement of xylem vulnerability to embolism**

219 Before performing the measurement, branch maximum xylem vessel lengths (MVL) were
220 estimated for each species to assess the minimum sample size useable to avoid the
221 introduction of air artifacts due to open xylem elements (Ennajeh et al., 2011; Martin-StPaul
222 et al., 2014). By using the air infiltration technique (Ewers & Fisher, 1989; Gao et al., 2019;
223 Perez-Harguindeguy et al., 2016), the estimation of MVL was made in the study sites on
224 three branches collected from the same individuals used for Ψ_{md} measurement. Branches
225 ranging between 0.6–1.0 m in length and 5–10 mm in diameter were cut, connected to a
226 rubber tubing with a syringe at the basal end, and immersed the other end in water. Then, a

227 small air pressure from a syringe was applied to the basal end, while the other end was
228 shortened at 1 cm intervals until the air bubbles emerged. The MVL was determined from the
229 remaining length plus 1–2 cm. Overall, the MVL of branches from all the selected tree
230 species was within the range of 15–50 cm. Thus, for each species, three straight branches
231 with similar diameter (5–10 mm) and length around 50 cm were collected and kept
232 immersing in cold water (~4 °C) before transporting to the laboratory for the measurement of
233 xylem embolism.

234 Xylem vulnerability to water stress-induced embolism was measured using air-
235 injection technique (Sperry & Saliendra, 1994) and xylem specific conductivity (K_s) was
236 determined following Melcher et al. (2012). The air pressure technique gave reliable results
237 because most of the studied species were diffuse-porous species, and the length of the
238 samples were at least four times the length of the pressure sleeve (Ennajeh et al., 2011). First,
239 the collected branch segments were flushed at pressure of 100 kPa for 25–30 minutes to
240 remove air emboli with perfusing solution, de-ionized and ultra-filtered water (PURELAB
241 Chorus 1 Complete, ELGA LabWater, Woodridge, IL, USA) that was degassed and adjusted
242 to an acidic pH (2–3) with HCl. This removal allowed the segments to restore their maximum
243 conductivity ($K_{s\max}$). Each segment was then connected to a tubing apparatus with the basal
244 end attached to the perfusing solution reservoir (upstream) and the other end connected to a
245 pipette (downstream). Next, the flow rate through the segment was measured and $K_{s\max}$ was
246 calculated according to Darcy's Law (Edwards & Jaris, 1982):

$$247 \quad K_s = \frac{Ql}{\Delta P A_s} \frac{\eta}{\eta_0} \quad (1)$$

248 where K_s is the xylem specific conductivity in $\text{kg m}^{-1} \text{ s}^{-1} \text{ MPa}^{-1}$, Q is the flow rate of fluid (kg
249 s^{-1}), l is the length of the segment (m), ΔP is the pressure difference between two ends of the
250 segment (MPa), A_s is the sapwood cross-sectional area (m^2), η is the viscosity of the fluid at
251 the temperature when the experiment is performed (N s m^{-2}), and η_0 is the reference viscosity

252 at 25 °C (N s m⁻²). After determining $K_{s\max}$, the segment was placed inside a double-ended
253 pressure sleeve (PMS Instrument Company, Albany, OR, USA). The chamber was then
254 connected to a pressure chamber (same instrument used for Ψ_{md} measurements) and
255 pressurized with N₂ to artificially induce embolism (Sperry & Ikeda, 1997). First, the
256 chamber was applied with a small pressure, 0.5 MPa, and maintained for at least two minutes
257 before reducing the pressure back to atmospheric level. After the pressurization, the segment
258 was rested for 10-30 minutes for the balanced system and K_s with induced embolism was
259 determined. This procedure was repeated by increasing the injection pressure from 0.5 or 1
260 MPa steps (depending on species), until more than 85% loss of K_s was reached. The
261 percentage loss of hydraulic conductivity (PLC) was calculated as:

$$262 \quad PLC = 100 \times \left(1 - \frac{K_s}{K_{s\max}}\right) \quad (2)$$

263 where K_s is the xylem specific conductivity following each step of increased pressure and
264 $K_{s\max}$ is the maximum conductivity measured after removal of embolism. Then, xylem
265 vulnerability curves were created by plotting PLC as a function of the applied pressures and
266 fitted by the following sigmoidal equation described by Pammeter and Vander Willigen
267 (1998) and modified by Domec and Gartner (2001):

$$268 \quad PLC = \frac{100}{(1 + \exp(S/25(P - P_{50})))} \quad (3)$$

269 where P is the applied pressure, and S is the slope of linear part of the curve centered on P_{50} ,
270 which is the pressure causing 50% loss of xylem conductivity and commonly used to
271 compare embolism resistance among and between species. The slope of the vulnerability
272 curve (S) represents the sensitivity of a species to embolism (Delzon et al., 2010; Trueba et
273 al., 2017). Additionally, the constructed vulnerability curves were also used to calculate the
274 percentage loss of hydraulic conductivity corresponding to midday leaf water potential during
275 the dry season (PLC_{dry}) to further assess the potential water transport efficiency during water-
276 limited conditions from each studied tree species.

277 **2.5 Data analysis**

278 To accomplish the first objective, two sets of analysis were performed to detect and confirm
279 significant differences in Ψ_{md} across successional stages and seasons. The first set was to test
280 for overall difference among successional stages using combined data from all dominant
281 species within each succession, while the second set was to further evaluate the difference
282 among forest stages by focusing only on the data from species found in multiple sites. For the
283 first set of the analysis, one-way analysis of variance (ANOVA) was performed to evaluate
284 the significant difference of Ψ_{md} among forest successions in the same season. Then, in each
285 succession, an independent sample *t-test* was used to test the significant difference in Ψ_{md}
286 between the wet and dry seasons. For the second set of the analysis, Ψ_{md} from the species
287 occupying in all study sites, i.e., *Symplocos cochinchinensis*, was tested for the significant
288 difference across the forest succession in each season by using one-way ANOVA, and tested
289 the significant difference in seasonal variation by using independent sample *t-test*. For the
290 species occupying in two sites, i.e., *Schima wallichii* in OF and IF and *Syzygium nervosum* in
291 IF and YF, significant differences in Ψ_{md} between the forest succession and seasons were
292 evaluated using independent sample *t-test*. Tukey's post hoc test was used after the one-way
293 ANOVA test to determine which pairwise comparisons are significantly different. To
294 characterize differences in xylem vulnerability to embolism between species and sites
295 (objective 2), regression analysis using sigmoidal equation (Eq. 3) was conducted to generate
296 P_{50} , S, PLC_{dry} for all selected tree species. P_{50} , S, and PLC_{dry} were also tested using one-way
297 ANOVA with Tukey's post-hoc test to evaluate the significant differences among forest
298 successions by using pooled data from the dominant tree species, and across the dominant
299 tree species within each forest succession. However, there was only one PLC_{dry} value for
300 each species and therefore was not appropriate for statistical comparisons among species
301 within each site. Thus, we descriptively compared the values in the discussion. All analyses

302 in this study were performed using R (version 4.0.3) and all statistical tests were considered
303 at the significance level of 0.05. All graphs and regression analysis were made by SigmaPlot
304 12.0 (Systat Software, Inc., San Jose, California, USA).

305

306 **3. Results**

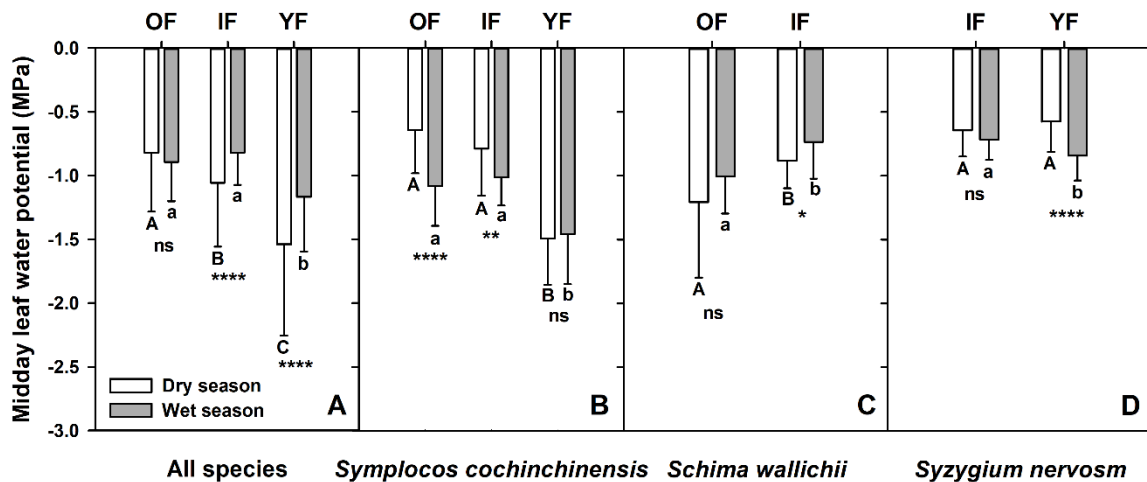
307 **3.1 Seasonal variation in midday leaf water potential of dominant tree species across forest
308 successions**

309 Overall, seasonal variation in Ψ_{md} differed among the successional stages (Figure 3A).
310 Within each forest stage, IF and YF showed significant seasonal variation in Ψ_{md}
311 (independent sample *t-test*, $p < 0.0001$), with a slightly larger difference in YF than in IF
312 (32% in YF vs. 29% in IF). However, insignificant seasonal difference in Ψ_{md} was found in
313 OF (independent sample *t-test*, $p = 0.10$). Focusing on each season, the differences in Ψ_{md}
314 were significant across forest successions in both seasons (one-way ANOVA, $p < 0.05$). It
315 was more pronounced during the dry season, in which YF had the lowest Ψ_{md} (-1.54 ± 0.72
316 MPa), followed by Ψ_{md} in IF (-1.06 ± 0.50 MPa) and OF (-0.82 ± 0.46 MPa), respectively.
317 During the wet season, YF also had the lowest Ψ_{md} (-1.17 ± 0.43 MPa) while Ψ_{md} in OF and
318 IF were comparable (-0.89 ± 0.31 MPa in OF and -0.82 ± 0.25 MPa in IF).

319 Species growing in multiple sites exhibited different variations in Ψ_{md} between the
320 seasons, and among the forest successions. For *S. cochinchinensis* (Figure 3B), significant
321 seasonal difference in Ψ_{md} was observed in OF and IF (independent sample *t-test*, $p < 0.0001$
322 in OF and $p = 0.006$ in IF), with a lower average in the wet season than in the dry season for
323 OF and IF by 69% and 28%, respectively. In contrast, no seasonal variation in Ψ_{md} of *S.*
324 *cochinchinensis* growing in YF was found (independent sample *t-test*, $p = 0.73$). For both
325 seasons, Ψ_{md} differed significantly among the forest successions (one-way ANOVA, $p <$
326 0.05), in which the lowest Ψ_{md} was found in YF, while it was similar in OF and IF. For *S.*

327 *wallichii*, seasonal difference in Ψ_{md} was detected only in IF (independent sample *t-test*, $p =$
 328 0.028), with a 19% lower Ψ_{md} during the dry season than in the wet season (Figure 3C). For
 329 both seasons, lower Ψ_{md} was found in OF than in IF (independent sample *t-test*, $p < 0.05$).
 330 Only *S. nervosum* in YF differed between seasons (independent sample *t-test*, $p < 0.0001$),
 331 with a 47% lower in Ψ_{md} during the wet season than in the dry season (Figure 3D). In the wet
 332 season, Ψ_{md} in YF was significantly lower than in IF (independent sample *t-test*, $p < 0.0001$),
 333 whereas no difference between the forest successions was observed in the dry season
 334 (independent sample *t-test*, $p = 0.134$).

335



336

337 **Figure 3** Midday leaf water potential (Ψ_{md}) from the old-growth (OF), intermediate (IF) and
 338 young (YF) forests during the dry (white bars) and wet (gray bars) season in (A) all species
 339 and those growing in multiple successions including (B) *Symplocos cochinchinensis*, (C)
 340 *Schima wallichii* and (D) *Syzygium nervosum*. Each bar represents the mean Ψ_{md} values for a
 341 total of 150 sampled leaves in (A), and 30 samples in (B - D). For each panel, different
 342 upper- and lower-case letters represent significant differences in the wet and dry seasons,
 343 respectively. Asterisks indicate significant seasonal differences within the same successional

344 stage based on independent sample *t-test*; ns = not significant, * $p < 0.05$, ** $p < 0.01$, *** p
345 < 0.001 , and **** $p < 0.0001$.

346

347 **3.2. Vulnerability to xylem embolism of dominant tree species from different successional
348 stages**

349 Considering all species within each forest stage, xylem vulnerability to embolism,
350 represented by the xylem pressure inducing 50% loss of hydraulic conductivity (P_{50}), did not
351 vary across forest successions (one-way ANOVA, $p = 0.123$, Table 2). However, significant
352 difference in sensitivity to xylem embolism, represented by slope of the vulnerability curve
353 (S), was observed among the successional forests (one-way ANOVA, $p < 0.05$, Table 2). At
354 the forest level, xylem vulnerability ranged from potentially more vulnerable in OF ($-2.87 \pm$
355 0.30 MPa) to less vulnerable in IF (-3.04 ± 0.18 MPa) and in YF (-3.71 ± 0.39 MPa).

356 Sensitivity to embolism was higher in OF ($73.70 \pm 21.60 \% \text{ MPa}^{-1}$) than in IF (26.80 ± 1.25
357 % MPa $^{-1}$) and YF ($23.40 \pm 1.05 \% \text{ MPa}^{-1}$). For the species occupying multiple forest stages,
358 vulnerability to xylem embolism was generally comparable across forest successions. *S.*

359 *cochinchinensis* exhibited similar P_{50} across successions (one-way ANOVA, $p = 0.687$), by
360 having P_{50} of -3.27 ± 0.04 MPa in OF, -3.39 ± 0.03 MPa in IF, and -3.24 ± 0.21 MPa in YF.

361 The same trend was also found in *S. nervosum* (independent sample *t-test*, $p = 0.762$), by
362 having P_{50} of -2.30 ± 0.17 and -2.24 ± 0.03 MPa in IF and YF, respectively. In contrast,
363 significant difference in P_{50} was found in *S. wallichii* between the two forest successions
364 (independent sample *t-test*, $p < 0.05$), with 0.45 MPa lower in OF than in IF.

365

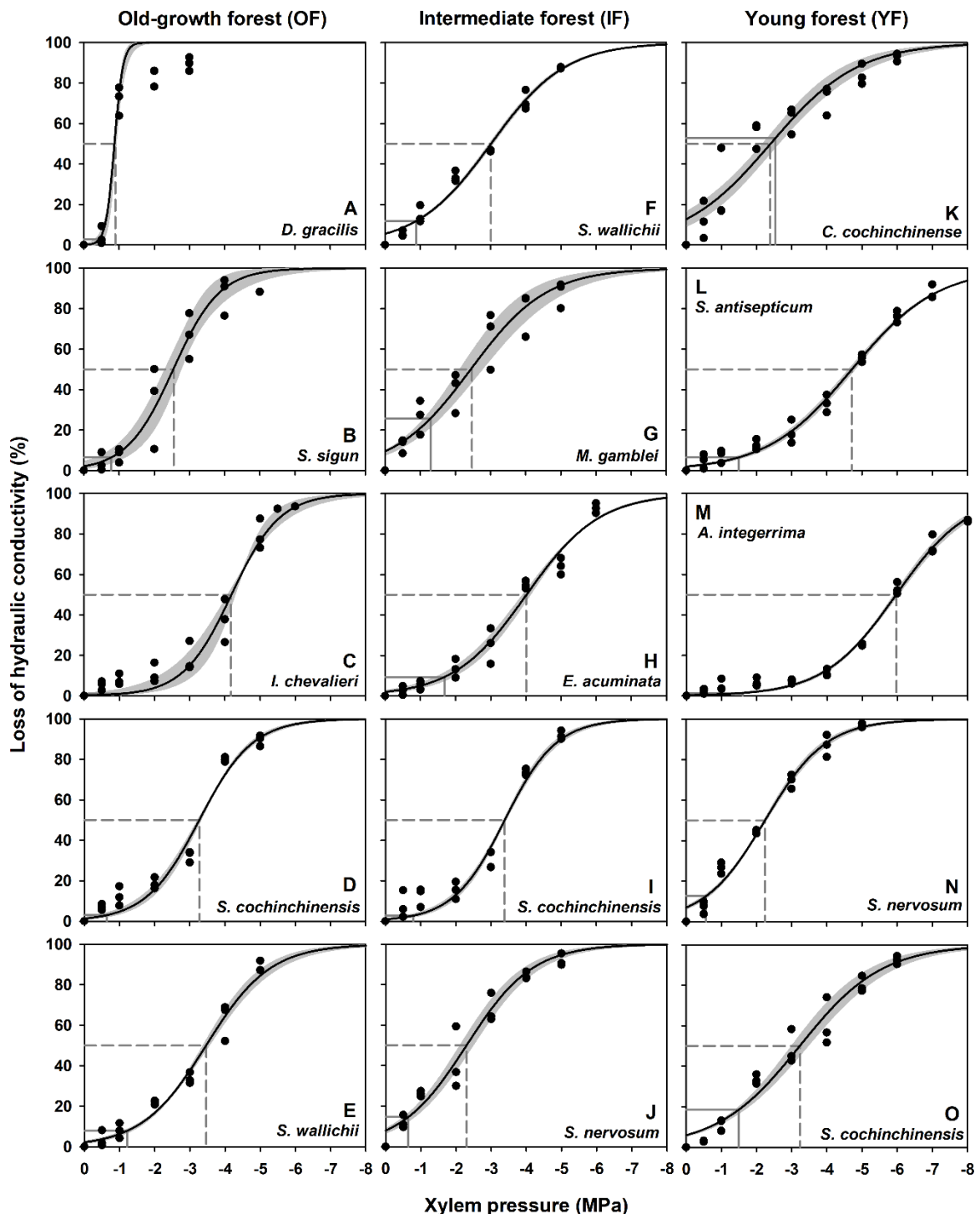
366 **Table 2** Vulnerability to xylem embolism, represented by xylem pressure at 50% loss of
367 hydraulic conductivity (P_{50}), slope of the vulnerability curve (S), and percentage loss of
368 hydraulic conductivity corresponding to midday leaf water potential during the dry season

369 (PLC_{dry}) of selected dominant tree species from different successions in Khao Yai National
 370 Park, Thailand. Values are means \pm one standard error with sample size of 3. Different upper-
 371 and lower-case letters represent significant differences among the forest successions and
 372 within each forest succession, respectively (One-way ANOVA with Tukey's post-hoc test,
 373 significance level of 0.05).

Species	P ₅₀ (MPa)	S (% MPa ⁻¹)	PLC _{dry} (%)
Old-growth forest (OF)			
<i>Dipterocarpus gracilis</i>	-2.87 \pm 0.30 A	73.70 \pm 21.60 A	4.22 \pm 1.25 A
<i>Sloanea sigun</i>	-0.89 \pm 0.01 d	222.56 \pm 45.72 b	2.81
<i>Ilex chevalieri</i>	-2.55 \pm 0.21 c	43.83 \pm 10.92 a	6.45
<i>Symplocos cochinchinensis</i>	-4.17 \pm 0.08 a	41.09 \pm 11.49 a	1.02
<i>Schima wallichii</i>	-3.27 \pm 0.04 b	33.34 \pm 2.73 a	3.03
	-3.46 \pm 0.08 b	27.81 \pm 2.17 a	7.78
Intermediate forest (IF)			
<i>Schima wallichii</i>	-3.04 \pm 0.18 A	26.80 \pm 1.25 B	12.90 \pm 3.77 A
<i>Machilus gamblei</i>	-3.01 \pm 0.05 bc	23.58 \pm 0.17 a	11.86
<i>Eurya acuminata</i>	-2.47 \pm 0.34 c	24.36 \pm 1.96 a	25.77
<i>Symplocos cochinchinensis</i>	-4.01 \pm 0.10 a	24.44 \pm 1.59 a	9.40
<i>Syzygium nervosum</i>	-3.39 \pm 0.03 ab	34.35 \pm 2.45 b	2.79
	-2.30 \pm 0.17 c	27.22 \pm 1.61 ab	14.65
Young forest (YF)			
<i>Cratoxylum cochinchinense</i>	-3.71 \pm 0.39 A	23.40 \pm 1.05 B	18.37 \pm 9.07 A
<i>Syzygium antisepticum</i>	-2.39 \pm 0.25 d	20.73 \pm 2.63 a	52.77
<i>Adinandra integerrima</i>	-4.71 \pm 0.08 b	20.74 \pm 0.44 a	6.48
<i>Syzygium nervosum</i>	-5.97 \pm 0.06 a	24.44 \pm 1.26 ab	1.40
<i>Symplocos cochinchinensis</i>	-2.24 \pm 0.03 d	29.05 \pm 1.64 b	12.71
	-3.24 \pm 0.21 c	21.87 \pm 1.54 ab	18.47

374
 375 Within each forest successional stage, xylem vulnerability varied greatly among the
 376 dominant tree species (one-way ANOVA, $p < 0.05$, Table 2, Figure 4). In OF, the lowest P₅₀
 377 was found in *I. chevalieri* (-4.17 \pm 0.08 MPa, Figure 4C) whereas the highest P₅₀ was found
 378 in *D. gracilis* (-0.89 \pm 0.01 MPa, Figure 4A). Slopes of vulnerability curves were comparable
 379 across the dominant tree species in OF, except for *D. gracilis* that had the steepest slope than
 380 the others. PLC_{dry} differed substantially across species in OF, in which *I. chevalieri*
 381 experienced relatively lower impact during the dry season (1.02 %, Figure 4C) while a
 382 greater impact was observed in *S. sigun* (6.45%, Figure 4B) and *S. wallichii* (7.78%, Figure
 383 4E). In IF, *E. acuminata* (Figure 4H) was the most while *S. nervosum* (Figure 4J) was the

384 least resistant to xylem embolism (-4.01 ± 0.10 MPa and -2.30 ± 0.17 MPa, respectively)
385 compared to other coexisting species. Sensitivity to xylem embolism was higher in *S.*
386 *cochinchinensis* than the rest of the species in IF. *S. cochinchinensis* in IF also responded less
387 to potentially dry conditions in the dry season by losing relatively small hydraulic
388 conductivity at midday (2.79 %, Figure 4I) while *M. gamblei* in IF reacted more by further
389 losing the hydraulic conductivity in the dry season (25.77 %, Figure 4G). In YF, *A.*
390 *integerrima* (Figure 4M) displayed the lowest P_{50} value at -5.97 ± 0.06 MPa, with low
391 response to dry conditions as observed from midday PLC_{dry} (1.40 %). *C. cochinchinense*
392 (Figure 4K), however, had the highest P_{50} (-2.39 ± 0.25 MPa), with the greatest response
393 from losing hydraulic conductivity in the dry season (52.77 %) compared to the other species.
394 The steepest slope of vulnerability curve in YF was measured in *S. nervosum*.



395

396 **Figure 4** Vulnerability of xylem to embolism of branches from dominant tree species from
 397 different successions in Khao Yai National Park, Thailand. Mean vulnerability curves are
 398 presented with shaded bands representing one standard error from 3 branches for a given
 399 species. The gray dashed and solid lines indicate the xylem pressure at 50% loss of hydraulic

400 conductivity (P_{50}) and percentage loss of hydraulic conductivity corresponding to midday leaf
401 water potential (Ψ_{md}) during the dry season (PLC_{dry}), respectively.

402

403 **4. Discussion**

404 ***4.1 Comparison of leaf water potential and xylem vulnerability with previous reported***
405 ***studies***

406 Midday leaf water potentials (Ψ_{md}) and xylem vulnerability curves, represented by the xylem
407 pressure at which 50% of hydraulic conductivity in branches or stems is lost (P_{50}), are
408 summarized from previous studies in tropical forests across the globe (Table 3). Due to
409 differences in experimental conditions and settings, these studies could not be directly
410 compared to the results from this study. Nonetheless, measured values of Ψ_{md} from this study
411 were within the ranges of those observed in Neotropics (Barros et al., 2019; Bittencourt et al.,
412 2020; Powell et al., 2017; Rowland et al., 2015), Australasia (Nolf et al., 2015; Trueba et al.,
413 2017), and Indomalaya (Chen et al., 2017; Tan et al., 2020; Zhu et al., 2017). For xylem
414 vulnerability, results from this study were within similar ranges of those from Neotropics
415 (Barros et al., 2019; Rowland et al., 2015) and Indomalaya (Tan et al., 2020; Zhu et al.,
416 2017), but were lower than those shown in the other studies in Table 3. In general, this
417 comparison reveals that leaf water potential and xylem vulnerability vary greatly within
418 tropical region, and they seem to be site-specific.

419 **Table 3** Literature survey of leaf water potential (Ψ , MPa) and xylem tension at 50% loss of hydraulic conductivity in branches or stems (P_{50} ,
 420 MPa) in tropical forests including this study. Values are shown as ranges. NA indicates not available data.

Location	Condition	Dominant tree species	Ψ (MPa)	P_{50} (MPa)	Reference	
Tropical rain forest in Caxiuaná National Forest, State of Pará, Brazil (1°43'S, 51°27'W)	Control	<i>Eschweilera</i> sp., <i>Licania</i> sp., <i>Pouteria</i> sp., <i>Protium</i> sp., <i>Swartzia</i> sp., and <i>Inga</i> sp.	NA	-0.80 to -4.50	Rowland et al. (2015)	
	Through-fall exclusion (TFE)					
Tropical rain forest in Caxiuaná National Forests, State of Pará, Brazil (1°44'13.2"S, 51°27'28.8"W)	Midday Ψ was measured in control (left in Ψ column) and TFE (right in Ψ column) experiments. P_{50} was estimated during throughfall exclusion experiment (TFE).	<i>Inga</i> sp., <i>Eschweilera</i> sp., <i>Protium</i> sp., and <i>Licania</i> sp.	-0.14 to -1.42	-0.35 to -1.95	-1.20 to -2.30	Powell et al. (2017)
Tropical rain forest in Tapajós National Forests, State of Pará, Brazil (2°53'49.2"S, 54°57'07.2"W)	Throughfall exclusion experiment (TFE)	<i>Inga</i> sp., <i>Eschweilera</i> sp., <i>Protium</i> sp., and <i>Licania</i> sp.	NA	-1.10 to -2.00		
Low seasonality forest: Cuieras Biological Reserve, Manaus, Amazonas, Brazil (2°61'S, 60°21'W)	Minimum Ψ was measured during the peak of the dry season of non-ENSO (left in Ψ column) and ENSO (right in Ψ column) years.	<i>Caryocar</i> sp., <i>Dypterix</i> sp., <i>Eschweilera</i> sp., <i>Gouphia</i> sp., <i>Gustavia</i> sp., <i>Lecyths</i> sp., <i>Maquira</i> sp., <i>Minquartia</i> sp., <i>Ocotea</i> sp., <i>Pouteria</i> sp., <i>Pouteria</i> sp., <i>Protium</i> sp., <i>Scleronema</i> sp., and <i>Zygia</i> sp.	-0.57 to -2.09	-1.10 to -2.89	-1.01 to -4.47	Barros et al. (2019)
High seasonality forest: Tapajós National Forest, Santarém, Pará, Brazil (2°51'S, 54°58'W)		<i>Amphyrrhox</i> sp., <i>Chamaecrista</i> sp., <i>Coussarea</i> sp., <i>Endopleura</i> sp., <i>Erisma</i> sp., <i>Manilkara</i> sp., <i>Mezilaurus</i> sp., <i>Miconia</i> sp., <i>Minquartia</i> sp., <i>Protium</i> sp., <i>Rinorea</i> sp., and <i>Tachigali</i> sp.	-1.06 to -2.68	-1.06 to -4.43	-1.52 to -5.02	
Tropical rain forest in Caxiuaná National Forest, State of Pará, Brazil (1°43'S, 51°27'W)	Control	<i>Aspidosperma</i> sp., <i>Eschweilera</i> sp., <i>Inga</i> sp., <i>Licania</i> sp., <i>Micropholis</i> sp., <i>Minquartia</i> sp., <i>Pouteria</i> sp., <i>Protium</i> sp., <i>Swartzia</i> sp., <i>Syzygiopsis</i> sp., <i>Virola</i> sp., and <i>Vouacapoua</i> sp.	-1.30 to -2.40	-1.40 to -3.10	Bittencourt et al. (2020)	
	Through-fall exclusion (TFE)					
Tropical rain forest in Daintree Rainforest Observatory Research Facility, Cape Tribulation, Queensland, Australia (16°06'14.4"S, 145°26'56.4"E)	-	<i>Dysoxylum</i> sp., <i>Elaeocarpus</i> sp., and <i>Syzygium</i> sp.	-1.23 to -1.62	-2.10 to -3.06	Nolf et al. (2015)	
Tropical rain forest in New Caledonia, the north of the Tropic of Capricorn in the southwest Pacific Ocean (21°30'S, 165°30'E)	-	<i>Amborella</i> sp., <i>Ascarina</i> sp., <i>Cryptocarya</i> sp., <i>Hedycarya</i> sp., <i>Hedycarya</i> sp., <i>Kibaropsis</i> sp., <i>Nemuaron</i> sp., <i>Paracryphia</i> sp., <i>Quintinia</i> sp., and <i>Zygogynum</i> sp.	NA	-2.10 to -4.00	Trueba et al. (2017)	

Location	Condition	Dominant tree species	Ψ (MPa)	P_{50} (MPa)	Reference
Xishuangbanna Tropical Botanical Garden, Yunnan Province, China (21°54'N, 101°46'E)	Lianas	<i>Celastrus</i> sp., <i>Marsdenia</i> sp., <i>Ventilago</i> sp., and <i>Mucuna</i> sp.	NA	-1.04 to -1.57	Chen et al. (2017)
	Trees	<i>Celtis</i> sp., <i>Ficus</i> sp., <i>Harpullia</i> sp., <i>Michelia</i> sp., and <i>Streblus</i> sp.	NA	-1.43 to -2.93	
Tropical non-karst and karst forests in Xishuangbanna Tropical Botanical Garden, Yunnan Province, China (21°54'N, 101°46'E)	Data collected in tropical non-karst forest	<i>Bauhinia</i> sp., <i>Bischofia</i> sp., <i>Castanopsis</i> sp., <i>Lagerstroemia</i> sp., <i>Millettia</i> sp., <i>Syzygium</i> sp., <i>Millettia</i> sp., <i>Uncaria</i> sp., and <i>Byttneria</i> sp.	NA	-1.10 to -2.00	Zhu et al. (2017)
	Data collected in tropical karst rain forest	<i>Alphonsea</i> sp., <i>Celtis</i> sp., <i>Cipadessa</i> sp., <i>Cleistanthus</i> sp., <i>Croton</i> sp., <i>Lasiococca</i> sp., <i>Pistacia</i> sp., <i>Turpinia</i> sp., <i>Combretum</i> sp., and <i>Ventilago</i> sp.	NA	-1.30 to -4.10	
Tropical karst forest in Xishuangbanna Tropical Botanical Garden, Yunnan Province, China (21°54'N, 101°46'E)	Minimum Ψ was measured in normal dry season (left in Ψ column) and extreme dry season (right in Ψ column).	Evergreen <i>Alphonsea</i> sp., <i>Celtis</i> sp., <i>Cleidion</i> sp., <i>Cleistanthus</i> sp., <i>Pistacia</i> sp., <i>Lasiococca</i> sp., and <i>Turpinia</i> sp.	-0.98 to -2.41	-2.13 to -6.55	Tan et al. (2020)
		Brevi-deciduous <i>Cipadessa</i> sp., <i>Croton</i> sp., <i>Ficus</i> sp., <i>Lagerstroemia</i> sp., <i>Mayodendron</i> sp.	-1.34 to -1.80	-1.10 to -2.68	
		Liana <i>Bauhinia</i> sp., <i>Combretum</i> sp., <i>Gnetum</i> sp., <i>Ventilago</i> sp.	-0.60 to -1.60	-0.65 to -2.95	
Seasonal evergreen forest Khao Yai National Park, Thailand (14°26'N, 101°22'E)	Midday leaf Ψ was measured in wet season (left in Ψ column) and dry season (right in Ψ column). P_{50} was done once throughout the study.	Old-growth forest <i>Dipterocarpus</i> sp., <i>Sloanea</i> sp., <i>Ilex</i> sp., <i>Symplocos</i> sp., and <i>Schima</i> sp.	-0.58 to -1.20	-0.36 to -1.28	This study
		Intermediate forest <i>Schima</i> sp., <i>Machilus</i> sp., <i>Eurya</i> sp., <i>Symplocos</i> sp., and <i>Syzygium</i> sp.	-0.57 to -1.07	-0.56 to -1.56	
		Young forest <i>Cratoxylum</i> sp., <i>Syzygium</i> sp., <i>Adinandra</i> sp., <i>Syzygium</i> sp., and <i>Symplocos</i> sp.	-0.43 to -1.60	-0.82 to -2.26	

423 **4.2 Variations in midday leaf water potential across forest successions and seasons.**

424 The dominant tree species across forest successions showed different seasonal variations in
425 Ψ_{md} . At forest level, YF exhibited lower Ψ_{md} in both wet and dry season and had greater
426 seasonal variation in Ψ_{md} compared to OF and IF (Figure 3A). This could imply that lower
427 Ψ_{md} during water-limited conditions, e.g., in the dry season, and higher variation in Ψ_{md}
428 induced by seasonal changes could occur frequently in the younger successions, consistent
429 with other studies (Barros et al., 2019; Marksteijn et al., 2010; Mitchell et al., 2008). In
430 contrast to late successional forests, early successions receive more direct solar heating owing
431 to more open canopy, leading to drier conditions in the atmosphere and higher temperature
432 (Lebrija-Trejos et al., 2011). A drier environment in early successional stage would introduce
433 greater water stress than in late succession and become more intensified during the onset of
434 dry season (Bretfeld et al., 2018), as seen by lower Ψ_{md} in drier YF site as compared to
435 moister OF and IF sites. Interestingly, studies have shown that species found in drier sites
436 have higher tolerance to desiccation, meaning the ability to remain active at lower water
437 potentials (Baltzer et al., 2008; Engelbrecht et al., 2007; Kursar et al., 2009). However,
438 allowing low Ψ_{md} in drier sites can also be detrimental for dehydration and hydraulic failure,
439 especially during the dry season, if the value decreases beyond the critical threshold of xylem
440 embolism (Blackman et al., 2019).

441 To further investigate the variations in Ψ_{md} by excluding potential confounding
442 effects from various intra-site species, species existing in multiple sites were examined. As
443 would be expected from its existence in drier environment, *S. cochinchinensis* in YF
444 exhibited the lowest Ψ_{md} in both seasons compared to OF and IF, with no significant seasonal
445 difference in Ψ_{md} (Figure 3B). *S. cochinchinensis* in OF and IF showed comparable Ψ_{md} in
446 both seasons; however, their Ψ_{md} during the wet season was lower than in the dry season,
447 despite the presumably better access to water in the wet season. This unexpected pattern also

448 occurred in *S. nervosum* in YF, when lower Ψ_{md} was found in the wet season compared to the
449 dry season (Figure 3D). Such unexpected patterns may be explained by that, during the wet
450 season, *S. cochinchinensis* in OF and IF and *S. nervosum* in YF adopted a less conservative
451 water use regulation when water is more abundant. This observation was also reported in
452 some previous studies (Bucci et al., 2005; Prado et al., 2004), with no clear explanation being
453 provided. In *S. wallichii*, lower Ψ_{md} was found in OF than in IF in both seasons (Figure 3C),
454 with no seasonal difference in OF but a slight change in IF in the dry season. Even though
455 they existed in a relatively wetter environment, the sampled trees of *S. wallichii* in OF grew
456 under a large gap created by tree falls. The higher intensity of light under the gap strongly
457 influence the microclimate, leading to higher air temperature and lower air humidity
458 compared to the adjacent area (Fletcher et al., 1985; McCarthy, 2001). Therefore, the leaf-
459 level water deficits resulted from canopy gap may contribute to the unexpectedly more
460 negative values of Ψ_{md} in OF than in IF. Different changes and patterns in Ψ_{md} induced by
461 seasonal changes found in this study seem to be species-specific. These different strategies
462 dealing with water-limited condition have a critical impact on xylem embolism (Sperry et al.,
463 2002; Zhu & Cao, 2009), and hence the potential risk of tree mortality resulted from water
464 stress-induced hydraulic failure.

465 **4.3 Xylem vulnerability to embolism of dominant tree species in successional forests.**

466 Many studies have documented that vulnerability to xylem embolism vary substantially
467 among trees from different habitats. Species occupying in drier sites are generally less
468 vulnerable to embolism than those occupying in wetter sites (Barros et al., 2019; Choat et al.,
469 2007; Vander Willigen et al., 2000; Vinya et al., 2013; Zhu et al., 2017). Our results revealed
470 a tendency for species at more xeric sites to have higher ability to resist xylem embolism,
471 despite non-statistical difference at the forest level (Table 2, Figure 4). The most vulnerable
472 species to xylem embolism was found in OF, a deciduous tree species *D. gracilis* with the

473 highest P_{50} of -0.89 MPa. On the other hand, *A. integerrima*, an evergreen tree species in YF,
474 had the lowest P_{50} , at -5.97 MPa, standing out from the rest of the studied tree species from
475 all forest successions. The presence of species with lower P_{50} in drier sites could imply the
476 adaptive importance of embolism resistance in response to the environments where water
477 stress is more pronounced (Maherali et al., 2004). In addition to this finding, the overall
478 sensitivity to xylem cavitation in OF was considerably higher than that in IF and YF,
479 potentially suggesting the higher rate of embolism occurrence for the species in the wetter
480 site. Nevertheless, species occupying in multiple forest stages, e.g., *S. cochinchinensis*,
481 exhibited comparable P_{50} , implying the similar embolism resistance across the forest
482 successions. The lack of difference in P_{50} along forest successions was also observed in a
483 tropical dry forest in Mexico (Pineda-Garcia et al., 2013). Great variations in the xylem
484 vulnerability among species imply that evaluating species' performance under water stress
485 should be carefully interpreted, as other mechanisms, e.g., stomatal regulation, sapwood
486 water storage, or leaf-shedding strategy, could also contribute to xylem resistance to
487 embolism (Barnard et al., 2011; Domec et al., 2006; Markesteijn et al., 2011; Rosner et al.,
488 2019).

489 In each forest succession, larger variations in embolism resistance were found in OF
490 and YF than in IF, based on their coefficients of variation (40.42%, 22.89%, and 40.43% in
491 OF, IF, and YF, respectively). Cartwright et al. (2020) suggested that substantial variability
492 in drought response within an ecosystem can be driven by endogenous factors (e.g.,
493 phenological characters) and by exogenous factors (e.g., topographic and hydrologic
494 characteristics). In this study, differences in leaf phenology among the dominant tree species
495 were observed in OF and YF. Compared to the other evergreen species within the same site,
496 deciduous tree species, *D. gracilis* in OF and *C. cochinchinense* in YF, exhibited lower
497 resistance to xylem embolism. Such difference in xylem vulnerability between deciduous and

498 evergreen tree species was also found in the studies from other tropical forests (Chen et al.,
499 2017; Choat et al., 2005; Markesteijn et al., 2011) and subtropical forests (Krober et al.,
500 2014). In addition, other exogenous factors may contribute to the variation in P_{50} , particularly
501 in OF. The variation in xylem vulnerability in OF could be explained by high microhabitat
502 heterogeneity in this area (Brockelman et al., 2017), that might lead to spatial distribution of
503 vegetation with varying sensitivity to water availability within the site. For example, species
504 with presumably better access to water, e.g., *S. sigun* which dominated in flat lowland near
505 streamside, showed higher vulnerability to xylem embolism among the others. In contrast,
506 species with limiting soil water, e.g., *I. chevalieri* which occupied in a hilly slope, showed
507 relatively less vulnerable to embolism compared to the rest of the species. Consistent with
508 this finding, Zhang et al. (2021) and Zhu et al. (2017) found a wide range of P_{50} in tropical
509 karst forests, in which species existing in the middle to top of hilly areas were more resistant
510 to embolism than species dominated in lowlands or valleys, resulting from soil water
511 gradient. Nevertheless, further investigations on hydraulic architecture, sapwood water
512 storage capacity, and rooting depth should be conducted to confirm such findings.

513 In terrestrial plants, the ability to sustain xylem water transport under water deficit
514 conditions is crucial for plant functions and survival. Our results showed that the dominant
515 tree species from each succession experienced midday leaf water potentials during the dry
516 season that could result in loss of hydraulic conductivity (PLC_{dry}) at different levels (Table 2,
517 Figure 4). Based on xylem vulnerability curves and Ψ_{md} , most of the studied tree species
518 operated well below or close to their P_{50} values. Species with higher resistance to xylem
519 embolism tended to lose lower hydraulic conductivity during the dry season across the
520 successions. For example, species with high embolism resistance, e.g., *I. chevalieri* in OF, *S.*
521 *cochinchinensis* in IF, and *A. integerrima* in YF, showed lower than 3% in PLC_{dry} . The
522 reverse was seen in species that were more vulnerable to embolism, e.g., *S. sigun* in OF, *M.*

523 *gamblei* in IF, *C. cochinchinense* in YF, which exhibited 7% to 53% in PLC_{dry}. The
524 probability of losing higher xylem water transport efficiency related to the tension
525 experienced during the dry season may be associated with species' performance to deal with
526 embolism, consistent with findings obtained from a karstic woodland (Nardini et al., 2013),
527 an Amazonian tropical forest (Markesteijn et al., 2011), and across forest biomes (Choat et
528 al., 2012). This result, thus, implies the significance of embolism resistance in determining
529 species risk of hydraulic dysfunction during low water availability (Barros et al., 2019;
530 Brodribb, 2017; Oliveira et al., 2019).

531 Understanding how plants respond to water stress from different tree species and
532 different forest successions is useful not only for the forest conservation and restoration
533 efforts, but also for the predictions of tree mortality across the successions. In accordance
534 with predicted warming atmosphere and more variable droughts, it is important for forest
535 restoration and conservation to consider the threshold at which tree mortality would occur
536 (Hérault & Gourlet-Fleury, 2016), in order to maintain and promote the species that could
537 adapt well in particular environments, under both current and future conditions. By selecting
538 species that could be well-adapted in a specific setting, e.g., using information derived from
539 P₅₀ and PLC_{dry}, the likelihood of success of forest restoration and conservation in a drier and
540 hotter future could be enhanced (Elliott et al., 2003; Hérault & Piponiot, 2018; Vieira &
541 Scariot, 2006).

542 **5. Author Contribution Statement**

543 W.U and P.T. planned and designed the study; W.U. collected the samples and conducted the
544 measurements with help from S.Y. and J.C.D.; W.U. and P.T. performed statistical analyses
545 and result interpretations; W.U. and P.T. wrote the first draft and A.N., Y.C., and J.C.D.
546 provided comments and revised the manuscript. All the authors jointly contributed to the
547 manuscript and gave final approval for publication.

548

549 **6. Data Availability Statement**

550 **We will archive the data in the Dryad Digital Repository and will update the link later.**

551

552 **7. Acknowledgements**

553 This work was financially supported by the National Science and Technology Development
554 Agency (NSTDA, P-18-51395), the Thailand Science Research and Innovation (TSRI,
555 RDG6230006), and the Agence Nationale de la Recherche projects CWSSEA-SEA Europe
556 and PRIMA-SWATCH (ANR-18-PRIM-0006 and ANR-17-ASIE-0007). W.U. was supported
557 by Thailand Graduate Institute of Science and Technology (TGIST), National Science and
558 Technology Development Agency through a postgraduate scholarship (SCA-CO-2562- 9778-
559 TH). We would like to thank Professor Warren Brockelman, Ph.D. and Associate Professor
560 Wirong Chanthorn, Ph.D. for facilitating field work, and Vijitra Jan-uthai, Nawatbhrist
561 Kitudom, and Napatsorn Somkhaoyai for field assistance.

562 **8. Reference**

563 Adams, H. D., Zeppel, M. J. B., Anderegg, W. R. L., Hartmann, H., . . . McDowell, N. G.

564 (2017). A multi-species synthesis of physiological mechanisms in drought-induced tree

565 mortality. *Nature Ecology & Evolution*, 1(9), 1285-1291.

566 <https://doi.org/10.1038/s41559-017-0248-x>

567 Allen, C. D., Macalady, A. K., Chenchouni, H., Bachelet, D., . . . Cobb, N. (2010). A global

568 overview of drought and heat-induced tree mortality reveals emerging climate change

569 risks for forests. *Forest Ecology and Management*, 259(4), 660-684.

570 <https://doi.org/10.1016/j.foreco.2009.09.001>

571 Baltzer, J. L., Davies, S. J., Bunyavejchewin, S., & Noor, N. S. M. (2008). The role of

572 desiccation tolerance in determining tree species distributions along the Malay-Thai

573 Peninsula. *Functional Ecology*, 22(2), 221-231. <https://doi.org/10.1111/j.1365-2435.2007.01374.x>

575 Barbeta, A., Mejia-Chang, M., Ogaya, R., Voltas, J., . . . Penuelas, J. (2015). The combined

576 effects of a long-term experimental drought and an extreme drought on the use of plant-

577 water sources in a Mediterranean forest. *Global Change Biology*, 21(3), 1213-1225.

578 <https://doi.org/10.1111/gcb.12785>

579 Barnard, D. M., Meinzer, F. C., Lachenbruch, B., McCulloh, K. A., . . . Woodruff, D. R.

580 (2011). Climate-related trends in sapwood biophysical properties in two conifers:

581 avoidance of hydraulic dysfunction through coordinated adjustments in xylem

582 efficiency, safety and capacitance. *Plant Cell Environ*, 34(4), 643-654.

583 <https://doi.org/10.1111/j.1365-3040.2010.02269.x>

584 Barros, F. D., Bittencourt, P. R. L., Brum, M., Restrepo-Coupe, N., . . . Oliveira, R. S. (2019).

585 Hydraulic traits explain differential responses of Amazonian forests to the 2015 El

586 Nino-induced drought. *New Phytologist*, 223(3), 1253-1266.

587 <https://doi.org/10.1111/nph.15909>

588 Bittencourt, P. R. L., Oliveira, R. S., da Costa, A. C. L., Giles, A. L., . . . Rowland, L. (2020).

589 Amazonia trees have limited capacity to acclimate plant hydraulic properties in

590 response to long-term drought. *Global Change Biology*, 26(6), 3569-3584.

591 <https://doi.org/https://doi.org/10.1111/gcb.15040>

592 Blackman, C. J., Creek, D., Maier, C., Aspinwall, M. J., . . . Choat, B. (2019). Drought

593 response strategies and hydraulic traits contribute to mechanistic understanding of plant

594 dry-down to hydraulic failure. *Tree Physiology*, 39(6), 910-924.

595 <https://doi.org/10.1093/treephys/tpz016>

596 Bretfeld, M., Ewers, B. E., & Hall, J. S. (2018). Plant water use responses along secondary

597 forest succession during the 2015-2016 El Nino drought in Panama. *New Phytologist*,

598 219(3), 885-899. <https://doi.org/10.1111/nph.15071>

599 Brockelman, W. Y., Nathalang, A., & Maxwell, J. F. (2017). Mo Singto Forest Dynamics

600 Plot: Flora and Ecology. National Science and Technology Development Agency.

601 Brodribb, T. J. (2017). Progressing from ‘functional’ to mechanistic traits. *New Phytologist*,

602 215(1), 9-11. <https://doi.org/https://doi.org/10.1111/nph.14620>

603 Bucci, S. J., Goldstein, G., Meinzer, F. C., Franco, A. C., . . . Scholz, F. G. (2005).

604 Mechanisms contributing to seasonal homeostasis of minimum leaf water potential and

605 predawn disequilibrium between soil and plant water potential in neotropical savanna

606 trees. *Trees-Structure and Function*, 19(3), 296-304. <https://doi.org/10.1007/s00468-004-0391-2>

608 Carnicer, J., Coll, M., Ninyerola, M., Pons, X., . . . Penuelas, J. (2011). Widespread crown

609 condition decline, food web disruption, and amplified tree mortality with increased

610 climate change-type drought. *Proceedings of the National Academy of Sciences of the*
611 *United States of America*, 108(4), 1474-1478. <https://doi.org/10.1073/pnas.1010070108>

612 Cartwright, J. M., Littlefield, C. E., Michalak, J. L., Lawler, J. J., . . . Dobrowski, S. Z.
613 (2020). Topographic, soil, and climate drivers of drought sensitivity in forests and
614 shrublands of the Pacific Northwest, USA. *Scientific Reports*, 10(1).
615 <https://doi.org/ARTN 1848610.1038/s41598-020-75273-5>

616 Chanthorn, W., Hartig, F., & Brockelman, W. Y. (2017). Structure and community
617 composition in a tropical forest suggest a change of ecological processes during stand
618 development. *Forest Ecology and Management*, 404, 100-107.
619 <https://doi.org/10.1016/j.foreco.2017.08.001>

620 Chanthorn, W., Ratanapongsai, Y., Brockelman, W., Allen, M., . . . Dubois, M.-A. (2016).
621 Viewing tropical forest succession as a three-dimensional dynamical system.
622 *Theoretical Ecology*, 9. <https://doi.org/10.1007/s12080-015-0278-4>

623 Chen, Y. J., Schnitzer, S. A., Zhang, Y. J., Fan, Z. X., . . . Cao, K. F. (2017). Physiological
624 regulation and efficient xylem water transport regulate diurnal water and carbon
625 balances of tropical lianas. *Functional Ecology*, 31(2), 306-317.
626 <https://doi.org/10.1111/1365-2435.12724>

627 Choat, B., Ball, M. C., Luly, J. G., & Holtum, J. A. M. (2005). Hydraulic architecture of
628 deciduous and evergreen dry rainforest tree species from north-eastern Australia. *Trees-*
629 *Structure and Function*, 19(3), 305-311. <https://doi.org/10.1007/s00468-004-0392-1>

630 Choat, B., Brodribb, T. J., Brodersen, C. R., Duursma, R. A., . . . Medlyn, B. E. (2018).
631 Triggers of tree mortality under drought. *Nature*, 558(7711), 531-539.
632 <https://doi.org/10.1038/s41586-018-0240-x>

633 Choat, B., Jansen, S., Brodribb, T. J., Cochard, H., . . . Zanne, A. E. (2012). Global
634 convergence in the vulnerability of forests to drought. *Nature*, 491(7426), 752-+.
635 <https://doi.org/10.1038/nature11688>

636 Choat, B., Sack, L., & Holbrook, N. M. (2007). Diversity of hydraulic traits in nine *Cordia*
637 species growing in tropical forests with contrasting precipitation. *New Phytologist*,
638 175(4), 686-698. <https://doi.org/10.1111/j.1469-8137.2007.02137.x>

639 Davies, S. J., Abiem, I., Abu Salim, K., Aguilar, S., . . . Zuleta, D. (2021). ForestGEO:
640 Understanding forest diversity and dynamics through a global observatory network.
641 *Biological Conservation*, 253, 108907.
642 <https://doi.org/https://doi.org/10.1016/j.biocon.2020.108907>

643 Delzon, S., Douthe, C., Sala, A., & Cochard, H. (2010). Mechanism of water-stress induced
644 cavitation in conifers: bordered pit structure and function support the hypothesis of seal
645 capillary-seeding. *Plant Cell and Environment*, 33(12), 2101-2111.
646 <https://doi.org/10.1111/j.1365-3040.2010.02208.x>

647 Domec, J.-C., & Gartner, B. L. (2001). Cavitation and water storage capacity in bole xylem
648 segments of mature and young Douglas-fir trees. *Trees*, 15(4), 204-214.
649 <https://doi.org/10.1007/s004680100095>

650 Domec, J. C., King, J. S., Ward, E., Oishi, A. C., . . . Noormets, A. (2015). Conversion of
651 natural forests to managed forest plantations decreases tree resistance to prolonged
652 droughts. *Forest Ecology and Management*, 355, 58-71.
653 <https://doi.org/10.1016/j.foreco.2015.04.012>

654 Domec, J. C., Scholz, F. G., Bucci, S. J., Meinzer, F. C., . . . Villalobos-Vega, R. (2006).
655 Diurnal and seasonal variation in root xylem embolism in neotropical savanna woody
656 species: impact on stomatal control of plant water status. *Plant Cell and Environment*,
657 29(1), 26-35. <https://doi.org/DOI 10.1111/j.1365-3040.2005.01397.x>

658 Edwards, W. R. N., & Jaris, P. G. (1982). Relations between water content, potential and
659 permeability in stems of conifers. *Plant, Cell & Environment*, 5(4), 271-277.
660 <https://doi.org/https://doi.org/10.1111/1365-3040.ep11572656>

661 Elliott, S., Navakitbumrung, P., Kuarak, C., Zangkum, S., . . . Blakesley, D. (2003). Selecting
662 framework tree species for restoring seasonally dry tropical forests in northern Thailand
663 based on field performance. *Forest Ecology and Management*, 184(1-3), 177-191.
664 [https://doi.org/10.1016/S0378-1127\(03\)00211-1](https://doi.org/10.1016/S0378-1127(03)00211-1)

665 Engelbrecht, B. M. J., Tyree, M. T., & Kursar, T. A. (2007). Visual assessment of wilting as
666 a measure of leaf water potential and seedling drought survival. *Journal of Tropical
667 Ecology*, 23, 497-500. <https://doi.org/10.1017/S026646740700421x>

668 Ennajeh, M., Simões, F., Khemira, H., & Cochard, H. (2011). How reliable is the double-
669 ended pressure sleeve technique for assessing xylem vulnerability to cavitation in
670 woody angiosperms? *Physiol Plant*, 142(3), 205-210. [https://doi.org/10.1111/j.1399-3054.2011.01470.x](https://doi.org/10.1111/j.1399-
671 3054.2011.01470.x)

672 Ewers, F. W., & Fisher, J. B. (1989). Techniques for Measuring Vessel Lengths and
673 Diameters in Stems of Woody Plants. *American Journal of Botany*, 76(5), 645-656.
674 <https://doi.org/10.2307/2444412>

675 Fetcher, N., Oberbauer, S. F., & Strain, B. R. (1985). Vegetation effects on microclimate in
676 lowland tropical forest in Costa Rica. *International Journal of Biometeorology*, 29(2),
677 145-155. <https://doi.org/10.1007/BF02189035>

678 Gao, H., Chen, Y.-J., Zhang, Y.-J., Maenpuen, P., . . . Zhang, J.-L. (2019). Vessel-length
679 determination using silicone and air injection: are there artifacts? *Tree Physiology*,
680 39(10), 1783-1791. <https://doi.org/10.1093/treephys/tpz064>

681 Heithecker, T. D., & Halpern, C. B. (2007). Edge-related gradients in microclimate in forest
682 aggregates following structural retention harvests in western Washington. *Forest*

683 *Ecology and Management*, 248(3), 163-173.

684 <https://doi.org/10.1016/j.foreco.2007.05.003>

685 Hérault, B., & Gourlet-Fleury, S. (2016). Will Tropical Rainforests Survive Climate Change?

686 In E. Torquebiau (Ed.), *Climate Change and Agriculture Worldwide* (pp. 183-196).

687 Springer Netherlands. https://doi.org/10.1007/978-94-017-7462-8_14

688 Hérault, B., & Piponiot, C. (2018). Key drivers of ecosystem recovery after disturbance in a

689 neotropical forest. *Forest Ecosystems*, 5(1), 2. <https://doi.org/10.1186/s40663-017-0126-7>

690 0126-7

691 Imai, N., Furukawa, T., Tsujino, R., Kitamura, S., . . . Yumoto, T. (2018). Factors affecting

692 forest area change in Southeast Asia during 1980-2010 (vol 13, e0197391, 2018). *Plos*

693 *One*, 13(6). <https://doi.org/ARTN e019990810.1371/journal.pone.0199908>

694 Krober, W., Zhang, S. R., Ehmig, M., & Bruelheide, H. (2014). Linking Xylem Hydraulic

695 Conductivity and Vulnerability to the Leaf Economics Spectrum-A Cross-Species

696 Study of 39 Evergreen and Deciduous Broadleaved Subtropical Tree Species. *Plos One*,

697 9(11). <https://doi.org/ARTN e1092110.1371/journal.pone.0109211>

698 Kursar, T. A., Engelbrecht, B. M. J., Burke, A., Tyree, M. T., . . . Giraldo, J. P. (2009).

699 Tolerance to low leaf water status of tropical tree seedlings is related to drought

700 performance and distribution. *Functional Ecology*, 23(1), 93-102.

701 <https://doi.org/10.1111/j.1365-2435.2008.01483.x>

702 Lebrija-Trejos, E., Perez-Garcia, E. A., Meave, J. A., Bongers, F., . . . Poorter, L. (2010).

703 Functional traits and environmental filtering drive community assembly in a species-

704 rich tropical system. *Ecology*, 91(2), 386-398. <https://doi.org/10.1890/08-1449.1>

705 Lebrija-Trejos, E., Perez-Garcia, E. A., Meave, J. A., Poorter, L., . . . Bongers, F. (2011).

706 Environmental changes during secondary succession in a tropical dry forest in Mexico.

707 *Journal of Tropical Ecology*, 27, 477-489. <https://doi.org/10.1017/S0266467411000253>

708 Lee, Y. K., Lee, D. K., Woo, S. Y., Abraham, E. R. G., . . . Park, C. (2006). Differences of
709 tree species composition and microclimate between a mahogany (*swietenia*
710 *macrophylla* king) plantation and a secondary forest in Mt. Makiling, Philippines.
711 *Forest Science and Technology*, 2(1), 1-12.
712 <https://doi.org/10.1080/21580103.2006.9656293>

713 Maherali, H., Pockman, W. T., & Jackson, R. B. (2004). Adaptive variation in the
714 vulnerability of woody plants to xylem cavitation. *Ecology*, 85(8), 2184-2199.
715 <https://doi.org/10.1890/02-0538>

716 Markesteijn, L., Iraipi, J., Bongers, F., & Poorter, L. (2010). Seasonal variation in soil and
717 plant water potentials in a Bolivian tropical moist and dry forest. *Journal of Tropical
718 Ecology*, 26, 497-508. <https://doi.org/10.1017/S0266467410000271>

719 Markesteijn, L., Poorter, L., Paz, H., Sack, L., . . . Bongers, F. (2011). Ecological
720 differentiation in xylem cavitation resistance is associated with stem and leaf structural
721 traits. *Plant Cell and Environment*, 34(1), 137-148. [https://doi.org/10.1111/j.1365-3040.2010.02231.x](https://doi.org/10.1111/j.1365-
722 3040.2010.02231.x)

723 Marthews, T. R., Burslem, D. F. R. P., Paton, S. R., Yanyuez, F., . . . Mullins, C. E. (2008).
724 Soil drying in a tropical forest: Three distinct environments controlled by gap size.
725 *Ecological Modelling*, 216(3-4), 369-384.
726 <https://doi.org/10.1016/j.ecolmodel.2008.05.011>

727 Martin-StPaul, N. K., Longepierre, D., Huc, R., Delzon, S., . . . Cochard, H. (2014). How
728 reliable are methods to assess xylem vulnerability to cavitation? The issue of 'open
729 vessel' artifact in oaks. *Tree Physiology*, 34(8), 894-905.
730 <https://doi.org/10.1093/treephys/tpu059>

731 Matheny, A. M., Fiorella, R. P., Bohrer, G., Poulsen, C. J., . . . Curtis, P. S. (2017).
732 Contrasting strategies of hydraulic control in two codominant temperate tree species.
733 *Ecohydrology*, 10(3). <https://doi.org/ARTN e181510.1002/eco.1815>

734 McCarthy, J. (2001). Gap dynamics of forest trees: A review with particular attention to
735 boreal forests. *Environmental Reviews* 9, 1-59. <https://doi.org/10.1139/er-9-1-1>

736 McDowell, N., Pockman, W. T., Allen, C. D., Breshears, D. D., . . . Yepez, E. A. (2008).
737 Mechanisms of plant survival and mortality during drought: why do some plants
738 survive while others succumb to drought? *New Phytologist*, 178(4), 719-739.
739 <https://doi.org/10.1111/j.1469-8137.2008.02436.x>

740 McDowell, N. G., Williams, A. P., Xu, C., Pockman, W. T., . . . Koven, C. (2016). Multi-
741 scale predictions of massive conifer mortality due to chronic temperature rise. *Nature
742 Climate Change*, 6(3), 295-300. <https://doi.org/10.1038/nclimate2873>

743 Melcher, P. J., Holbrook, N. M., Burns, M. J., Zwieniecki, M. A., . . . Sack, L. (2012).
744 Measurements of stem xylem hydraulic conductivity in the laboratory and field.
745 *Methods in Ecology and Evolution*, 3(4), 685-694. [https://doi.org/10.1111/j.2041-210X.2012.00204.x](https://doi.org/10.1111/j.2041-
746 210X.2012.00204.x)

747 Mitchell, P. J., Veneklaas, E. J., Lambers, H., & Burgess, S. S. O. (2008). Leaf water
748 relations during summer water deficit: differential responses in turgor maintenance and
749 variation in leaf structure among different plant communities in south-western
750 Australia. *Plant, Cell & Environment*, 31(12), 1791-1802.
751 <https://doi.org/https://doi.org/10.1111/j.1365-3040.2008.01882.x>

752 Mueller, R. C., Scudder, C. M., Porter, M. E., Trotter, R. T., . . . Whitham, T. G. (2005).
753 Differential tree mortality in response to severe drought: evidence for long-term
754 vegetation shifts. *Journal of Ecology*, 93(6), 1085-1093. [https://doi.org/10.1111/j.1365-2745.2005.01042.x](https://doi.org/10.1111/j.1365-
755 2745.2005.01042.x)

756 Nardini, A., Battistuzzo, M., & Savi, T. (2013). Shoot desiccation and hydraulic failure in
757 temperate woody angiosperms during an extreme summer drought. *New Phytologist*,
758 200(2), 322-329. <https://doi.org/10.1111/nph.12288>

759 Nolf, M., Creek, D., Duursma, R., Holtum, J., . . . Choat, B. (2015). Stem and leaf hydraulic
760 properties are finely coordinated in three tropical rain forest tree species. *Plant Cell and*
761 *Environment*, 38(12), 2652-2661. <https://doi.org/10.1111/pce.12581>

762 Oliveira, R. S., Costa, F. R. C., van Baalen, E., de Jonge, A., . . . Poorter, L. (2019).
763 Embolism resistance drives the distribution of Amazonian rainforest tree species along
764 hydro-topographic gradients. *New Phytologist*, 221(3), 1457-1465.
765 <https://doi.org/https://doi.org/10.1111/nph.15463>

766 Pammenter, N. W., & Vander Willigen, C. (1998). A mathematical and statistical analysis of
767 the curves illustrating vulnerability of xylem to cavitation. *Tree Physiology*, 18(8-9),
768 589-593. <https://doi.org/DOI 10.1093/treephys/18.8-9.589>

769 Perez-Harguindeguy, N., Diaz, S., Garnier, E., Lavorel, S., . . . Cornelissen, J. H. C. (2016).
770 New handbook for standardised measurement of plant functional traits worldwide
771 *Australian Journal of Botany*, 64(7-8), 715-716. https://doi.org/10.1071/Bt12225_Co

772 Pineda-Garcia, F., Paz, H., & Meinzer, F. C. (2013). Drought resistance in early and late
773 secondary successional species from a tropical dry forest: the interplay between xylem
774 resistance to embolism, sapwood water storage and leaf shedding. *Plant Cell and*
775 *Environment*, 36(2), 405-418. <https://doi.org/10.1111/j.1365-3040.2012.02582.x>

776 Pineda-Garcia, F., Paz, H., Meinzer, F. C., & Angeles, G. (2016). Exploiting water versus
777 tolerating drought: water-use strategies of trees in a secondary successional tropical dry
778 forest. *Tree Physiology*, 36(2), 208-217. <https://doi.org/10.1093/treephys/tpv124>

779 Powell, T. L., Wheeler, J. K., de Oliveira, A. A. R., da Costa, A. C. L., . . . Moorcroft, P. R.
780 (2017). Differences in xylem and leaf hydraulic traits explain differences in drought

781 tolerance among mature Amazon rainforest trees. *Global Change Biology*, 23(10),
782 4280-4293. <https://doi.org/10.1111/gcb.13731>

783 Prado, C. H. B. d. A., Wenhui, Z., Cardoza Rojas, M. H., & Souza, G. M. (2004). Seasonal
784 leaf gas exchange and water potential in a woody cerrado species community. *Brazilian*
785 *Journal of Plant Physiology*, 161(1), 7-16. <https://doi.org/10.1590/S1677->
786 04202004000100002

787 Reichstein, M., Bahn, M., Ciais, P., Frank, D., . . . Wattenbach, M. (2013). Climate extremes
788 and the carbon cycle. *Nature*, 500(7462), 287-295. <https://doi.org/10.1038/nature12350>

789 Rodtassana, C., Unawong, W., Yaemphum, S., Chanthorn, W., . . . Tor-ngern, P. (2021).
790 Different responses of soil respiration to environmental factors across forest stages in a
791 Southeast Asian forest. *Ecology and Evolution*. <https://doi.org/10.1002/ece3.8248>

792 Rosner, S., Heinze, B., Savi, T., & Dalla-Salda, G. (2019). Prediction of hydraulic
793 conductivity loss from relative water loss: new insights into water storage of tree stems
794 and branches. *Physiologia Plantarum*, 165(4), 843-854.
795 <https://doi.org/10.1111/ppl.12790>

796 Rowland, L., da Costa, A. C. L., Galbraith, D. R., Oliveira, R. S., . . . Meir, P. (2015). Death
797 from drought in tropical forests is triggered by hydraulics not carbon starvation. *Nature*,
798 528(7580), 119-122. <https://doi.org/10.1038/nature15539>

799 Ruiz-Benito, P., Ratcliffe, S., Zavala, M. A., Martinez-Vilalta, J., . . . Jump, A. S. (2017).
800 Climate- and successional-related changes in functional composition of European
801 forests are strongly driven by tree mortality. *Global Change Biology*, 23(10), 4162-
802 4176. <https://doi.org/10.1111/gcb.13728>

803 Shaw, J. D., Steed, B. E., & DeBlander, L. T. (2005). Forest Inventory and Analysis (FIA)
804 annual inventory answers the question: What is happening to pinyon-juniper

805 woodlands? *Journal of Forestry*, 103(6), 280-285. <Go to
806 ISI>://WOS:000232416300004

807 Skelton, R. P., West, A. G., & Dawson, T. E. (2015). Predicting plant vulnerability to drought
808 in biodiverse regions using functional traits. *Proceedings of the National Academy of
809 Sciences of the United States of America*, 112(18), 5744-5749.
810 <https://doi.org/10.1073/pnas.1503376112>

811 Sperry, J. S., Hacke, U. G., Oren, R., & Comstock, J. P. (2002). Water deficits and hydraulic
812 limits to leaf water supply. *Plant Cell and Environment*, 25(2), 251-263.
813 <https://doi.org/DOI 10.1046/j.0016-8025.2001.00799.x>

814 Sperry, J. S., & Ikeda, T. (1997). Xylem cavitation in roots and stems of Douglas-fir and
815 white fir. *Tree Physiology*, 17(4), 275-280. <https://doi.org/10.1093/treephys/17.4.275>

816 Sperry, J. S., & Saliendra, N. Z. (1994). Intra-Plant and Inter-Plant Variation in Xylem
817 Cavitation in *Betula-Occidentalis*. *Plant Cell and Environment*, 17(11), 1233-1241.
818 <https://doi.org/DOI 10.1111/j.1365-3040.1994.tb02021.x>

819 Steppe, K. (2018). The potential of the tree water potential. *Tree Physiology*, 38(7), 937-940.
820 <https://doi.org/10.1093/treephys/tpy064>

821 Stibig, H. J., Achard, F., Carboni, S., Rasi, R., . . . Miettinen, J. (2014). Change in tropical
822 forest cover of Southeast Asia from 1990 to 2010. *Biogeosciences*, 11(2), 247-258.
823 <https://doi.org/10.5194/bg-11-247-2014>

824 Taiz, L., & Zeiger, E. (2003). Plant physiology. 3rd edn. *Annals of Botany*, 91.
825 <https://doi.org/10.1093/aob/mcg079>

826 Tan, F. S., Song, H. Q., Fu, P. L., Chen, Y. J., . . . Zhu, S. D. (2020). Hydraulic safety
827 margins of co-occurring woody plants in a tropical karst forest experiencing frequent
828 extreme droughts. *Agricultural and Forest Meteorology*, 292. <https://doi.org/ARTN 10810710.1016/j.agrformet.2020.108107>

830 Tor-ngern, P., Chart-asa, C., Chanthorn, W., Rodtassana, C., . . . Hasselquist, N. J. (2021).
831 Variation of leaf-level gas exchange rates and leaf functional traits of dominant trees
832 across three successional stages in a Southeast Asian tropical forest. *Forest Ecology*
833 and Management, 489. <https://doi.org/ARTN 11910110.1016/j.foreco.2021.119101>

834 Trueba, S., Pouteau, R., Lens, F., Feild, T. S., . . . Delzon, S. (2017). Vulnerability to xylem
835 embolism as a major correlate of the environmental distribution of rain forest species
836 on a tropical island. *Plant Cell and Environment*, 40(2), 277-289.
837 <https://doi.org/10.1111/pce.12859>

838 Vander Willigen, C., Sherwin, H. W., & Pammerer, N. W. (2000). Xylem hydraulic
839 characteristics of subtropical trees from contrasting habitats grown under identical
840 environmental conditions. *New Phytologist*, 145(1), 51-59. <https://doi.org/DOI 10.1046/j.1469-8137.2000.00549.x>

841 Vieira, D. L. M., & Scariot, A. (2006). Principles of natural regeneration of tropical dry
842 forests for restoration. *Restoration Ecology*, 14(1), 11-20. <https://doi.org/DOI 10.1111/j.1526-100X.2006.00100.x>

843 Vinya, R., Malhi, Y., Fisher, J. B., Brown, N., . . . Aragao, L. E. (2013). Xylem cavitation
844 vulnerability influences tree species' habitat preferences in miombo woodlands.
845 *Oecologia*, 173(3), 711-720. <https://doi.org/10.1007/s00442-013-2671-2>

846 Wilcove, D. S., Giam, X., Edwards, D. P., Fisher, B., . . . Koh, L. P. (2013). Navjot's
847 nightmare revisited: logging, agriculture, and biodiversity in Southeast Asia. *Trends in
848 Ecology & Evolution*, 28(9), 531-540. <https://doi.org/10.1016/j.tree.2013.04.005>

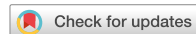
849 Zeng, Z. Z., Estes, L., Ziegler, A. D., Chen, A. P., . . . Wood, E. F. (2018). Highland cropland
850 expansion and forest loss in Southeast Asia in the twenty-first century. *Nature
851 Geoscience*, 11(8), 556-. <https://doi.org/10.1038/s41561-018-0166-9>

854 Zhang, Q. W., Zhu, S. D., Jansen, S., & Cao, K. F. (2021). Topography strongly affects
855 drought stress and xylem embolism resistance in woody plants from a karst forest in
856 Southwest China. *Functional Ecology*, 35(3), 566-577. <https://doi.org/10.1111/1365-2435.13731>

858 Zhu, S. D., & Cao, K. F. (2009). Hydraulic properties and photosynthetic rates in co-
859 occurring lianas and trees in a seasonal tropical rainforest in southwestern China. *Plant
860 Ecology*, 204(2), 295-304. <https://doi.org/10.1007/s11258-009-9592-5>

861 Zhu, S. D., Chen, Y. J., Fu, P. L., & Cao, K. F. (2017). Different hydraulic traits of woody
862 plants from tropical forests with contrasting soil water availability. *Tree Physiology*,
863 37(11), 1469-1477. <https://doi.org/10.1093/treephys/tpx094>

864



OPEN

Comparison of water-use characteristics of tropical tree saplings with implications for forest restoration

Tushar Andriyas¹, Nisa Leksungnoen² & Pantana Tor-ngern^{3,4,5}✉

Tropical forests are experiencing reduced productivity and will need restoration with suitable species. Knowledge of species-specific responses to changing environments during early stage can help identify the appropriate species for sustainable planting. Hence, we investigated the variability in whole-tree canopy conductance and transpiration (G_t and E_t) in potted saplings of common urban species in Thailand, viz., *Pterocarpus indicus*, *Lagerstroemia speciosa*, and *Swietenia macrophylla*, across wet and dry seasons in 2017–2018. Using a Bayesian modeling framework, G_t and E_t were estimated from sap flux density, informed by the soil, atmospheric and tree measurements. Subsequently, we evaluated their variations with changing vapor pressure deficit (VPD) and soil moisture across timescales and season. We found that G_t and E_t were higher and highly variable in *L. speciosa* across seasons than *S. macrophylla* and *P. indicus*. Our results implied that water-use in these species was sensitive to seasonal VPD. *L. speciosa* may be suitable under future climate variability, given its higher G_t and E_t across atmospheric and soil moisture conditions. With their lower G_t and E_t , *P. indicus* and *S. macrophylla* may photosynthesize throughout the year, maintaining their stomatal opening even under high VPD. These findings benefit reforestation and reclamation programs of degraded lands.

Tropical forests are one of the largest carbon sinks in terrestrial ecosystems¹. Climate change has been predicted to result in more intense with protracted dry or wet spells, with varying duration, intensity, frequency, and spatiotemporal spread in different parts of the world^{2,3}. In fact, drought-induced mortality of global tropical forests has been recently documented⁴. Species mortality caused by anthropogenic factors can be important⁵ and can result in a loss of carbon storage, leading to a cyclical downturn of increasing temperatures and further mortality. Therefore, many countries are taking preemptive action to reduce such impacts through reforestation. Reforestation includes planting trees on previously degraded lands, which can be demanding on newly planted trees. Under the predicted intensification of climate change, reforested trees may experience harsh conditions, resulting in an unsuccessful establishment. To ensure successful establishment in degraded lands, species robustness to seasonal variations, especially under a climate change scenario is needed. Because trees in urban conditions likely experience extreme environmental stresses from heat, drought, and flood, another interesting approach is to study the tolerance and resilience of urban tree species to climate variability which will infer the physiological responses of trees and their vulnerability to climate extremes^{5,6}.

In Bangkok, street tree species differ in leaf phenology (i.e., deciduous or evergreen), habitat (ranging from hill evergreen forest to mangrove forest), and origin (native or exotic)⁷, with the most common street tree species being *Pterocarpus indicus*, *Lagerstroemia speciosa*, and *Swietenia macrophylla*⁸. *P. indicus* is a fast-growing medium-size tree native to Asia and can be either deciduous or facultative evergreen, depending on the availability of soil moisture and the openness of the growth area. *L. speciosa* is a fast-growing medium-size tree native to Southeast Asia and is a deciduous species, usually found in mixed deciduous forests. *S. macrophylla* is an

¹Graduate School, Chulalongkorn University, Bangkok 10330, Thailand. ²Department of Forest Biology, Faculty of Forestry, Kasetsart University, Bangkok 10900, Thailand. ³Department of Environmental Science, Faculty of Science, Chulalongkorn University, Bangkok 10330, Thailand. ⁴Environment, Health and Social Data Analytics Research Group, Chulalongkorn University, Bangkok 10330, Thailand. ⁵Water Science and Technology for Sustainable Environment Research Group, Chulalongkorn University, Bangkok 10330, Thailand. ✉email: Pantana.t@chula.ac.th

evergreen species native to South and Central America and was introduced into Thailand due to its fast growth and adaptability to various environmental conditions.

The robustness of a given tree species for forest establishment is inferred by investigating its physiological responses to variations in atmospheric demand (i.e., seasonal variations) and soil water availability, especially during the early stages of growth. Variability in soil water availability and atmospheric demand make it essential to estimate the variations in plant ecohydrological process/processes⁹. Some relevant variables for estimating such responses are transpiration and photosynthesis, which represent water use and carbon gain of trees. Many investigations have been widely conducted in trees of various growing stages by measuring leaf level transpiration and photosynthesis^{10–13}. However, during leaf-level experiments, it can be difficult to monitor the continual changes in variables, limiting the amount of useful information that can be gained by estimating such responses. Moreover, physiological responses at leaf scale may not directly translate to those at the canopy scale^{14–17}. An alternative approach is to analyze the whole-tree transpiration and photosynthesis in response to changing environmental conditions. However, whole-tree photosynthesis is usually difficult to estimate without detailed measurements of biochemical photosynthetic parameters and leaf nutrients, as required in most photosynthesis models^{18,19}. Instead, canopy conductance may be used to infer a tree's ability in capturing the atmospheric carbon dioxide and to impute the responses of whole-tree photosynthesis to environmental changes.

Common techniques for estimating such parameters include sap flux probes which continuously detect changes in water flow rates in stems and are of various designs (Heat dissipation^{20,21}, Heat pulse²², Heat ratio²³, Heat balance²⁴). Data from sap flux probes can be scaled from a point measurement in the stem to whole-tree transpiration and canopy conductance^{25–28}. As such, proper scaling is needed to estimate the canopy conductance^{29,30}, transpiration³¹, and carbon assimilation³². However, there are inherent errors and uncertainties involved in the scaling process. Additionally, errors can result from failing to account for capacitance in stems, which causes a time lag between both fluxes and atmospheric evaporative demand^{33,34}. Another issue is missing data which come from unexpected sensor failure. This can result in an inability to obtain a continuous data set for analyses across temporal scales.

Normally, gap filling of missing data is performed by applying relationships between the measured sap flux data and environmental factors such as vapor pressure deficit (VPD) and soil moisture³⁵. However, such an approach may not capture the true physiological responses of trees and is unable to recover continuous data when the environmental data are also missing. Therefore, a coherent probabilistic specification is needed to account for uncertainty resulting from sensor failure³⁶, as unusable data points can cause scaling errors (from sap flux measurements to canopy processes)^{37,38}. To overcome these limitations, a method based on hierarchical Bayesian statistics, called State-Space Canopy Conductance (StaCC) model, was developed recently³¹. The StaCC model uses sap flux density (point observation in stems) to infer transpiration and canopy conductance (at whole-tree or canopy scale) by explicitly accounting for the above uncertainties associated with the internal tree hydraulics and measurement errors occurred during observation. While estimating the canopy transpiration and conductance, the model also allows simultaneous gap-filling of missing sap flux data based on prior inference on canopy processes. The model substantially improves the estimation of canopy parameters compared to traditional scaling methods³¹.

With this context, we estimated whole-tree canopy conductance (G_t) and transpiration (E_t) of saplings of three common street tree species in Bangkok, Thailand, and evaluated their variations with atmospheric and soil moisture, with implications for potential establishment in degraded lands. The specific aims were to (1) determine the seasonal and interspecific difference in G_t and E_t in potted saplings of *P. indicus*, *L. speciosa*, and *S. macrophylla* (2) assess the extent to which such differences are a response to soil moisture and atmospheric evaporative demand (i.e., VPD). Additionally, we performed analysis across temporal scales, ranging from daily to monthly, to gain insights into the difference in physiological responses among the species, if exist, and whether it preserves across timescales. To estimate G_t and E_t , a joint specification of tree-level (sap flux density, sapwood area, and leaf area) and environmental (air temperature, VPD, and soil moisture) data, together with model uncertainty was used to build an inference³⁶. We employed the StaCC model on sap flux density data that were monitored on these saplings for 6 months (from 25th July 2017 to 11th February 2018), covering parts of a dry and a wet season. Findings from this study will benefit the selection of tree species for reforestation of lands, formerly under agriculture and logged forests, which can sometimes be found adjacent to national parks in Thailand. Such areas may be preserved to act as a buffer zone between the protected area and community lands.

Results

Model performance. An initial sensitivity analysis was done to determine the capacitance parameter, β (i.e., β was varied between 0.22 and 1 or a storage time between 120 to 0 min), as indicated by high R^2 and significant p values. The β parameter represents the water storage capacity in stems which can be discharged through transpiration, buffering its daily fluctuations. In the context of our analysis, the response in sap flux density can be dampened by lags in stomatal response and capacitance (i.e., water storage). Additionally, we also ensured that model parameters converged to clear posterior distributions. These were obtained at different values of β for the three species, during a given season. Additionally, based on our analysis, keeping the prior on β weak (i.e., non-informative prior) improved the model predictions further. Hence, for a given species and season, we initialized the simulation with a given β value, which stabilized to a final value within the first 1000 iterations. Table 1 indicates the values with which the simulation was initialized (as determined through the sensitivity analysis) and the mean value obtained after removing the burn-in. For *P. indicus* and *L. speciosa* during the wet season, the variations in sap flux density were best explained by storage time which was around half of that during the dry season, while *S. macrophylla* had a higher storage time in the wet season. A lower storage time means

Species	β Wet [initial, mean]	β Dry [initial, mean]	Mean storage time, wet, dry [Mins]
<i>P. indicus</i>	0.63, 0.83	0.63, 0.63	17, 30
<i>L. speciosa</i>	0.63, 0.81	0.86, 0.65	18, 29
<i>S. macrophylla</i>	0.86, 0.72	0.86, 0.86	23, 15

Table 1. Initial and mean values of the species capacitance parameter during wet and dry seasons. The last column indicates the storage time in minutes based on the mean β value.

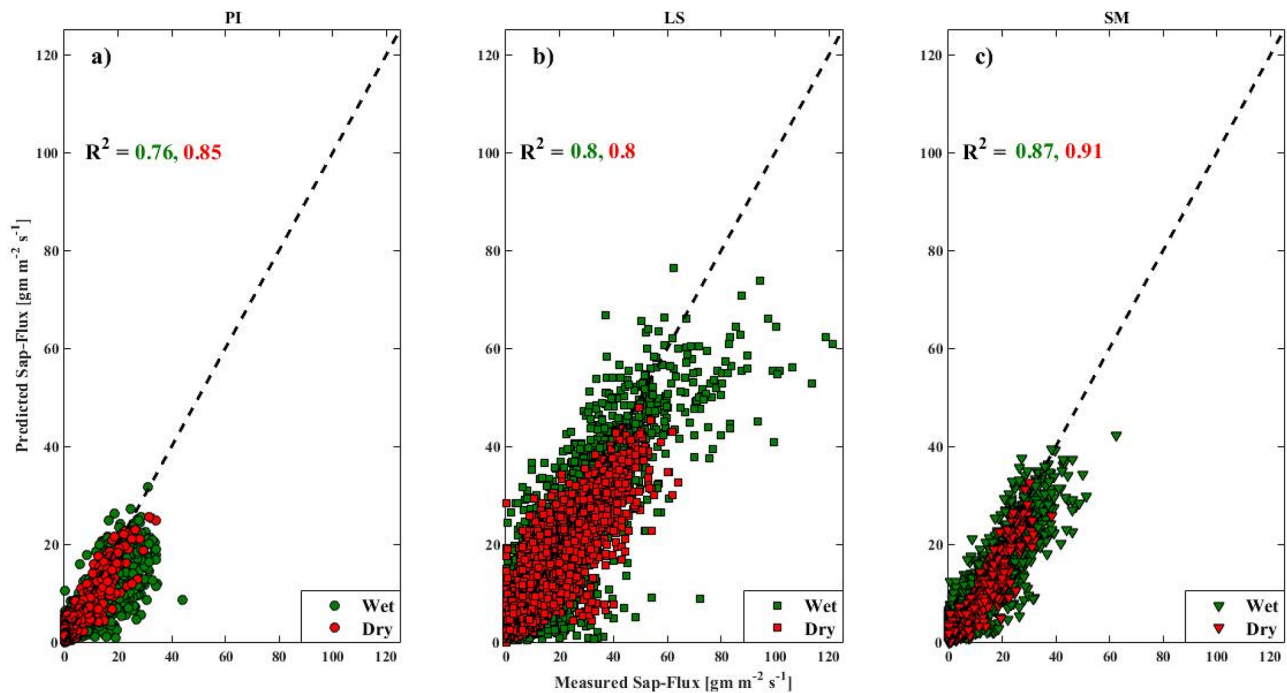


Figure 1. The best model of sap flux density prediction for (a) *Pterocarpus indicus* (PI), (b) *Lagerstroemia speciosa* (LS), and (c) *Swietenia macrophylla* (SM). The green (red) filled circles represent sap flux density data during the wet (dry) season. The corresponding R^2 value for each season is also indicated. The black dashed line is the 1:1 line. This figure was generated using MATLAB version 7.12.0 R2017a (https://www.mathworks.com/products/new_products/release2017a.html).

that the lag between the stored water and the transpirational water is short, causing a relatively fast response to low soil moisture.

Prediction of sap flux density. The model performance varied with species and seasons, with predictions being the closest for *S. macrophylla*, intermediate in *P. indicus*, and the lowest for *L. speciosa*. Also, the model performance was relatively better during the wet season. The R^2 values of the relationship between modeled and measured sap flux density during the wet (dry) season ranged 0.44–0.76 (0.40–0.85) for *P. indicus*, 0.46–0.80 (0.39–0.80) for *L. speciosa*, and 0.75–0.87 (0.61–0.91) for *S. macrophylla*, while the corresponding mean R^2 values were 0.64 (0.65) for *P. indicus*, 0.70 (0.57) for *L. speciosa*, and 0.81 (0.78) for *S. macrophylla*. The corresponding average root mean squared error (RMSE) was 2.73 (2.10), 4.00 (2.71), and 3.36 (2.57) g m⁻² s⁻¹ for *P. indicus*, *L. speciosa*, and *S. macrophylla*, respectively. The residuals, which indicate the difference between predicted and measured sap flux values, did not deviate appreciably from a normal distribution. The scatter plots of the best sap flux density's predictions (as indicated by the highest R^2 value) are plotted in Fig. 1. Around the highest 1 to 3.5% daytime and the lowest nighttime, sap flux values, on average, were under and overestimated by the model, respectively. This prediction behavior may be associated with the unused PAR sub-model, but this did not influence our results as previously explained about the indifference between model runs with and without the PAR sub-model. On average, the model was able to capture the diurnal trends in sap flux density with the residuals not having an inherent bias.

Canopy conductance and transpiration. Sap flux measurements indicate that water consumption is different among the species and seasons. We observed a large degree of variation in seasonal and interspecific magnitude of reference conductance (G_{ref}) and relative stomatal sensitivity to VPD was observed (figure not shown). *P. indicus* had similar G_{ref} in both seasons, but was highly sensitive to VPD during the dry season. As

Species	Season	Daily G_t (mmol m ⁻² s ⁻¹)	Weekly G_t (mmol m ⁻² s ⁻¹)	Monthly G_t (mmol m ⁻² s ⁻¹)	Daily E_L (mmol m ⁻² s ⁻¹)	Weekly E_L (mmol m ⁻² s ⁻¹)	Monthly E_L (mmol m ⁻² s ⁻¹)
<i>P. indicus</i>	Wet	9.4 ± 3 ^E	9 ± 2.3 ^C	8.9 ± 1.8 ^C	0.30 ± 0.1 ^C	0.29 ± 0.1 ^C	0.31 ± 0.03 ^C
	Dry	6.7 ± 3.4 ^F	6.6 ± 2.5 ^C	6.8 ± 0.9 ^C	0.23 ± 0.1 ^D	0.22 ± 0.1 ^C	0.23 ± 0.04 ^C
<i>L. speciosa</i>	Wet	77.1 ± 19.6 ^A	73.6 ± 20.1 ^A	71.6 ± 18 ^A	0.76 ± 0.2 ^A	0.73 ± 0.2 ^A	0.73 ± 0.2 ^A
	Dry	40.2 ± 11.9 ^B	39.9 ± 8.04 ^A	40.5 ± 2.4 ^A	0.40 ± 0.1 ^B	0.40 ± 0.1 ^A	0.41 ± 0.02 ^A
<i>S. macrophylla</i>	Wet	20 ± 4.3 ^C	19.2 ± 4.5 ^B	19.1 ± 3.1 ^B	0.44 ± 0.1 ^B	0.43 ± 0.1 ^B	0.45 ± 0.1 ^B
	Dry	12.4 ± 4.3 ^D	12.4 ± 3 ^B	12.9 ± 1.8 ^B	0.28 ± 0.1 ^C	0.28 ± 0.1 ^B	0.29 ± 0.04 ^B
Species		<0.0001	<0.0001**	<0.0001**	<0.0001	<0.0001**	<0.0001**
Seasons		<0.0001	<0.0001**	<0.0001**	<0.0001	<0.0001**	<0.0001**
Species × seasons		<0.0001**	0.409	0.334	<0.0001**	0.202	0.230
Remarks			Wet>dry	Wet>dry		Wet>dry	Wet>dry

Table 2. Mean stomatal sensitivity along with mean daily, weekly and monthly G_t and E_L (\pm SD) for the three investigated species during the wet and the dry season. The same alphabetical superscript indicates no significant difference from each other and vice versa at 5% significant level. P -values in bold and having ** indicate a statistically significant difference between means of the main factors and the interaction between the main factors.

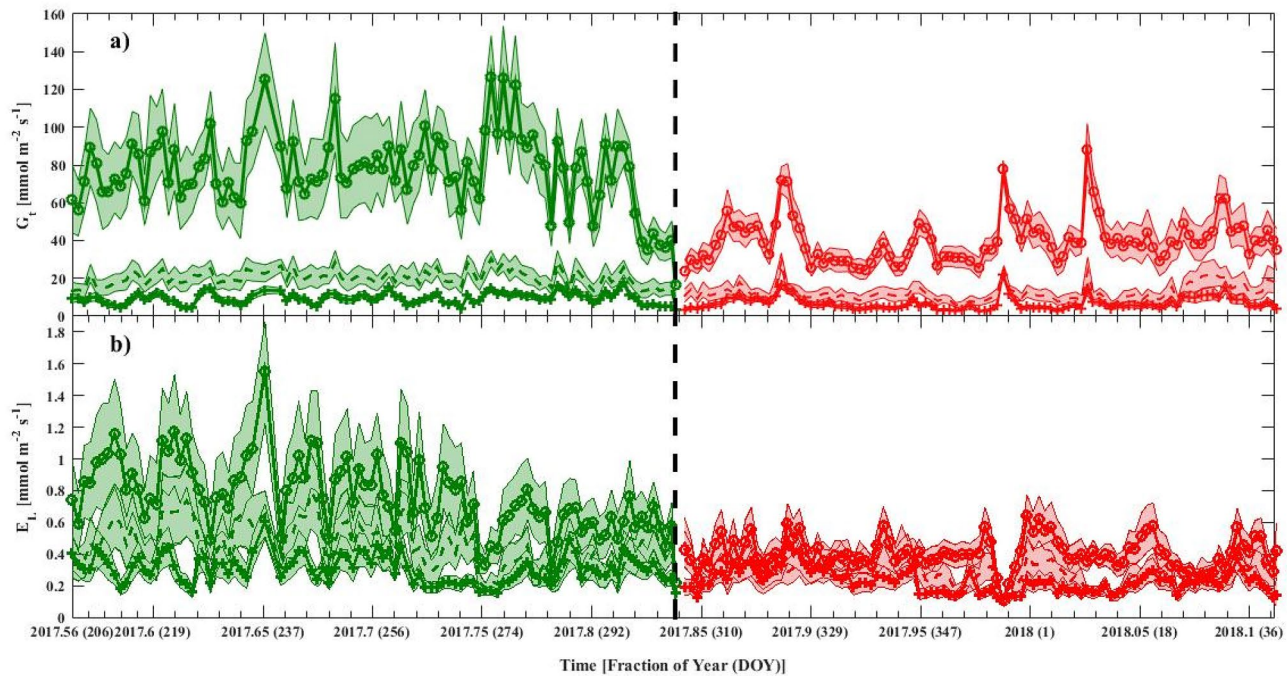


Figure 2. Estimated daily averaged (a) canopy conductance (G_t) and (b) leaf transpiration (E_L) during the wet (green) and dry (red) season. The vertical dash line indicates the ending of the wet season (DOY 305 or November 1st, 2017). Plots for *P. indicus* are depicted in +, *L. speciosa* in o-, and *S. macrophylla* in—markers, respectively. The shaded regions represent the 95% confidence intervals. This figure was generated using MATLAB version 7.12.0 R2017a (https://www.mathworks.com/products/new_products/release2017a.html).

indicated in Table 2, whole-tree canopy conductance varied the greatest in *L. speciosa* with the relative sensitivity to natural log of VPD being low ($\lambda/G_{ref} < 0.50$) during both seasons for all the species, with only exception being *P. indicus* during the dry season ($\lambda/G_{ref} > 0.70$). Both G_t and E_L showed similar seasonal variation for a given species but with varying intensity (Fig. 2). The uncertainty in daily G_t and E_L averages was high during the wet season, indicating that the variability in VPD and soil moisture contributed greatly, relative to the model error. Such errors can be amplified further at much shorter, half-hourly timescale, as indicated by the variable R^2 for the three species (Fig. 1).

Overall, the mean values of both G_t and E_L were statistically different among species and between seasons. *L. speciosa* had the highest G_t and E_L while *P. indicus* had the lowest values. Both G_t and E_L were significantly higher in wet season than in dry season. This difference was more pronounced in G_t , where, for *L. speciosa*, it was about 10 times higher than *P. indicus*, while E_L was approximately 2 times higher. However, only the mean daily values indicated a significant interaction between species and seasons. This may be attributed to the lower

number of samples in the weekly and monthly analysis, leading to a large variation and undetected difference in the ANOVA test.

Daily, weekly, and monthly G_t and E_L were the greatest in *L. speciosa* in either of the season and were the lowest for *P. indicus* (Table 2). The mean G_t and E_L for *L. speciosa* during the wet season was around $77 \text{ mmol m}^{-2} \text{ s}^{-1}$ and $0.76 \text{ mmol m}^{-2} \text{ s}^{-1}$, respectively and reached their maximum value (around $140 \text{ mmol m}^{-2} \text{ s}^{-1}$ and $1.6 \text{ mmol m}^{-2} \text{ s}^{-1}$, respectively) around mid-July, 2017. This can be attributed to the low total leaf area of *L. speciosa* (averaged 2.55 m^2) compared to *P. indicus* and *S. macrophylla*, which had similar leaf areas (averaged $\sim 3 \text{ m}^2$). In general, G_t declined drastically for *L. speciosa*, with the other two species experiencing marginal declines as time progressed from wet to dry season, till the end of the study period.

Diurnal variations. During both seasons, VPD variations over the day were between 0.7 and 2.0 kPa, with VPD being significantly higher during the wet season than in the dry season from 8:00 to 17:00 local time (LT) (Fig. 3a). The soil moisture content measured in each species was lower during the dry season (Fig. 3b). The course of hourly G_t and E_L (averages from 6:00 to 18:00 LT) are plotted for the three species (Fig. 3c and d, respectively). A uni-modal pattern was observed in both G_t and E_L in the three species, showing peaks between 8:00 and 14:00 LT (Fig. 3c and d). Maximum G_t was reached early in the day (around 9:00 LT) for *L. speciosa*, while the E_L rates peaked approximately 2 h later during the wet season. A sudden rise to high values during the early hours was more pronounced during the wet season. After this, both parameters declined relatively consistently, during both seasons. Overall, G_t and E_L were consistently higher during the wet season, with the estimated E_L values for *L. speciosa* being twice that of the dry season. A plateau during the wet season (less pronounced in the dry season), was observed for *S. macrophylla* (from 9:00 to 13:00 LT).

Over various time scales (weekly and monthly not shown), E_L was positively correlated with G_t within both wet and dry seasons (Fig. 4 showing daily estimates only). The significant relationships revealed that, on average over both seasons, a unit change in G_t caused a change of 0.45, 1.16, and 0.76 units in E_L for *P. indicus*, *L. speciosa*, and *S. macrophylla*, respectively.

Atmospheric and soil demand. Responses of daily E_L to atmospheric evaporative demand, represented by VPD, and soil moisture, were different between the two seasons and species (Fig. 5). Generally, E_L increased with increasing VPD (Fig. 5a–c) in all species. The sensitivity of E_L to VPD was relatively higher during the wet season and highly pronounced for *L. speciosa* and *S. macrophylla* (compare green and red lines in Fig. 5b and c), while that for *P. indicus* was similar in both seasons (Fig. 5a). Strong decreases in E_L with increasing soil moisture was observed during the wet season for *L. speciosa* and *S. macrophylla*, while the effect was highly suppressed in *P. indicus* (green lines in Fig. 5d–f). The observed trends of decreasing E_L with increasing soil water indicated possible flooding condition during the wet season. Some extra rainfalls may contribute to this, although we had no access to rainfall data at the site to confirm it. However, the range of soil moisture during the wet season was relatively small with differences between the maximum and the minimum around $0.1 \text{ m}^3 \text{ m}^{-3}$ for both species (Fig. 5e, f) and the significant trends may be driven by the ‘extreme’ value such as the data point at the lowest soil moisture of *S. macrophylla* (the leftmost green symbol in Fig. 5f). During the dry season, E_L did not change significantly for both *L. speciosa* and *S. macrophylla* but it increased marginally with increasing soil moisture for *P. indicus*.

Discussion

Model performance to predict sap flux density in saplings. Using the Bayesian modeling technique³¹, we estimated G_t and E_L from sap flux density measured in saplings of three common urban species in Bangkok. The sap flux rates were closely related to the weather variations, particularly VPD. Previous studies have indicated that the stomatal response is sensitive to VPD as it directly affects the leaf water loss which, together with plant hydraulic system, controls leaf water potential and turgor pressure^{39–42}. The best model performance was obtained by uniquely parameterizing each species and season with variable dampening effects (as indicated by the β parameters in Table 1), based on the dependence of water storage and hence transpiration on changes in soil and plant water status⁴³. Given many uncertainties related to measurement errors (e.g., those in measuring environmental data), the overall agreement between the model estimates and the data was sufficiently accurate, as indicated by the respective R^2 and RMSE values, implying that the model estimates of G_t and E_L were reliable. Furthermore, VPD and soil moisture could explain a large portion of the variability in the sap flux density of the three species, as indicated by mean R^2 during wet (dry) seasons; 0.64 (0.65) for *P. indicus*, 0.70 (0.57) for *L. speciosa*, and 0.81 (0.78).

While the model output gives reasonable values of sap flux density which allows good estimates of G_t and E_L across the three species, certain important caveats need to be considered. In our study, assumptions were made while predicting J_b , G_b and E_L from the sensor data, soil moisture, and environmental variables. First, we assumed that there were no radial or azimuthal variations in sap flux density, due to the small stem size. Additionally, as the non-conducting wood (pith) was negligible, it was assumed that the sapwood covered the entire stem. Thus, the estimated values are for potted saplings and more mature individuals could have a relatively modest variation between the estimated values of G_t and E_L , due to a higher stomatal sensitivity to VPD^{44,45}. The difference between present study and the previous study³¹ that employed the StaCC model is that their estimations were based on sap flux density in mature trees and were closely related to the total leaf area index of the crown, without the need to individually quantify the leaves that constitute it. Also, due to many unusable data points, we did not use the PAR to generate the estimates. However, we tested the model run with the data provided by the original model³¹, including and excluding the PAR sub-model, resulting in an approximately 2% difference between the two scenarios (0.86 with PAR and 0.88 without PAR). The model setup and parameterization

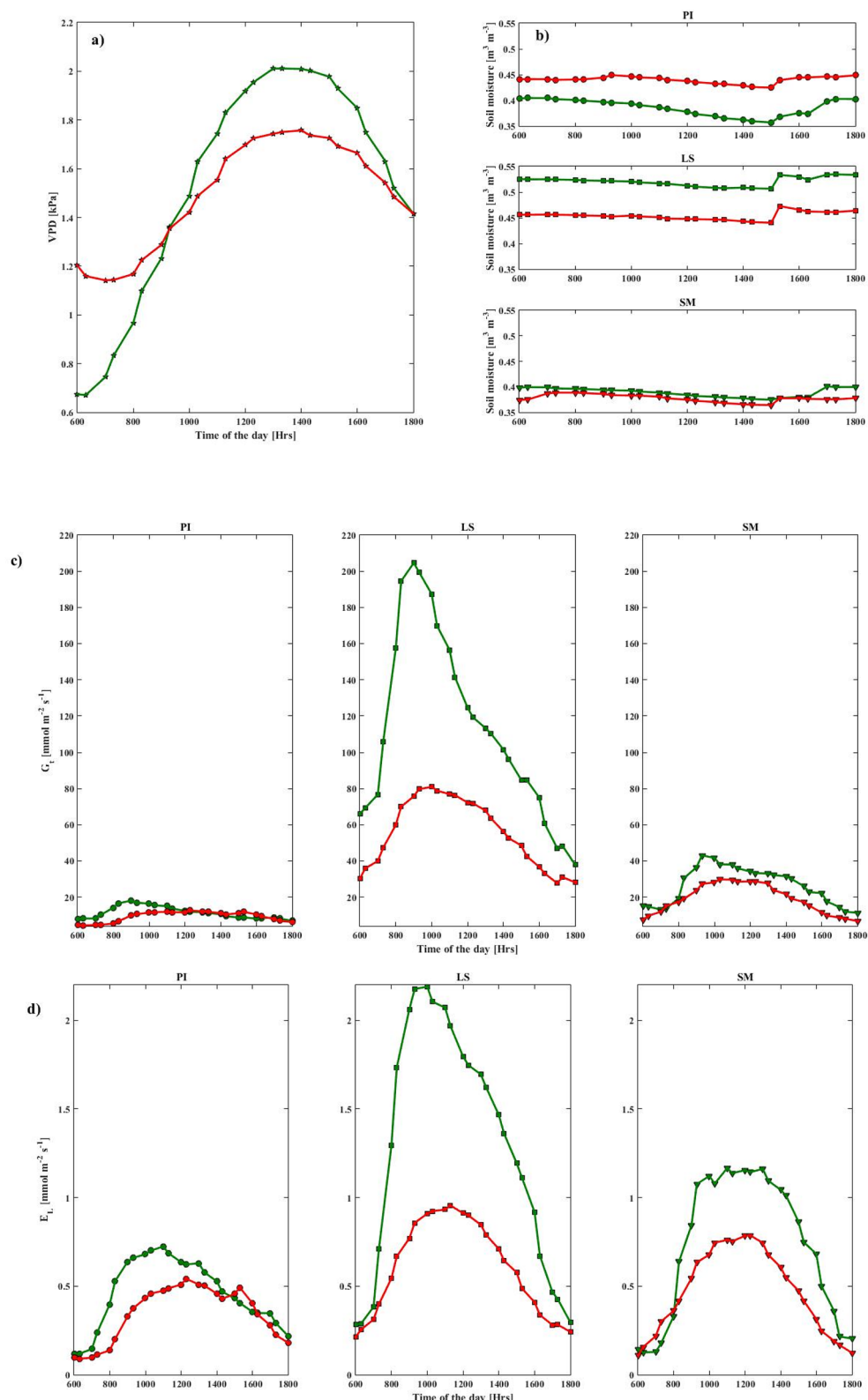


Figure 3. Hourly variations in (a) vapor pressure deficit (VPD; kPa), (b) soil moisture ($\text{m}^3 \text{m}^{-3}$), (c) canopy conductance (G_p ; $\text{mmol m}^{-2} \text{s}^{-1}$) and (d) whole-tree transpiration (E_L ; $\text{mmol m}^{-2} \text{s}^{-1}$), averaged over 6 AM to 6 PM LT of all days in the study period, during the dry and wet season. Columns correspond to the three species (*P. indicus* (PI); leftmost panel, *L. speciosa* (LS); middle panel, and *S. macrophylla* (SM); right panel) and seasons plotted in green (wet) and red (dry) symbols. This figure was generated using MATLAB version 7.12.0 R2017a (https://www.mathworks.com/products/new_products/release2017a.html).

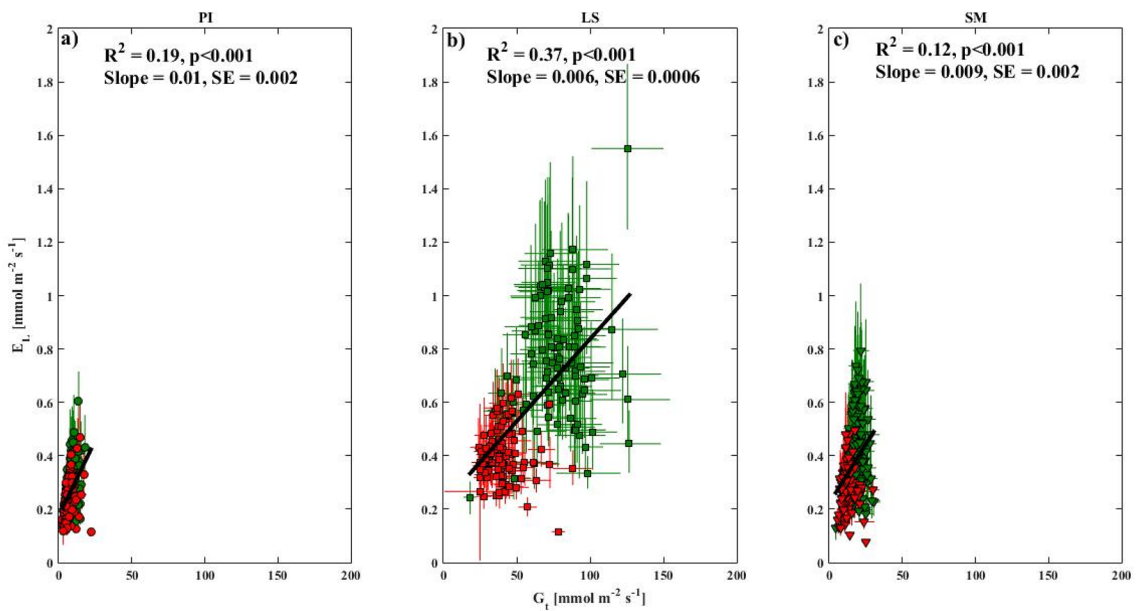


Figure 4. Daily averages of transpiration (E_L) plotted against canopy conductance (G_t) for (a) *P. indicus* (PI), (b) *L. speciosa* (LS), and (c) *S. macrophylla* (SM) and seasons plotted in green (wet) and red (dry) symbols. The black lines are linear fits, with the corresponding regression statistics indicated in each panel. This figure was generated using MATLAB version 7.12.0 R2017a (https://www.mathworks.com/products/new_products/release2017a.html).

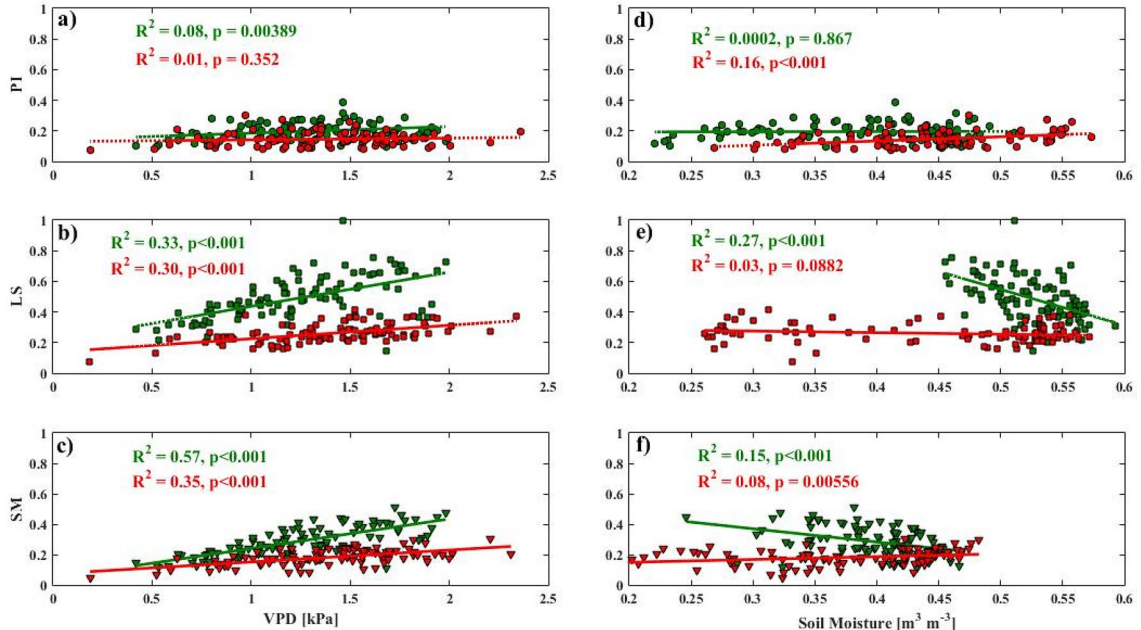


Figure 5. Daily averages of transpiration (E_L) plotted against VPD (a-c) and soil moisture (d-f) with the rows corresponding to the three species: *P. indicus* (PI), *L. speciosa* (LS), and *S. macrophylla* (SM), and seasons plotted in green (wet) and red (dry) symbols. This figure was generated using MATLAB version 7.12.0 R2017a (https://www.mathworks.com/products/new_products/release2017a.html).

may thus hide errors associated with such assumptions on canopy structure and missing information through appropriate parameter values. As indicated by the R^2 and RMSE values, the model G_t and E_L estimates could be generated without a substantial loss in model performance.

Canopy conductance and transpiration. The distribution of G_t was observed to be much broader for *L. speciosa*, relative to *P. indicus* and *S. macrophylla*, and approaching maximum G_t during the wet season (Table 2

and Fig. 2). Species-specific stomatal response is sensitive to environmental drivers, including atmospheric and soil moisture conditions, in addition to species phenology, which may promote a greater water flux during specific periods. The observation of relatively high levels of G_t in *L. speciosa* (deciduous species⁷) may be attributed to the fact that drought deciduous species tend to maximize carbon gain during the growing season (wet season), at the cost of a shorter leaf longevity compared to dry evergreen species⁴⁶. *P. indicus* and *S. macrophylla*, which are evergreen species, had relatively lower values of G_t and E_L when compared to the deciduous *L. speciosa*, during the study period. The evergreen species are able to photosynthesize all year round⁴⁷, without losing all the leaves in the canopy during any season⁴⁸. Therefore, opened stomata for photosynthesis can be maintained at the same rate throughout the seasons (Table 2).

During the wet period, we found that the atmospheric demand (VPD) was higher than in the dry period from 10 am to 6 pm (Fig. 3a) resulting in a higher canopy conductance and transpiration. Typically, VPD during the dry period should be higher than the wet period. However, in our experiments, saplings were placed on the roof top of a building, which could have had some confounding effect of heat dissipation from the building or the cement floor resulting in a high VPD during the wet season.

In the present study, as the saplings were potted, isolated, well ventilated, and placed on the balcony of a building, the variability in G_t was closely related to the atmospheric demand, with an approximate but weak linear relationship observed between daily variability in G_t and E_L (Fig. 5)⁴⁹. During the dry season, G_t and E_L were greatly reduced in all three species, which could indicate a moderation in the internal water potential, with the most prominent decrease in *L. speciosa*. The diurnal course of G_t and E_L was also variable between the three species (Fig. 5). In a previous study⁵⁰, it was reported that the sap flux density peaked just before noon and then decreased gradually throughout the late afternoon. This could be explained by a relatively higher stomatal closure in all species under high evaporative demand.

Soil and atmospheric demand. Stomatal response to VPD is usually optimized by minimizing water loss for a given amount of carbon assimilation⁵¹. Apart from sustaining a high rate of assimilation, this adaptability also helps in maintaining optimum leaf temperatures⁵². A reduction in the available soil moisture can lead to stomatal closure, reducing the evaporative demand on the internal water potential and decreasing the rate of depletion in root zone water⁵³. Similar relationships with soil moisture have been observed in the Amazonian⁵⁴ and Bornean rain forests⁵⁵ and may reflect a response mechanism to counteract short-term water stress induced by partial drying of root zone during dry periods.

A previous study⁵⁶ reported that *S. macrophylla* was able to extract water at relatively lower levels of soil water content. However, our study was on potted saplings, whose root expansion was limited in a container, where *S. macrophylla* was able to extract most water in the container until the soil moisture reached $0.2 \text{ m}^3 \text{ m}^{-3}$ in dry period (Fig. 5b). The highest transpiration rates estimated for *L. speciosa* might indicate a low xylem resistance to water flow and a deep root system⁵⁷ to maintain the water flow during dry season. Soil moisture used by *L. speciosa* during the dry season was also the highest among the three species and was above $0.25 \text{ m}^3 \text{ m}^{-3}$ even during times when the estimated transpiration rate was the highest. This could be due to the total leaf area of *L. speciosa* being the lowest, such that the rate of water depletion in the container was lower than that for *S. macrophylla* and *P. indicus*.

Suitable species for restoration under a future climate change scenario. Tropical species may be susceptible to variation in temperature, with a relatively small change in mean temperature causing a disproportionately large change in plant function due to heat related stresses. Additionally, extreme weather events due to erratic precipitation patterns can lead to an increased likelihood of excessive precipitation or protracted dry spells. The adaptability of a species to respond to such occurrences would strongly impact their survival. This trade-off can cause susceptibility to drought conditions in those plants that have been growing in waterlogged conditions and vice versa⁵⁸. Such large variations in temporal difference in soil moisture conditions may be detrimental for endangered species having narrow physiological tolerances⁵⁹ or poor competitors⁶⁰.

Forests degraded due to prolonged mono-crop practice, from fires, or a high mortality rate resulting from climate change, can be restored back from a state of being totally razed. Buffer zones around national parks fall under a sensitive land use criterion, and are treated as a protected area. But native people residing in such areas are allowed to live of the land while being under strict regulatory supervision. Illegal deforestation and ill-effects of climate change have resulted in a high mortality rate of forest species. One strategy for devising a restoration plan is to choose native species because the introduced alien species may easily spread and are harmful to the native species.

Deciduous species exhibit higher levels of transpiration and greater cooling and drought avoidance through leaf loss, relative to evergreen species, which have a limited physiological and morphological adaptability to survive wider swings in water and temperature ranges^{61,62}. While evergreen species, mostly native to wetter environments, can have fine roots concentrated near the soil surface during the dry season as nutrients and water are readily available on the soil surface. Therefore, when water is not a limiting factor on the forest floor, evergreen species compete for nitrogen and light resources⁶³, which under a restoration scenario, apart from soil water and nutrients are key limiting factors determining plant survival.

All three species in this study are native to tropical regions and can be considered for establishment under a restoration program. Moreover, since all of them are fast-growing species, they can also be pioneer species in degraded or barren lands as they would provide shade for other species. Under circumstances of low soil nutrition and the need for high rate of nutrient cycling, *L. speciosa* could be a suitable choice for restoration as it tends to photosynthesize rapidly, as indicated by higher canopy conductance and transpiration (Table 2 and

Fig. 2). Furthermore, given its deciduous nature, it would shed leaves during the dry season resulting in higher return rates of soil nutrient recycling.

Under a climate change scenario with higher temperatures and drier atmosphere and soil water stress, *P. indicus* is likely to be suitable choice under the restoration program, as it maintained a steady canopy conductance and transpiration during both wet and dry season soil moisture and air vapor demand (Fig. 3). This suggests that *P. indicus* would maintain a steady growth rate, independent of how dry the soil or air is. In other words, the stomata of *P. indicus* are relatively less sensitive to air and soil moisture demands when compared to *L. speciosa* and *S. macrophylla*. Also, *P. indicus* would be able to survive even if the future climate is predicted to be wetter than at present. However, the only downside of considering *P. indicus* is its potentially relatively slow growth rate due to low stomatal opening for photosynthesis but if the annual growth is to be accounted for, it may not be much different from the other two species.

Conclusions

We report the model estimates of G_t and E_L for the three potted sapling tree species across temporal scales during the wet and dry season using the StaCC model, which has been previously used only with the mature tree species. With our unique parameterization for species and season, we concluded that the model was able to perform well with the sapling data and could be used further to provide meaningful estimates of G_t and E_L for saplings. As the estimated transpiration rates of the studied species were variable, it is possible to select the most suitable species to be planted accordingly to restore degraded lands for effective reforestation. Transpiration per unit leaf area was the highest in *L. speciosa* while that in *S. macrophylla* and *P. indicus* was lower in both seasons. During the wet season with high VPD, higher amount of water loss through transpiration occurred compared to the dry season with a lower VPD. *P. indicus* is likely to be insensitive to changes of soil moisture and atmospheric demands, while *L. speciosa* responded to even small variations in the weather conditions. Leaf phenology might play a crucial role in G_t and E_L due to differences in the species' behavior. Being a deciduous species, *L. speciosa* would have a stronger stomatal control, while *P. indicus* and *S. macrophylla*, as evergreen species, tended to have low water use, given the ability to photosynthesize all year round, and would be able to maintain their stomatal opening even under the high atmospheric demand. Nevertheless, future studies on field-grown trees should be performed to confirm the findings.

Methods

Experimental setup and environmental measurement. The study site was established on the balcony of the 4th floor of a building in Chulalongkorn University, Bangkok ($13^{\circ} 44' 2.9''$ N $100^{\circ} 31' 54.1''$ E). Based on the 30-year- record (1981–2010) of climate data from a Bangkok metropolis station (Thai Meteorological Department), mean annual air temperature was 28.6° C and mean annual precipitation was 1648 mm. This study was undertaken from 25th July 2017 to 11th February 2018, which included both the wet (25th July–31st October 2017) and dry season (1st November 2017 to 11th February 2018). Ten trees for each species were bought from a nursery (Chatuchak market) and an automatic irrigation system was used to water the trees once a day. Despite the daily irrigation, the fluctuations of soil moisture may be large enough to affect any physiological responses of the potted saplings, hence we considered soil moisture as a covariate in this study. A detailed description of the experimental setup and the measurements can be found in a previous study⁵⁰ which mainly reported the observed sap flux density without scaling up to canopy conductance. We measured half-hourly air temperature ($^{\circ}$ C) and relative humidity (RH in %) with a probe (HC23-L, Campbell Scientific, Logan UT, USA), which were used to calculate VPD (kPa)⁶⁴. Photosynthetically active radiation (PAR, $\text{umol m}^{-2} \text{ s}^{-1}$) was measured using a quantum sensor (LI190R-L, Li-COR Biosciences, Lincoln, NE, USA). All these instruments were installed at approximately 2 m above the saplings. Volumetric soil moisture (% by volume) was monitored using Time-Domain Reflectometry (TDR) probes (CS 616, Campbell Scientific, Logan UT, USA), with the default factory calibration, installed in 2 pots for *L. speciosa* and *S. macrophylla* and 3 pots for *P. indicus*.

Tree biometric data. Tree data, including girth at breast height (GBH in cm), and leaf area were also measured to parameterize the model. The GBH was converted to diameter at breast height (DBH), assuming the stems were circular. Sapwood area was estimated from the measured GBH using the equation for calculating a circle, assuming negligible non-conducting wood (pith) due to small stem size (GBH ranged 7.3–10.7 cm). The assumption of negligible pith was confirmed from cutting some stems in the previous experiment and found that 98% of the basal area was sapwood area. For leaf area, we sampled 5 leaves from the upper and lower half of the crown of each sapling, scanned using a scanner (EPSON L3110 model) and analyzed the areas using ImageJ⁶⁵. Total leaf area of each sapling was then determined by multiplying the average measured leaf areas with the number of leaves in the respective crown layer. For scaling purposes using the model, leaf area and sapwood area were determined at the beginning of the study. We realized that leaf shedding may occur in some species, which could change the leaf areas of the studied saplings. However, since the study period was of 6 months, we could not get significant change in leaf area. Also, we considered to preserve the leaves because collecting them for the measurement may influence the sap flux measurements through changing transpirational area. Mean values ($\pm \text{SD}$) of total leaf area of the saplings were $3 \pm 0.34 \text{ m}^2$ for *P. indicus*, $2.55 \pm 0.18 \text{ m}^2$ for *L. speciosa* and $2.97 \pm 0.28 \text{ m}^2$ for *S. macrophylla*.

Sap flux measurement. To measure sap flux density ($J_s; \text{ g m}^{-2} \text{ s}^{-1}$), of the saplings, Granier-type thermal dissipation probes^{20,21} (TDPs) were constructed. Each T-type thermocouple (copper-constantan) was encapsulated within a steel needle making up the probe. A data logger (used to measure temperature difference between the two probes) was connected to each copper end with the constantan ends connected to each. The sap flux rate

was measured continuously by tracking the difference between the unheated (upstream or lower probe) and the heated (downstream or upper probe). The temperature difference was converted to sap flux density using the Baseline program version 4.0⁶⁶. All environmental sensors and sap flux probes were connected to a datalogger (CR1000, Campbell Scientific, Logan, UT, USA) which recorded 30-min average data throughout the study period. However, due to sensor failure for a relatively long time, we could not obtain continuous PAR record, with gaps covering 39% of the period. Consequently, the PAR data were not considered in further analysis after finding only 2% difference between running the model with and without the PAR sub-model.

Model description. We used the State-Space Canopy Conductance (StaCC) model to gap-fill the missing sap flow measurements using Bayesian inference, and to estimate the latent variables such as canopy stomatal conductance (G_c), transpiration per unit leaf area (E_L), and canopy transpiration (E_c)³¹. The model utilizes a combination of sap flux data and canopy conductance models while accounting for random errors associated with individual sensors. The final hierarchical Bayesian construct is a joint distribution accounting for sap flux measurement, latent states (transpiration and canopy conductance), and model parameters. The data model uses the measured sap flux density to estimate sap flux rate in probe i at time t as:

$$J_{it} \sim N(J_t Z(d_i) a_i, S) \quad (1)$$

where J_t is the average sap flux at time t , $Z(d_i)$ is the sapwood depth sub-model, a_i is the random effect due to probe i and S is the observational variance. As the sap flux was measured on potted saplings with small stem size (GBH \sim 7.3–10.7 cm), the sapwood depth sub-model was not used in this study. The model estimates canopy conductance (G_c) and transpiration per unit leaf area (E_L). The steady-state conductance at instant t ($G_{s,t}$, mmol m $^{-2}$ s $^{-1}$) is modeled semi-mechanistically^{67,68} through multiplicative nonlinear functions of environmental covariates, including vapor pressure deficit (D_t), photosynthetically active radiation (Q_t), and volumetric soil moisture (M_t) as:

$$G_{s,t} = f(D_t)g(Q_t)h(M_t) \quad (2)$$

The sub-model estimating the effect of D_t on $G_{s,t}$ has the form:

$$f(D_t) = G_{ref} - \lambda \ln(D_t) \quad (3)$$

where G_{ref} is the reference conductance (or the canopy conductance at $D_t = 1$ kPa) and λ is the stomatal sensitivity to D_t ⁶⁸. The dependence of $G_{s,t}$ on light is incorporated through the sub-model:

$$g(Q_t) = 1 - \alpha_1 \exp(Q_t/\alpha_2) \quad (4)$$

where, α_1 accounts for nighttime conductance and α_2 is the sensitivity to Q_t . However, because of the large gaps in PAR record, we did not use this light sub-model, as explained previously. The soil moisture sub-model has the form:

$$h(M_t) = \exp(-0.5(M_t - \alpha_3)^2/\alpha_4^2) \quad \text{if } M_t \leq \alpha_3 \quad (5)$$

or $h(M_t) = 1 \quad \text{if } M_t > \alpha_3$,

where α_3 is the threshold below which M_t reduces $G_{s,t}$ and α_4 controls the sensitivity of the reduction in $G_{s,t}$ with decrease in M_t below threshold. $G_{s,t}$ is used to calculate actual canopy conductance (G_t) using the state equation:

$$G_t = G_{t-dt} + (G_{s,t} - G_{t-dt})V_t, \quad (6)$$

with the assumption that G_t depends on the conductance at previous time step $t-dt$ and $dt = 30$ min and $V_t = 1 - \exp(-dt/\tau)$. The V_t term accounts for stomatal lags and $\tau = 10$ min³¹. Canopy conductance is then scaled to calculate E_L (kg m $^{-2}$ s $^{-1}$) as:

$$E_{L,t} = G_t q_t \quad (7)$$

where q_t is a composite variable. We kept a weak prior on the species-specific lags in the capacitance sub-model described in the previous study³¹. Additionally, wherever possible, the same priors for the data and process models were used³¹. A separate model analysis was implemented for each of the three species and the two seasons. The Gibbs sampler was run for 10,000 iterations and the first 3000 iterations were discarded as burn-in. The model generated J_t , G_t , and E_L estimates at each time step and was used to evaluate the differences in water flux among species and across the wet and dry seasons. Daily, weekly, and monthly averages of J_t , G_t , and E_L , were calculated for each species to evaluate the variability in water flux across temporal scales. We then estimated the relationship between daily G_t and E_L and environmental variables (VPD and soil moisture) using linear regression analyses. The analyses and visualization were carried out on MATLAB 7.12.0 R2017a (The MathWorks, Inc., Natick, Massachusetts, USA). To determine the interspecific and inter-seasonal differences, ANOVA and multiple regressions associated with mean parameters were performed, using the MATLAB program.

Data availability

The datasets generated during and/or analyzed during the current study are available from the corresponding author on reasonable request.

Received: 9 June 2020; Accepted: 6 January 2021
 Published online: 18 January 2021

References

- Pan, Y. *et al.* A large and persistent carbon sink in the world's forests. *Science* **333**, 988–993 (2011).
- Blenkinsop, S. & Fowler, H. J. Changes in drought frequency, severity and duration for the British Isles projected by the PRUDENCE regional climate models. *J. Hydrol.* **342**, 50–71 (2007).
- Guardiola-Claramonte, M. *et al.* Decreased streamflow in semi-arid basins following drought-induced tree die-off: a counter-intuitive and indirect climate impact on hydrology. *J. Hydrol.* **406**, 225–233 (2011).
- Hartmann, H. *et al.* Research frontiers for improving our understanding of drought-induced tree and forest mortality. *New Phytol.* **218**, 15–28 (2018).
- Chaturvedi, R. K., Raghubanshi, A. S., Tomlinson, K. & Singh, J. S. Impacts of human disturbance in tropical dry forests increase with soil moisture stress. *J. Veg. Sci.* **28**, 997–1007 (2017).
- Sjöman, H., Hiron, A. D. & Bassuk, N. L. Improving confidence in tree species selection for challenging urban sites: a role for leaf turgor loss. *Urban Ecosyst.* **21**, 1171–1188 (2018).
- Esperon-Rodriguez, M. *et al.* Assessing the vulnerability of Australia's urban forests to climate extremes. *Plants People Planet.* **1**, 387–397 (2019).
- Thaiutsa, B., Puangchit, L., Kjelgren, R. & Arunpraparut, W. Urban green space, street tree and heritage large tree assessment in Bangkok, Thailand. *Urban For. Urban Green.* **7**, 219–229 (2008).
- Chaturvedi, R. K., Tripathi, A., Raghubanshi, A. S. & Singh, J. S. Functional traits indicate a continuum of tree drought strategies across a soil water availability gradient in a tropical dry forest. *For. Ecol. Manag.* **2020** (In press).
- Chaturvedi, R. K., Raghubanshi, A. S. & Singh, J. S. Growth of tree seedlings in a tropical dry forest in relation to soil moisture and leaf traits. *J. Plant Ecol.* **6**, 158–170 (2013).
- Krauss, K. W., Twilley, R. R., Doyle, T. W. & Gardiner, E. S. Leaf gas exchange characteristics of three neotropical mangrove species in response to varying hydroperiod. *Tree Physiol.* **26**, 959–968 (2006).
- Yan, M.-J., Yamanaka, N., Yamamoto, F. & Du, S. Responses of leaf gas exchange, water relations, and water consumption in seedlings of four semiarid tree species to soil drying. *Acta Physiol. Plant.* **32**, 183–189 (2010).
- Yan, W., Zheng, S., Zhong, Y. & Shangguan, Z. Contrasting dynamics of leaf potential and gas exchange during progressive drought cycles and recovery in *Amorpha fruticosa* and *Robinia pseudoacacia*. *Sci. Rep.* **7**, 4470 (2017).
- Medlyn, B. E. *et al.* Stomatal conductance of forest species after long-term exposure to elevated CO₂ concentration: a synthesis. *New Phytol.* **149**, 247–264 (2001).
- Wullschleger, S. D., Gunderson, C. A., Hanson, P. J., Wilson, K. B. & Norby, R. J. Sensitivity of stomatal and canopy conductance to elevated CO₂ concentration: interacting variables and perspectives of scale. *New Phytol.* **153**, 485–496 (2002).
- Ainsworth, E. A. & Rogers, A. The response of photosynthesis and stomatal conductance to rising [CO₂]: mechanisms and environmental interactions. *Plant. Cell Environ.* **30**, 258–270. <https://doi.org/10.1111/j.1365-3040.2007.01641.x> (2007).
- Tor-ngern, P. *et al.* Increases in atmospheric CO₂ have little influence on transpiration of a temperate forest canopy. *New Phytol.* **205**, 518–525 (2015).
- Schäfer, K. V. R. *et al.* Exposure to an enriched CO₂ atmosphere alters carbon assimilation and allocation in a pine forest ecosystem. *Glob. Chang. Biol.* **9**, 1378–1400 (2003).
- Williams, M. *et al.* Modelling the soil-plant-atmosphere continuum in a *Quercus*-*Acer* stand at Harvard Forest: the regulation of stomatal conductance by light, nitrogen and soil/plant hydraulic properties. *Plant. Cell Environ.* **19**, 911–927 (1996).
- Granier, A. Une nouvelle méthode pour la mesure du flux de sève brute dans le tronc des arbres. *Ann. For. Sci.* **42**, 193–200 (1985).
- Granier, A. Evaluation of transpiration in a Douglas-fir stand by means of sap flow measurements. *Tree Physiol.* **3**, 309–320 (1987).
- Green, S., Clothier, B. & Jardine, B. Theory and practical application of heat pulse to measure sap flow. *Agron. J.* **95**, 1371–1379 (2003).
- Burgess, S. S. O. *et al.* An improved heat pulse method to measure low and reverse rates of sap flow in woody plants. *Tree Physiol.* **21**, 589–598 (2001).
- Sakurata, T. A Heat balance method for measuring water flux in the stem of intact plants. *J. Agric. Meteorol.* **37**, 9–17 (1981).
- Chang, X., Zhao, W., Zhang, Z. & Su, Y. Sap flow and tree conductance of shelter-belt in arid region of China. *Agric. For. Meteorol.* **138**, 132–141 (2006).
- Ewers, B. E., Oren, R., Phillips, N., Strömgren, M. & Linder, S. Mean canopy stomatal conductance responses to water and nutrient availabilities in *Picea abies* and *Pinus taeda*. *Tree Physiol.* **21**, 841–850 (2001).
- Pataki, D. E., Oren, R. & Phillips, N. Responses of sap flux and stomatal conductance of *Pinus taeda* L. trees to stepwise reductions in leaf area. *J. Exp. Bot.* **49**, 871–878 (1998).
- Ryan, M. G. *et al.* Transpiration and whole-tree conductance in ponderosa pine trees of different heights. *Oecologia* **124**, 553–560 (2000).
- Oishi, A. C., Oren, R., Novick, K. A., Palmroth, S. & Katul, G. G. Interannual invariability of forest evapotranspiration and its consequence to water flow downstream. *Ecosystems* **13**, 421–436 (2010).
- Oishi, A. C., Oren, R. & Stoy, P. C. Estimating components of forest evapotranspiration: a footprint approach for scaling sap flux measurements. *Agric. For. Meteorol.* **148**, 1719–1732 (2008).
- Bell, D. M. *et al.* A state-space modeling approach to estimating canopy conductance and associated uncertainties from sap flux density data. *Tree Physiol.* **35**, 792–802 (2015).
- Kim, H.-S., Oren, R. & Hinckley, T. M. Actual and potential transpiration and carbon assimilation in an irrigated poplar plantation. *Tree Physiol.* **28**, 559–577 (2008).
- Meinzer, F. C., James, S. A. & Goldstein, G. Dynamics of transpiration, sap flow and use of stored water in tropical forest canopy trees. *Tree Physiol.* **24**, 901–909 (2004).
- Phillips, N., Nagchaudhuri, A., Oren, R. & Katul, G. Time constant for water transport in loblolly pine trees estimated from time series of evaporative demand and stem sapflow. *Trees* **11**, 412–419 (1997).
- Tor-ngern, P. *et al.* Ecophysiological variation of transpiration of pine forests: synthesis of new and published results. *Ecol. Appl.* **27**, 118–133 (2017).
- Clark, J. S. *et al.* Inferential ecosystem models, from network data to prediction. *Ecol. Appl.* **21**, 1523–1536 (2011).
- Lu, P., Urban, L. & Zhao, P. Granier's thermal dissipation probe (TDP) method for measuring sap flow in trees: theory and practice. *Acta Bot. Sin.* **46**, 631–646 (2004).
- Ewers, B. & Oren, R. Analyses of assumptions and errors in the calculation of stomatal conductance from sap flux measurements. *Tree Physiol.* **20**, 579–589 (2000).
- Ward, E. J., Oren, R., Sigurdsson, B. D., Jarvis, P. G. & Linder, S. Fertilization effects on mean stomatal conductance are mediated through changes in the hydraulic attributes of mature Norway spruce trees. *Tree Physiol.* **28**, 579–596 (2008).
- Addington, R. N., Mitchell, R. J., Oren, R. & Donovan, L. A. Stomatal sensitivity to vapor pressure deficit and its relationship to hydraulic conductance in *Pinus palustris*. *Tree Physiol.* **24**, 561–569 (2004).

41. Leuning, R. A critical appraisal of a combined stomatal-photosynthesis model for C3 plants. *Plant. Cell Environ.* **18**, 339–355 (1995).
42. Meinzer, F. C., Hinckley, T. M. & Ceulemans, R. Apparent responses of stomata to transpiration and humidity in a hybrid poplar canopy. *Plant. Cell Environ.* **20**, 1301–1308 (1997).
43. Monteith, J. L. A reinterpretation of stomatal responses to humidity. *Plant. Cell Environ.* **18**, 357–364 (1995).
44. Loustau, D. *et al.* Transpiration of a 64-year-old maritime pine stand in Portugal. *Oecologia* **107**, 33–42 (1996).
45. Domec, J.-C. & Gartner, B. L. Cavitation and water storage capacity in bole xylem segments of mature and young Douglas-fir trees. *Trees* **15**, 204–214 (2001).
46. Moore, G. W., Bond, B. J., Jones, J. A., Phillips, N. & Meinzer, F. C. Structural and compositional controls on transpiration in 40- and 450-year-old riparian forests in western Oregon, USA. *Tree Physiol.* **24**, 481–491 (2004).
47. Leigh, A., Sevanto, S., Close, J. D. & Nicotra, A. B. The influence of leaf size and shape on leaf thermal dynamics: does theory hold up under natural conditions? *Plant. Cell Environ.* **40**, 237–248 (2017).
48. Brodribb, T. J., Holbrook, N. M., Edwards, E. J. & Gutierrez, M. V. Relations between stomatal closure, leaf turgor and xylem vulnerability in eight tropical dry forest trees. *Plant. Cell Environ.* **26**, 443–450 (2003).
49. Choat, B., Ball, M., Luly, J., Donnelly, C. & Holtum, J. Seasonal patterns of leaf gas exchange and water relations in dry rain forest trees of contrasting leaf phenology. *Tree Physiol.* **26**, 657–664 (2006).
50. Tor-ngern, P. & Puangchit, L. Effects of varying soil and atmospheric water deficit on water use characteristics of tropical street tree species. *Urban For. Urban Green.* **36**, 76–83 (2018).
51. Jarvis, P. G. Transpiration and assimilation of tree and agricultural crops: the omega factor. In *Attributes of Trees as Crop Plants* (eds Cannel, M. G. R. & Jackson, J. E.) 460–480 (Institute of Terrestrial Ecology Huntingdon, UK, 1985).
52. Marchin, R. M., Broadhead, A. A., Bostic, L. E., Dunn, R. R. & Hoffmann, W. A. Stomatal acclimation to vapour pressure deficit doubles transpiration of small tree seedlings with warming. *Plant. Cell Environ.* **39**, 2221–2234 (2016).
53. Mahan, J. R. & Upchurch, D. R. Maintenance of constant leaf temperature by plants—I Hypothesis-limited homeothermy. *Environ. Exp. Bot.* **28**, 351–357 (1988).
54. Schultz, H. R. Differences in hydraulic architecture account for near-isohydric and anisohydric behaviour of two field-grown *Vitis vinifera* L. cultivars during drought. *Plant. Cell Environ.* **26**, 1393–1405 (2003).
55. Harris, P. P., Huntingford, C., Cox, P. M., Gash, J. H. C. & Malhi, Y. Effect of soil moisture on canopy conductance of Amazonian rainforest. *Agric. For. Meteorol.* **122**, 215–227 (2004).
56. Kjelgren, R., Joyce, D. & Doley, D. Subtropical-tropical urban tree water relations and drought stress response strategies. *Arboric. Urban For.* **39**, 125–131 (2013).
57. West, A. G., Hultine, K. R., Jackson, T. L. & Ehleringer, J. R. Differential summer water use by *Pinus edulis* and *Juniperus osteosperma* reflects contrasting hydraulic characteristics. *Tree Physiol.* **27**, 1711–1720 (2007).
58. Hatfield, J. L. & Prueger, J. H. Temperature extremes: effect on plant growth and development. *Weather Clim. Extrem.* **10**, 4–10 (2015).
59. Suratna, R. R. & Yamauchi, A. Root growth, aerenchyma development, and oxygen transport in rice genotypes subjected to drought and waterlogging. *Environ. Exp. Bot.* **64**, 75–82 (2008).
60. Lawler, J. J. *et al.* The scope and treatment of threats in endangered species recovery plans. *Ecol. Appl.* **12**, 663–667 (2002).
61. Liu, H., Lin, J., Zhang, M., Lin, Z. & Wen, T. Extinction of poorest competitors and temporal heterogeneity of habitat destruction. *Ecol. Model.* **219**, 30–38 (2008).
62. Baltzer, J. L., Grégoire, D. M., Bunyavejchewin, S., Noor, N. S. M. & Davies, S. J. Coordination of foliar and wood anatomical traits contributes to tropical tree distributions and productivity along the Malay-Thai Peninsula. *Am. J. Bot.* **96**, 2214–2223 (2009).
63. Kursar, T. A. *et al.* Tolerance to low leaf water status of tropical tree seedlings is related to drought performance and distribution. *Funct. Ecol.* **23**, 93–102 (2009).
64. Monteith, J. L. & Unsworth, M. H. *Principles of Environmental Physics* 287 (Butterworth-Heinemann, Oxford, 1990).
65. Schneider, C. A., Rasband, W. S. & Eliceiri, K. W. NIH Image to ImageJ: 25 years of image analysis. *Nat. Methods.* **9**(7), 671–675 (2012).
66. Oishi, A. C., Hawthorne, D. A. & Oren, R. Baseline: an open-source, interactive tool for processing sap flux data from thermal dissipation probes. *Software X* **5**, 139–143 (2016).
67. Ball, J., Woodrow, I. & Berry, J. A model predicting stomatal conductance and its contribution to the control of photosynthesis under different environmental conditions. *Prog. Photosynth. Res.* **4**, 221–224 (1987).
68. Jarvis, P. G. The interpretation of the variations in leaf water potential and stomatal conductance found in canopies in the field. *Philos. Trans. R. Soc. London. B Biol. Sci.* **273**, 593–610 (1976).

Acknowledgements

We thank Dr. Eric J. Ward for guidance in using the StaCC model. This research was supported by the Ratchadapisek Somphot Fund for Postdoctoral Fellowship, Chulalongkorn University. PT would like to thank the National Science and Technology Development Agency (NSTDA, P-18-51395) and the Thailand Science Research and Innovation (TSRI, RDG6230006) for financial support.

Author contributions

P.T. conceived and designed the study and collected the data. T.A. performed all data and modeling analyses. N.L. provided insights into the result interpretations. T.A. wrote the first draft and made all revisions. P.T. and N.L. helped comment the manuscript.

Competing interests

The authors declare no competing interests.

Additional information

Correspondence and requests for materials should be addressed to P.T.

Reprints and permissions information is available at www.nature.com/reprints.

Publisher's note Springer Nature remains neutral with regard to jurisdictional claims in published maps and institutional affiliations.



Open Access This article is licensed under a Creative Commons Attribution 4.0 International License, which permits use, sharing, adaptation, distribution and reproduction in any medium or format, as long as you give appropriate credit to the original author(s) and the source, provide a link to the Creative Commons licence, and indicate if changes were made. The images or other third party material in this article are included in the article's Creative Commons licence, unless indicated otherwise in a credit line to the material. If material is not included in the article's Creative Commons licence and your intended use is not permitted by statutory regulation or exceeds the permitted use, you will need to obtain permission directly from the copyright holder. To view a copy of this licence, visit <http://creativecommons.org/licenses/by/4.0/>.

© The Author(s) 2021

Objective	Proposed activities	Actual activities	Outputs
1. Study the past responses of tree growth to climate change	1. Collect tree ring samples in Thai and Chinese forests and analyze ring widths and their relationship with climatic variables.	1. Collected tree ring samples in a Thai forest and analyzed tree rings and their relationship with climate variables including temperature and precipitation.	1. A manuscript titled “Growth-climate relationships and long-term growth trend of <i>Choerospondias axillaris</i> at Mosingto, Khao Yai National Park, Central Thailand” accepted by <i>Forests</i> (Q1 SCOPUS).
2. Study the present responses of forests to climate variability and assess the vulnerability and resilience of forests	1. Measure water and carbon flows in forests. 2. Perform analysis of the variations of the water and carbon flows with climate variability. 3. Collect samples and analyze tree hydraulic and plant functional traits. 4. Perform data analysis and interpretations.	1. Set up sap flow measurement net work on trees in Thai forests and began data collection during the last period of the project. 2. Tested a model that was developed to estimate canopy conductance of forests from sap flow data using previously collected sap flow data from saplings of tropical tree species. 3. Measured and analyzed leaf gas exchange parameters including leaf photosynthesis and stomatal conductance of dominant tree species in Thai forests of various successional stages.	1. Half-hourly continuous data until the present. 2. A publication titled “Comparison of water-use characteristics of tropical tree saplings with implications for forest restoration” published in <i>Scientific Reports</i> (Tier 1 SCOPUS) 3. A publication titled “Variation of leaf-level gas exchange rates and leaf functional traits of dominant trees across three successional stages in a Southeast Asian tropical forest” published in

		<p>4. Measured and analyzed tree hydraulic parameters to study the seasonal variations of dominant tree species among successional forests and assessed their vulnerability to drought with implications for future climate change impact, such as drought, on the species.</p> <p>5. Developed allometric equations for estimating sapwood area of trees in the Thai forests. These equations were used in combination with sap flow data to preliminary calculate canopy transpiration of the forests.</p> <p>6. Measured and analyzed soil respiration of three successional forests in Thailand across seasons and investigated different environmental factors that may contribute to its variations.</p> <p>7. Measured and analyzed litterfall and litter</p>	<p><i>Forest Ecology and Management</i> (Tier 1 SCOPUS)</p> <p>4. A manuscript titled “Variations in leaf water status and drought tolerance of dominant tree species among three successional forests in Southeast Asia” submitted to <i>Journal of Ecology</i> (Tier 1 SCOPUS)</p> <p>5. A manuscript titled “Sapwood area ~DBH allometries for 14 common tree species in a successional tropical forest in Thailand” was accepted by <i>Forestry: An International Journal of Forest Research</i> (Q1 SCOPUS)</p> <p>6. A publication titled “Different responses of soil respiration to environmental factors across forest stages in a Southeast Asian forest” published in <i>Ecology and Evolution</i> (Q1 SCOPUS)</p> <p>7. A manuscript titled “Litter dynamics across successional</p>
--	--	--	--

		decomposition of three successional forests in Thailand.	stages of evergreen seasonal tropical forests: seasonal patterns and productivity" is being prepared
3. Study the future impacts of climate change on forest biomass, productivity, and diversity.	<ol style="list-style-type: none"> 1. Use and validate a dynamic global vegetation model (LPJmL-FIT model) using the past response results. 2. Perform analysis of future impacts of climate change on the forests in the next century. 	<p>1. Due to difficulty and challenges in obtaining data for model parameterization and collaborative work between partners, we could not achieve the originally proposed plan. However, we did our best to obtain data related to vulnerability to drought of tree species in both Thai and Chinese forests and perform a synthetic analysis to investigate the relationship between the parameter related to drought tolerance of trees and site conditions of the forests along the latitudinal gradient.</p>	<p>1. Preliminary results which call for further investigation in the future.</p>

(Associate Professor Pantana Tor-ngern, Ph.D.)

Principal Investigator

Date: